NASA CONTRACTOR REPORT

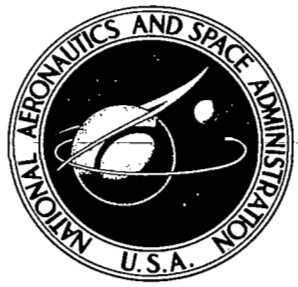

NASA CR-1933

MOTION EFFECTS ON AN IFR HOVERING TASK — ANALYTICAL PREDICTIONS AND EXPERIMENTAL RESULTS

by R. F. Ringland, R. L. Stapleford, and R. E. Magdaleno

Prepared by
SYSTEMS TECHNOLOGY, INC.
Hawthorne, Calif. 90250
for Ames Research Center

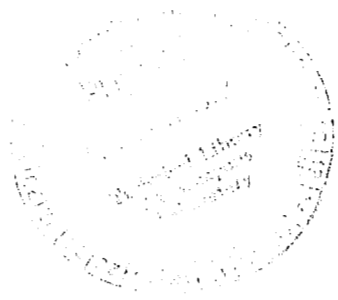

NATIONAL AERONAUTICS AND SPACE ADMINISTRATION • WASHINGTON, D. C. • NOVEMBER 1971

1. Report No.	2. Government Accession No.	3. Recipient's Catalog No.
NASA CR-1933		

4. Title and Subtitle	5. Report Date
Motion Effects on an IFR Hovering Task--Analytical Predictions and Experimental Results	November 1971
	6. Performing Organization Code

7. Author(s)	8. Performing Organization Report No.
R.F. Ringland, R.L. Stapleford & R.E. Magdaleno	
	10. Work Unit No.

9. Performing Organization Name and Address	11. Contract or Grant No.
Systems Technology, Inc. 13766 South Hawthorne Boulevard Hawthorne, Ca. 90250	NAS 2-5261
	13. Type of Report and Period Covered
12. Sponsoring Agency Name and Address	Contractor Report
National Aeronautics & Space Administration Washington, D.C. 20546	14. Sponsoring Agency Code

15. Supplementary Notes

16. Abstract

An analytical pilot model incorporating the effects of motion cues and display scanning and sampling is tested by comparing predictions against experimental results on a moving base simulator. The simulated task is that of precision hovering of a VTOL having varying amounts of rate damping, and using separated instrument displays. Motion cue effects are investigated by running the experiment under fixed and moving base conditions, the latter in two modes -- full motion, and angular motion only. Display scanning behavior is measured on some of the runs.

The results of the program show that performance is best with angular motion only, most probably because of a g-vector tilt cue is available to the pilot in this motion condition. This provides an attitude indication even when not visually fixating the attitude display. Vestibular threshold effects are also present in the results because of the display scaling used to permit hovering position control within the motion simulator limits -- no washouts are used in the simulator drive signals. The IFR nature of the task results in large decrements in pilot opinion and performance relative to VFR conditions because of the scanning workload. Measurements of scanning behavior are sensitive to motion conditions and show more attention to attitude control under fixed base conditions.

17. Key Words (Suggested by Author(s))	18. Distribution Statement
Motion Simulation Pilot Models Tracking Performance Pilot Ratings Display Scanning	UNCLASSIFIED-UNLIMITED

19. Security Classif. (of this report)	20. Security Classif. (of this page)	21. No. of Pages	22. Price*
UNCLASSIFIED	UNCLASSIFIED	203	$3.00

*For sale by the National Technical Information Service, Springfield, Virginia 22151

FOREWORD

The research reported here was sponsored by the Man/Machine Integration Branch, Biotechnology Division, Ames Research Center, National Aeronautics and Space Administration. It was conducted by Systems Technology, Inc., Hawthorne, California, under Contract No. NAS2-5261 with NASA support for the experiments. The NASA Project Monitor was John D. Stewart. The contractor's Technical Director was Duane T. McRuer and the Project Engineer was Robert L. Stapleford.

The authors would like to express their gratitude to the NASA personnel for their excellent cooperation throughout the experiments.

ABSTRACT

An analytical pilot model incorporating the effects of motion cues and display scanning and sampling is tested by comparing predictions against experimental results on a moving base simulator. The simulated task is that of precision hovering of a VTOL having varying amounts of rate damping, and using separated instrument displays. Motion cue effects are investigated by running the experiment under fixed and moving base conditions, the latter in two modes — full motion, and angular motion only. Display scanning behavior is measured on some of the runs.

The results of the program show that performance is best with angular motion only, most probably because a g-vector tilt cue is available to the pilot in this motion condition. This provides an attitude indication even when not visually fixating the attitude display. Vestibular threshold effects are also present in the results because of the display scaling used to permit hovering position control within the motion simulator limits — no washouts are used in the simulator drive signals. The IFR nature of the task results in large decrements in pilot opinion and performance relative to VFR conditions because of the scanning workload. Measurements of scanning behavior are sensitive to motion conditions and show more attention to attitude control under fixed base conditions.

CONTENTS

FIGURES

TABLES

SYMBOLS

a	Gain in pilot's motion (vestibular) channel
b	Inverse time constant of motion fidelity filter
f_s	Overall look (scan) rate
$\bar{f}_s$	Average look (scan) frequency
F	Motion fidelity filter transfer function
g	Graviataional acceleration
$G(j\omega)$ or $G(\sigma)$	Open-loop transfer function
H	Display motion synchronization filter transfer function
K_m	Gain margin
K_p	Pilot describing function gain
ℓ_x	Pilot location forward of vehicle center of gravity
L_p	Roll acceleration per unit roll rate
L_v	Roll acceleration per unit lateral velocity
L_{δ_a}	Roll acceleration per unit aileron deflection
M_q	Pitch acceleration per unit pitch rate
M_u	Pitch acceleration per unit longitudinal velocity
M_{δ_e}	Pitch acceleration per unit elevator deflection
N	Number of looks during a run
P_c	$\frac{2\pi}{\omega_{c_a}}$
PR	Pilot rating
q	Pitch rate
s	Laplace transform variable
S	Sampling parameter (Appendix A)
T	Time constant
$\bar{T}_d$	Average dwell time

T_{d_e}	Effective display dwell time
T_D	Time constant, display motion synchronization filter
T_L	Pilot discribing function lead time constant
T_{L_V}	Visual lead time constant
T_o	Minimum sample interval
T_R	Run length
$\overline{T}_s$	Average look interval
T_{sp}	Short-period time constant in VTOL attitude dynamics
u	Longitudinal velocity
u_g	Longitudinal gust velocity
v	Lateral velocity
v_g	Lateral gust velocity
w	Vertical velocity
w_g	Vertical gust velocity
x	Longitudinal displacement of vehicle center of gravity
x_i, y_i, z_i	Ideal cab displacements
x_{ref}	Longitudinal position reference (Fig. A-1)
x_ϵ	Longitudinal position error (Fig. A-1)
X_D, Y_D, Z_D	Displayed values of VTOL displacements
X_u	Longitudinal acceleration per unit longitudinal velocity
y	Lateral displacement of vehicle center of gravity
Y_p	Pilot describing function
Y_v	Lateral acceleration per unit lateral velocity
z	Vertical displacement of vehicle center of gravity
Z_w	Vertical acceleration per unit vertical velocity (aerodynamic)
Z_w'	Vertical acceleration per unit vertical velocity (stability augmentor)

Z_{δ_e}	Vertical acceleration per unit collective deflection
δ	Display sampling variability parameter (Eq. 6)
δ_a	Aileron deflection (lateral cyclic)
δ_c	Collective deflection
δ_e	Elevator deflection (longitudinal cyclic)
Δ	Indicates increment in a quantity
ζ	Damping ratio
ζ_D	Damping ratio, display motion synchronization filter
ζ_p	Phugoid damping ratio
ζ_{sp}'	Short-period damping ratio (when attitude loop closed)
ζ_1	See Eq. A-5
η	Dwell fraction (foveal)
η_e	Effective dwell fraction
θ	Pitch attitude
θ_D, Φ_D	Displayed values of pitch and roll attitudes
θ_ϵ	Pilot's internally generated pitch attitude error (Fig. A-1)
θ_x	Pilot's internally generated pitch attitude command (Fig. A-1)
ν	Look fraction
σ_D	Root mean square value of display motion
σ_{disp}	Vector position error (Eq. 5)
σ_k	Root mean square value of k, where k is any motion variable
σ_{n_D}	rms noise level introduced by subject as a result of display scanning
σ_{T_d}	Standard deviation of dwell time
τ	Pilot describing function time delay
τ_m	Time delay in pilot's motion (vestibular) channel

τ_s	Display fixation delay
τ_1	Incremental delay
φ	Roll attitude
ϕ	Phase angle
ϕ_m	Phase margin at crossover
$\Phi_{nn}(\omega)$	Power spectral density
ω	Circular frequency
ω_c	Crossover frequency
ω_{c_a}	Average crossover frequency
ω_{cp}	Parafoveal crossover frequency (Appendix A)
ω_{c_f}	Foveal crossover frequency (Appendix A)
ω_D	Natural frequency, display motion synchronization filter
ω_M	Frequency at which visual channel and motion channel gains are equal (Appendix A)
ω_p	Phugoid frequency, attitude dynamics
ω_s	Display sampling frequency
ω_{sp}'	Short-period frequency (when attitude loop closed)
ω_1	See Eq. A-5
Ω	Parafoveal-to-foveal gain ratio

SUBSCRIPTS

i	Refers to display number (1, 2, or 4) or to loop closure (θ, φ, x, y, or z)

SECTION I

INTRODUCTION

A. BACKGROUND

Motion cues can often have an important effect on the manual control of aerospace vehicles. Designers and researchers in the field of manual control are therefore interested in analytical pilot models which are useful in predicting these effects. In an earlier study (Ref. 1) the existing data on motion cue effects was surveyed and such a model — the multimodality pilot model — was developed. The overall purpose of the experimental research discussed in this report was to provide a test of this model in a realistic manual control situation. Additional data were sought as well in these areas where the multimodality pilot model rests on relatively few data points.

The major goals of this program are, in the order of their importance, as follows:

- To test the application of the multimodality pilot model for a typical realistic task.
- To provide additional experimental data on the role of linear motion cues.
- To provide additional experimental data on the effects of the fidelity of the motion simulation.
- To obtain a limited amount of data on the effect of motion cues on pilot display scanning and sampling.

These four goals constitute the objectives of the Priority I, II, III, and IV runs discussed in this report.

The initial phase of the program was devoted to the selection of an experimental situation capable of satisfying these objectives, and an analysis to predict the experimental results. The analysis was based upon the multimodality pilot model together with recent results, Refs. 2, 3, and 4, concerning display scanning and sampling behavior. This analytical work was completed while the shakedown and early training runs were taking place and without knowledge of the early experimental results.

VTOL hovering in gusty air was selected as the experimental task. The simulated vehicle dynamics were programmed on an analog computer,

signals from which drove the angular and linear degrees of freedom of a moving-base simulator. The three subjects manipulated controls in the enclosed simulator cab in response to motion variables displayed on separate instruments, and to the cab motions themselves. The subjects were all pilots qualified in VTOL-type vehicles and for instrument flight. The simulator drive signals were all compensated for the known dynamic lags of the simulator — no washout circuits were used to limit cab motions. The two principal experimental variables (other than subject) were first, the motion itself (three conditions: fixed base, moving base with angular and linear cab motions, and moving base with angular motion only) and the configuration of the vehicle dynamics (several degrees of difficulty and corresponding sensitivity to the presence of motion cues). Differences in configuration were presented to the subjects in random order, different for each subject. Similarly, the motion conditions for each configuration were presented in random order, different for each subject. On a few runs, a fourth variable was introduced, a lag deliberately inserted in the simulator drive signals.

Various of the simulated motion variables were recorded on strip charts, and for most of the runs, on FM tape for possible later describing function analysis. The variances of these quantities were recorded for each run as indicators of task performance. On some of the runs, pilot scanning behavior was measured using the Eye-Point-of-Regard system developed at Systems Technology, Inc. Pilot ratings were given and pilot commentary was recorded (and later transcribed) for most of the experimental runs.

The performance and pilot opinion data were extensively analyzed relative to preexperimental predictions. Much of the scanning measurements were reduced and a few example runs were analyzed for pilot describing functions. The results revealed large differences between VFR and IFR performance and opinion, and a preference for the angular motion only condition — apparently because the pilot can effectively respond to the utricular (or proprioceptive) sensation of tilt. The data also showed the influence of vestibular threshold effects — in this experiment the angular rates were subthreshold for much of the time, rendering motion cues less effective than anticipated.

B. REPORT OUTLINE

The task selection, experimental setup, and procedures used in the experiment are discussed in Section II. This section notes the modifications made as a result of the experience gained in the early shakedown and subject training runs. The principal modifications were to the attitude display gains and control sensitivities. These changes were necessary to permit hovering within the linear motion limits of the simulator.

Section III presents the pilot opinion, commentary, and performance results, and their interpretation. Particular attention is paid to differences in subject, configuration, and motion condition. The results of a "target of opportunity" experiment are also given — this brief experiment was intended to ascertain performance differences ascribable to VFR-IFR differences, and the influence of input disturbance magnitude on performance.

Section IV describes the eye-point-of-regard data. Subject, configuration and motion condition influences on these data are emphasized.

Section V presents the results of the brief describing function analysis with emphasis on motion condition differences.

Section VI is a summary of the major findings of the experimental program.

Appendix A describes the pilot models used and the techniques used in the preexperimental prediction of the experimental results. This appendix is also an example of nearly all facets of the current theory on pilot vehicle analysis. Multiloop, multimodality, and display scanning effects are included. The analytical predictions include performance, pilot ratings, and pilot comments.

Appendix B contains a run-by-run listing of most of the performance data (the rest is given in Section III) and that portion of the eye-point-of-regard data which was reduced (34 runs out of 53). Appendix C contains additional describing function data.

SECTION II

EXPERIMENTAL CONDITIONS AND DATA-TAKING PROCEDURES

Selection of the test conditions was guided by the following essentials:

- The piloting task should be a multiaxis task to permit testing of the multimodality pilot model in a multiaxis situation.
- It should be similar to tasks used in past work to provide a basis for comparison of results.
- It should be variable over a range of sensitivity to the presence (or absence) of motion cues.
- It should permit measurement of pilot display scanning and sampling behavior.

With these needs in mind, a VTOL hovering task using separated instrument displays was selected. The display aspects of the task were quite similar to the "conventional instrument display" of Ref. 5, while the dynamics of the hovering vehicle were similar to those used in earlier studies (Refs. 6, 7, and 8).

A. SIMULATION DESCRIPTION

The general task presented to the subjects was to hover over a spot in mildly gusty air. They were instructed to keep their position (fore-and-aft and side-to-side) and altitude excursions to a minimum. The experiments were conducted on the NASA Ames six-degrees-of-freedom simulator (Fig. 1). In response to displayed visual and motion cues, the pilot manipulated a two-axis centerstick and a collective control. The controller positions were fed to an analog computer which was used to simulate the VTOL dynamics and compensate for motion simulator lags. Signals from the computer drove both the motion simulator and the displays in the simulator cab. The computer (actually, two EAI 231R consoles) was also used for taking the performance measures and providing signal conditioning for FM recording (see Fig. 2). The following paragraphs describe the various elements in the experimental setup.

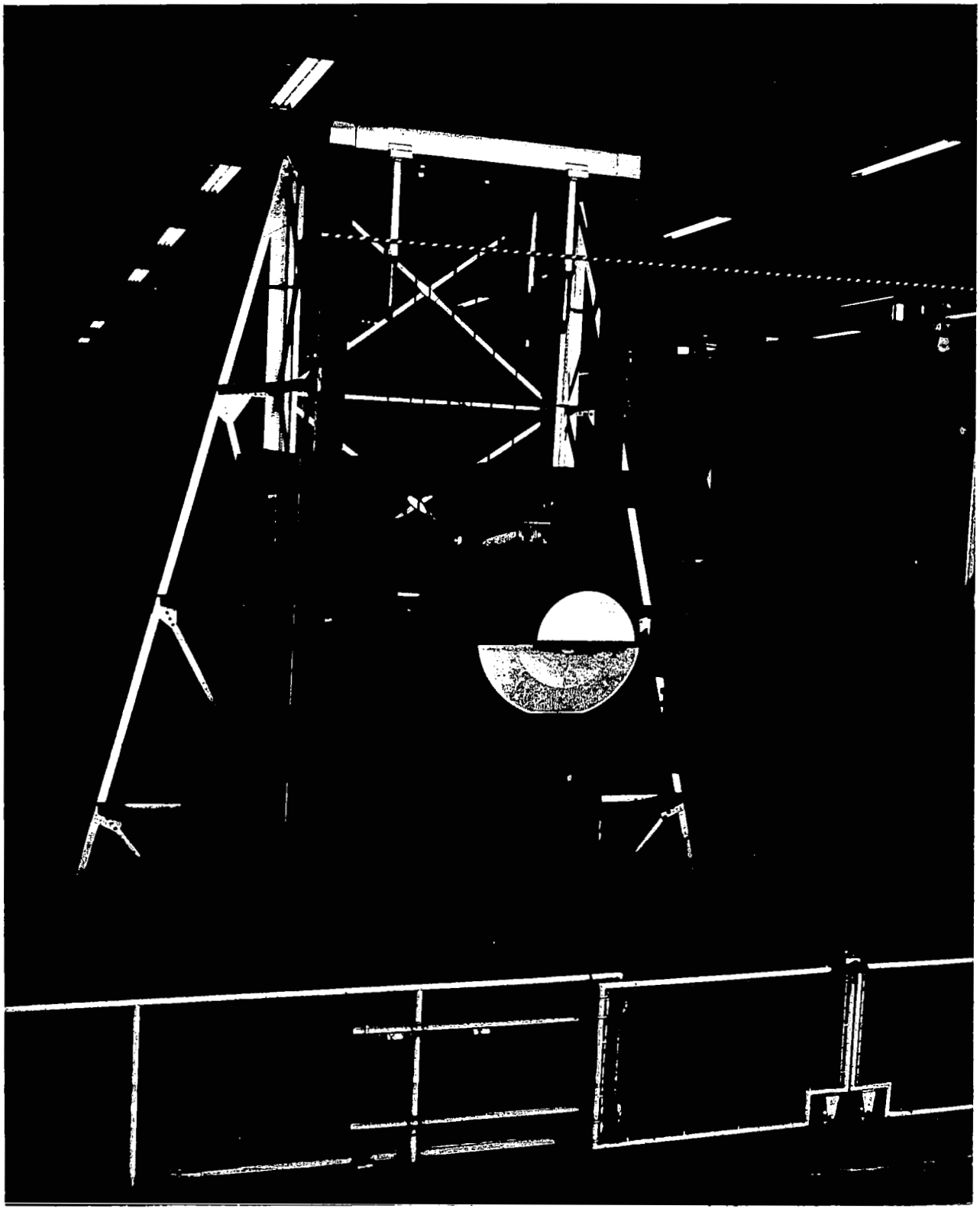

Figure 1. Six-Degrees-of-Freedom Simulator

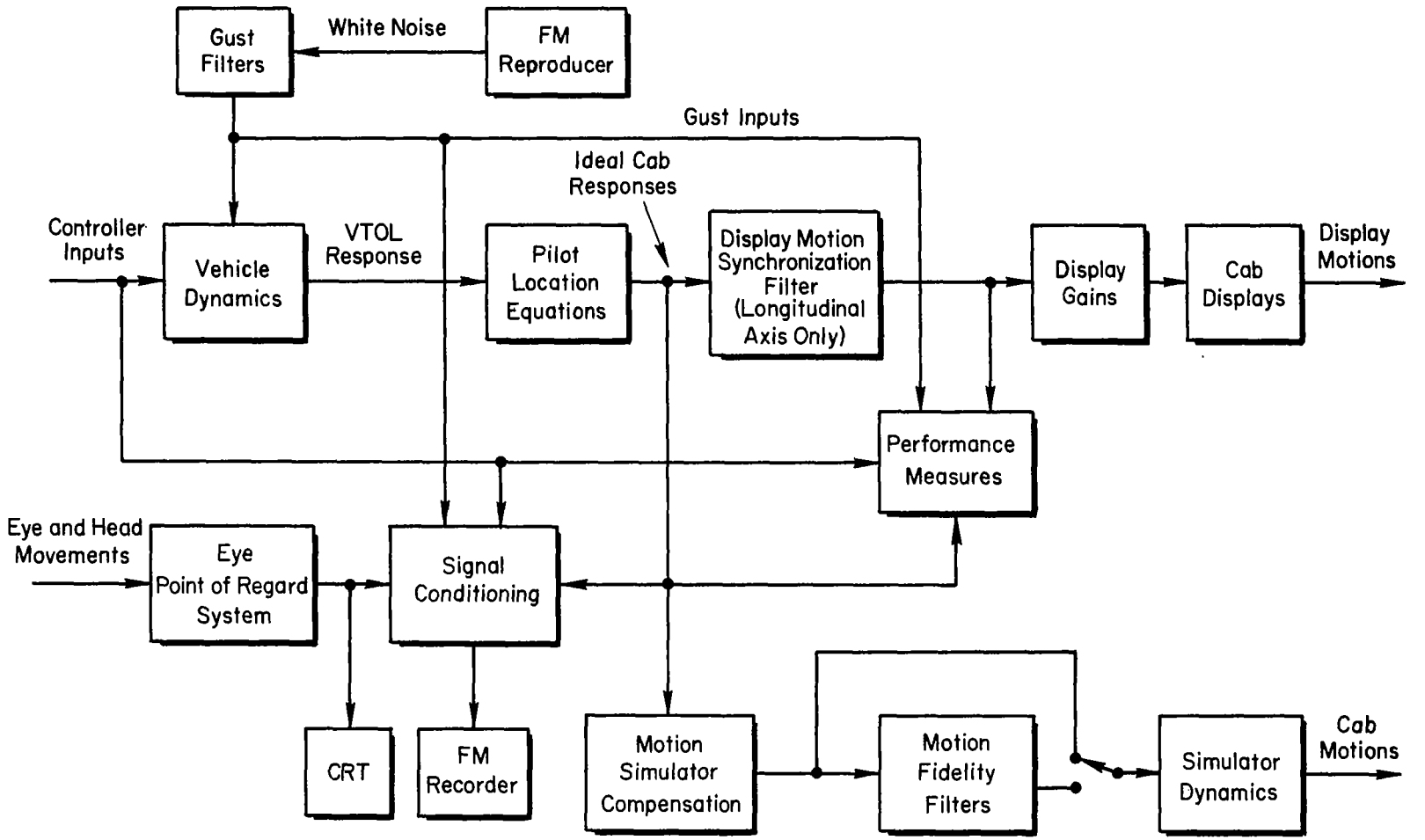

Figure 2. Simulation Schematic

1. Controllers

The force-versus-displacement characteristics for the centerstick control of pitch and roll are shown in Fig. 3. The displacements were measured at the center of the handgrip. The subjects felt the controller configuration to be quite acceptable with pleasingly light force levels.

The collective, located to the left of the pilot's seat, was a pure friction control requiring about 5 lb force to get it moving and somewhat less to keep it moving. This stiction characteristic and the relatively high friction level were quite objectionable to the pilots, who felt that it made small corrections on the altitude control task quite difficult.

2. Displays and Display Gains

The pilot viewed the instrument panel in the closed motion simulator cab from a distance of approximately 30 in. The display panel was arranged as shown in Fig. 4, with the instruments being separated by approximately 6 in. center-to-center, both horizontally and vertically. The altitude display at the upper left was a simple moving needle display having a full-scale deflection of ±1.5 in. representing ±10 ft. Unlike the other two displays, it had a measurable lag in the frequency range of interest — about 0.15 sec. The attitude display at the upper right was a 5 in. Lear ball. As originally set up, the gain of this display was one-to-one. Shakedown run results confirmed those of Ref. 5 which showed that the linear motion excursions for instrument hovering using conventional instruments are quite large — well in excess of the Ames motion simulator limits. The reason is that the pilot cannot discern from the conventional attitude ball display the small attitude changes which are needed to hold the lateral and longitudinal excursions within narrow limits. The gain was therefore increased to five-to-one, i.e., 5 deg of ball motion represented 1 deg of cab motion in both pitch and roll.

The position display was a 3 in. CRT located below the ball display on which horizontal and vertical lines were displayed. As originally set up, the intersection of the horizontal and vertical lines represented the spot on the ground over which the pilot was to hover. Leftward motion of the vertical line meant the cab was going to the right, while upward motion

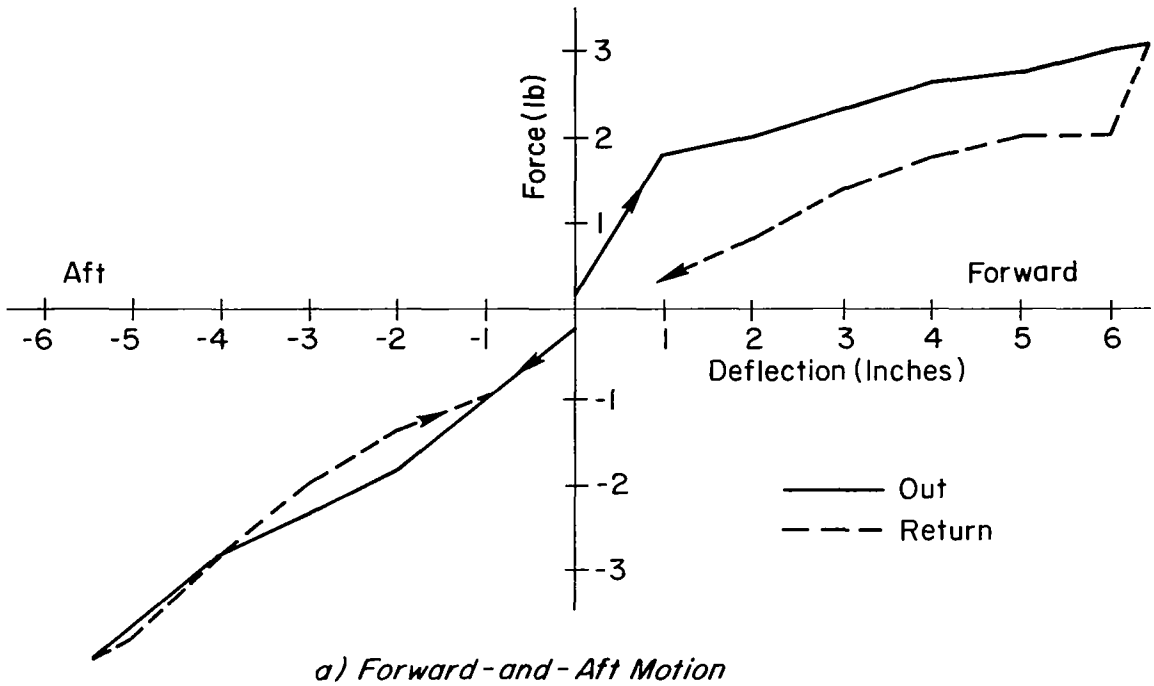

a) Forward-and-Aft Motion

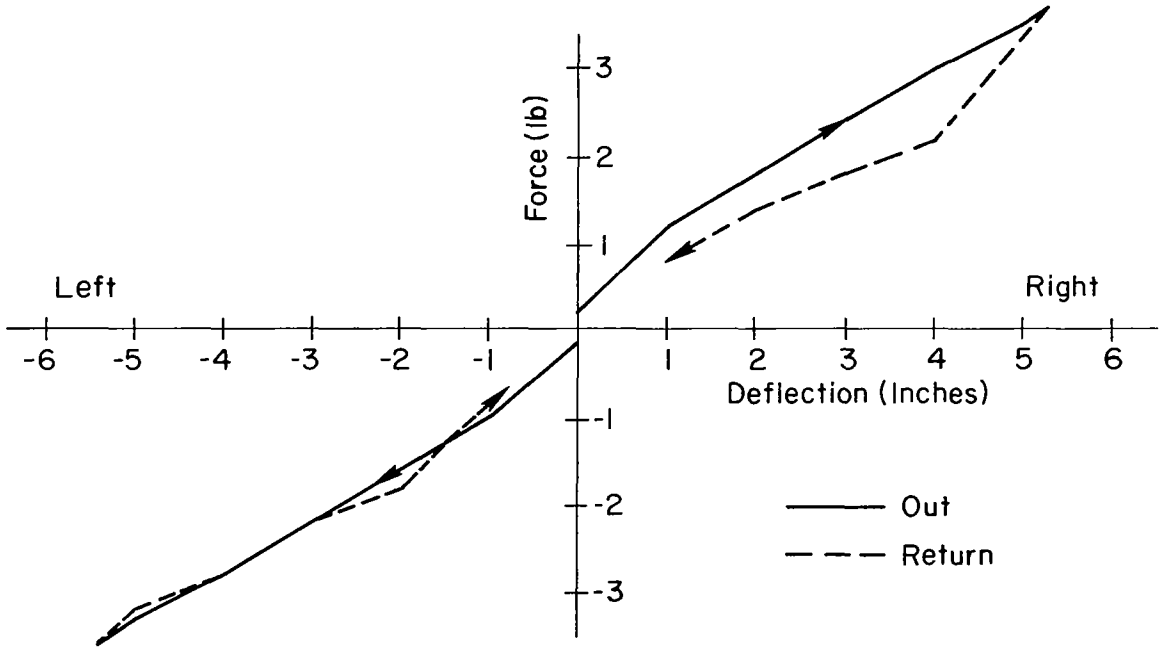

b) Side-to-Side Motion

Figure 3. Centerstick Force Versus Displacement

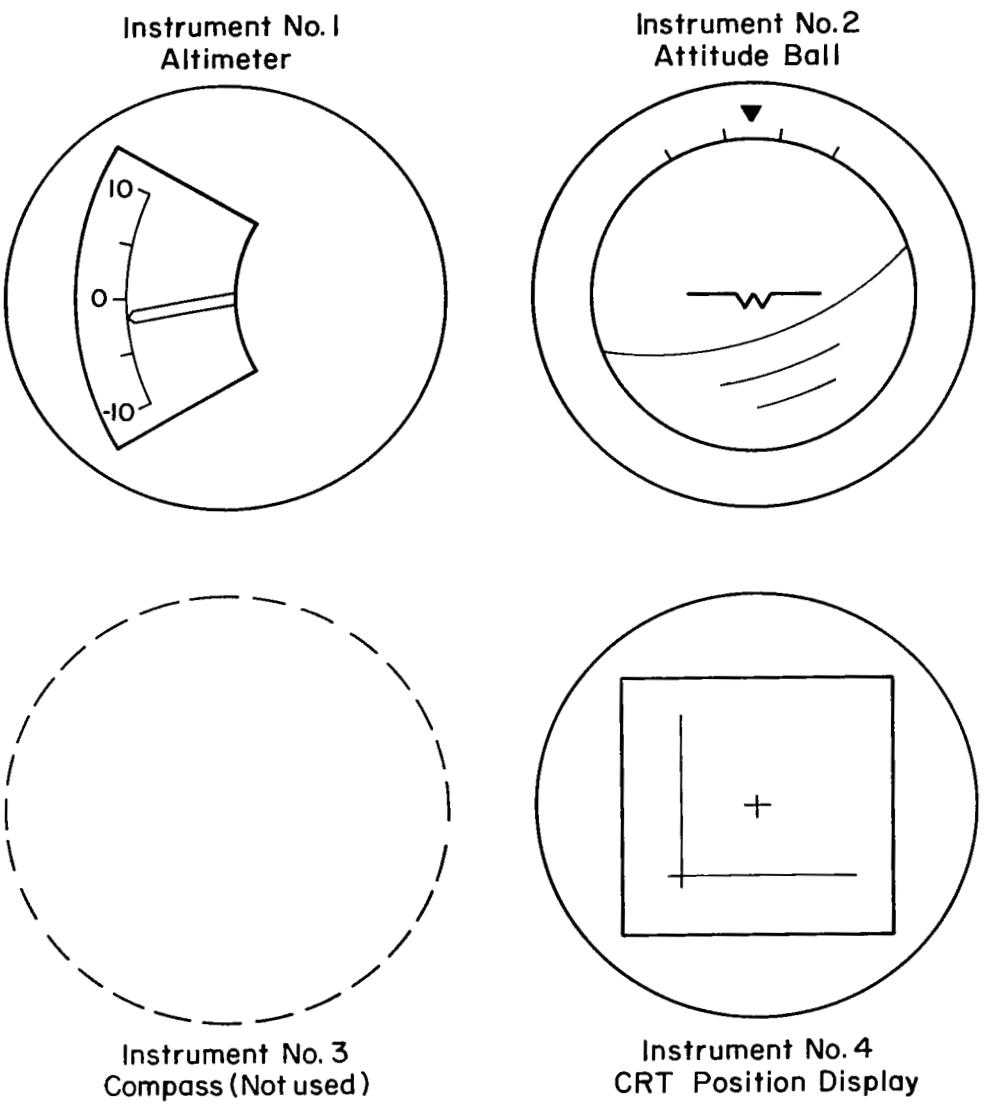

Figure 4. Display Panel Arrangement

of the horizontal line implied that the cab was moving aft. Full-scale motion of approximately ±1.0 in. implied position excursions of ±9.1 ft, the motion simulator limits. The small cross at the center of the display therefore represented the VTOL's position with respect to the desired point on the ground, represented by the intersection of the horizontal and vertical lines.

The subject pilots had difficulty with this setup because the horizontal line moved in the opposite direction in response to a stick deflection than would be expected if the lines were interpreted as ILS needles. A forward stick deflection caused the vehicle to pitch down and move forward — the horizontal line moved down the screen. An ILS needle would move in the opposite direction in response to a forward stick deflection. To expedite the training process for two of the pilots, EF and RG, the drive signal deflecting the horizontal line was reversed; the third pilot, GB, used the original setup.

A directional control task (compass display at lower left on the panel, rudder pedals for control) was originally planned for these experiments but was deleted because shakedown run results showed that the pilots were unable to maintain small yaw attitude excursions due to the high attention levels required for the longitudinal and lateral tasks. Large yaw attitude excursions resulted in erroneous motion cues because of the small angle approximations used in the equations of motion and in the simulator drive signals.

3. Vehicle Dynamics

The equations of motion for the vehicle are given below:

- Longitudinal

$$\left.\begin{aligned} s(s - X_u)x + g\theta &= -X_u u_g \\ -M_u s x + s(s - M_q)\theta &= M_{\delta_e}\delta_e - M_u u_g \end{aligned}\right\} \qquad (1)$$

- Lateral

$$\left.\begin{aligned} s(s - Y_v)y - g\varphi &= -Y_v v_g \\ -L_v s y + s(s - L_p)\varphi &= L_{\delta_a}\delta_a - L_v v_g \end{aligned}\right\} \qquad (2)$$

- Vertical

$$s(s - Z_w - Z_{\dot{w}}')z = Z_{\delta_c}\delta_c - Z_w w_g \tag{3}$$

- Pilot Location

$$\left.\begin{aligned} x_i &= x \\ y_i &= y \\ z_i &= z - \ell_x\theta \end{aligned}\right\} \tag{4}$$

The intersection of the motion simulator's pitch and roll axes was the simulated center-of-gravity location of the vehicle except when ℓ_x was nonzero. The numerical values of the various parameters are given in Table I. The vehicle dynamic configurations are defined in Table II. Each of these 11 configurations of vehicle dynamics were to be flown fixed-base (FB), moving-base with only angular motion (MBA), and moving-base with both angular and linear motion (MBL).

The first six configurations were intended to explore the effects of increasing longitudinal task difficulty for two different levels of lateral task difficulty. The results presented in Ref. 7 would indicate that the most difficult longitudinal task ($M_q = 0$) would be quite sensitive to the presence or absence of motion cues, while the least difficult ($M_q = -4$) would show little change going from fixed- to moving-base.

Configurations 7 through 11 were intended to explore the effects of linear motion cues. Configurations 7 and 8 had degraded vertical task stability and were meant to reveal (by comparison of fixed- and moving-base performance) the effects of translational motion on vertical task performance — there are no rotational aspects to this task. Configurations 9, 10, and 11 were intended to explore the effects of vertical motion on pitch attitude control. Relative to Configurations 1, 2, and 3, the pilot is moved 20 ft ahead of the center of gravity so that pitch angular accelerations add to vertical accelerations. This can conceivably have an effect on pitch tracking and secondarily (because of pitch motions showing up on the altitude display) on vertical task performance.

TABLE I

VEHICLE DYNAMIC PARAMETERS

Longitudinal Dynamics

Fixed Parameters:

$$gM_u = 0.2 \text{ sec}^{-3} \quad , \quad X_u = -0.1 \text{ sec}^{-1}$$

Variable Parameters:

M_q (sec^{-1})	Descriptor
−4.0	"Good"
−1.0	"Mediocre"
0	"Bad"

Lateral Dynamics

Fixed Parameters:

$$gL_v = -0.2 \text{ sec}^{-3} \quad , \quad Y_v = -0.1 \text{ sec}^{-1}$$

Variable Parameters:

L_p (sec^{-1})	Descriptor
−4.0	"Good"
−0.5	"Bad"

Vertical Dynamics

Variable Parameters:

Z_w (sec^{-1})	Z'_w (sec^{-1})	Descriptor
−1.00	−3.00	"Good"
−1.00	−0.00	"Mediocre"
−0.25	0	"Bad"

Pilot Location

ℓ_x = 0 ft , 20 ft

TABLE II

VEHICLE CONFIGURATIONS

CONFIG. NO.	LONGITUDINAL	LATERAL	VERTICAL	ℓ_x
1	"Good"	"Good"	"Good"	0 ft
2	"Mediocre"	↓	↓	↓
3	"Bad"	↓	↓	↓
4	"Good"	"Bad"	↓	↓
5	"Mediocre"	↓	↓	↓
6	"Bad"	↓	↓	↓
7	"Good"	"Good"	"Mediocre"	↓
8	"Good"	↓	"Bad"	↓
9	"Good"	↓	"Good"	20 ft
10	"Mediocre"	↓	↓	↓
11	"Bad"	↓	↓	↓

Table III lists the control sensitivities used by the three subjects together with the estimated optimum values derived from those given in Ref. 8. The longitudinal and lateral gains are a factor of five lower than those quoted in this reference to account for the increased attitude ball sensitivity. The initial values (i.e., those values set prior to modifications at the subject's request) of these gains were selected based upon the optimum values of Ref. 8 using estimated values of the stick travel (the actual calibrations of stick force versus displacement and output voltage were unavailable until later in the program). During the training runs the subjects were asked to select better gains as they saw fit. The results were as shown in Table III; the control sensitivities for the "good" configurations for lateral and longitudinal dynamics were the only ones modified. The sensitivities for the more difficult configurations were left unchanged, although one subject, RG, later complained of low sensitivity in pitch — after he had considerable experience with the more difficult configurations.

The very low collective control sensitivity, Z_{δ_c}, for the "bad" vertical dynamics came about as a result of an inadvertent miscalibration of the pertinent potentiometer on the computer. This error was not "caught"

TABLE III

CONTROL SENSITIVITIES

a) Longitudinal Task, M_{δ_e} $(\frac{rad/sec^2}{inch})$

CONFIG. DESCRIPTOR	OPTIMUM GAIN*	SUBJECT		
		RG	EF	GB
"Good"	0.066	0.066	0.070	0.043
"Mediocre"	0.047	0.037	→	
"Bad"	0.042	0.031	→	

b) Lateral Task, L_{δ_a} $(\frac{rad/sec^2}{inch})$

CONFIG. DESCRIPTOR	OPTIMUM GAIN*	SUBJECT		
		RG	EF	GB
"Good"	0.074	0.089	0.095	0.053
"Bad"	0.040	0.039	→	

c) Vertical Task, Z_{δ_c} $(\frac{ft/sec^2}{inch})$

CONFIG. DESCRIPTOR	OPTIMUM GAIN*	SUBJECT		
		RG	EF	GB
"Good"	-4.3	-4.91	→	
"Mediocre"	-2.9	-3.10	→	
"Bad"	-2.2	-0.77	→	

*Based on data in Ref. 8.

by the pilots because they interpreted the resultant vertical task sluggishness as part of the intentional task degradation and (apparently) because their opinions of this task were masked by the poor collective force characteristics. None of the subjects requested any change in the control sensitivity for any of the vertical task configurations.

4. Gust Inputs

The three gust inputs were simulated by feeding prerecorded noise through "gust filters" having a first-order lag characteristic with

τ = 1.0 sec. In order to get repeatable rms level measurements (measured over a 100 sec time interval) the prerecorded noise consisted of a 100 sec white noise sample repeated over and over — a different sample for each of the three inputs. The simulated rms gust levels used were as follows (mean values are zero in all cases):

$$\sigma_{u_g} = 1.0 \text{ ft/sec}$$

$$\sigma_{v_g} = 1.4 \text{ ft/sec}$$

$$\sigma_{w_g} = 1.6 \text{ ft/sec}$$

These gust levels are lower than the originally intended level of 3 ft/sec in all three axes. The shakedown runs and early training runs revealed that the position excursions could not be reliably controlled within the simulator limits for gust levels this high, and the level was reduced to that indicated. Pilot ratings (based on past data, see Ref. 7) are relatively insensitive to the precise level of gust excitation with the values of M_u and L_v used in this experiment.

5. Simulator Dynamics and Compensation

Table IV lists the position, velocity, and acceleration limits of the motion simulator degrees of freedom used. The drive signals from the analog computer were limited at levels corresponding to the position limits. The yaw axis was not used.

TABLE IV

SIX-DEGREES-OF-FREEDOM SIMULATOR LIMITS

AXIS	POSITION	VELOCITY	ACCELERATION
Roll, φ	±45 deg	218 deg/sec	688 deg/sec^2
Pitch, θ	±45 deg	132 deg/sec	344 deg/sec^2
Longitudinal, x	±9.1 ft	11.4 ft/sec	6 ft/sec^2
Lateral, y	±9.1 ft	11.4 ft/sec	7 ft/sec^2
Vertical, z	±8.4 ft	13.2 ft/sec	10 ft/sec^2

The frequency responses for all but the yaw axis of the simulator are shown in Figures 5 through 9. Those data are taken from Refs. 9 and 10. In Ref. 9 lead compensation is used to improve the fidelity of the motion simulator response out to approximately 12.5 rad/sec. In the present case it was felt that a more restricted range was appropriate in view of the low frequency character of the hovering VTOL dynamics. Second-order compensation, listed in Table V, was used in all axes and was based on the "uncompensated" results of Refs. 9 and 10. The computed effects of this compensation are shown in these same figures. In the longitudinal axis the compensation was less than perfect, resulting in a phase characteristic approximating a single-order lag having a time constant of 0.1 sec (see Fig. 7). Additional lead was avoided in this axis because of the undesirable amplitude peaking which would result.

TABLE V

SECOND-ORDER LEAD COMPENSATION FOR MOTION SIMULATOR

AXIS	ω (RAD/SEC)	ζ
Roll, φ	10.0	0.6
Pitch, θ	8.0	0.6
Longitudinal, x	6.5	0.5
Lateral, y	6.0	0.9
Vertical, z	5.5	0.9

The net lag in the longitudinal axis has two consequences: first, the motion of the cab lags the displayed value of x; and second, the longitudinal acceleration of the cab due to pitch motion will lag the desired acceleration. In this simulation a display motion synchronization filter was used to lag the displayed value of x by an amount equal to the motion lag. The second effect was ignored as being small relative to the errors introduced by the angular resolution of the simulator (approximately 0.25 deg in pitch, 0.10 deg in roll). The compensation (Table V) used for the angular degrees of freedom is based on large amplitude results — large relative to those actually observed in the experiment.

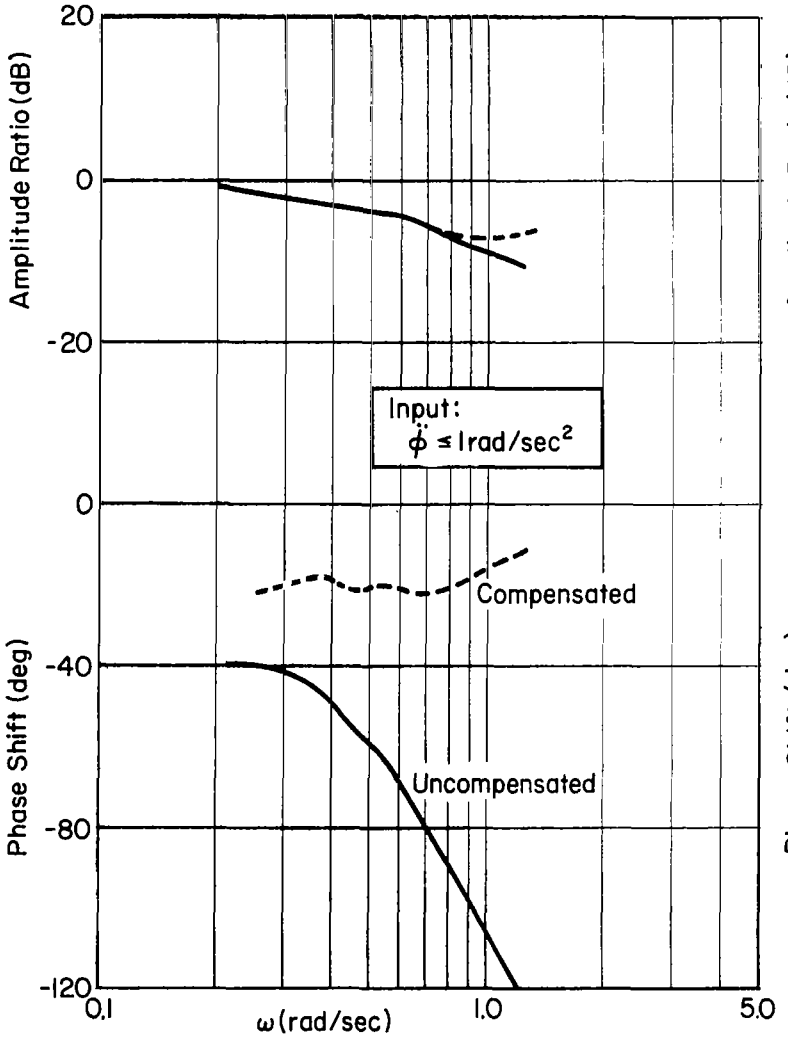

Figure 5. Roll Axis Simulator Response

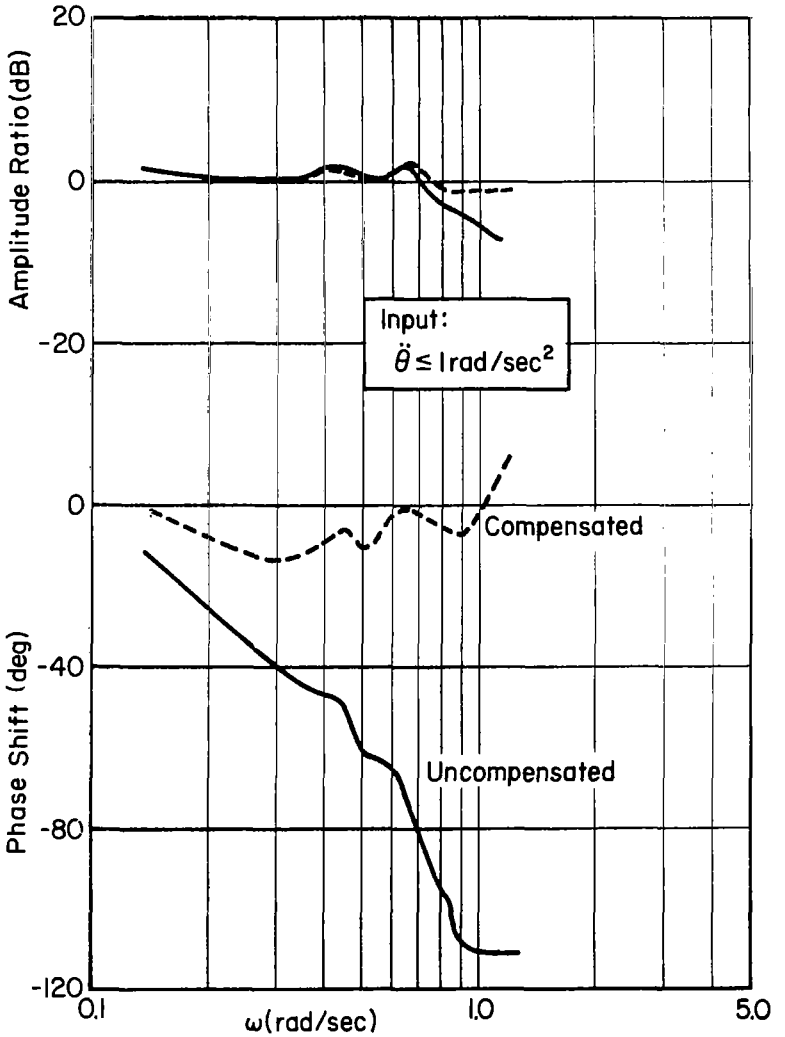

Figure 6. Pitch Axis Simulator Response

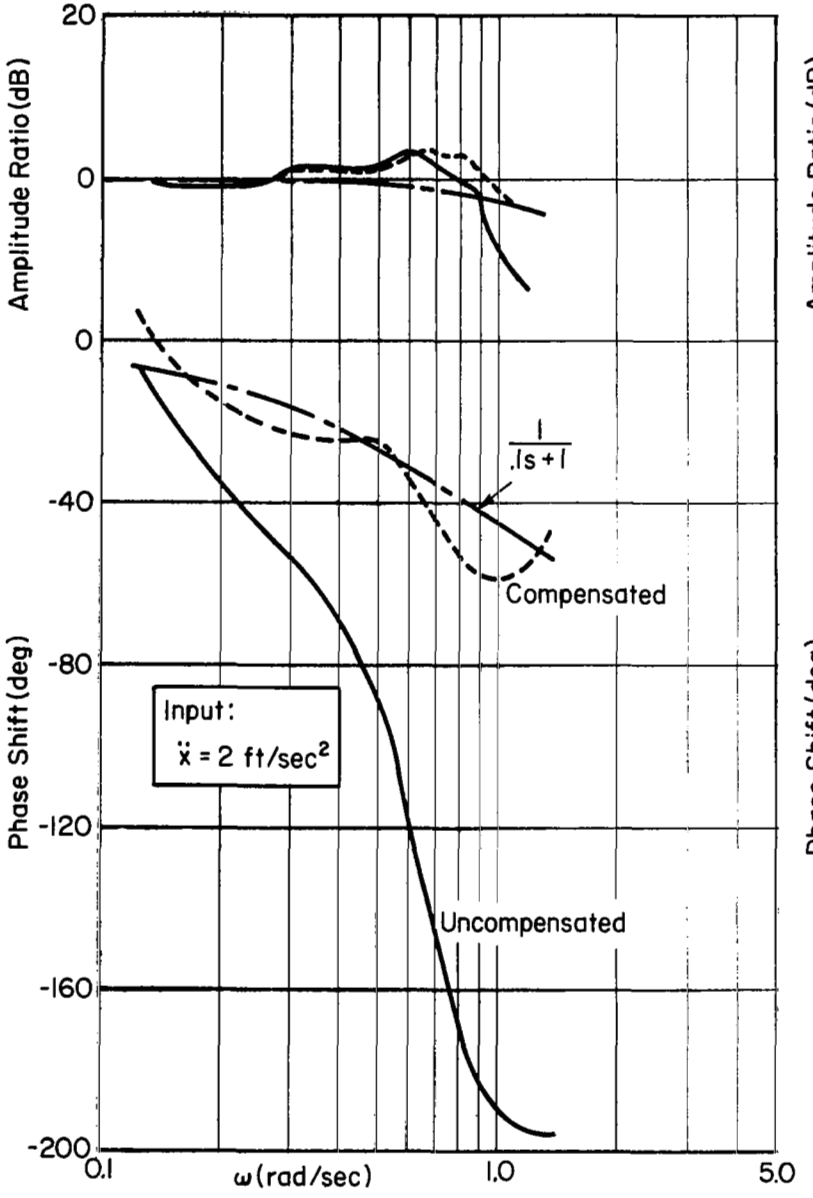

Figure 7. Longitudinal Axis Simulator Response

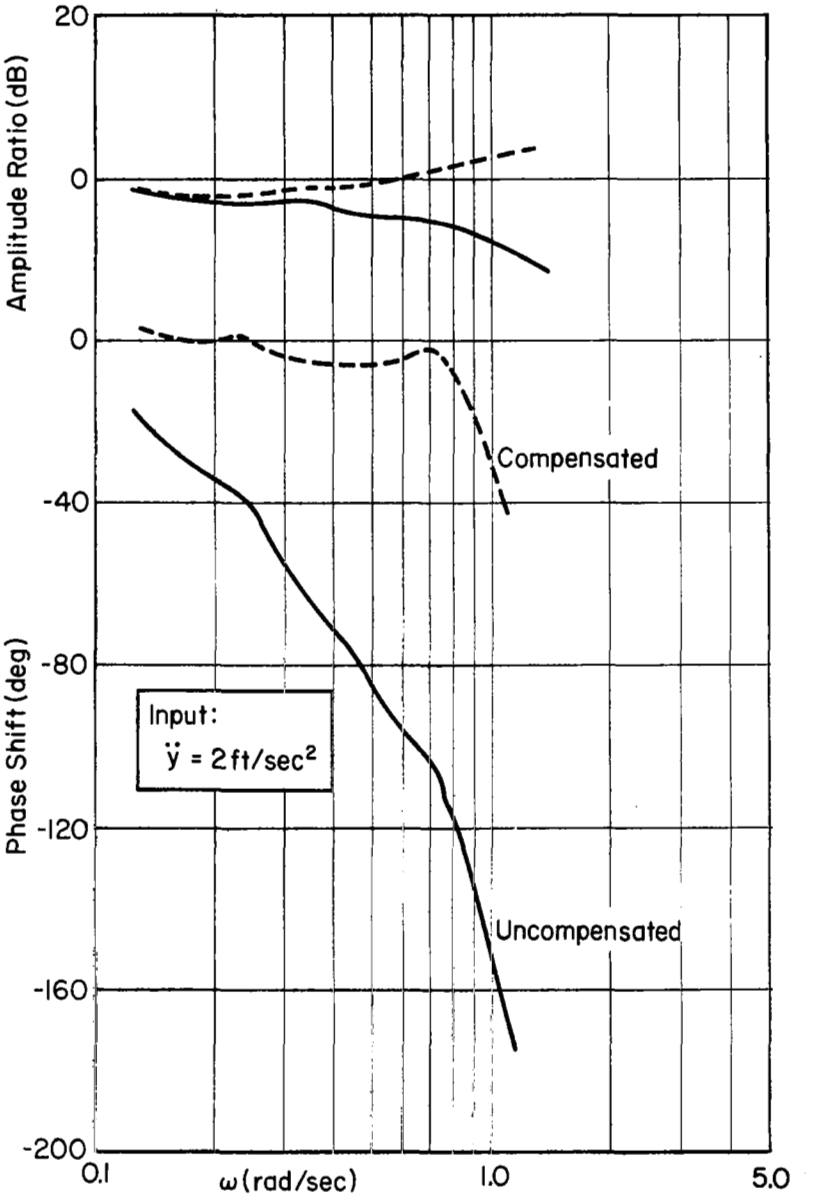

Figure 8. Lateral Axis Simulator Response

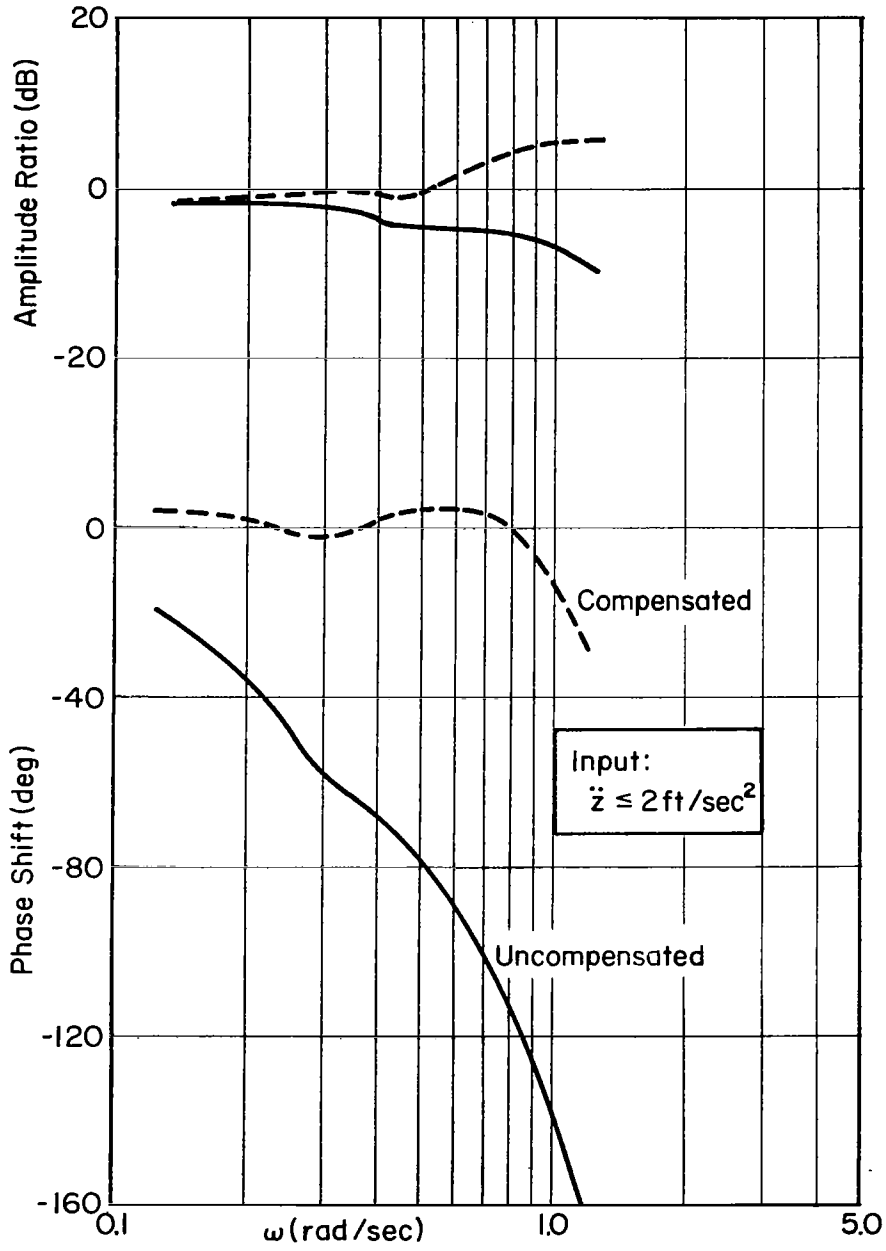

Figure 9. Vertical Axis Simulator Response

6. Motion Fidelity Filters

For the Priority III runs, first-order lags in the angular motion were introduced to determine the magnitude of lag tolerable in motion simulation of this type. The experimental variable is the time constant of the filter.

7. Performance Measures

The integrated mean square values of 14 motion quantities were measured at the end of each run as a measure of pilot performance. A switch operated by the experimenter started the integration which was automatically stopped 100 sec later. These measures defined the rms levels of the gust inputs (σ_{u_g}, σ_{v_g}, σ_{w_g}); the controller deflections (σ_{δ_e}, σ_{δ_a}, σ_{δ_c}); the displayed pitch and roll angles (σ_θ, σ_φ), the position excursions (σ_x, σ_y, σ_z); and the pitch, longitudinal, and vertical velocities (σ_q, σ_x, σ_w).

8. Signal Conditioning

These circuits were used to attenuate and limit the voltage levels of the same 14 motion quantity signals going into the FM recorder as well as providing overload protection for the recorder.

9. Eye-Point-of-Regard System

For some of the runs the pilot's eye point-of-regard on the panel was measured using the Eye-Point-of-Regard System developed at Systems Technology, Inc. This system measures both pilot head movement with respect to the panel and pilot eye movement with respect to the head, and combines the two to yield a determination of where the pilot is looking on the panel. The system's description and theory of operation is more fully discussed in Ref. 3. The electronics associated with the measuring transducers were mounted in the simulator cab. Signals indicative of the horizontal and vertical coordinates of the pilot's point-of-regard were monitored using a CRT on the computer console and recorded on FM tape. The monitoring allowed calibration of the system without the need of docking the simulator; the subject would adjust knobs in response to the experimenter's desires while the latter observed the CRT.

10. Strip Chart and Voice Recording

All signals recorded on FM were also recorded (without signal conditioning) on strip charts together with an indication of the performance integration time interval and the simulator cab motions (feedback potentiometers in the simulator drive servos).

Pilot commentary was recorded using a voice-operated magnetic tape recorder connected to the intercom system which provided the voice communication link between experimenter, subject, and motion simulator operator.

B. EXPERIMENTAL PROCEDURE

Three pilot subjects were used throughout the experimental program; their pertinent backgrounds are summarized in Table VI. Because of his extensive research experience and limited availability, subject RG was used as a point of reference for the other two pilots who were inexperienced in giving pilot opinion ratings and commentary. Subjects GB and EF were relied upon for most of the data taken.

TABLE VI

SUBJECT BACKGROUNDS

GB:	Airline flight engineer and pilot, approximately 800 hr; former USAF pilot with 650 hr as instrument instructor, approximately 4,300 hr in helicopters in U. S.
EF:	Airline flight engineer, approximately 200 hr; former USMC pilot with 1,550 hr as primary flight instructor, 1,500 hr in helicopters in Vietnam.
RG:	NASA research pilot; approximately 4,200 hr total, mostly in single-engine fighters; more than 500 hr in helicopters and VTOL aircraft.

Subjects GB and EF each received five days of training totaling approximately 85 to 90 runs of 2 min or more duration for each subject. They were exposed to all configurations used in the experimental program. These trials were under both fixed-base (FB) and moving-base with linear

and angular motion (MBL). The angular motion only condition (MBA) was not flown in these trials as it was initially felt to be intermediate in difficulty between the other two motion conditions. Subject RG had three training sessions of ten trials or more each and was similarly exposed to FB and MBL motion conditions for the various configurations. Performance records were kept on all subjects throughout the training period. These records, together with those taken in the experimental runs, reveal that pilot performance for all subjects continued to improve slowly throughout the program.

Initial plans called for running both GB and EF through all 11 configurations for fixed-base, moving-base (angular motion only), and moving-base (linear and angular motion) conditions. During the course of the training runs it became apparent that pilot location effects were, at most, very small, and that the variations in the vertical task difficulty would yield little information. The reasons for this are that the vertical motions due to center of gravity location (ℓ_x effects) are very small because of the small pitch attitude excursions, and that the vertical task is much less difficult than any of the others — an increase in the task difficulty is a small increment in the overall task difficulty. The Priority I runs therefore followed the matrix in Table VII; originally planned runs on Configurations 7 and 10 were deleted. Some of the moving-base (angular motion only) runs were deleted for intermediate levels of difficulty (2 and 5) or where primary interest was on the effects of the vertical motion (7, 9, and 11). The order of presentation was different for both pilots; they flew the configurations in random order and the two or three motion conditions for a particular configuration in random order.

Except for the Priority III and IV runs in the last three days of the experimental program, all subjects had four trial runs on the best and worst configurations at the beginning of the day. The first two were on Configuration 1, both fixed- and moving base; the second two on Configuration 6, both fixed- and moving base. The moving-base trial runs were with both linear and angular motion cues. The subjects were in the simulator for periods of time up to an hour and a half, although actually "flying" for only part of the time. The rest of the time was spent in

TABLE VII

EXPERIMENTAL MATRIX, PRIORITY I RUNS

CONFIG.	MOTION SIMULATOR CONDITION		
	FIXED-BASE	MOVING-BASE (ANGULAR MOTION ONLY)	MOVING-BASE (LINEAR & ANGULAR MOTION)
1	×	×	×
2	×		×
3	×	×	×
4	×	×	×
5	×		×
6	×	×	×
7			
8	×		×
9	×		×
10			
11	×		×

taking data, annotating charts, recording pilot commentary, and changing over the configuration for the next run.

With the changes made during the shakedown runs noted earlier (i.e., deletion of the directional control task, increased attitude display gain with correspondingly reduced stick gain, and reversal of sense in the longitudinal display for two of the subjects) the motion simulator was "flyable," but with very poor pilot opinion. This had an adverse effect on the ability to distinguish between the subjective difficulty of the various tasks (as defined by the controlled element dynamics and the presence or absence of motion cues). Consequently, the pilots were instructed to rate the simulation as flyable [pilot opinion rating (Cooper-Harper scale, Fig. 10) better than 10.0] if they were able to keep the position excursions within the motion simulator limits for the duration of the run, barring momentary exceedances. Under these circumstances, the most experienced subject, RG, rated Configuration 1 between 6.0 and 7.0. This rating is still considerably poorer than those obtained (Refs. 6 and 7) with an integrated visual (real-world) display and the same task dynamics. This

HANDLING QUALITIES RATING SCALE

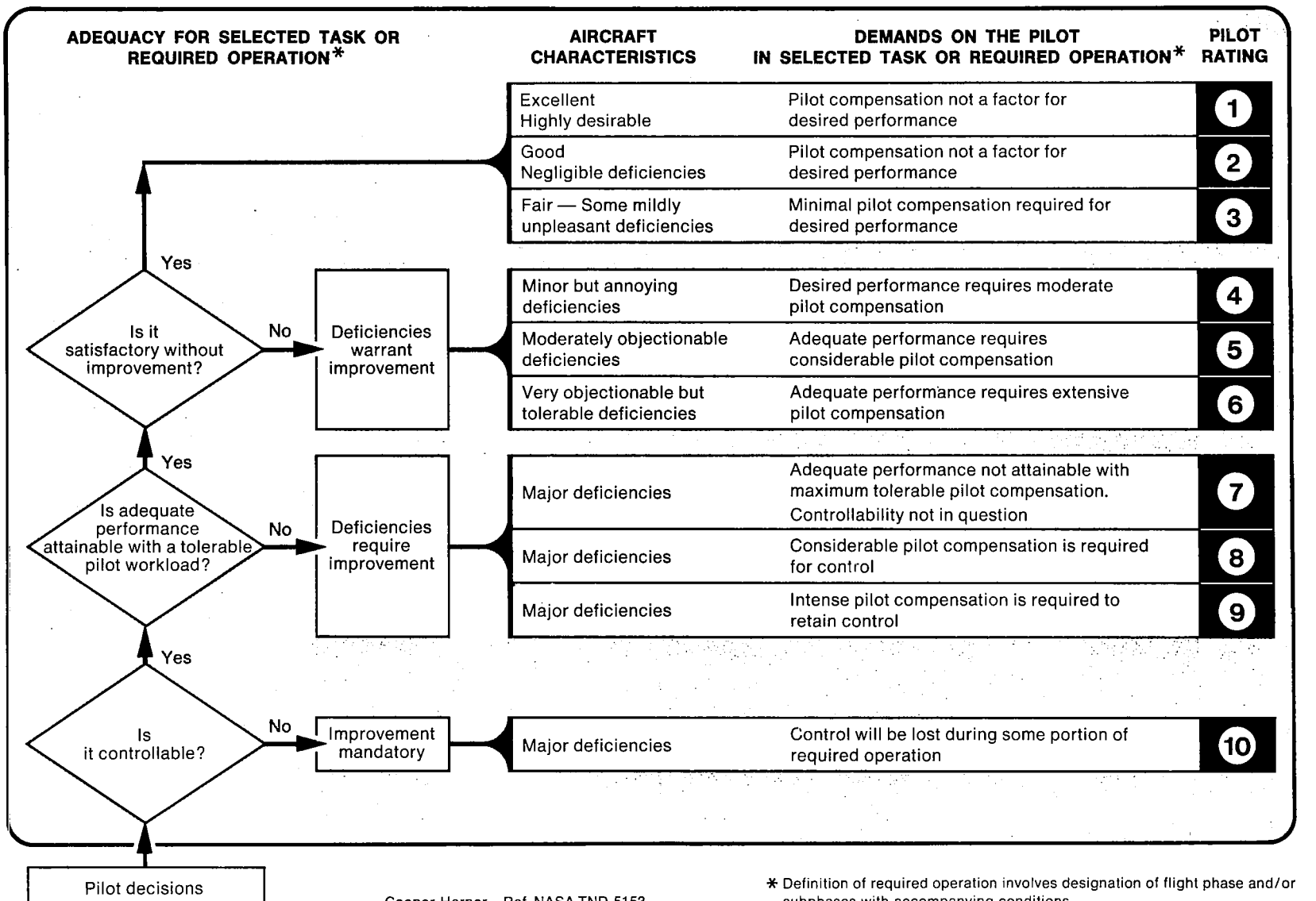

Cooper-Harper Ref. NASA TND-5153

* Definition of required operation involves designation of flight phase and/or subphases with accompanying conditions.

Figure 10. Cooper-Harper Rating Scale

decrement is judged to be due to the VFR-IFR differences between the earlier work and the experimental task with separated instrument displays.

The procedure in the Priority I runs called for two runs in succession on a given combination of configuration and motion conditions during which the pilot was asked to minimize his position and altitude errors. The first run was intended to provide the pilot with plenty of time to identify the configuration and to stabilize his tracking behavior. He was asked to comment on the configuration and to give a pilot rating according to the rating scale (posted in the simulator cab) after this run. The second run was recorded on FM tape for possible later analysis of pilot tracking behavior, and any additional comments were recorded. In all cases he was not informed of the configuration, only of the motion condition. Measurement of pilot performance started approximately 15 sec after starting the simulator. This procedure was dropped for the remaining runs when the performance data indicated no significant performance difference between the first and second runs in a set, and because the pilots had no trouble in identifying the configurations — typically within a few seconds after start.

An examination of the performance and pilot rating data, together with the pilot commentary from these runs, indicated considerable scatter in the data and a tendency for the pilots to prefer the moving-base with angular motion only (MBA) condition. Pilot location effects were negligible (they couldn't tell the difference between Configurations 1 and 9, or 3 and 11) and there was no discernible change due to motion (or its absence) on the vertical task performance in Configuration 8. It was decided to get additional data on Configurations 1, 3, 4, and 6 under all motion conditions for all three pilots, the purpose being to explore the reasons for preferring angular motion only to linear and angular motion. This constituted the objective of the Priority II runs.

The procedure for these Priority II runs was similar to that of Priority I, except that there was only one run on each combination of configuration and motion conditions (12 in all for each pilot subject). The pilot was instructed to indicate when to start measuring performance, the objective being to allow him time to accustom himself to the new

configuration. The motion conditions for each configuration were run in succession, in random order, different for each pilot. In his commentary the pilot was asked to pay special attention to the effects of motion, i.e., to compare the relative merits of the three motion conditions. All runs were recorded on FM for possible later analysis.

The Priority III runs had the objective of determining the motion simulator lags tolerable for simulators having only angular degrees of freedom. Configurations 4 and 6 were used; Subjects EF and RG were used in the experiment. In these runs the subjects were not informed of the nature of the changes in the motion fidelity filters, and were asked to identify any changes they could discern. No FM recordings were taken.

The Priority IV runs had the objective of obtaining eye-point-of-regard data. The procedure was identical to that of the Priority II runs, except that two runs for Configurations 1, 4, and 6, and one run for Configuration 3 was made for Subjects EF and GB for all three motion conditions. Subject RG only flew Configurations 1 and 6 because of limited time. All runs were recorded on FM with the two EPR data channels later being played back on high-speed strip charts for data reduction.

C. DATA REDUCTION

The raw data obtained in this experimental program consists of the following:

- Magnetic tape recordings (voice) of pilot opinion and commentary for each run.
- Performance measures (see subsection A-7) for each experimental run, as well as the "warm-up" runs.
- Magnetic tape recordings (FM) of the major motion variables (disturbance inputs, control deflections, and displayed variables) as well as the EPR data for the Priority IV runs.
- Strip chart recordings of these variables plus simulator motions.
- High-speed (50 mm/sec) strip chart recordings of the EPR data.

The original intent was to rely on pilot commentary transcriptions, pilot opinion and performance, together with the results of the pre-experimental analysis (Appendix A) for validation of the multimodality pilot model by inference, i.e., comparison of actual versus predicted performance and opinion. The results obtained did not contradict the model, but did preclude a point-by-point comparison (Section III). Consequently, it was decided to reduce some of the EPR data from the high-speed strip charts and perform limited describing function analysis on a few of the Priority IV runs. The EPR data was reduced using the techniques described in Ref. 3, while the describing functions were obtained by NASA-Ames personnel using the methods described in Ref. 11.

SECTION III

PERFORMANCE DATA AND PILOT COMMENTARY

In the course of training and early experimental runs, it was possible to make certain qualitative assessments of the manner in which the three subjects "flew" the simulated VTOL. These evaluations are set down by way of an introduction to the discussion of the data.

All the subjects felt that attitude control was of primary importance. Poor control of attitude leads to rapid divergences in position which cannot be arrested with a high degree of confidence. Thus all subjects controlled attitude closely with looser control of position. The key criterion expressed by the subjects was to maintain attitude excursions (as seen on the attitude ball) within plus or minus 5 to 10 degrees (±1 or 2 degrees of simulated VTOL attitude changes). Altitude control was regarded as of tertiary importance.

Three different techniques were used in the control of altitude. EF tended to use rather large collective position changes to affect control. In fact, he caused the simulator to shut down on one or two occasions in the course of his training runs — the large collective deflections coupled with the second-order lead compensation of the simulator's vertical axis, caused acceleration overloads. The result was that EF complained of jerky collective response which he felt to be "disconcerting." Warned of this, RG used his "seat-of-pants" feel to regulate the magnitude of his collective inputs. Subject GB adopted a technique where he would "hunt" for a "centered" collective position which would result in subsequent attitude deviations within a couple of feet. When he couldn't find it, he tended to down rate the configuration. Further, his collective deflections were very small, and he couldn't feel the vertical motion. Presumably, one could expect less reliable pilot performance and ratings from this subject as a result of his technique.

All subjects felt that the first run of the day, moving base with both angular and linear motion, to be "strange", "disconcerting", etc. Further, in the training and early experimental runs, there were frequent episodes of hitting the simulator limits in this motion condition (but not violently

enough to cause simulator overload and shutdown). When this happened, the cues were regarded as very disconcerting — there is a jerk when hitting the limits, and another when coming off. The noise, vibration, and rumble of the simulator in this MBL condition was felt to be "distracting" in all cases.

The subjects frequently commented to the fact that position excursions in one axis were not necessarily indicative of the task difficulty in that axis, but could also be due to reduced attention caused by increased effort on another task. For example, large lateral excursions on Configuration 3 would fall into this category. Consequently the overall performance referred to in the discussion which follow is taken to be the rms vector position error, viz.,

$$\sigma_{disp} = \sqrt{\sigma_x^2 + \sigma_y^2 + \sigma_z^2} \tag{5}$$

and thus includes all effects.

The results of several runs are averaged to provide an indicator of performance for a particular configuration, subject, and motion condition, even though in many cases, there is an obvious learning trend evident. Averaging rms error measures instead of (more correctly) taking the square root of the average variance tends to weight the smaller errors more heavily, and thus is closer to an asymptotic performance measure, i.e., closer to values typical of a high level of training.

With regard to the statistical significance of the overall performance measures presented in this section, the appropriate test is the F test for equality of variances (Ref. 12). This would be applied to each of the three mean-square error measures, σ_x, σ_y, and σ_z, in a 100 sec run length. The number of degrees of freedom associated with a single run is between 3 and 10, assuming the bandwidth of the process to be equivalent to the outer-loop crossover frequencies which vary over a range of 0.10 rad/sec to 0.30 rad/sec, based on the limited describing function measures made (Section V). The number of degrees of freedom can be increased by applying the test to the average variance determined from several runs with the same subject, configuration, and motion condition.

Only a few approximate calculations were made in this fashion. These suggest that significant overall performance differences (at the 95 percent level of confidence) most often can be established for those configurations having a relatively large number of repeated runs, and which are relatively sensitive to motion cues. For the variance in attitude, the larger bandwidth of the inner loops permit establishing significances with fewer runs. It is concluded, therefore, that the differences in performance (as indicated in this section by the average rms levels of each variable for several runs) are usually significant at a relatively high level of confidence for most of the data. The data were not analyzed to determine the level of confidence associated with each individual pair of motion conditions, although the data given in Appendix A (with appropriate assumptions concerning process bandwidth) is sufficient to make these calculations.

Subsections A through E illustrate and discuss the performance data and commentary pertinent to each of the configurations tested. By way of summary of these five subsections for those readers who would prefer to avoid wading through some 30 pages of tables, figures, and discussion, the significant (i.e., at least two, preferably three or more runs included in the averaging process) results are these:

- The MBA motion condition is rated best by all pilots for all configurations with performance confirming this for all but GB, who is postulated to "relax" — his performance is worst, his rating best, in this motion condition for all configurations.

- The MBL motion condition is rated at an intermediate level between the FB and MBA conditions by all pilots for all configurations with the exception of the easiest (Nos. 1 and 9) where EF and GB rate the MBL condition worse than FB. Pilot performance confirms this trend.

- The above trends are strongest for configurations of intermediate difficulty (e.g., Nos. 3, 4, and 11), less so for the most difficult (i.e., No. 6), and least of all for the easiest (Nos. 1 and 9).

- Pilot commentary indicates the MBL condition to be subjectively "strange," "confusing," "distracting," etc., suggesting a tendency to vertigo in this motion condition. The MBA condition was subjectively better because of the "unmistakable" g-vector tilt cue and the absence of the "distractions," etc., of the MBL motion condition.

- The above results are largely based on Configuration Nos. 1, 3, 4, and 6; the data base is too limited or the performance/opinion differences from the above "baseline" summary too small to permit drawing significant conclusions from the results of the other configurations tested.

Further interpretation of these results is deferred to subsections I and J.

A. CONFIGURATION NO. 1

Table VIII lists the averaged performance for all three subjects and motion conditions for this, the easiest configuration. These averages (as well as similar ones for Configuration No. 6) include the performance measured in the warmup runs; the warmup performance does not appear significantly different from that measured in the more formal experimental runs. Relative to the preexperimental predictions also listed (see Appendix A), the experimental results show comparable or better attitude control, but poorer position control, especially on the altitude control task. Differences between subjects are also substantial with GB showing tighter attitude control than the other two subjects and RG the best control over altitude. These intersubject differences are reflected in the more difficult configurations as well.

These performance measures and the scatter in these measures are illustrated graphically in Fig. 11, while Table IX summarizes some of the pertinent commentary. For subject RG, both performance and pilot rating show a small advantage of either of the two moving-base conditions over fixed base. The advantage in rating is roughly 0.3 of a rating point. Significant differences in overall performance among the three

TABLE VIII

AVERAGED PERFORMANCE, CONFIGURATION NO. 1

PERFORMANCE VARIABLE	MOTION CONDITION	SUBJECT			PREEXPERIMENTAL PREDICTION
		RG	EF	GB	
σ_q (deg/sec)	FB	0.22	0.27	0.08	0.19‡
	MBL	0.21	0.34	0.08	0.17‡
	MBA	0.22†	0.36	0.10	
σ_θ (deg)	FB	0.44	0.37	0.20	0.38
	MBL	0.34	0.47	0.22	0.48
	MBA	0.40†	0.40	0.24	
σ_u (ft/sec)	FB	0.66	0.52	0.47	0.31‡
	MBL	0.54	0.59	0.52	0.28‡
	MBA	0.54†	0.48	0.51	
σ_x (ft)	FB	2.5*	1.8	2.6	0.98
	MBL	1.8	1.9	2.9	0.82
	MBA	2.0†	1.5	3.0	
σ_φ (deg)	FB	0.51	0.57	0.32	0.78
	MBL	0.36	0.64	0.32	0.68
	MBA	0.46†	0.52	0.33	
σ_y (ft)	FB	1.7*	1.7	2.3	1.4
	MBL	1.5*	2.1	2.4	1.2
	MBA	1.4†	1.7	2.6	
σ_w (ft/sec)	FB	0.48	0.55	0.43	0.09
	MBL	0.42	0.53	0.44	
	MBA	0.47†	0.52	0.42	
σ_z (ft)	FB	1.0	1.7	1.7	0.16
	MBL	1.0	1.9	2.0	
	MBA	0.9†	1.5	1.9	
σ_{disp} (ft)	FB	3.0*	3.0	4.0	1.7
	MBL	2.6*	3.4	4.3	1.5
	MBA	2.6†	2.7	4.5	
PR	FB	6.7	4.2	4.8	4.0
	MBL	6.4	4.2	4.9	2.5
	MBA	6.4†	4.1	4.5	

*Pronounced Learning Trend.

†Only 2 data points.

‡Exclusive of scanning remnant.

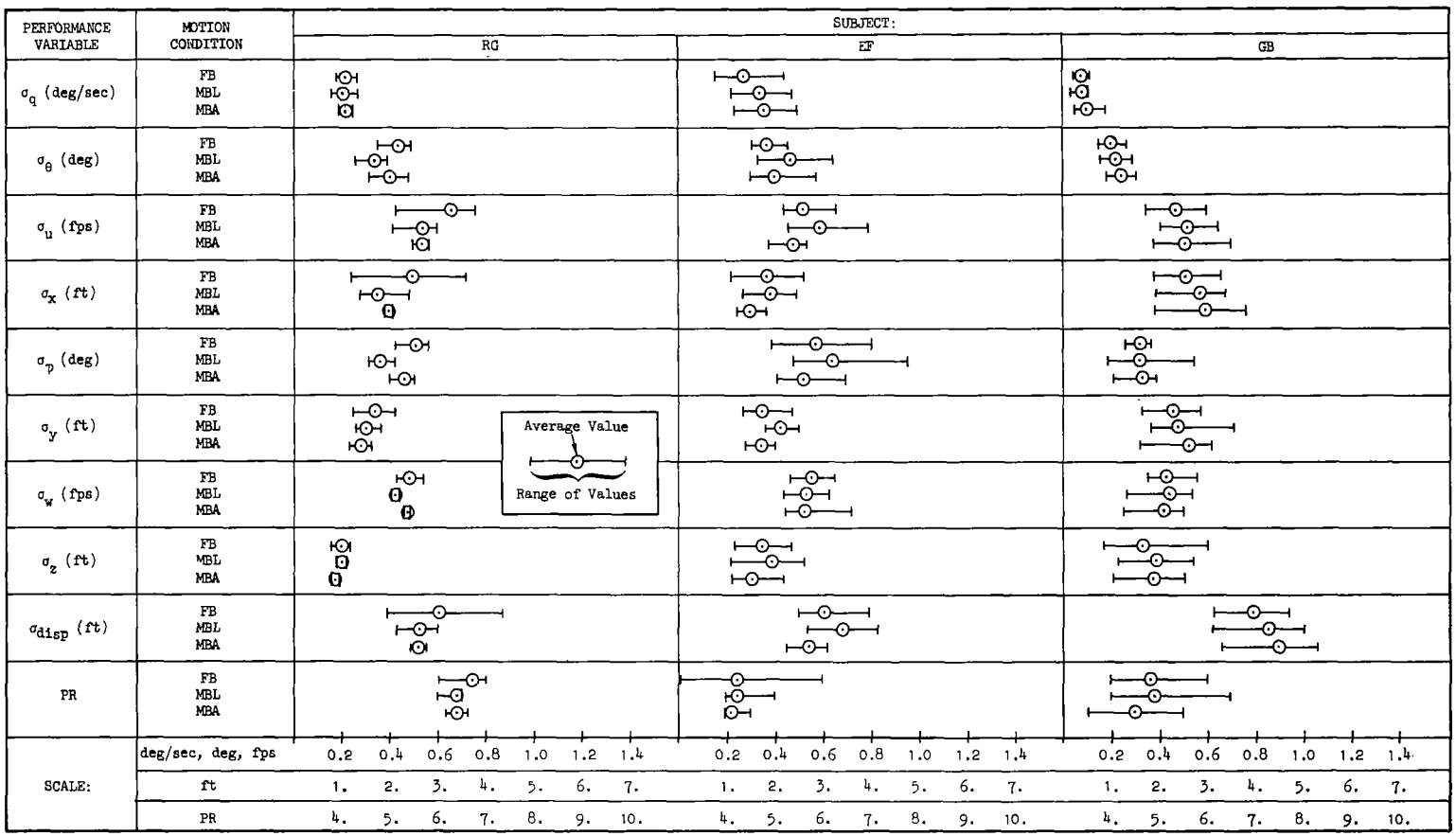

Figure 11. Performance and Pilot Rating Data, Configuration No. 1

TABLE IX

SUMMARY OF SUBJECT COMMENTARY, CONFIGURATION NO. 1

TOPIC	PILOT SUBJECT		
	RG	EF	GB
General Remarks	It requires a great deal of attention to keep the errors minimized; you can't get it to settle down. I am concerned about overcontrolling.	You have to keep right after it, and requires constant attention to keep it close to center. It seems slightly unstable, longitudinally and laterally, and appears to have more than a reasonable lag between input and result.	Unless the altitude error exceeds ±2 ft, I don't mess with it. The altitude task is very annoying, trying to figure out where the center point is (i.e., where further corrections are unnecessary).†
MBL Motion Condition	The MBL condition, at least the first thing in the morning, seems a little strange or confusing, and suggests a little bit of vertigo. But it makes it a little easier to keep the errors down — I work just as hard but do better.	The easier configurations are actually a little easier to fly without all the motion. In the MBL condition, the motion laterally and vertically* seems a little disconcerting, especially the first time in the morning. The motion doesn't help enough to offset the distraction of the simulator rumble because your excursions aren't as rapid on this configuration.	I don't see any advantage in all that motion. When you ignore attitude for a little bit, it doesn't result in such a drastic deviation as on Configuration 6. The lateral motion is distracting, but I can't feel the vertical motion at all.† I like it better in the fixed-base condition.
MBA Motion Condition	The more I fly the MBA condition, the better I like it. The MBL condition appears to confuse rather than help.	The angular motion alone is a nice help and very comfortable. It gives you a feel of pitch angle and bank angle, and a more immediate indication of what the deviation is and what correction to make. But it feels a little artificial relative to the MBL condition, although not as artificial as fixed base.	I like this motion condition better than any other.
FB Condition		It seems more sensitive to attitude corrections than it does in the MBL condition.	

*This subject uses relatively large corrections on the collective, for all configurations.

†This subject would downrate a particular run if he couldn't "find" the centerpoint.

†Very small, often inadequate collective corrections are used in controlling the altitude task by this subject.

motion conditions are difficult to establish because of the small number of runs for this subject. It is clear that the fixed-base condition has the most scatter primarily as a result of the scatter in the performance of the longitudinal task. His commentary suggests that the benefits of the MBL condition in improving his performance outweigh the detrimental effects of vertigo. As his experience increased, he tended to prefer the MBA condition over MBL although this is not reflected in his performance.

Subject EF shows negligible difference in pilot rating between the FB and MBL conditions, and a small preference (approximately 0.1 of a rating point) for the MBA condition. His commentary suggests a decrement in the MBL condition — apparently the vertigo and/or "distraction" of the simulator noise negate any motion benefits for this subject. On the other hand, performance improves in the MBA condition, apparently due to the absence of vertigo and the "unmistakable" angular position cue as well as the angular rate cue.

For subject GB there is a similar decrement in performance and pilot rating for the MBL condition relative to FB. The rating decrement is roughly 0.1 of a rating point. Presumably, the same reasoning holds — vertigo and "distraction" outweigh the beneficial effects of the angular rate cues. For the MBA condition, the rating (relative to fixed base) improves by roughly 0.3 of a rating point but the performance deteriorates, even relative to the MBL condition. If his commentary is accepted at face value, it can only be concluded that the MBA motion condition provides him with enough additional cues permitting him to relax his attention — he can allow larger deviations with confidence because he knows he can catch them.

There are other factors which suggest that this subject is atypical. First is his manner of controlling altitude already described. Second, his pitch attitude control is such that σ_θ is roughly equivalent to the angular resolution of the simulator (all performance measures are taken from computed motions, not those of the simulator) meaning that his angular and angular rate cues in pitch are of low fidelity relative to the other two subjects. This tighter pitch attitude control may also reflect the position display for this subject which is "backwards"

relative to an ILS display. The very tight attitude closure implies low rates of longitudinal position divergence — giving him time to "think" about the reversed display (?). In retrospect, the decision to leave the position display unchanged for this subject may have been a poor one.

In summary, Configuration 1 shows much less advantage, in terms of pilot rating, for moving base (MBL) over fixed base relative to predictions (Table VIII). However, this is in accord with data given in Ref. 7 in that the vehicle dynamics fall in a range where fixed base-moving base differences are quite small. For subjects relatively unfamiliar with the artifacts, etc., of moving base simulators, there is an apparent decrement due to either the distraction of the noise and rumble caused by its motion, or due to vertigo — the g-vector tilt felt by the pilot is not in accord with the attitude display. Finally, in the MBA condition, the pilots may use the g-vector tilt cue to aid in the simulated hovering task. This, plus the absence of simulator noise distraction may explain the preference for this motion condition mentioned by all subjects.

B. CONFIGURATION NO. 3

This configuration has deteriorated longitudinal task stability relative to Configuration No. 1. Table X lists the averaged performance data for all subjects and motion conditions. As with Configuration No. 1, performance achieved is worse than predictions with regard to position control, while attitude performance is comparable or better than predictions. Subject RG has the poorest longitudinal task performance, principally because of his limited experience with this configuration at the time the data was taken. His data are therefore an unsuitable basis for conclusions. The performance data for all subjects is shown graphically in Fig. 12 and a summary of the pilot commentary is given in Table XI. RG's commentary indicates a preference for the MBA condition.

For subject EF, these data indicate a rating advantage over fixed base of approximately 0.6 for MBL, and 0.7 for MBA. The overall performance shows an even greater advantage for the MBA condition which shows up in all three control tasks. Note also that the scatter in attitude

TABLE X

AVERAGED PERFORMANCE, CONFIGURATION NO. 3

PERFORMANCE VARIABLE	MOTION CONDITION	SUBJECT			PREEXPERIMENTAL PREDICTION
		RG*	EF	GB	
σ_q (deg/sec)	FB	1.12	1.15	0.90	0.94†
	MBL	0.66	1.08	0.70	0.35‡
	MBA	0.66	0.89	0.68	
σ_θ (deg)	FB	1.35	0.96	0.84	0.80†
	MBL	0.61	0.76	0.66	0.73
	MBA	0.72	0.67	0.58	
σ_u (ft/sec)	FB	1.19	0.83	0.72	0.52†
	MBL	0.68	0.70	0.76	0.45‡
	MBA	0.93	0.67	0.72	
σ_x (ft)	FB	4.1	2.7	2.9	1.1†
	MBL	3.1	2.5	3.0	1.3
	MBA	3.5	2.4	3.2	
σ_φ (deg)	FB	0.58	0.43	0.37	0.77
	MBL	0.37	0.39	0.34	0.68
	MBA	0.52	0.34	0.35	
σ_y (ft)	FB	2.4	2.5	2.9	1.4
	MBL	1.8	2.4	2.5	1.2
	MBA	2.4	2.3	2.8	
σ_w (ft/sec)	FB	0.42	0.56	0.50	0.09
	MBL	0.44	0.61	0.44	
	MBA	0.49	0.60	0.48	
σ_z (ft)	FB	1.1	2.0	1.9	0.16
	MBL	1.5	1.9	2.0	
	MBA	1.4	1.7	2.3	
σ_{disp} (ft)	FB	4.9	4.2	4.5	1.8†
	MBL	3.9	4.0	4.4	1.7
	MBA	4.5	3.7	4.8	
PR	FB	9.5	7.5	8.0	8.0
	MBL	9.0	6.9	7.0	6.0
	MBA	9.3	6.8	6.1	

*Only one run for this subject, each motion condition.

†Exclusive of scanning remnant.

‡Predicted scanning behavior for longitudinal task, fixed base was such that coherence matrix was unstable; thus no scanning remnant is included for these figures (see Appendix A)

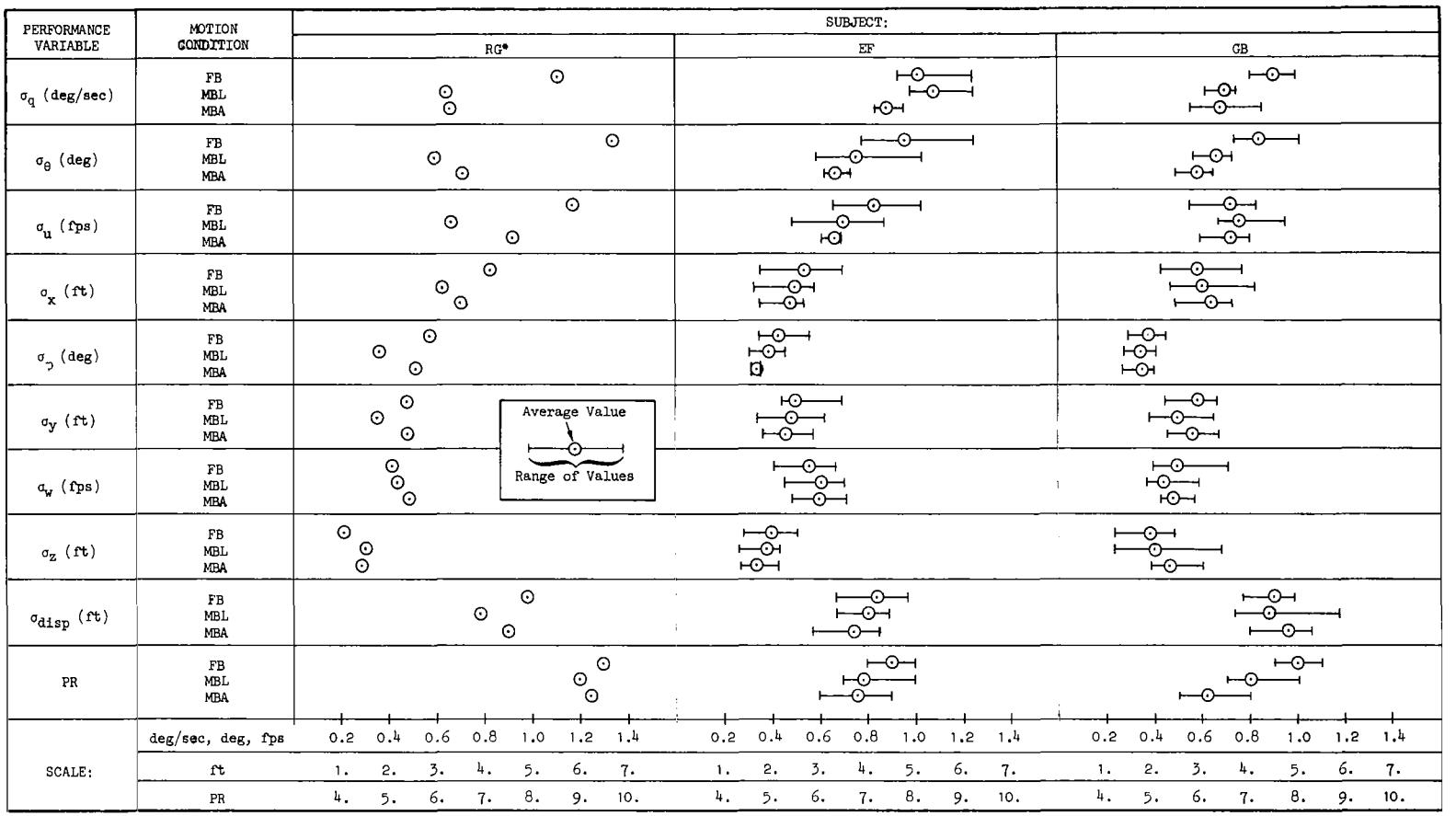

*Only one run for each motion condition.

Figure 12. Performance and Pilot Rating Data, Configuration No. 3

TABLE XI

SUMMARY OF SUBJECT COMMENTARY, CONFIGURATION NO. 3

TOPIC	PILOT SUBJECT		
	RG	EF	GB
General Remarks	The longitudinal task is a lot harder than the lateral task is on Configuration 4.	It's only slightly unstable laterally and very unstable longitudinally — it wanted to slip away from you real quick. The vertical task was no problem. My primary attention is to the attitude display, then almost as much to the CRT (position display) and least of all to the altitude display. You can pick up altitude pretty well with your peripheral vision. A split second's inattention to attitude and it's gone.	With the longitudinal task being more unstable, moving the control stick, then immediately taking your correction out is more effective than just holding it. The fore-and-aft instability sometimes throws off my lateral control. I don't really look at the altitude display that often, and when I do, it throws off my lateral and longitudinal control. The altitude task gives me a lot of trouble because of this.
MBL Motion Condition	Motion really helps because it helps you avoid large attitude changes due to disturbances. It quickens your response to attitude disturbances. Vertically, I use seat of pants to assess my collective input.	The motion is definitely a help. It makes it much easier to pick up attitude changes which might cause trouble. The vertical motion cues I find disorienting because of the jerkiness with which they happen.†	With the motion, it is definitely easier than fixed base. I think MBL helps more on the intermediate configurations (3 and 4) rather than the extreme — on Configuration 1 it is distracting, while on Configuration 6 it is alarming.
MBA Motion Condition	I can see an improvement (over the MBL condition). I don't get vertigo. I think I use the g vector as an attitude cue, so I don't mind the absence of the linear cues — in fact, my performances is better.*	It's easier with the angular motion cues only (relative to MBL).	I find it easier to fly in the MBA condition. Angular cues only is easiest, then linear and angular, and then fixed base.

*It isn't for the Priority 2 run data (one run).

†Large collective inputs.

performance is least for this condition, suggesting greater precision of attitude control.

GB's data indicate tighter attitude control, but poorer position control relative to EF. In agreement with EF, there are rating advantages due to motion. However, they are greater. For MBL relative to FB conditions, the rating advantage is a full point, and for MBA relative to MBL it is another 0.9 of a rating point. But the MBA performance doesn't jibe with this. We are left with the earlier explanation — this subject relaxes when he can.

The limited number of runs on this configuration as well as disagreements among subjects makes it difficult to establish a quantitative rating advantage of moving base over fixed base. It is estimated, based on the data given, that the MBA condition rates on the order of a point better than fixed base, with the MBL condition falling in between. The configuration is so difficult to fly that its numerical rating falls at the high end of the scale (recall the "biasing" of the scale discussed in Section II) where relatively large differences in relative ease show up as small increments in rating.

C. CONFIGURATION NO. 4

Relative to the easiest configuration (No. 1) this configuration of VTOL dynamics has deteriorated lateral task stability, although the deterioration is not as great as the longitudinal task deterioration in Configuration No. 3. The averaged performance and pilot ratings for Configuration No. 4 are listed in Table XII. As before, the pre-experimental position control performance predictions are optimistic. For subject RG the MBA condition is best, in terms of both pilot rating, and performance while for the other two conditions (only two runs) the performance and rating are contradictory. His commentary (Table XIII) suggests use of the g-vector tilt cue in the MBA condition.

For subject EF, both pilot rating and performance agree to the MBA condition being best and FB worst. The scatter in the MBA rating data (Fig. 13) reflects a change in the relative preference of MBA and MBL conditions — in the Priority I runs, he felt MBL to be best while in

TABLE XII

AVERAGED PERFORMANCE, CONFIGURATION NO. 4

PERFORMANCE VARIABLE	MOTION CONDITION	SUBJECT			PREEXPERIMENTAL PREDICTION
		RG	EF	GB	
σ_q (deg/sec)	FB	0.19*	0.33	0.08	0.19†
	MBL	0.30*	0.41	0.09	0.17†
	MBA	0.24	0.35	0.09	
σ_θ (deg)	FB	0.34*	0.33	0.22	0.55
	MBL	0.58*	0.44	0.24	0.48
	MBA	0.42	0.33	0.25	
σ_u (ft/sec)	FB	0.54*	0.56	0.52	0.38
	MBL	0.93*	0.63	0.53	0.28†
	MBA	0.71	0.47	0.57	
σ_x (ft)	FB	2.0*	2.6	3.0	0.98
	MBL	2.9*	2.3	2.9	0.82
	MBA	2.7	2.0	3.0	
σ_φ (deg)	FB	1.59*	1.08	0.79	1.28
	MBL	0.66*	0.93	0.61	0.97
	MBA	0.61	0.77	0.55	
σ_y (ft)	FB	2.9*	2.2	2.6	1.8
	MBL	2.7*	1.8	2.3	1.8
	MBA	1.8	1.8	2.3	
σ_w (ft/sec)	FB	0.50*	0.64	0.46	0.09
	MBL	0.50*	0.51	0.44	
	MBA	0.50	0.57	0.44	
σ_z (ft)	FB	1.8*	1.6	2.1	0.16
	MBL	1.6*	1.5	2.1	
	MBA	1.2	1.5	2.2	
σ_{disp} (ft)	FB	4.0*	3.8	4.6	2.1
	MBL	4.3*	3.5	4.3	2.0
	MBA	3.5	3.1	4.4	
PR	FB	9.8*	7.5	7.3	7.0
	MBL	9.0*	6.8	6.8	5.5
	MBA	8.5	6.1	6.2	

*Represents a single run.

†Exclusive of scanning remnant.

TABLE XIII

SUMMARY OF SUBJECT COMMENTARY, CONFIGURATION NO. 4

TOPIC	PILOT SUBJECT		
	RG	EF	GB
General Remarks	Intense pilot concentration is required to retain control. In normal instrument flying you have to scan at a fairly rapid rate, but things aren't squirrelly like they are here. I find I have to use peripheral scanning — not even looking at altitude except peripherally.* I have more difficulty with the longitudinal axis than I should. The attitude-display may be the cause.	The lateral task damping just doesn't seem to be there, it's very difficult to control. Longitudinally it seems relatively stable and the vertical task is no particular problem. I think an instability in the lateral axis is more easily controlled than the same amount longitudinally. It's impossible to hold any kind of stabilized attitude.	I have a tendency to ignore the altitude task when I know I shouldn't because I know I can't get into trouble on it.
MBL Motion Condition	I do better in the lateral task with motion, but the difference between MBL and FB is small as far as improvement is concerned. I cannot feel the pitch rate, or even its onset. Linear motion degrades or saturates the rotational. This may be the reason why one prefers MBA because of the nature of the task — attitude control.	The angular and linear motion condition is more difficult than with the angular motion only, but feels more comfortable and slightly easier than fixed base.	Motion is a definite advantage — it warns you that you'd best be doing something, but the rumbling around distracts me. You can tell that you're moving, but not in which direction. I get more benefit out of the way the cab tilts (in MBA) than the way it slides from side to side (in MBL).
MBA Motion Condition	I am definitely using the side g due to leaning for attitude and using the roll rate for roll rate. I may not be able to do it as well, longitudinally — I may be more sensitive to roll angles than to pitch angles from a seat of the pants standpoint.	The motion cues, MBA, seemed to be a more definite indication of what is taking place. Linear motion detracts from the angular cues. This condition has a small advantage over MBL and a tremendous advantage over fixed base.	On the lateral control, the cab rocking a little bit gave me an indication that I'd better take a look at things, and I was able to get more lead on the lateral motion. MBA is easier than MBL.
FB Condition	Take the motion away and you can really see the deterioration in the lateral axis.	If anything, the vertical task is easier without the motion (MBL).†	

*This must be true only subjectively, as the EPR data shows more frequent looks at the altitude display than any other subject, by a factor of roughly 2.

†Probably due to this subject's collective control technique which uses fairly large collective corrections, resulting in a jerky vertical response of the simulator because of the lead compensation employed.

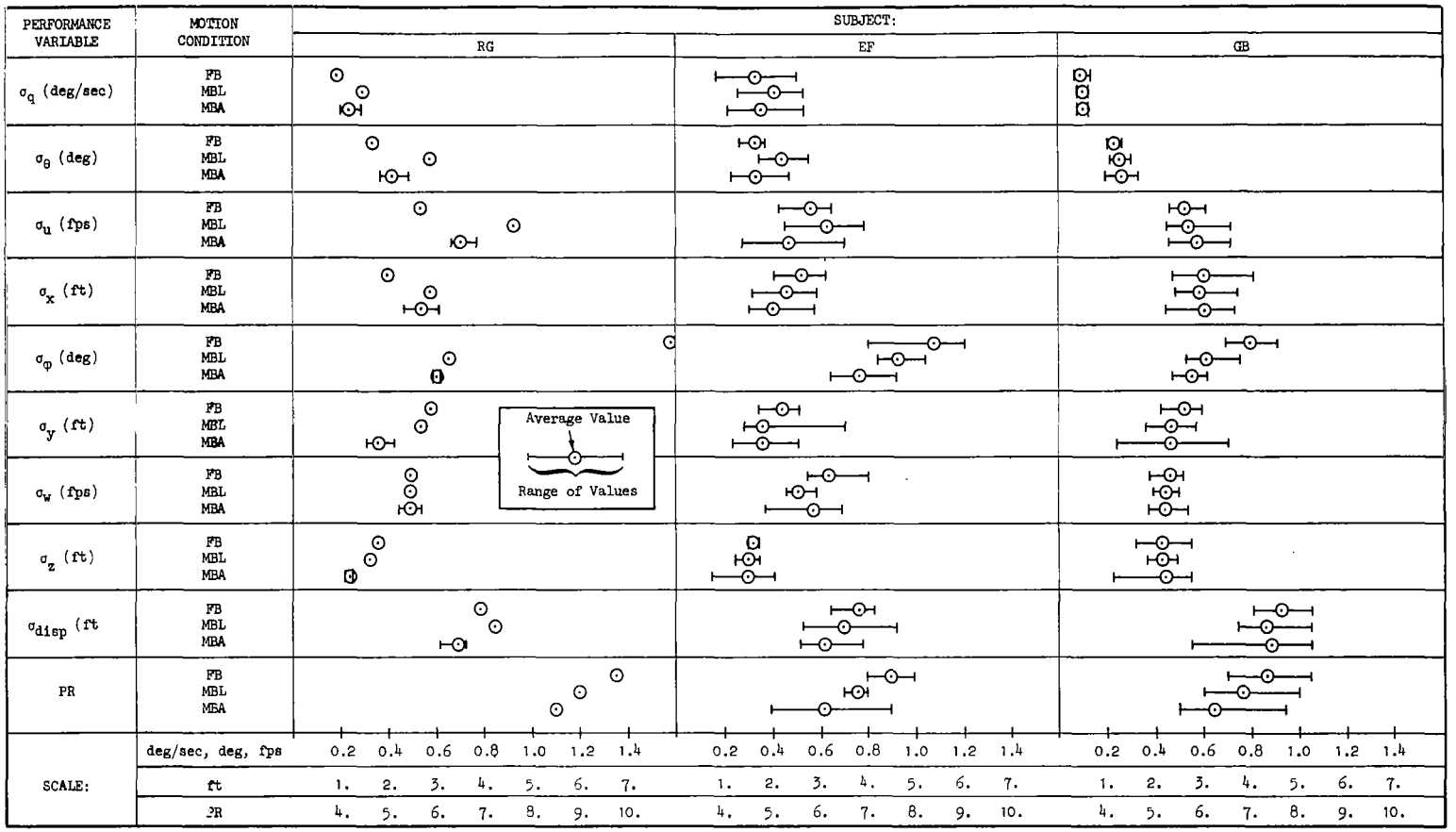

Figure 13. Performance and Pilot Rating Data, Configuration No. 4

later runs the MBA condition was preferred (see Appendix B for the run by run performance listing). The rating advantage is 0.7 of a rating point for MBL over FB, and another 0.7 of a rating point for MBA over MBL. These increments are similar to those of subject RG.

Subject GB's data similarly rates MBA best (by 0.6 rating points over MBL) and FB worst (0.5 of a rating point poorer than MBL), however, his performance doesn't follow this trend. The performance decrement, going from MBL to MBA probably reflects this subject's tendency, observed on the other configurations, to relax attention in this motion condition.

Considering the data and commentary for all subjects for this configuration, there appears to be a significant advantage for the angular motion only (MBA) condition relative to fixed base or the MBL condition. In terms of pilot rating, the increment is on the order of 1.4 for MBA over FB, and about half this for MBL over FB.

D. CONFIGURATION NO. 6

This configuration has deteriorated dynamics in both the lateral and longitudinal axes, and thus represents the most difficult configuration to fly. Table XIV lists the averaged performance data for this configuration, together with the preexperimental predictions of performance. As before, position control performance is worse than predictions, while attitude control is comparable to the predicted performance. Figure 14 illustrates the pilot performance graphically and Table XV summarizes some of the pertinent commentary.

Subject RG shows an advantage of 0.4 of a rating point for MBL over FB and 0.7 of a point for MBA over FB; both of which are reflected in his performance in each task. His commentary suggests it to be more difficult to judge the relative merits of the three motion conditions because the simulated VTOL is so difficult to fly — the ratings are all clustered near the uncontrollable end of the scale.

For subject EF, the same trends are present. The MBA condition is best by 1.6 rating points over fixed base, while the MBL condition rates a 0.8 point advantage. Performance in all tasks follows the ratings.

TABLE XIV

AVERAGED PERFORMANCE, CONFIGURATION NO. 6

PERFORMANCE VARIABLE	MOTION CONDITION	SUBJECT			PREEXPERIMENTAL PREDICTION
		RG	EF	GB	
σ_q (deg/sec)	FB	0.85	1.02	1.06	0.94‡
	MBL	0.69	0.91	0.77	0.35†
	MBA	0.61*	0.87	0.67	
σ_θ (deg)	FB	0.90	0.99	0.99	0.80
	MBL	0.69	0.73	0.73	0.73
	MBA	0.54*	0.65	0.58	
σ_u (ft/sec)	FB	0.78	0.93	0.97	0.52‡
	MBL	0.72	0.73	0.81	0.45†
	MBA	0.58*	0.62	0.71	
σ_x (ft)	FB	3.2	3.1	3.1	1.1‡
	MBL	2.5	2.8	2.8	1.3
	MBA	2.1*	2.7	3.1	
σ_φ (deg)	FB	0.96	1.06	0.94	1.28
	MBL	0.66	0.73	0.68	0.97
	MBA	0.65*	0.62	0.62	
σ_y (ft)	FB	2.3	3.2	2.6	1.8
	MBL	2.2	2.9	2.3	1.8
	MBA	2.2*	2.3	2.5	
σ_w (ft/sec)	FB	0.50	0.54	0.45	0.09
	MBL	0.43	0.57	0.44	
	MBA	0.43*	0.58	0.48	
σ_z (ft)	FB	1.7	2.6	2.4	0.16
	MBL	1.4	2.5	2.3	
	MBA	1.0*	2.3	2.7	
σ_{disp} (ft)	FB	4.4	5.2	4.7	2.1†
	MBL	3.7	4.8	4.3	2.2
	MBA	3.2*	4.3	4.9	
PR	FB	9.8	8.6	9.2	9-10
	MBL	9.4	7.8	8.5	8.5
	MBA	9.1*	7.0	8.5	

*Only 2 data points.

†Scanning remnant effects not included.

‡Predicted scanning behavior for longitudinal task, fixed base, was such that coherence matrix was unstable; thus no scanning remnant included in these figures (see Appendix A).

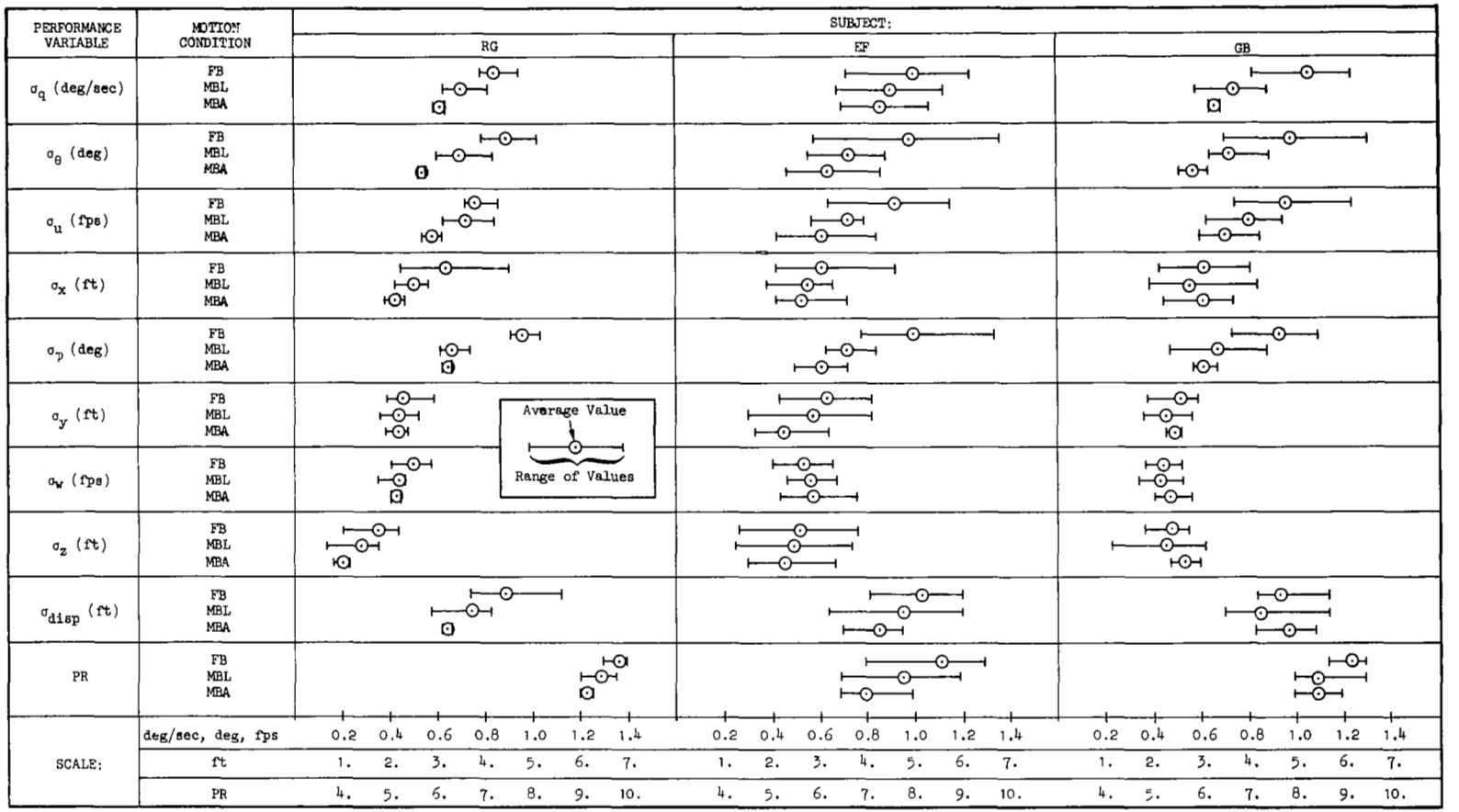

Figure 14. Performance and Pilot Rating Data, Configuration No. 6

TABLE XV

SUMMARY OF SUBJECT COMMENTARY, CONFIGURATION NO. 6

TOPIC	PILOT SUBJECT		
	RG	EF	GB
General Remarks	You can't take your eye off the attitude indicator for even half a second. You have to use your peripheral vision to watch your error signals and maintain 90 percent of your scan on attitude* to keep the attitude excursions as small as possible.	It's extremely unstable, longitudinally, and slightly less so, laterally. Even with small corrections it just won't hold any semblance of stabilized attitude. Large excursions vertically occur because you are tied up with attitude control. On this configuration you just get tired after awhile, and can't hold it like you should.	I look at the CRT, and if the line is to the right, I put the stick to the right, and then look at the attitude indicator to see how much I have it to the right. If I look at the attitude indicator first, then make the correction, it's too late.
MBL Motion Condition	I think the motion helps me, but it's difficult to assess. If you have an extreme attitude variance, you can feel the cab pitch angle, not the pitch rate, the pitch angle. It is difficult to tell if this condition is significantly better than fixed base. It is definitely not as good as with the angular cues only.	With the motion, it's definitely easier, but it's initially disconcerting. The motion makes it easier to catch up with attitude excursions.	It's easier with motion, and I think it's because when it starts to move, I can anticipate that I've got to take out whatever attitude change I have made. It's a little more difficult than the MBA condition, perhaps because the noise of the simulator on its tracks distracts me.
MBA Motion Condition	I detect an improvement in this motion condition. Just the roll attitude was beneficial in helping me tighten up on the lateral tracking error. I think the benefits of the angular cues show up better in the lateral task.	The angular cues were of tremendous value to me in controlling the oscillatory longitudinal task. You can feel it pitching and rolling — it feels so good, that everything else feels poor by comparison. With the angular cues only, you get the feeling of greatest stability.	It feels like it's easier to fly when I only have angular motion.
FB Condition		It's barely controllable. I get the impression that it's much more unstable laterally than it is with the motion going. There seems to be considerable lag in the response to control deflections, primarily in pitch, but also in roll.	

*The largest scanning dwell fraction measured was for this subject and configuration, fixed base ($\eta_2 = 0.699$).

The rating increments are greater than for RG probably because of EF's generally more optimistic ratings.

GB's data is less consistent. While his attitude control performance shows, and commentary suggests, the MBA condition to be best, his averaged performance shows MBA worst with negligible rating advantage over MBL. His commentary agrees with RG in that the relative merits of the three motion conditions are much less distinct. As with the easier configurations, it is postulated that he relaxes his attention in the angular motion only condition.

Considering all the Configuration 6 data, the tentative conclusion is that the MBA condition is better than FB by something less than a full rating point, with the MBL condition falling about halfway between. The smaller increment due to motion is attributed to the overall difficulty of the task.

E. ADDITIONAL CONFIGURATIONS, PRIORITY I RUNS

In the exploratory Priority I runs, several additional configurations were tested in the fixed-base condition, and in the moving-base condition with both linear and angular simulator motion. The level of training in these runs is not very high.

1. Configurations Nos. 9 and 11

These configurations differ from 1 and 3, respectively, only in that the pilot was moved 20 ft ahead of the c.g. of the simulated VTOL. The purpose of these runs was to see if the additional vertical accelerations produced would affect control. The performance data is listed in Tables XVI through XIX.

On Configuration 9 for both subjects, the data shows a performance improvement for the FB condition. Since there are no motion cues, this must be due to random scatter in performance (fixed base, one would expect a performance decrement, if anything, because of the pitch task cross coupling into altitude). Since the performance decrement in the MBL condition relative to Configuration 1 is of smaller magnitude than the performance improvement, FB, one can similarly conclude the

TABLE XVI

CONFIGURATION NO. 9 PERFORMANCE DATA, SUBJECT EF

PERFORMANCE VARIABLE	MOTION CONDITION	CONFIG. 1 AVERAGE	CONFIG. 9 10 DEC. 1969		CONFIG. 9 AVERAGE
Run No.	FB		59	60	
	MBL		57	58	
σ_q (deg/sec)	FB	0.27	0.214	0.226	0.22
	MBL	0.34	0.375	0.432	0.40
σ_θ (deg)	FB	0.37	0.394	0.364	0.38
	MBL	0.47	0.616	0.638	0.63
σ_u (ft/sec)	FB	0.52	0.529	0.443	0.49
	MBL	0.59	0.777	0.717	0.75
σ_x (ft)	FB	1.8	1.559	1.100	1.3
	MBL	1.9	2.419	1.908	2.2
σ_φ (deg)	FB	0.57	0.653	0.544	0.60
	MBL	0.64	0.730	0.959	0.84
σ_y (ft)	FB	1.7	1.536	1.552	1.5
	MBL	2.1	1.843	2.288	2.1
σ_w (ft/sec)	FB	0.55	0.490	0.515	0.50
	MBL	0.53	0.474	0.538	0.51
σ_z (ft)	FB	1.7	1.783	1.584	1.7
	MBL	1.9	2.310	2.260	2.3
σ_{disp} (ft)	FB	3.0	2.823	2.476	2.6
	MBL	3.4	3.819	3.739	3.8
PR	FB	4.2	3.5	3.5	3.5
	MBL	4.2	4.5	4.0	4.3

TABLE XVII

CONFIGURATION NO. 9 PERFORMANCE DATA, SUBJECT GB

PERFORMANCE VARIABLE	MOTION CONDITION	CONFIG. 1 AVERAGE	CONFIG. 9 12 DEC. 1969				CONFIG. 9 AVERAGE
Run. No.	FB		103	104	125*		
	MBL		105	106	123*	126*	
	MBA				124*		
σ_q (deg/sec)	FB	0.08	0.047	0.092	0.073		0.07
	MBL	0.08	0.061	0.087	0.079	0.037	0.07
	MBA	0.10			0.052		0.05
σ_θ (deg)	FB	0.20	0.144	0.205	0.174		0.17
	MBL	0.22	0.229	0.237	0.288	0.157	0.23
	MBA	0.24			0.177		0.18
σ_u (ft/sec)	FB	0.47	0.351	0.436	0.360		0.38
	MBL	0.52	0.555	0.539	0.655	0.480	0.56
	MBA	0.51			0.377		0.38
σ_x (ft)	FB	2.6	2.191	2.493	2.071		2.3
	MBL	2.9	3.233	2.695	3.469	3.339	3.2
	MBA	3.0			2.308		2.3
σ_φ (deg)	FB	0.32	0.296	0.372	0.350		0.34
	MBL	0.32	0.298	0.313	0.430	0.349	0.35
	MBA	0.33			0.324		0.32
σ_y (ft)	FB	2.3	2.781	2.360	1.794		2.3
	MBL	2.4	1.867	2.269	2.985	2.465	2.4
	MBA	2.6			3.120		3.1
σ_w (ft/sec)	FB	0.43	0.364	0.486	0.486		0.45
	MBL	0.44	0.488	0.503	0.509	0.476	0.49
	MBA	0.42			0.437		0.44
σ_z (ft)	FB	1.7	1.077	1.704	2.293		1.7
	MBL	2.0	1.793	2.439	1.966	2.751	2.2
	MBA	1.9			2.322		2.3
σ_{disp} (ft)	FB	4.0	3.701	3.832	3.573		3.7
	MBL	4.3	4.142	4.285	4.981	4.979	4.6
	MBA	4.5			4.522		4.5
PR	FB	4.8	4.5	4.5	5.5		4.8
	MBL	4.9	4.0	4.5	6.5	5.5	5.1
	MBA	4.5			5.0		5.0

*These runs at subject's request.

TABLE XVIII

CONFIGURATION NO. 11 PERFORMANCE DATA, SUBJECT EF

PERFORMANCE VARIABLE	MOTION CONDITION	CONFIG. 3 AVERAGE	CONFIG. 11 11 DEC. 1969		CONFIG. 11 AVERAGE
Run No.	FB MBL		77 79	78 80	
σ_q (deg/sec)	FB	1.15	1.128	1.242	1.19
	MBL	1.08	1.129	1.117	1.12
σ_θ (deg)	FB	0.96	0.811	1.061	0.91
	MBL	0.76	0.660	0.735	0.70
σ_u (ft/sec)	FB	0.83	0.662	0.914	0.79
	MBL	0.70	0.686	0.703	0.69
σ_x (ft)	FB	2.7	1.844	3.520	2.7
	MBL	2.5	2.758	2.431	2.6
σ_φ (deg)	FB	0.43	0.483	0.351	0.42
	MBL	0.39	0.364	0.404	0.38
σ_y (ft)	FB	2.5	2.238	2.217	2.2
	MBL	2.4	2.730	1.776	2.3
σ_w (ft/sec)	FB	0.56	0.663	0.672	0.67
	MBL	0.61	0.710	0.663	0.69
σ_z (ft)	FB	2.0	2.234	2.563	2.4
	MBL	1.9	2.185	2.073	2.1
σ_{disp} (ft)	FB	4.2	3.660	4.886	4.3
	MBL	4.0	4.454	3.655	4.1
PR	FB	7.5	7.0	7.5	7.3
	MBL	6.9	7.0	6.5	6.8

TABLE XIX

CONFIGURATION NO. 11 PERFORMANCE DATA, SUBJECT GB

PERFORMANCE VARIABLE	MOTION CONDITION	CONFIG. 3 AVERAGE	CONFIG. 11 10 DEC. 1969		CONFIG. 11 AVERAGE
Run No.	FB		49	50	
	MBL		51	52	
σ_q (deg/sec)	FB	0.90	0.860	0.951	0.91
	MBL	0.70	0.685	0.681	0.68
σ_θ (deg)	FB	0.84	0.814	0.897	0.86
	MBL	0.66	0.624	0.684	0.65
σ_u (ft/sec)	FB	0.72	0.765	0.829	0.80
	MBL	0.76	0.676	0.811	0.74
σ_x (ft)	FB	2.9	3.207	2.939	3.1
	MBL	3.0	2.378	3.022	2.7
σ_φ (deg)	FB	0.37	0.420	0.419	0.42
	MBL	0.34	0.354	0.339	0.35
σ_y (ft)	FB	2.9	3.301	2.757	3.0
	MBL	2.5	2.528	2.207	2.4
σ_w (ft/sec)	FB	0.50	0.504	0.497	0.50
	MBL	0.44	0.395	0.507	0.45
σ_z (ft)	FB	1.9	1.814	2.075	1.9
	MBL	2.0	1.173	2.095	1.6
σ_{disp} (ft)	FB	4.5	4.947	4.523	4.7
	MBL	4.4	3.663	4.288	4.0
PR	FB	8.0	8.5	7.5	8.0
	MBL	7.0	8.0	6.5	7.3

difference to be data scatter. On this basis, the Configuration 9 data was treated as being similar to Configuration No. 1 in all the performance averages.

For Configuration 11, EF shows a decrement relative to Configuration 3 in both the FB and MBL conditions. The decrement is small and is attributed to data scatter — certainly no significance can be attached to it in view of the small number of runs. For subject GB, there is a performance improvement, MBL, and a decrement, FB over the averaged Configuration 3 data. This "trend" would suggest that this subject may be using vertical acceleration cues. On the other hand, the performance achieved and the pilot rating obtained for the two moving-base runs disagree (poorer performance had a better rating) suggesting that the subject was working harder than usual for him on the run where the best performance was achieved. Consequently, this trend is not judged significant and the Configuration 11 data was lumped with the Configuration 3 data in the performance averages.

One concludes that significant "ℓ_x effects" cannot be established by the limited data sample taken. This is reasonable in view of the relatively small excursions in pitch — there is little discernible difference between $\ell_x = 0$ and $\ell_x = 20$ as far as the pilot is concerned with the small pitch angles, velocities, and accelerations experienced. Certainly the effect is negligible with regard to its influence on vertical task performance because of the low attention level on that task. On one occasion during the training runs, the value of ℓ_x was deliberately changed several times between the two values of 0 and 20 ft on a moving-base run with no discernible difference to the pilot — he could barely detect the momentary transient and couldn't detect any difference between the two configurations.

2. Configurations Nos. 2 and 5

These configurations are intermediate in longitudinal task difficulty between 1 and 3, and 4 and 6, respectively. The data for these runs is listed with averaged performance in the easier and more difficult tasks in Tables XX through XXIII. Most of the data falls at an intermediate level between the two extremes, the outstanding exception being GB's

TABLE XX

CONFIGURATION NO. 2 PERFORMANCE DATA, SUBJECT EF

PERFORMANCE VARIABLE	MOTION CONDITION	CONFIG. 1 AVERAGE	CONFIG. 2 10 DEC. 1969		CONFIG. 2 AVERAGE	CONFIG. 3 AVERAGE
Run No.	FB MBL		63 61	64 62		
σ_q (deg/sec)	FB MBL	0.27 0.34	0.556 0.480	0.468 0.476	0.51 0.48	1.15 1.08
σ_θ (deg)	FB MBL	0.37 0.47	0.882 0.578	0.616 0.602	0.75 0.59	0.96 0.76
σ_u (ft/sec)	FB MBL	0.52 0.59	1.009 0.556	0.664 0.646	0.84 0.60	0.83 0.70
σ_x (ft)	FB MBL	1.8 1.9	2.916 1.765	1.741 1.996	2.3 1.9	2.7 2.5
σ_φ (deg)	FB MBL	0.57 0.64	0.533 0.443	0.408 0.421	0.47 0.43	0.43 0.39
σ_y (ft)	FB MBL	1.7 2.1	3.231 2.447	1.681 1.832	2.4 2.1	2.5 2.4
σ_w (ft/sec)	FB MBL	0.55 0.53	0.361 0.425	0.450 0.387	0.41 0.41	0.56 0.61
σ_z (ft)	FB MBL	1.7 1.9	1.745 1.398	2.032 1.101	1.9 1.2	2.0 1.9
σ_{disp} (ft)	FB MBL	3.0 3.4	4.689 3.326	3.160 2.924	3.9 3.1	4.2 4.0
PR	FB MBL	4.2 4.2	6.0 5.0	6.0 5.5	6.0 5.3	7.5 6.9

TABLE XXI

CONFIGURATION NO. 2 PERFORMANCE DATA, SUBJECT GB

PERFORMANCE VARIABLE	MOTION CONDITION	CONFIG. 1 AVERAGE	CONFIG. 2 12 DEC. 1969		CONFIG. 2 AVERAGE	CONFIG. 3 AVERAGE
Run No.	FB MBL		93 95	94 96		
σ_q (deg/sec)	FB MBL	0.08 0.08	0.329 0.384	0.367 0.359	0.35 0.37	0.90 0.70
σ_θ (deg)	FB MBL	0.20 0.22	0.420 0.430	0.435 0.361	0.43 0.40	0.84 0.66
σ_u (ft/sec)	FB MBL	0.47 0.52	0.660 0.650	0.697 0.430	0.68 0.54	0.72 0.76
σ_x (ft)	FB MBL	2.6 2.9	2.942 2.576	3.048 1.411	3.0 2.0	2.9 3.0
σ_φ (deg)	FB MBL	0.32 0.32	0.327 0.378	0.425 0.275	0.38 0.33	0.37 0.34
σ_y (ft)	FB MBL	2.3 2.4	2.381 2.360	2.828 2.379	2.6 2.4	2.9 2.5
σ_w (ft/sec)	FB MBL	0.43 0.44	0.367 0.513	0.513 0.498	0.44 0.51	0.50 0.44
σ_z (ft)	FB MBL	1.7 2.0	1.439 2.378	2.355 2.212	1.9 2.3	1.9 2.0
σ_{disp} (ft)	FB MBL	4.0 4.3	4.049 4.226	4.778 3.542	4.4 3.9	4.5 4.4
PR	FB MBL	4.8 4.9	5.5 5.5	6.0 5.0	5.8 5.3	8.0 7.0

TABLE XXII

CONFIGURATION NO. 5 PERFORMANCE DATA, SUBJECT EF

PERFORMANCE VARIABLE	MOTION CONDITION	CONFIG. 4 AVERAGE	CONFIG. 5 9 DEC. 1969		CONFIG. 5 AVERAGE	CONFIG. 6 AVERAGE
Run No.	FB MBL		31 33	32 34		
σ_q (deg/sec)	FB	0.33	0.498	0.541	0.52	1.02
	MBL	0.41	0.555	0.509	0.53	0.91
σ_θ (deg)	FB	0.33	0.747	0.701	0.72	0.99
	MBL	0.44	0.695	0.584	0.64	0.73
σ_u (ft/sec)	FB	0.56	0.815	0.693	0.75	0.93
	MBL	0.63	0.768	0.641	0.70	0.73
σ_x (ft)	FB	2.6	1.777	1.769	1.8	3.1
	MBL	2.3	2.474	2.272	2.4	2.8
σ_φ (deg)	FB	1.08	0.615	1.484	1.05	1.06
	MBL	0.93	0.993	1.036	1.01	0.73
σ_y (ft)	FB	2.2	2.436	2.852	2.6	3.2
	MBL	1.8	2.793	2.718	2.8	2.9
σ_w (ft/sec)	FB	0.64	0.559	0.523	0.54	0.54
	MBL	0.51	0.491	0.596	0.54	0.57
σ_z (ft)	FB	1.6	2.573	2.334	2.5	2.6
	MBL	1.5	2.370	2.853	2.6	2.5
σ_{disp} (ft)	FB	3.8	3.965	4.088	4.0	5.2
	MBL	3.5	4.421	4.555	4.5	4.8
PR	FB	7.5	6.5	6.0	6.3	8.6
	MBL	6.8	6.0	6.0	6.0	7.8

TABLE XXIII

CONFIGURATION NO. 5 PERFORMANCE DATA, SUBJECT GB

PERFORMANCE VARIABLE	MOTION CONDITION	CONFIG. 4 AVERAGE	CONFIG. 5 12 DEC. 1969		CONFIG. 5 AVERAGE	CONFIG. 6 AVERAGE
Run No.	FB		109	110		
	MBL		107	108		
	MBA		111*	112*		
σ_q (deg/sec)	FB	0.08	0.349	0.415	0.38	1.06
	MBL	0.09	0.450	0.405	0.43	0.77
	MBA	0.09	0.389	0.372	0.38	0.67
σ_θ (deg)	FB	0.22	0.421	0.441	0.43	0.99
	MBL	0.24	0.474	0.397	0.44	0.73
	MBA	0.25	0.396	0.401	0.40	0.58
σ_u (ft/sec)	FB	0.52	0.630	0.668	0.65	0.97
	MBL	0.53	0.585	0.559	0.57	0.81
	MBA	0.57	0.639	0.640	0.64	0.71
σ_x (ft)	FB	3.0	2.547	3.020	2.8	3.1
	MBL	2.9	2.420	2.460	2.5	2.8
	MBA	3.0	2.713	2.574	2.6	3.1
σ_φ (deg)	FB	0.79	0.904	1.005	0.95	0.94
	MBL	0.61	0.762	0.696	0.73	0.68
	MBA	0.55	0.469	0.544	0.51	0.62
σ_y (ft)	FB	2.6	2.227	2.236	2.2	2.6
	MBL	2.3	1.985	1.903	1.9	2.3
	MBA	2.3	2.338	1.876	2.1	2.5
σ_w (ft/sec)	FB	0.46	0.447	0.426	0.44	0.45
	MBL	0.44	0.464	0.419	0.44	0.44
	MBA	0.44	0.471	0.468	0.47	0.48
σ_z (ft)	FB	2.1	2.476	1.980	2.2	2.4
	MBL	2.1	2.479	1.716	2.1	2.3
	MBA	2.2	2.612	2.248	2.4	2.7
σ_{disp} (ft)	FB	4.6	4.192	4.248	4.2	4.7
	MBL	4.3	3.992	3.552	3.8	4.3
	MBA	4.4	4.432	3.898	4.2	4.9
PR	FB	7.3	8.0	8.0	8.0	9.2
	MBL	6.8	6.0	6.0	6.0	8.5
	MBA	6.2	6.5	6.5	6.5	8.5

*These runs at subject's request.

data for Configuration 5. Here, performance is better than either extreme, both overall (σ_{disp}) and in the longitudinal and lateral tasks (σ_x and σ_y). A possible explanation for this lies in the run sequence causing a change in the subject's "set." Earlier in the day, GB "flew" Configuration 6 wherein the value of the roll damping was (inadvertently) set to zero, making it more difficult than No. 6. This caused him to come very close to losing control (he did lose control on one of the fixed-base runs). He wasn't informed of the error until after the conclusion of the runs that day. Consequently, he probably increased his efforts substantially when next confronted with a difficult configuration, in this case, No. 5.

RG flew Configuration No. 5 in the course of his training when "working up" to No. 6. His comment (see Table XXIV) was similar to other remarks made later, concerning the relative difficulty of the roll and pitch tasks. On this configuration, the pitch damping is greater than the roll damping. Considering the display differences, and differences in the control sensitivity (and simulator motion differences such as angular resolution and pilot location relative to the motion axis, as well as pilot physiological differences) between pitch and roll one has several possible reasons as to why the longitudinal task rates as more difficult than the lateral task. The obvious difference is the difference in task damping, but the display (and other) differences also contribute.

3. Configuration No. 8

This configuration has deteriorated vertical task stability and low control sensitivity relative to Configuration No. 1. The performance data for this configuration is listed in Tables XXV and XXVI. It is clear that for EF, motion apparently is an advantage, unlike the situation for Configuration No. 1. There were two reasons for this mentioned by the subjects. First, an abrupt collective deflection could be felt, to the lead compensation of the simulator motion — if large enough it could be felt as a jolt and acted to inhibit large collective deflections. (Note: The collective control is such that it remains wherever it is set — thus the deflection time history looks like a

TABLE XXIV. SUMMARY OF SUBJECT COMMENTARY, CONFIGURATIONS 2, 5, AND 8

	PILOT SUBJECT		
	RG	EF	GB
Config. 2	(No runs on this configuration.)	By keeping my attitude excursions within ±5 deg on the attitude ball (±1 deg simulator motion), it was very controllable. It was more unstable longitudinally than laterally. The instability is aggravated with the lack of motion — the more difficult the task, the more the motion seems to help.	The fore-and-aft task was the one that was varying (i.e., deteriorated stability). I cannot find a zero on the collective task, or a point where the excursions will stay within ±2 ft. You don't get the real advantages of motion until you get to the more difficult configurations. .On the easier ones it is more distracting than beneficial, especially the lateral motion.
Config. 5	I can see an improvement, moving base. The pilot compensation required was a bit less. (Training run.) I seem to have more trouble with the longitudinal or the pitch task. It is harder because of the way the display is set up — I think you can degrade further in roll and still control it to a certain degree than you can in pitch. (Training run.)	It required a lot of concentration, both longitudinal and lateral tasks were difficult. I seemed to have more difficulty with the roll task. The vertical task more or less took care of itself with minimal attention.	The rate of display movement has a lot to do with how much correction you put in — a rapid movement requires a large correction. I get a definite benefit with the MBL condition — several times I felt it move, and my eye was directed to the CRT. I like the MBA condition the best.
Config. 8	(No runs on this configuration.)	The collective response is quite sluggish, but seems unstable in the sense that once you get an oscillation going it is hard to get it bracketed. The collective task detracts from the longitudinal and lateral control. You get some rather disconcerting motion cues when you hit the simulator limits, then jerk off these limits. If you can keep it within the limits, then the motion cues are helpful.	The moving base (MBL) condition is easier. The collective task is the same either way, but on moving base my body tells me when things are starting to change in the longitudinal and lateral tasks. I can't feel it go up and down, even with these large excursions; the only time I can feel it is when I make an abrupt change on the collective. Then I can feel it jump.

TABLE XXV

CONFIGURATION NO. 8 PERFORMANCE DATA, SUBJECT EF

PERFORMANCE VARIABLE	MOTION CONDITION	CONFIG. 1 AVERAGE	CONFIG. 8 9 DEC. 1969		CONFIG. 8 AVERAGE
Run No.	FB MBL		27 29	28 30	
σ_q (deg/sec)	FB	0.27	0.316	0.260	0.29
	MBL	0.34	0.324	0.312	0.32
σ_θ (deg)	FB	0.37	0.541	0.512	0.53
	MBL	0.47	0.543	0.469	0.51
σ_u (ft/sec)	FB	0.52	0.812	0.745	0.78
	MBL	0.59	0.728	0.612	0.67
σ_x (ft)	FB	1.8	2.376	2.449	2.4
	MBL	1.9	2.814	2.108	2.5
σ_φ (deg)	FB	0.57	0.727	0.563	0.65
	MBL	0.64	0.639	0.428	0.53
σ_y (ft)	FB	1.7	1.694	2.118	1.9
	MBL	2.1	1.922	1.545	1.7
σ_w (ft/sec)	FB	0.55	1.308	1.103	1.21
	MBL	0.53	1.515	0.847	1.18
σ_z (ft)	FB	1.7	4.043	3.742	3.9
	MBL	1.9	4.713	2.703	3.7
σ_{disp} (ft)	FB	3.0	4.986	4.947	5.0
	MBL	3.4	5.817	3.761	4.8
PR	FB	4.2	7.0	7.0	7.0
	MBL	4.2	8.0*	5.0	6.5

TABLE XXVI

CONFIGURATION NO. 8 PERFORMANCE DATA, SUBJECT GB

PERFORMANCE VARIABLE	MOTION CONDITION	CONFIG. 1 AVERAGE	CONFIG. 8 12 DEC. 1969		CONFIG. 8 AVERAGE
Run No.	FB MBL		115 113	116 114	
σ_q (deg/sec)	FB MBL	0.08 0.08	0.110 0.095	0.064 0.077	0.09 0.09
σ_θ (deg)	FB MBL	0.20 0.22	0.281 0.276	0.212 0.205	0.25 0.24
σ_u (ft/sec)	FB MBL	0.47 0.52	0.629 0.686	0.518 0.480	0.57 0.58
σ_x (ft)	FB MBL	2.6 2.9	3.669 3.474	3.328 2.655	3.5 3.1
σ_φ (deg)	FB MBL	0.32 0.32	0.368 0.353	0.391 0.393	0.38 0.37
σ_y (ft)	FB MBL	2.3 2.4	2.978 3.348	3.036 3.139	3.0 3.2
σ_w (ft/sec)	FB MBL	0.43 0.44	0.813 0.847	1.087 0.963	0.95 0.91
σ_z (ft)	FB MBL	1.7 2.0	2.098 2.917	2.844 2.946	2.5 2.9
σ_{disp} (ft)	FB MBL	4.0 4.3	5.170 5.638	5.327 5.058	5.2 5.3
PR	FB MBL	4.8 4.9	7.0 7.0	7.0 6.5	7.0 6.8

series of steps of random amplitude and timing.) Second, both subjects felt that the presence of motion enabled them to pay less attention to the longitudinal and lateral tasks, and devote more time to the vertical task.

However, GB's data doesn't confirm this trend — the MBL condition shows a performance decrement in both the vertical control task and overall performance for both Configuration 1 and 8. In any case, both subjects felt that the vertical task was still minor relative to lateral and longitudinal tasks. One concludes that the data taken is insufficient to establish the benefits (if any) of linear motion on control of a lightly damped vertical control task having low control sensitivity, probably because the other tasks are so demanding.

F. PRIORITY III RUNS

The intent in these runs was to define the permissible lags in the simulator motion which are tolerable in the simulated task. The time constant of a low-pass filter was varied — the filter acting only on the simulator drive signals. The experiment was run in the MBA condition on Configurations 4 and 6. The procedure called for two runs with the lag equal to zero, then several more with varying amounts of lag.

A summary of the pertinent comments and the pilot rating is given in Table XXVII. Configuration 4 is listed first, then Configuration 6. The effects on performance, shown in Fig. 15, are not consistent — the run-to-run scatter is greater than the effects of motion lag for low values of the motion fidelity filter time constant. However, there was a sharp, definable drop in performance in going from a lag of 0.2 sec to 0.4 sec for both subjects on Configuration No. 6. For Configuration No. 4, subject RG had a sharp drop in performance at the same level of lag; but EF was more sensitive to the lag, showing a substantial drop in performance going from 0.1 to 0.2 sec of lag.

These results would suggest that both subjects were somewhat less sensitive to motion lags than the preexperimental analyses would predict (i.e., that 0.1 sec lag would be significant). This would suggest that these subjects are closing the attitude loop at a somewhat lower

TABLE XXVII

SUMMARY OF PILOT OPINION AND COMMENTARY, PRIORITY III EXPERIMENT

TIME CONSTANT	SUBJECT RG		SUBJECT EF	
	PR	COMMENTARY	PR	COMMENTARY
0	8.5	The lateral task seems more stable than it does on No. 6. I get the impression that I'm spending just as much time on the longitudinal task as the lateral.	5.0	Seems as if there are very momentary lags in pitch and roll motion — it would hang up very momentarily, then come back the way it's supposed to.*
0.05	8.25	It seemed a little harder to fly, laterally. I got the impression that you're cutting down on the roll sensitivity.	5.0 — 5.25	It seems as though the motion damping has been reduced a little bit, a slight hesitation. It seemed just a little slow, but not adverse to performance.
0.10	8.5 — 9.0	I can't see much, if any, difference.	6.0	The lateral task seemed to have varying stability — more unstable than the last run. I cannot detect any change in the longitudinal task.
0.20	8.5 — 9.0	I can't see a great deal of difference.	8.5	Laterally, the motion cues are unreliable; difficult to describe, but it does change the stability characteristics. Longitudinally it doesn't feel quite right either. It wouldn't respond.†
0.40	9.0 — 9.5	I still get the impression that the amount of bank angle going into the motion has been cut down. I'm beginning to notice a deterioration in the lateral response.	—	
0	9.0	Yes, that is No. 6. It's pretty bad.	7.0 — 7.5	It felt about normal for No. 6. I felt the pitch instability most — I'm much more aware of the longitudinal instability after flying No. 4.
0.05	—		7.0 — 7.5	Any changes made were very subtle. Pitch is the whole task. It seemed a little bit more stable than the last run.‡
0.10	9.0	No obvious change, perhaps a slight degradation in performance.	7.0 — 7.5	Nothing of real significance, there. The changes were very subtle. It's very difficult to spot changes in this configuration.
0.20	9.0	I can't assess whether I am doing any better or any worse. No obvious change. The pitch is harder to control than roll.	7.5	(Early in the run.) It seems a little more unstable in pitch. (Toward the end.) Now it seems more stable than it did earlier. The change is very small, if any.
0.40	9.5 — 9.75	Now I see a difference. I had to put in large, probably overcontrolling inputs. I worked harder. Seems as if control power is being reduced. Sluggish from a feel standpoint.	8.5	There is a small lag in the movement — it seems more unstable than the earlier runs. This run it was a lot tougher.

*Probably a reference to the angular resolution of the simulator.

†Subject commented that he had more difficulty at the beginning of the run than toward the end.

‡Effects of practice?

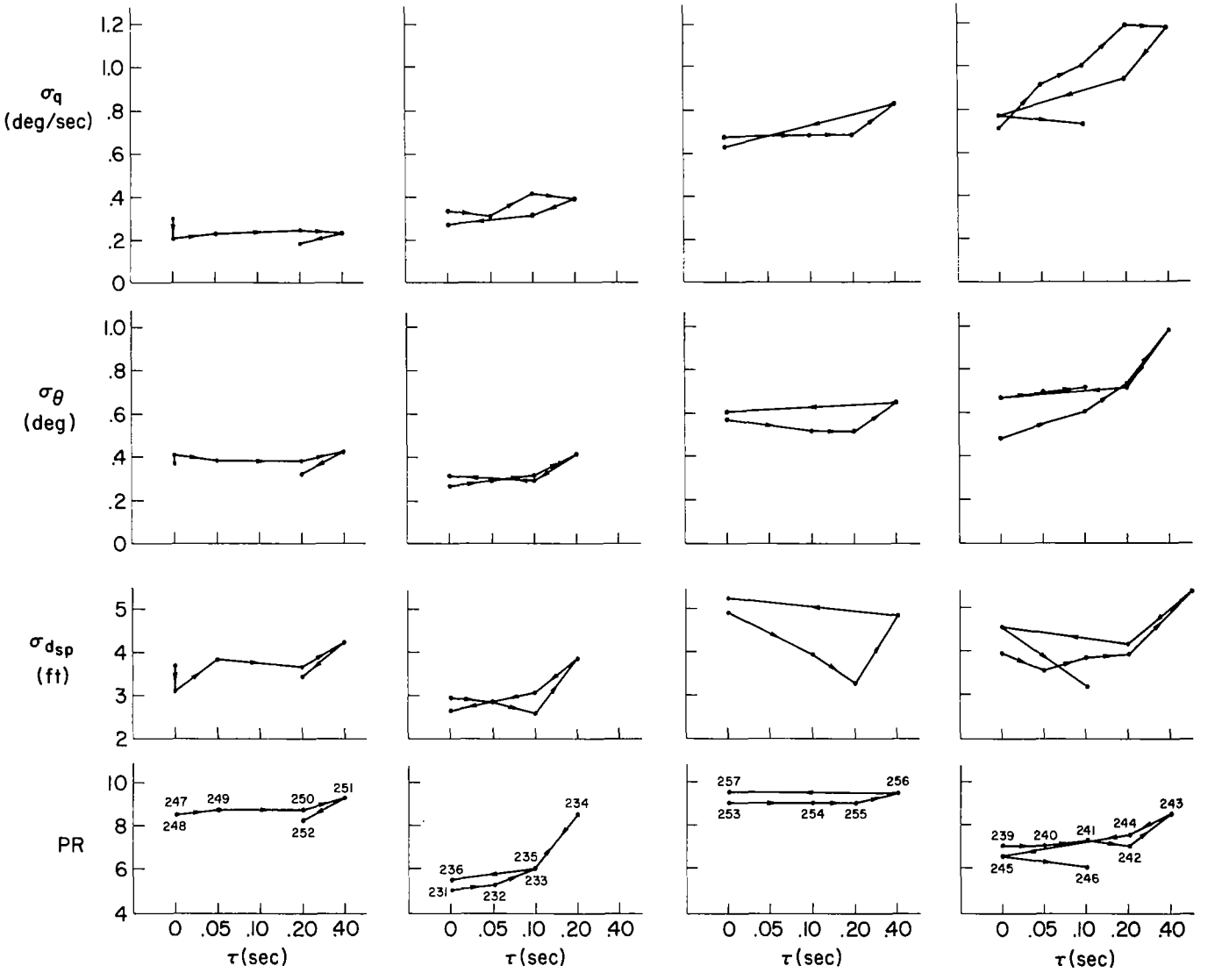

Figure 15. Effect of Motion Fidelity Filter Lag on Performance, Priority III Runs.

frequency — on the order of one half the predicted crossover frequency of 2.25 rad/sec. At the lower crossover frequency, the effects of the lag on the motion phase are correspondingly reduced — it takes twice the lag at half the frequency to produce the same decrement in phase margin.

G. VFR-IFR DIFFERENCES

During the shakedown and early training runs it became quite obvious that the simulated task differed strongly from both predicted results as well as past data in similar tasks. The major difference lies in the use of separated instrument displays. Virtually all past data (upon which the predictions of such things as pilot rating are predicated) is based on use of a contact analog display as a close approach to VFR conditions.

At about the midpoint of the experimental program, an opportunity presented itself to briefly evaluate what these differences are. Two successive moving base (MBL) runs were made, the first under VFR conditions wherein the control sensitivities were increased by a factor of five from their nominal values to restore the desired cab angular motion sensitivity. The hatch on one side of the cab was removed. On the next run, the hatch was closed, and the control gains restored to their former values. The results of these two runs are listed in Table XXVIII with other comparable results and predictions. The hovering position control performance improves by a factor of about three, while the vehicle attitude deviations in pitch increase by a similar amount. These runs were made with the same level of gust excitation used throughout the program.

This table reveals a much closer correspondence between the VFR data and overall performance predictions, although it is clear that the prediction assumes much closer attention to altitude deviations than is actually the case. The pilot endeavors to make each of his three position errors roughly equal — a factor not taken into account in the predictions.

The major point of difference between the VFR and IFR runs is the much tighter control of hovering position error obtained by using much larger attitude excursions for control of this error under VFR conditions.

TABLE XXVIII

VFR-IFR DIFFERENCES, CONFIGURATION NO. 1, SUBJECT GB

PERFORMANCE VARIABLE	UNITS	MBL RUN AVERAGE*	RUN 166 (IFR)	RUN 165 (VFR)	PREEXPERIMENTAL PREDICTIONS	UARL DATA†
σ_q	deg/sec	0.08	0.11	1.17†	0.17*	1.74
σ_θ	deg	0.22	0.28	0.78†	0.48	2.42
σ_w	ft/sec	0.52	0.58	0.40	0.28*	0.75
σ_x	ft	2.9	3.1	0.7	0.82	1.10
σ_φ	deg	0.32	0.58	0.65	0.68	—
σ_y	ft	2.4	2.6	0.8	1.2	—
σ_w	ft/sec	0.44	0.44	0.29	0.09	—
σ_z	ft	2.0	1.9	0.8	0.16	—
σ_{disp}	ft	4.3	4.4	1.3	1.5	—
PR	—	4.9	4.0	3.5†	2.5	3.25

*Exclusive of scanning remnant.

†The subject commented on the fact that he didn't have a good visual cue in pitch — the front of the cab was still enclosed.

‡From Ref. 8 for UARL Configuration PH 12 where $gM_u = 0.67$, $M_q = -5$, $X_u = -0.1$, $\sigma_{u_g} = 5.1$, $gL_v = -0.1$, $Y_v = -0.1$, $L_p = -3$, $\sigma_{v_g} = 1.3$, under fixed base conditions using a contact analog display.

His outer loop gain and crossover frequency are higher, VFR. Under IFR conditions, the separated instrument displays force him to use a loop closure criteria in which the position error buildup occurs relatively slowly because he can't be looking at the position error at all times. This implies small attitude excursions and relatively large position excursions; he uses a lower outer loop gain and crossover frequency under IFR conditions.

The last column in Table XXVIII taken from Ref. 8 is presented to show that the current experimental results are not unreasonable as a VFR task. Precise comparisons are not possible because of differences between the two tasks, e.g., the controlled element dynamics, gust excitation magnitude and real world versus contact analog display differences.

In an earlier experimental program oriented toward developing a contact analog display for use in hovering (Ref. 5) similar sorts of changes in the performance achieved were noted when going from a conventional instrument display to the integrated display (on a TV screen). In this experiment, run fixed base, altitude and lateral position control improved substantially while the roll angle excursions increased when the integrated display was used. Direct comparisons are not possible in view of the many other differences between the current experiment and that of Ref. 5 (e.g., controlled element dynamics, instrument configuration, etc.). Nevertheless it is clear that VFR-IFR differences are quite large.

H. EFFECT OF INPUT DISTURBANCE

During the same series of runs discussed above, an additional run was made to assess the importance of the input disturbance on performance under IFR conditions. Table XXIX lists the results of that run (Configuration No. 1, MBL condition) together with a comparable run with input disturbance, and the average of all runs made with this subject, motion condition, and configuration. The run with no input is representative of this subject's best efforts, to judge by his commentary at the time, "I bet I can hold this thing right on center."

The results are clear — the subject's own remnant (due to scanning, cross talk between lateral and longitudinal stick deflections, etc.) comprises at least half the performance variable magnitude (one quarter of the power) in all three tasks with input disturbance on this, the easiest configuration. Presumably, this ratio worsens for the more difficult configurations and motion conditions, and gives some idea of the difficulty of the task.

TABLE XXIX

EFFECT OF INPUT GUST, CONFIGURATION NO. 1, SUBJECT GB

PERFORMANCE VARIABLE	UNITS	MBL RUN AVERAGE	RUN 166 (INPUT)	RUN 162 (NO INPUT)
σ_q	deg/sec	0.08	0.11	0.04
σ_θ	deg	0.22	0.28	0.15
σ_u	ft/sec	0.52	0.58	0.33
σ_x	ft	2.9	3.1	1.5
σ_φ	deg	0.32	0.58	0.16
σ_y	ft	2.4	2.6	0.91
σ_w	ft/sec	0.44	0.44	0.11
σ_z	ft	2.0	1.9	0.95
σ_{disp}	ft	4.3	4.4	2.0
PR	—	4.9	4.0	3.0

I. COMPARISON WITH PAST DATA — THRESHOLD EFFECTS

Reference 8 gives some performance data obtained in a precision hovering experiment conducted on the Norair simulator in both fixed and moving base conditions. The tasks are dissimilar, having different dynamics and a substantially different display (a contact analog type integrated display), nevertheless, the fixed base-moving base differences in performance observed in those experiments serve as comparable data.

The data comparison is listed in Table XXX, Configuration No. 3 being chosen as the most comparable. In view of the considerable differences in tasks, the major point of comparison is in the change in going from moving-base to fixed-base. With the exception of the

TABLE XXX

STI-UARL DATA COMPARISON

PERFORMANCE VARIABLE	MOTION CONDITION (CHANGE)	UARL DATA*		CONFIG. NO. 3		
		PH 10	PH 12	RG†	EF	GB
σ_q (deg/sec)	MBL	3.56	2.44	0.66	1.08	0.70
	FB	4.05	2.79	1.12	1.15	0.90
	Δ (%)	+13.9	+13.3	+69.5	+6.5	+28.6
σ_θ (deg)	MBL	2.18	1.94	0.61	0.76	0.66
	FB	2.76	2.26	1.35	0.96	0.84
	Δ (%)	+26.6	+16.5	+121.2	+26.3	+27.2
σ_u (ft/sec)	MBL	0.912	0.839	0.68	0.70	0.76
	FB	1.541	1.259	1.19	0.83	0.72
	Δ (%)	+68.8	+50.0	+75.0	+18.6	−5.3
σ_x (ft)	MBL	1.86	1.83	3.1	2.5	3.0
	FB	3.33	3.16	4.1	2.7	2.9
	Δ (%)	77.5	72.9	+32.2	+8.0	−3.4
PR	MBL	5.0	3.0	9.0	6.9	7.0
	FB	8.0	5.0	9.5	7.5	8.0
	Δ	3.0	2.0	0.5	0.6	1.0

*Ref. 8, Configuration PH 10 is listed as having longitudinal and lateral tasks with the following dynamics:

a) Longitudinal

$M_u g = 0.67$, $X_u = -0.1$, $M_q = -1.0$, $\sigma_{u_g} = 5.1$

b) Lateral

$L_v g = -0.1$, $Y_v = -0.1$, $L_p = -3.0$, $\sigma_{v_g} = 1.3$

Configuration PH 12 is the same, with $M_q = -5.0$.

†Only one run in each motion condition.

limited data for RG, the changes in pitch attitude control precision (σ_θ) are comparable, while the position control (σ_χ) and pilot rating data are not. These latter data show the current experiment to be much less sensitive to motion condition, even though the unstable nature of the longitudinal task dynamics would suggest greater sensitivity, all other things being equal.

At least a portion of this difference is attributed to the lower pitch and roll rate magnitudes in the current experiment. The pilot's effective vestibular system threshold in the simulator flying task (a function of the attention demands made upon him, the "masking" effect of extraneous cues such as simulator noise and vibration, as well as his measurable vestibular system threshold) is exceeded a smaller fraction of the time in the current experiment. In effect, the MBL condition in the current experiment is closer to the FB condition as far as vestibular sensing is concerned because of the near-absence of a tilt cue (the simulated vehicle is quite close to being perfectly coordinated) and the angular rates being subthreshold much of the time.

As further evidence of the presence of vestibular (and utricular) threshold effects, Ref. 13 describes an experiment wherein the magnitude of the motion cues entering an angular motion simulator were progressively varied from a no motion condition up to full motion while the visual task is invariant (attitude ball display). The task was two axis (pitch and yaw) attitude control in the presence of random noise of an approximate 1 rad/sec bandwidth introduced at the pilot's control stick input to the controlled element. The controlled element was the simulator dynamics — a second-order system with a well damped ($\zeta \doteq 0.87$) response and a natural frequency in excess of 6 rad/sec.

These data indicate that vestibular and utricular threshold effects begin to be evident for rms pitch motions on the order of 1.5 to 2.0 deg (Ref. 14). For rms pitch motions on the order of one degree, the precision of attitude control (attitude ball motions) has deteriorated by 50 percent. The no motion condition shows a deterioration relative to the full motion (MBA) condition such that σ_θ has more than doubled. One can conclude that

the small magnitude of angular motions in the current experiment is such that threshold effects reduce the beneficial effects of motion in the MBA condition on the order of 50 percent, perhaps more considering the more demanding nature of the task. This reduction carries over to the MBL condition as well.

In passing, it is noted that the effective utricular threshold of 0.01g per Ref. 1 (implies angular tilt in the MBA condition of 0.573 deg) is about half the rms angles experienced for the unstable configurations. Thus utricular threshold effects (assuming utricular cues are used in the MBA condition) are of a smaller magnitude. The simulator angular thresholds are less than this (0.1 deg, roll; 0.25 deg, pitch). In the MBA condition, the utricular cue is therefore reasonably free of threshold phenomena for the more difficult configurations, particularly in roll.

J. IMPLICATIONS OF THE PERFORMANCE DATA

Table XXXI shows the various cues available to the pilot in the three motion conditions investigated in this program. The data presented in this section indicate a strong preference for the angular motion only (MBA) condition over full motion (MBL). This preference is attributed to the absence of auditory cues and simulator vibration in the MBA condition relative to MBL, and/or the presence and pilot's use of the g-vector tilt cue in the MBA condition. The latter point of view is confirmed by pilot commentary taken at face value, while the former is certainly a factor in the easier configurations, which would ordinarily be expected to show little advantage accruing to the presence of motion. The g-vector tilt cue as an indicator of attitude, present only in the MBA condition, is apparently used by the pilot in addition to his attitude display. It can give him an attitude indication when he is looking elsewhere which can be used at least to alert him to a changing situation, and perhaps even to provide some measure of closed-loop control. The apparent g-vector tilt experienced in the MBL condition is related weakly to attitude and strongly to the simulated gust excitation. It can't help him in control of attitude and, because of the restricted visual world inside the simulator cab (in particular, the absence of an approximation to a real world display which would aid his perception of orientation), can presumably lead to vertigo. Consequently, a moving base simulator with angular motion only gives the pilot an additional cue not present in the

TABLE XXXI

SIMULATOR MOTION CONDITIONS AND PILOT SENSORY MODALITIES

SIMULATOR CONDITION / PILOT MODALITY	VISION	AUDITION	VESTIBULAR		OTHER PROPRIOCEPTIVE
			CANALS	UTRICLE	
Fixed Base (FB)	Displays				
Moving Base, Angular Motions Only (MBA)	Displays		Angular velocities near effective threshold level.	1. G-vector tilt. 2. Pilot's head not at center of cab rotation (simulated c.g.)*	G-vector tilt
Moving Base, Angular and Linear Motions (MBL)	Displays	1. Simulator rumble. 2. Amplidyne whine (only in training and early experimental runs where motions are large).	Angular velocities near effective threshold level.	1. G-vector tilt only when linear motion limits exceeded. 2. Pilot's head not at center of cab rotation (simulated c.g.)*	1. G-vector tilt only when linear motion limits exceeded. 2. Simulator vibration in linear degrees of freedom.

*Therefore angular accelerations produce linear accelerations at pilot's head.

real world. If this cue can be used advantageously, as it apparently can in the simulated task where attitude control is of paramount importance and separated instrument displays are employed, then the results obtained will be optimistic relative to full motion simulation.

The experimental program was not successful in establishing the importance of linear acceleration cues in those cases where it was postulated that they could be, that is, on Configurations 8, 9, and 11. In the case of Configuration 8, the demands of the longitudinal and lateral tasks "swamp" any effects (beneficial or otherwise) of motion on the vertical task, at least for the limited data available. For Configurations 9 and 11, the data base is again too small, further, the angular accelerations are very low and the higher frequency (due to pitch attitude changes) perturbations on the altitude display would be ignored in view of the minimal attention paid to this task.

The effects of angular motion lags in the Priority III runs are somewhat less than predicted. The general level of performance would suggest attitude loop crossover frequencies less than predicted (attitude control performance is poorer than predictions on the more difficult configurations, as is position control) implying that the effects of high frequency motion lag are less important.

It is clear that VFR-IFR differences are of paramount importance in this task. The multimodality model used in making the performance predictions was successful in predicting a 5 to 10 percent performance improvement in the MBL condition over fixed base, but the general level of performance was much worse than predictions. This suggests that the loop closing criteria used and/or the pilot scanning model used is faulty — the pilot does not, quantitatively, behave as predicted. The scanning model in particular is at an early stage in its development, being based on a relatively limited number of earlier experiments. The next section examines some of the eye-point-of-regard data in the light of the predicted scanning behavior.

Finally, the relatively small fixed base moving base differences are ascribed to the low levels of angular rate being subthreshold much of the

time. These low rates are made possible by the display scaling used; in turn motivated by the need for hovering position performance within the bounds of the simulator's linear motion capability at the apparent low values of position loop gain adopted by the pilots under IFR conditions with separated displays.

SECTION IV

EYE-POINT-OF-REGARD DATA

The Priority IV runs consisted of 55 runs made in two days under all three motion conditions with all three subjects on Configuration Nos. 1, 3, 4, and 6. Two of these runs were lost due to procedural errors. Of the remaining, 25 runs were made with subject GB, 21 with EF, and 7 with RG. Because of GB's tendency to ignore the altitude control task (on at least one run, no activity was observed on the collective) or to become "annoyed" at the task when it wouldn't respond as he wanted (on several runs, his looks at the altitude display were observed to be bunched at some point in the run, rather than more or less evenly distributed throughout) his EPR data was regarded as the least reliable of the three subjects. Consequently, the EPR data reduction effort was concentrated on the other two subjects, although six of GB's runs on Configuration No. 6 were reduced. Reference 3 describes the data reduction procedure used, and Appendix A describes the scanning behavior measures discussed in this section.

During the course of the experiment, the subjects were observed to spend most of their time glancing back and forth between the attitude and position displays, with considerably fewer looks from attitude to altitude and back again. The number of looks between altitude and position displays was very small, perhaps once or twice in the course of the run. The stress level was such that there were very few blinks — in many cases, none throughout the course of a run. The looks at the altitude display are strongly correlated with the stepwise collective deflection — they would occur almost simultaneously, although there is some evidence for parafoveal viewing of this display in that deflections of the collective occasionally occurred between looks, especially for RG.

The overall impression gained during the experimental runs was one of tightly constrained, almost patterned scanning behavior with the altitude control task receiving the least attention and the attitude display the most.

Rigorous tests of statistical significance in scanning behavior across motion conditions are difficult to apply because of the limited number of data points for comparison, or because of the generally non-normal probability density functions (e.g., for dwell times on a particular instrument in a given run). The t test for significant differences in the sample means was applied (nonrigorously) to $\overline{T}_d$ across the spectrum of configurations, subjects and motion conditions with ambiguous results. The ambiguity results from the run-to-run changes in scanning behavior not ascribable to these differences — several instances were found where two runs for identical conditions (except time of day) showed highly significant differences in the mean attitude display dwell time, for example. In this section, the scanning data is presented in the form of averages across configurations and motion conditions as being indicative of the trends in the scanning behavior with these two variables.

A. SUBJECT DIFFERENCES IN SCANNING BEHAVIOR

The averaged scanning statistics (see symbology and Appendix A for definitions) for the runs analyzed are listed for each subject in Table XXXII. These data are compiled from the individual run statistics listed in Appendix B. The major differences among subjects are most apparent in the attention paid to the fixed (across the spectrum of configurations tested) altitude control task. The look fraction, ν_1, and the dwell fraction, η_1, are proportional to one another because the mean dwell times for the three subjects are approximately equal. Either is inversely related to altitude performance; across the three subjects, the better performance (lower value of σ_z) is associated with the larger dwell fraction, as one would expect.

Other strong differences between subjects show up in the overall scanning frequency, f_s, the attitude display scanning frequency, $\overline{f}_{s2}$, and the (inversely related to these frequencies) mean attitude display dwell times, $\overline{T}_{d_2}$. The attitude display look fraction, ν_2, is close to the maximum allowable value for any one display for two of the subjects and slightly lower (implying more looks between altitude and position displays) for RG.

TABLE XXXII

SUBJECT DIFFERENCES IN SCANNING BEHAVIOR

DISPLAY	SYMBOL	UNITS	RG (N = 7)	EF (N = 21)	GB (N = 5)†
All	f_s	sec^{-1}	1.550	1.810*	1.353
Attitude (θ, φ)	$\overline{T}_{d_2}$	sec	0.78	0.64	0.93
	$\sigma_{T_{d_2}}$	sec	0.37	0.23	0.49
	η_2	—	0.550	0.567	0.619
	ν_2	—	0.460	0.495	0.497
	$\overline{f}_{s_2}$	sec^{-1}	0.713	0.896*	0.673
Position (x, y)	$\overline{T}_{d_4}$	sec	0.60	0.51	0.59
	$\sigma_{T_{d_4}}$	sec	0.10	0.10	0.15
	η_4	—	0.330	0.378	0.347
	ν_4	—	0.355	0.413	0.436
	$\overline{f}_{s_4}$	sec^{-1}	0.550	0.747*	0.591
Altitude (z)	$\overline{T}_{d_1}$	sec	0.42	0.34	0.38
	$\sigma_{T_{d_1}}$	sec	0.09	0.07	0.12
	η_1	—	0.115	0.052	0.033
	ν_1	—	0.173	0.086	0.065
	$\overline{f}_{s_1}$	sec^{-1}	0.296	0.156*	0.088

*Scanning frequency showed steady increase with time over the course of the Priority 4 experiment.

†Represents 5 runs out of the 6 analyzed, all on Configuration No. 6. The sixth run showed a sharp increase in the altitude task dwell and look fractions, with a corresponding decrease in the position display dwell and look fractions, hence was judged atypical and discarded in the averages. A comparison based only on Configuration 6 results for all subjects shows the same trends illustrated here; see Tables XXXIII and XXXIV.

The high overall scanning frequency, f_s, is felt to be indicative of the subject's efforts to improve error coherence in the simulated task. The trend in this parameter with time shown by EF (see Fig. 16) may be an additional indication of these efforts. All the subjects commented on the need for a rapid scan of the panel to control the simulated VTOL. The scanning frequency observed in normal instrument flying is generally somewhat less than that shown here. Reference 3, which gives scanning statistics during simulated instrument approaches (without flight director), measured an overall scanning frequency of about 1.1 looks per second as compared with the averaged scanning frequencies measured here.

The importance of the attitude control task is indicated by the large dwell and look fractions, and the high scanning frequency associated with this task common to all subjects as well as preexperimental predictions. However, the differences between the various subjects suggest that a relatively wide range of scanning behavior can be adopted while still successfully controlling the simulated VTOL. To judge by the performance obtained that scanning behavior adopted by RG is probably closest to optimum.

B. CONFIGURATION DIFFERENCES IN SCANNING BEHAVIOR

The next most significant factor affecting the scanning behavior is the difference between one configuration and the next. Tables XXXIII and XXXIV list the averaged scanning statistics for RG and EF for the four configurations of simulated VTOL dynamics tested.

For subject RG, it is clear that Configuration No. 6 is more difficult than Configuration No. 1 because of the greater dwell fraction, average dwell time, look fraction and look rate on the attitude display for No. 6. There is a corresponding reduction in these variables for both the position and altitude displays when going from Configuration 1 to 6. The pattern is apparently one of devoting increased attention to attitude control as the configuration becomes more difficult, thus sacrificing precision in hovering position.

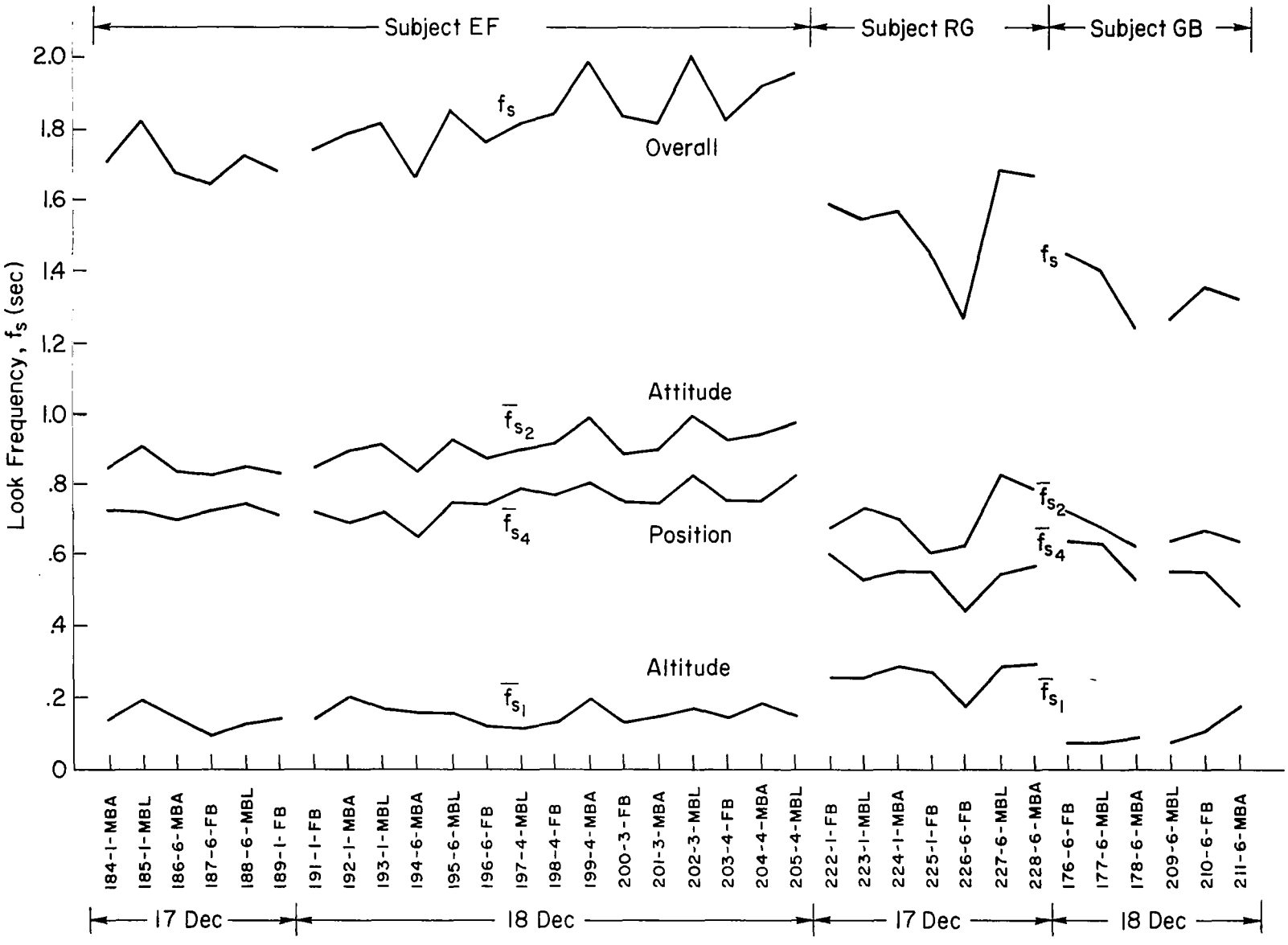

Figure 16. Run-to-Run History of Average Look Frequencies

TABLE XXXIII

CONFIGURATION DIFFERENCES IN SCANNING BEHAVIOR (RG)

DISPLAY	SYMBOL	UNITS	CONFIGURATION	
			1 (N = 4)	6 (N = 3)
All	f_s	sec^{-1}	1.550	1.551
Attitude (θ, φ)	$\overline{T}_{d_2}$	sec	0.74	0.84
	$\sigma_{T_{d_2}}$	sec	0.31	0.45
	η_2	—	0.506	0.610
	ν_2	—	0.443	0.483
	$\overline{f}_{s_2}$	sec^{-1}	0.686	0.749
Position (x, y)	$\overline{T}_{d_4}$	sec	0.64	0.55
	$\sigma_{T_{d_4}}$	sec	0.10	0.09
	η_4	—	0.362	0.288
	ν_4	—	0.366	0.341
	$\overline{f}_{s_4}$	sec^{-1}	0.567	0.528
Altitude (z)	$\overline{T}_{d_1}$	sec	0.46	0.38
	$\sigma_{T_{d_1}}$	sec	0.09	0.08
	η_1	—	0.128	0.098
	ν_1	—	0.179	0.163
	$\overline{f}_{s_1}$	sec^{-1}	0.277	0.257

TABLE XXXIV

CONFIGURATION DIFFERENCES IN SCANNING BEHAVIOR (EF)

DISPLAY	SYMBOL	UNITS	CONFIGURATION			
			1 (N = 6)	3 (N = 3)	4 (N = 6)	6 (N = 6)
All	f_s	sec^{-1}	1.764	1.896*	1.899*	1.727
Attitude (θ, φ)	$\bar{T}_{d_2}$	sec	0.60	0.61*	0.58*	0.74
	$\sigma_{T_{d_2}}$	sec	0.18	0.23	0.19	0.33
	η_2	—	0.521	0.562	0.545	0.636
	ν_2	—	0.494	0.489	0.496	0.497
	$\bar{f}_{s_2}$	sec^{-1}	0.871	0.927*	0.941*	0.859
Position (x, y)	$\bar{T}_{d_4}$	sec	0.58	0.48*	0.51*	0.45
	$\sigma_{T_{d_4}}$	sec	0.12	0.11	0.10	0.08
	η_4	—	0.413	0.377	0.401	0.321
	ν_4	—	0.406	0.410	0.415	0.419
	$\bar{f}_{s_4}$	sec^{-1}	0.716	0.777*	0.787*	0.723
Altitude (z)	$\bar{T}_{d_1}$	sec	0.38	0.33	0.32	0.30
	$\sigma_{T_{d_1}}$	sec	0.11	0.06	0.06	0.04
	η_1	—	0.064	0.056	0.051	0.042
	ν_1	—	0.096	0.084	0.084	0.080
	$\bar{f}_{s_1}$	sec^{-1}	0.170	0.159	0.160	0.139

*Gradual increase in scanning frequency over time shows up here. Last 9 runs were Configurations 3 and 4.

Subject EF shows the same trend in these variables when going from Configuration 1 to 6. The comparison is not so readily made for the intermediate configurations because these runs were the last 9 runs for this subject where the overall scanning frequency, as well as attitude and position display scanning frequencies, were highest. This higher scan rate implies shorter mean dwell times than would otherwise be the case. But the attitude display dwell fraction, η_2, clearly indicates their relative difficulty — Configuration No. 1 is easiest, followed by 4, 3, and 6. The incremental difficulty between Configurations 3 and 4 is quite small. The opposite trend is exhibited in the position display dwell fraction. The altitude display statistics (chiefly η_1) would indicate that the altitude control task on Configuration No. 3 is more difficult than No. 4. However the difference is small, and the number of looks (at this display in a given run) is limited, suggesting that this difference is probably insignificant. If it is significant, it might be related to the vertical acceleration cues caused by the subject being a small distance ahead of the simulator pitch axis — unstable longitudinal task dynamics in the case of Configuration No. 3 result in a slightly higher level of vertical acceleration at the pilot's station. This in turn may cause him to look at the altitude display a slightly greater fraction of the time.

C. MOTION DIFFERENCES IN SCANNING BEHAVIOR

The third most significant variable affecting the scanning statistics is the motion condition. The preexperimental scanning traffic predictions concentrated on these differences (Appendix A) to the exclusion of differences in configuration, and correctly predict the trend in overall scanning frequency, and attitude display average dwell time. Tables XXXV, XXXVI, and XXXVII list the averaged scanning statistics across configurations for each subject and motion condition.

Subject EF shows the lowest scan frequency and longest attitude display mean dwell time for the fixed base condition while the MBL condition shows the highest scan frequency and shortest attitude display mean dwell time. The attitude display dwell fraction is lowest for the MBL condition;

TABLE XXXV

MOTION DIFFERENCES IN SCANNING BEHAVIOR (EF)

DISPLAY	SYMBOL	UNITS	MOTION CONDITION		
			FB (N = 7)	MBA (N = 7)	MBL (N = 7)
All	f_s	sec^{-1}	1.768	1.802	1.864
Attitude (θ, φ)	$\bar{T}_{d_2}$	sec	0.68	0.63	0.60
	$\sigma_{T_{d_2}}$	sec	0.26	0.23	0.20
	η_2	—	0.592	0.559	0.549
	ν_2	—	0.494	0.495	0.495
	$\bar{f}_{s_2}$	sec^{-1}	0.872	0.893	0.922
Position (x, y)	$\bar{T}_{d_4}$	sec	0.48	0.52	0.51
	$\sigma_{T_{d_4}}$	sec	0.10	0.10	0.10
	η_4	—	0.355	0.383	0.396
	ν_4	—	0.421	0.404	0.413
	$\bar{f}_{s_4}$	sec^{-1}	0.743	0.728	0.770
Altitude (z)	$\bar{T}_{d_1}$	sec	0.35	0.33	0.32
	$\sigma_{T_{d_1}}$	sec	0.09	0.06	0.06
	η_1	—	0.048	0.057	0.053
	ν_1	—	0.076	0.096	0.087
	$\bar{f}_{s_1}$	sec^{-1}	0.135	0.173	0.162

TABLE XXXVI

MOTION DIFFERENCES IN SCANNING BEHAVIOR (RG)

DISPLAY	SYMBOL	UNITS	MOTION CONDITION		
			FB (N = 3)	MBA (N = 2)	MBL (N = 2)
All	f_s	sec^{-1}	1.446	1.631	1.626
Attitude (θ, φ)	$\overline{T}_{d_2}$	sec	0.88	0.70	0.72
	$\sigma_{T_{d_2}}$	sec	0.46	0.31	0.30
	η_2	—	0.559	0.524	0.564
	ν_2	—	0.445	0.460	0.483
	$\overline{f}_{s_2}$	sec^{-1}	0.640	0.750	0.786
Position (x, y)	$\overline{T}_{d_4}$	sec	0.61	0.61	0.58
	$\sigma_{T_{d_4}}$	sec	0.10	0.09	0.10
	η_4	—	0.333	0.344	0.312
	ν_4	—	0.372	0.350	0.336
	$\overline{f}_{s_4}$	sec^{-1}	0.540	0.570	0.595
Altitude (z)	$\overline{T}_{d_1}$	sec	0.41	0.44	0.43
	$\sigma_{T_{d_1}}$	sec	0.09	0.08	0.10
	η_1	—	0.102	0.129	0.121
	ν_1	—	0.167	0.182	0.163
	$\overline{f}_{s_1}$	sec^{-1}	0.243	0.295	0.280

TABLE XXXVII

MOTION DIFFERENCES IN SCANNING BEHAVIOR (GB)

DISPLAY	SYMBOL	UNITS	MOTION CONDITION		
			FB (N = 2)	MBA (N = 1)*	MBL (N = 2)
All	f_s	sec^{-1}	1.412	1.254	1.345
Attitude (θ, φ)	$\bar{T}_{d_2}$	sec	0.90	0.96	0.94
	$\sigma_{T_{d_2}}$	sec	0.43	0.61	0.49
	η_2	—	0.627	0.600	0.621
	ν_2	—	0.498	0.500	0.495
	$\bar{f}_{s_2}$	sec^{-1}	0.704	0.627	0.665
Position (x, y)	$\bar{T}_{d_4}$	sec	0.55	0.68	0.59
	$\sigma_{T_{d_4}}$	sec	0.13	0.23	0.14
	η_4	—	0.337	0.364	0.350
	ν_4	—	0.431	0.429	0.446
	$\bar{f}_{s_4}$	sec^{-1}	0.609	0.537	0.601
Altitude (z)	$\bar{T}_{d_1}$	sec	0.37	0.41	0.37
	$\sigma_{T_{d_1}}$	sec	0.11	0.15	0.11
	η_1	—	0.036	0.036	0.029
	ν_1	—	0.068	0.071	0.060
	$\bar{f}_{s_1}$	sec^{-1}	0.095	0.090	0.080

*The second run for this condition showed the sharp increase in altitude display dwell and look fraction, and was therefore excluded.

highest for FB, while the look fraction is essentially fixed at close to its maximum attainable value across the spectrum of motion conditions. The position display statistics generally show the opposite trend between fixed and moving base, only here the MBA condition shows the smallest look rate by a small amount. The altitude display scanning statistics would indicate the greatest dwell fraction, look fraction, and look frequency for the MBA condition, apparently indicative of the increased time available for attention to this task, or perhaps the absence of vertical acceleration cues requiring closer visual attention. The advantage of the MBA condition over MBL does not show up clearly in the data for this subject. Both attitude and altitude receive more attention MBA than MBL, while position receives less. Yet all measured performance variables except pitch rate (and probably roll rate as well, although not measured) show MBA to be better than MBL for EF.

For subject RG, where there are fewer data points (only 2 runs), similar results are shown for fixed base versus moving base; however the MBA condition has the lowest attitude display dwell fraction and average dwell time — more in accord with what might be expected based upon his performance and commentary. The MBA condition shows the highest dwell fraction on both position and altitude, indicative of the greater efforts possible in this motion condition for minimizing hovering position error.

Figure 17 graphically shows the link vectors and dwell fractions for the last three Priority IV runs for subject RG. The width of the arrow between two instruments represents the value of the link vector, i.e., the percentage of all transitions (including blinks) between pairs of displays. The area of the shaded portion of the circles represents the dwell fraction, η, pertinent to the particular instrument. There are relatively few transitions between instrument No. 1 (attitude) and No. 4 (altitude), implying that the look fraction for the attitude display is close to 0.5. Between 55 and 70 percent of the time is spent on attitude for these runs; fixed base shows the most and moving base, angular motion only shows the least.

Other differences in motion conditions for these same three runs are shown in Figs. 18, 19, and 20 illustrating histograms for the dwell times

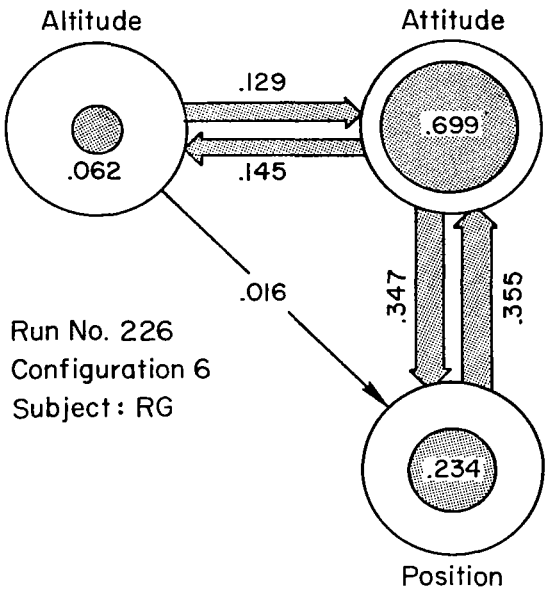

a) Fixed Base

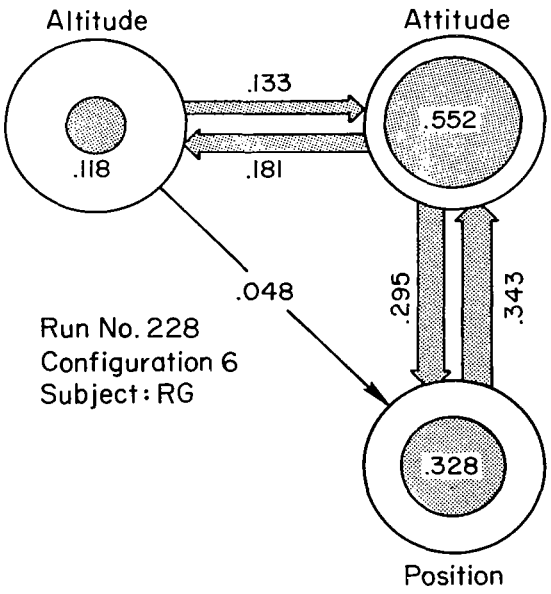

b) Moving Base, Angular Motion

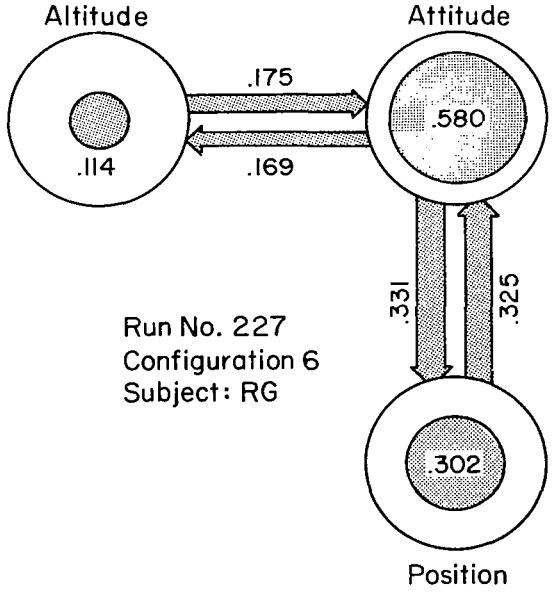

c) Moving Base, Linear and Angular

Figure 17. Transition Link Vectors and Dwell Fractions

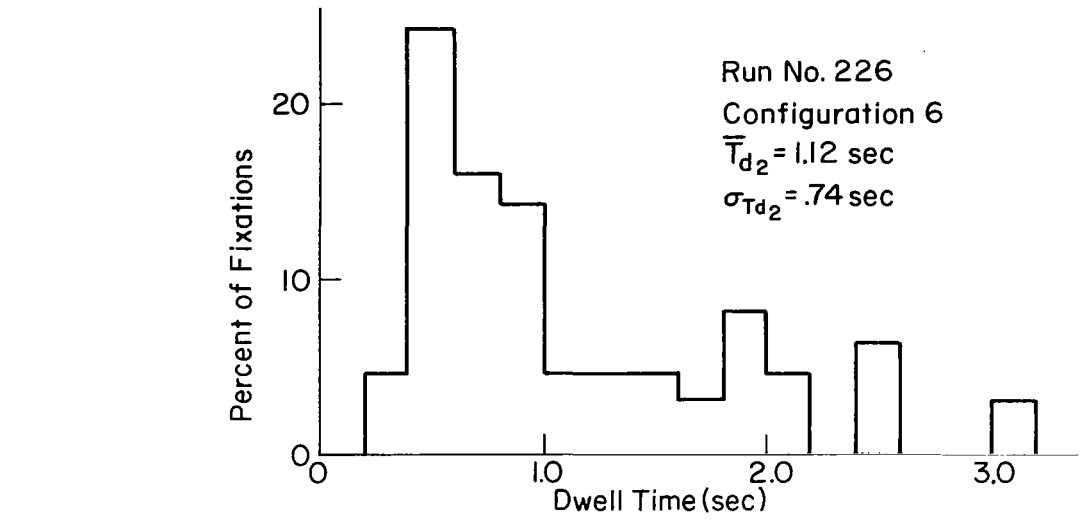

a) Fixed Base

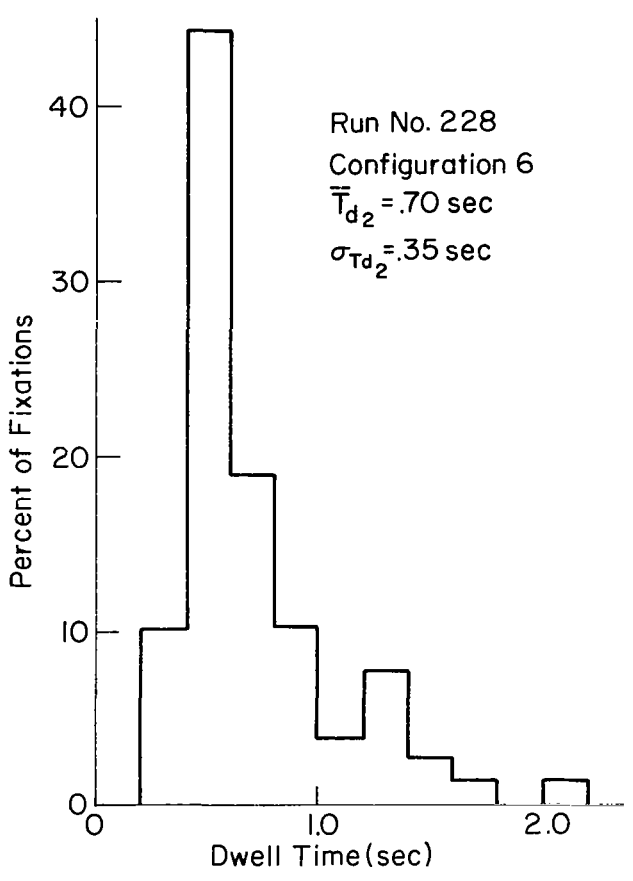

b) Moving Base, Angular Motion Only

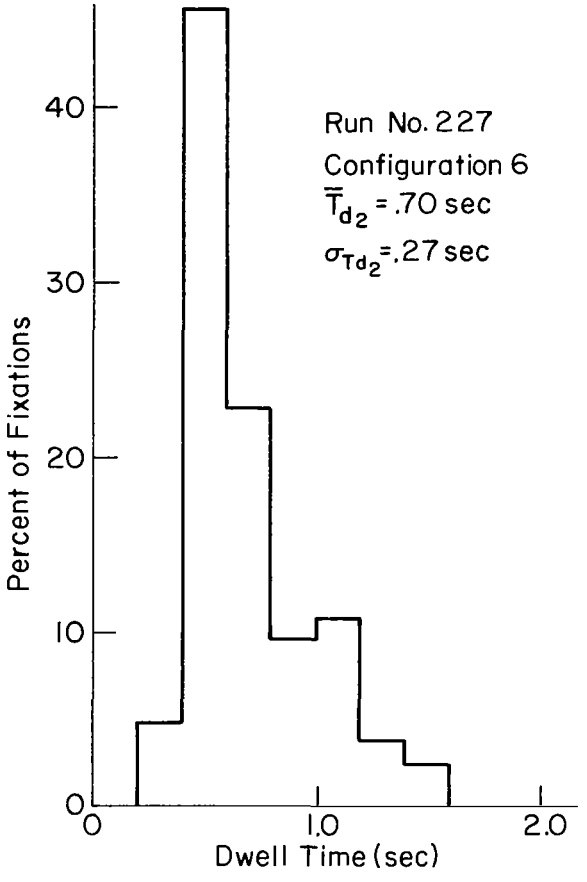

c) Moving Base, Angular and Linear Motion

Figure 18. Attitude Display Dwell Time Histogram

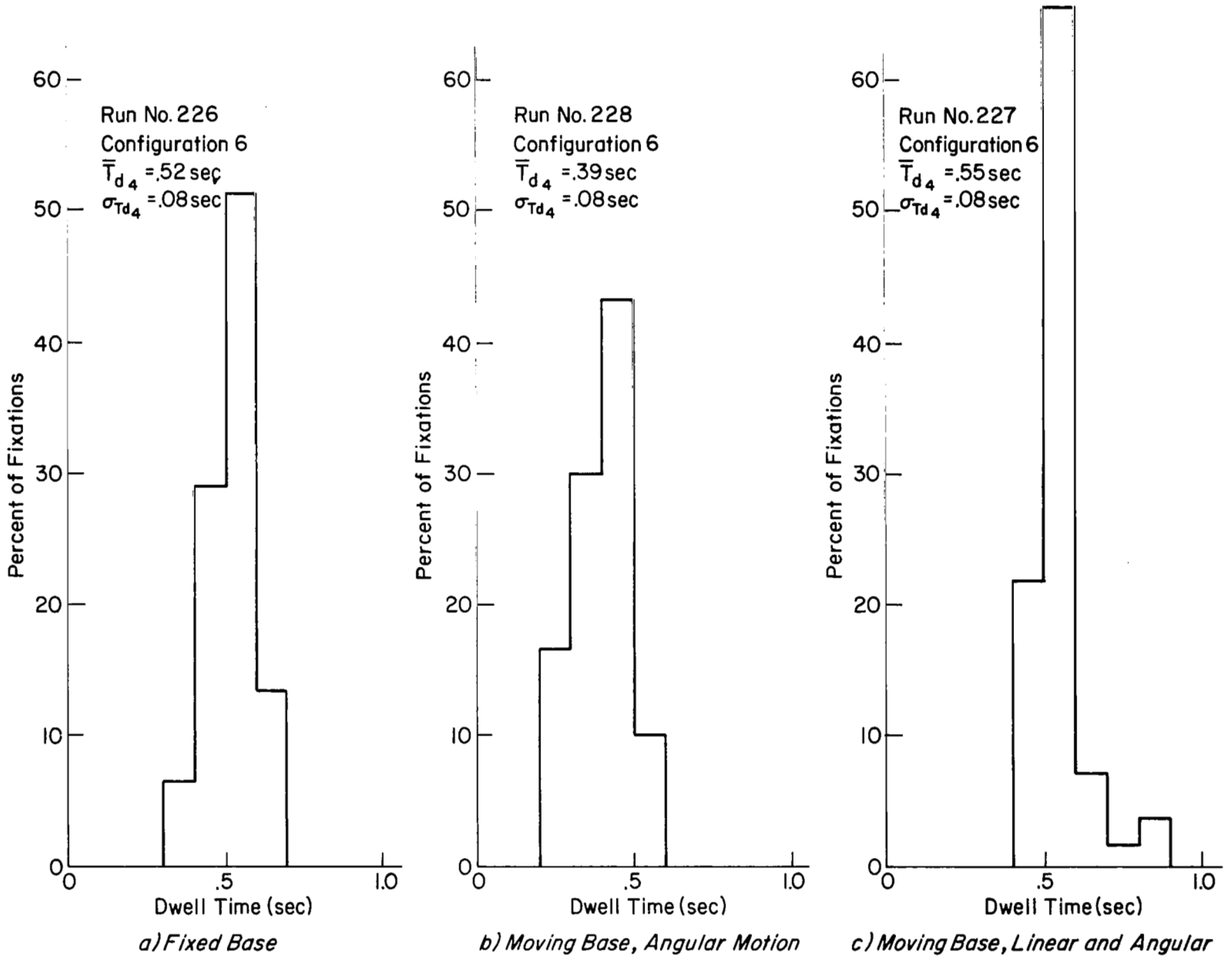

Figure 19. Position Display Dwell Time Histograms

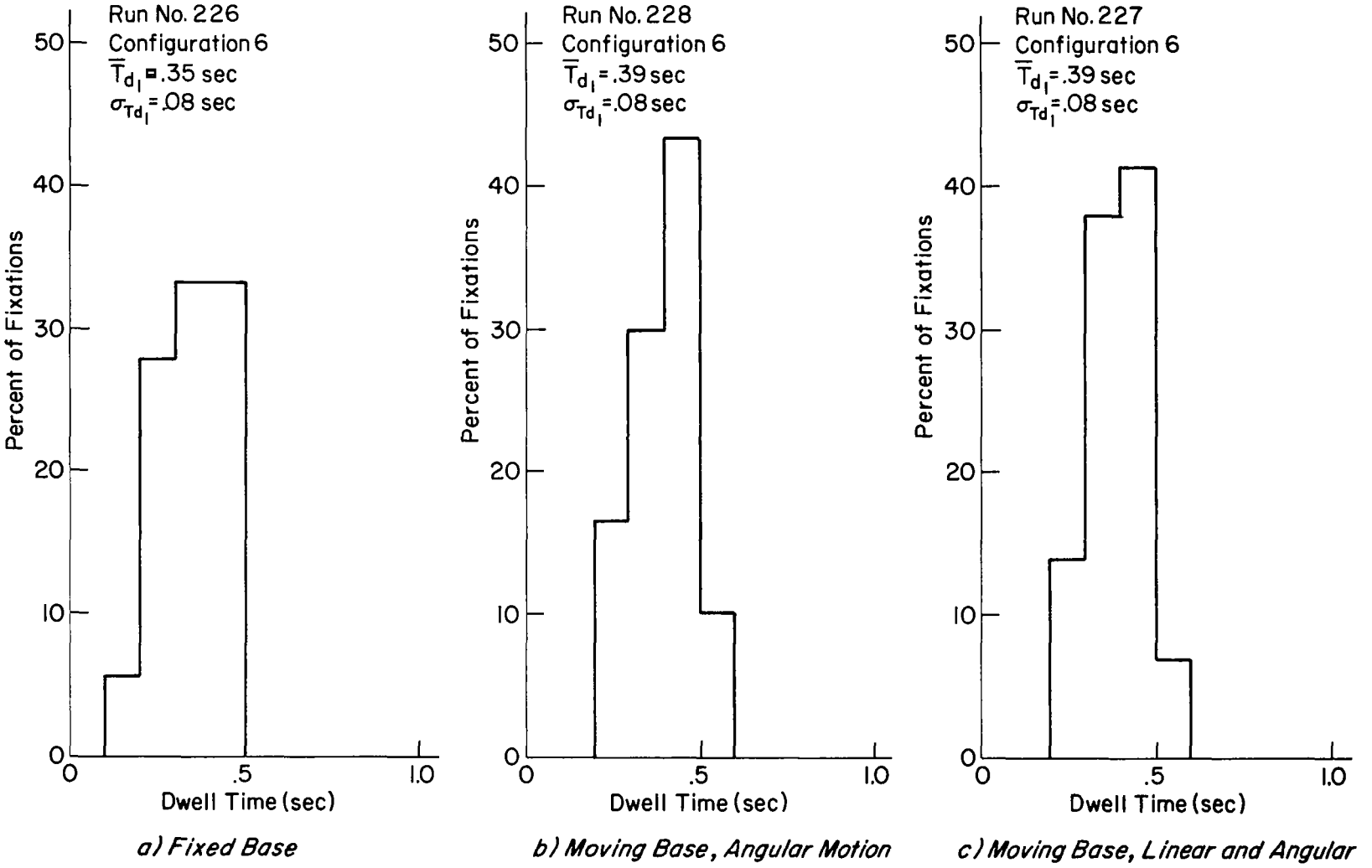

Figure 20. Altitude Display Dwell Time Histograms

on each of the three displays. The attitude display, fixed base, shows the widest variation in dwell time while the other two motion conditions show a somewhat narrower distribution. Both altitude and position displays show relatively narrow distributions for dwell time for all three motion conditions. The altitude display dwells in particular are very short, especially fixed base. Dwells this short are typical of monitoring, as opposed to control tasks (Refs. 2 and 4) and for this configuration, are indicative of the subject's reluctance to spend much time away from the attitude display.

Histograms for the sample intervals for these same three runs are shown in Figs. 21, 22, and 23. The regularity of the sample interval (i.e., the time interval between successive initial fixations of the same display) is related to the remnant introduced by display scanning, per current theories on scanning behavior, c.f. Ref. 2 and Appendix A. Briefly speaking, the sampling remnant is related to the probability density function for the sampling interval, T_s. Past experiments have shown that the measured probability distributions for T_s can be closely approximated by one of the Pearson Type III modified gamma functions. This probability density function is describable in terms of a variable skewness factor, n, and by a sampling variability parameter, δ, given by:

$$\delta = \frac{T_o}{\overline{T}_s} \tag{6}$$

where T_o is the minimum sampling interval, and $\overline{T}_s$ the mean sampling interval.

The remnant introduced by the scanning (which leads, by definition, to output power which is uncorrelated with the input) is related to the amplitude of display motions according to:

$$\frac{\sigma_{n_D}}{\sigma_D} = \sqrt{\frac{(1-\eta_e)(1-\delta)}{\eta_e}} \tag{7}$$

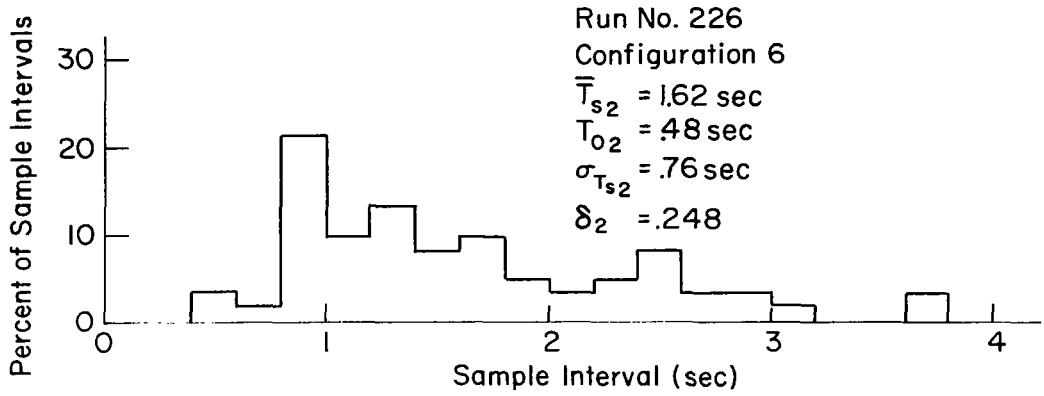

a) Fixed Base

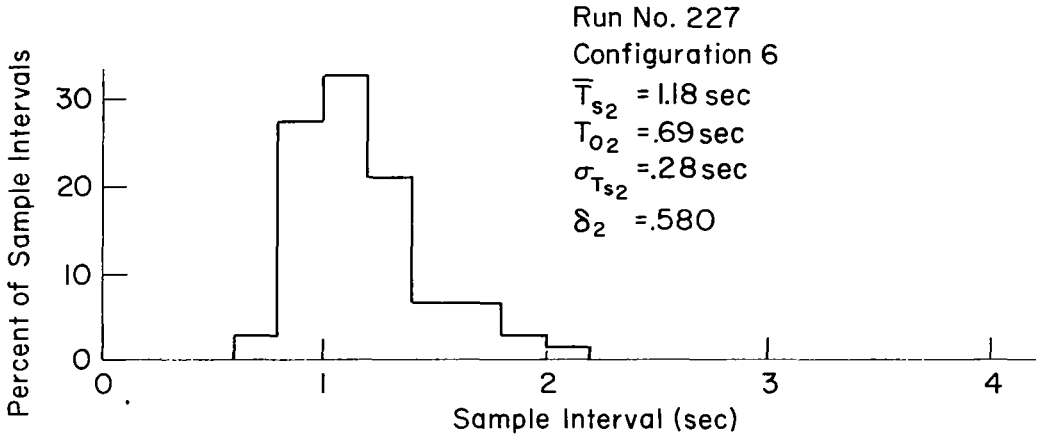

b) Moving Base, Linear and Angular Motion

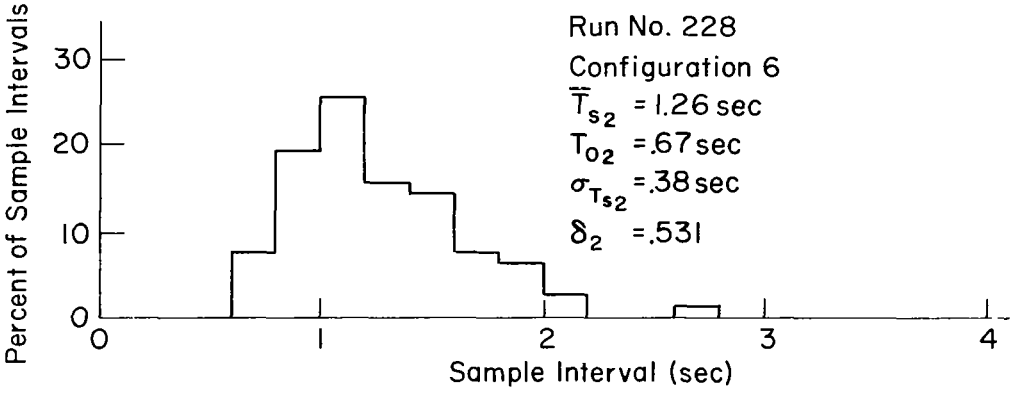

c) Moving Base, Angular Motion

Figure 21. Attitude Display Sample Interval Histograms

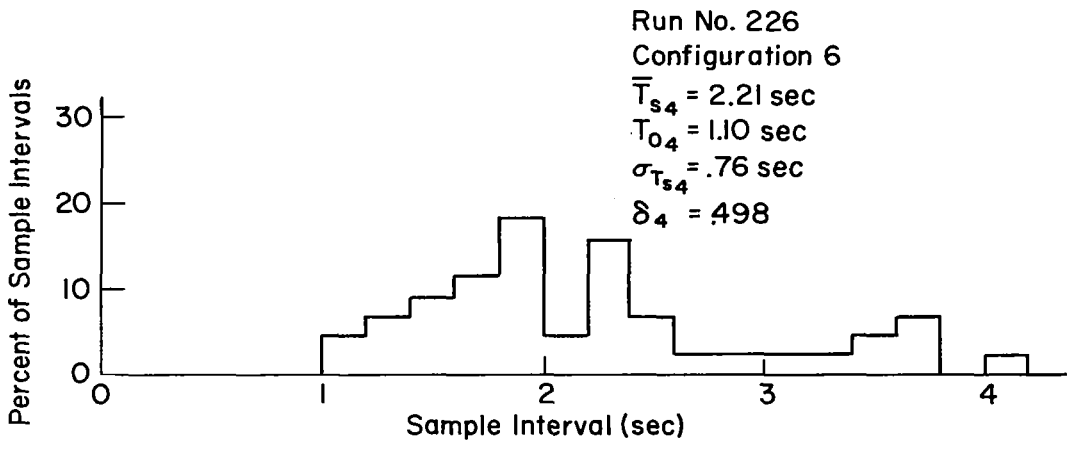

a) Fixed Base

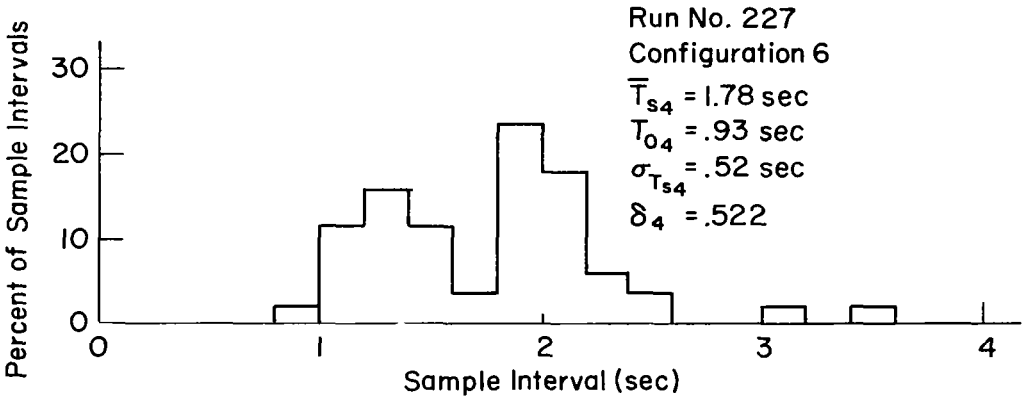

b) Moving Base, Linear and Angular Motion

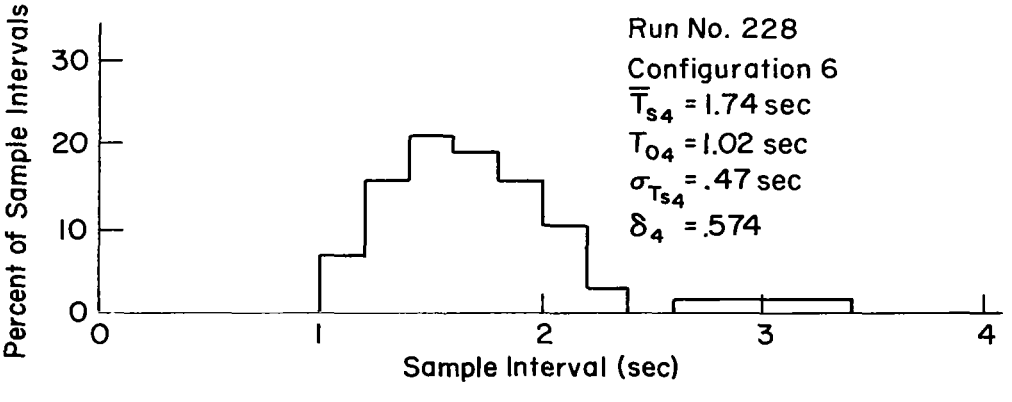

c) Moving Base, Angular Motion

Figure 22. Position Display Sample Interval Histograms

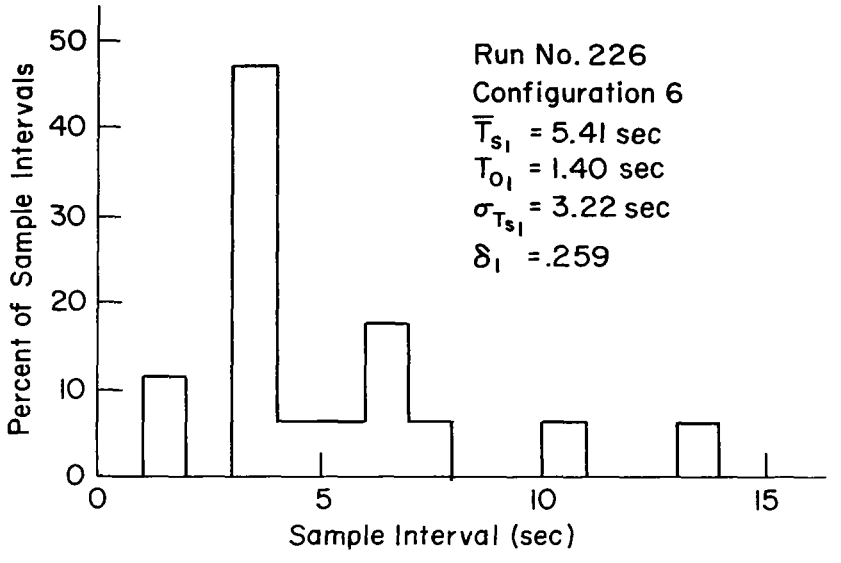

a) Fixed Base

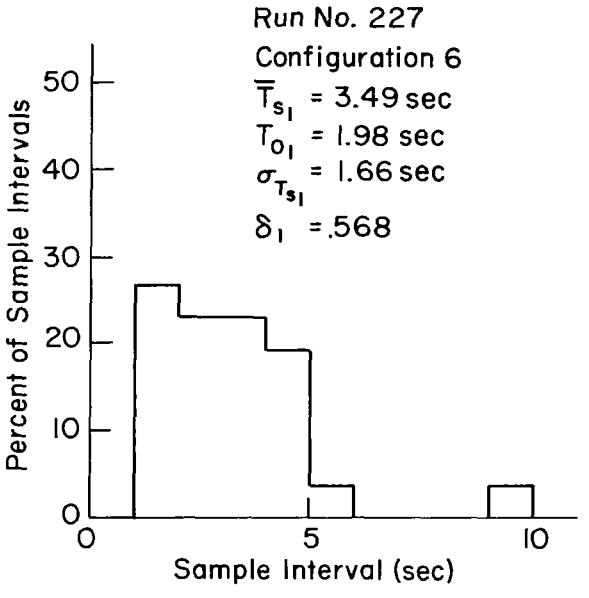

b) Moving Base, Linear and Angular

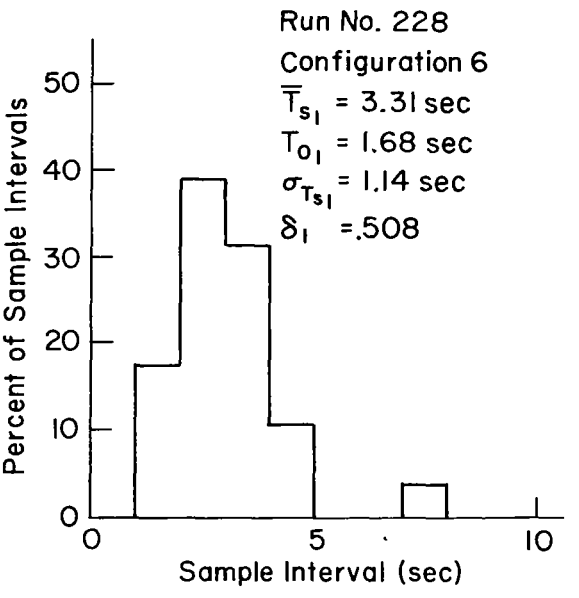

c) Moving Base, Angular Motion

Figure 23. Attitude Display Sample Interval Histograms

where η_e is the effective dwell fraction (see Appendix A), σ_{n_D} is the rms noise level (remnant) introduced by the subject, and σ_D is the rms level of the display motion. Thus as δ, the sampling variability parameter, approaches unity, meaning that the display sampling behavior becomes more regular (i.e., approaches periodic sampling), the uncorrelated (with the display motion) noise introduced by the subject due to scanning (residual remnant is not included), decreases. In other words, the coherence between input disturbance and output response increases as δ increases with increasing regularity of sample interval.

The data given in Figs. 21, 22, and 23 therefore indicate relatively low coherence on attitude and altitude control tasks for the fixed base case while the position display shows a relatively high coherence for all motion conditions, highest for the MBA condition. However, this level is low relative to the value of $\delta = 0.7$ used in the preexperimental predictions for all displays and motion conditions. This is, in part, indicative of the poorer performance exhibited by the subjects relative to the predictions.

These figures also permit some qualitative judgments concerning the "fit" of the histograms to the Pearson Type III distribution. The attitude display sample interval histograms (Fig. 21) have the expected appearance, but the position and altitude displays (Figs. 22 and 23) have varying degrees of distortion, qualitatively speaking. In particular Fig. 22b shows a tendency to be bimodal. This may be suggestive of the constraining nature of the task. Certain past experiments (Ref. 2) have shown significant departures from the expected sample interval distributions when another task forces a particular scanning technique (e.g., a maximum allowable time away from a given display). It is felt that this more detailed examination of RG's scanning for three of his Priority IV runs indicates, at least qualitatively, that his scanning behavior is compatible with existing theories of display scanning, sampling, and reconstruction.

For subject GB on Configuration 6, the trend in scanning behavior for motion versus no motion shows the highest scanning frequency and lowest attitude display dwell times for the fixed base condition—

a trend diametrically opposed to preexperimental predictions and the behavior of the other two subjects. For GB the MBA condition shows the lowest frequency of scan and the longest average dwell times on all three displays. However, the attitude display dwell fraction would indicate that attitude control is easiest, MBA, and most difficult, FB. This scanning behavior "correlates" with this subject's performance in that both are atypical relative to the trends exhibited by the other subjects. His scanning as well as his performance indicates that he relaxes when he can — there is no other account for his opinion that the MBA condition is easiest to fly.

D. IMPLICATIONS OF THE SCANNING DATA

In view of the range of scanning behavior exhibited, both among subjects and for the same subject, configuration and motion condition but different runs, it is clear that a wide range of scanning behavior is possible while still controlling successfully, and/or that a stable performance level was not achieved in the Priority IV runs. In particular, the trend in scanning frequency with time shown by EF suggests that an optimum is still being sought. The data would also suggest that a relatively high look rate, f_s, is required for these simulated dynamics but that the tradeoff between a high attitude display look frequency, $\overline{f}_{s_2}$, and a long attitude display mean dwell time, $\overline{T}_{d_2}$, is not clear cut from a subjective standpoint. One subject, EF, opted for a generally high look rate and short mean dwell, particularly on attitude, while another (GB) went to the opposite extreme.

The scanning data also suggest that attitude control requirements largely constrain the adopted behavior. The subjects cannot stay away from the attitude display for long ($\overline{T}_{s_2}$ is relatively short) and the visual lead generating requirements are such that the dwells must be of relatively long duration. These two factors constrain the position display scanning to relatively short dwells at frequent intervals so as to obtain the dwell fraction necessary for outer loop control. This in turn suggests that visual lead generating capabilities for the outer loops of the longitudinal and lateral control tasks are relatively

limited. The altitude task is monitored only often enough to maintain the altitude error at a level compatible with errors in the lateral and longitudinal position. η_1 is therefore small and $\overline{T}_{d_1}$ is short (because $\overline{T}_{d_2}$ is long and $\overline{T}_{s_2}$ short). The overall task difficulty is largely a function of attitude stabilization requirements — η_2 increases as the configuration (or motion condition) increases in difficulty.

These data also confirm the performance and pilot rating data in that the fixed-base condition renders attitude control more difficult (higher η_2 is required) relative to moving base. However, the preference for the MBA condition (as opposed to MBL) is not clearly indicated. In some cases the MBL condition has the longer dwells on attitude, in others, the MBA condition has the longer dwells. The data base is insufficient to establish a clear-cut trend in scanning behavior one way or the other.

Pilot performance, commentary, and rating data all suggest the MBA condition to be superior to MBL because of the better attitude cue and the reduced tendency to vertigo or "confusion". These reasons both suggest a reduced level of visual attention to be possible in the MBA condition — less visual gain is required and he needn't check attitude as much. On the other hand, the visual lead requirements might go up in the MBA condition because of the higher crossover frequencies made possible by the increased attitude gain, and/or because of the relatively poor fidelity of the angular rate cues (low angular motion amplitudes). This could imply longer dwell times for the MBA condition as opposed to MBL.

The scanning data presented in this section also suggest certain revisions to the criteria upon which the preexperimental predictions of scanning behavior were based — these predictions (Appendix A) missed the mark in that the predicted look frequencies were low and the dwell times on altitude and position were for too long, while the predicted dwell fraction on the position display was too small. A comparison of these predictions, the experimentally observed behavior, and the results of a revised series of calculations are presented in Table XXXVIII. While these calculations are in the nature of second guesses to fit

TABLE XXXVIII

EPR DATA COMPARISON

DISPLAY	SYMBOL	UNITS	ORIGINAL CALCULATION*		SUBJECT			CURRENT CALCULATION
			FB	MB	RG (N = 7)†	EF (N = 21)‡	GB (N = 5)§	
All	f_s	sec^{-1}	1.082	1.309	1.550	1.810	1.353	1.590
Attitude (θ, φ)	$\overline{T}_{d_2}$	sec	1.15	0.771	0.78	0.64	0.93	0.735
	$\sigma_{T_{d_2}}$	sec	—	—	0.37	0.23	0.49	—
	η_2	—	0.525	0.525	0.550	0.567	0.619	0.584
	ν_2	—	0.420	0.519	0.460	0.495	0.497	0.500
	$\overline{f}_{s_2}$	sec^{-1}	0.455	0.682	0.713	0.896	0.673	0.796
Position (x, y)	$\overline{T}_{d_4}$	sec	1.07	1.07	0.60	0.51	0.59	0.555
	$\sigma_{T_{d_4}}$	sec	—	—	0.10	0.10	0.15	—
	η_4	—	0.254	0.254	0.330	0.378	0.347	0.351
	ν_4	—	0.218	0.181	0.355	0.413	0.436	0.398
	$\overline{f}_{s_4}$	sec^{-1}	0.237	0.237	0.550	0.747	0.591	0.633
Altitude (z)	$\overline{T}_{d_1}$	sec	0.695	0.695	0.42	0.34	0.38	0.400
	$\sigma_{T_{d_1}}$	sec	—	—	0.09	0.07	0.12	—
	η_1	—	0.150	0.150	0.115	0.052	0.033	0.065
	ν_1	—	0.198	0.165	0.173	0.086	0.065	0.102
	$\overline{f}_{s_1}$	sec^{-1}	0.216	0.216	0.296	0.156	0.088	0.163

*Included a directional task.
†Four runs on Configuration 1, three on Configuration 6.
‡Configurations 1, 3, 4, and 6.
§Configuration 6.

the data, the assumptions by which they were arrived at are worth noting. These are listed in Table XXXIX. The major points to be noted are the adjustments in the direction of improved coherency within the limitations imposed by the separated instrument display scanning and the overriding (and constraining) demands of the attitude control task.

TABLE XXXIX

BASIS FOR REVISED SCANNING CALCULATIONS

PARAMETER	BASIS OR JUSTIFICATION
a. $\eta_{e_2} = 0.75$	The effective attitude display dwell fraction is based on a foveal crossover frequency of 2.0 rad/sec for a similar task, VFR, per Ref. 7 (which shows that the pilot adopts attitude lead sufficient to cancel the short-period root at $1/T_{sp}$) and an average crossover frequency, ω_{ca_2}, of 1.5 rad/sec to achieve maximum phase margin — pertinent to this situation of low coherency (high scanning remnant). (Eq. A-25)
b. $\Omega_2 = 0.4$	The pilot is assumed to be unable to achieve a higher parafoveal gain because of the relatively wide display separation. Past studies (Refs. 2 and 18) suggest that $0 \leq \Omega \leq 0.5$ be the criterion.
c. $\nu_2 = 0.5$	The look fraction is taken to be its maximum allowable value for the attitude display — the pilot must return to this display every other look (or closely approach this condition) to retain control.
d. $S_2 = 8.0$	The sampling parameter for the attitude display is taken to be at the high end of the criterion range, $4 \leq S \leq 8$ because of efforts to improve coherency. Past data (Ref. 2) indicates that S increases in stressful or demanding tasks. S_2, η_2, ν_2, and the crossover frequency define the attitude display sample interval, $\overline{T}_{s_2} = 1.257$ sec, the mean dwell time on attitude, $\overline{T}_{d_2} = 0.735$ sec, and the overall scanning frequency, $\overline{f}_s = 1.59$ looks/sec.
e. $\overline{T}_{d_1} = 0.40$ sec	The mean dwell time on the altitude display is taken as the minimum observed value in past data (Ref. 2) in minimal demand tasks. For such tasks, 0.35 sec $\leq \overline{T}_s \leq$ 0.45 sec.
f. $\eta_{e_4} = 0.416$	The effective position display dwell fraction is based on a foveal crossover frequency of 0.6 rad/sec, based on outer-loop crossovers for a similar task, VFR, per Ref. 7 (which assumes no outer-loop lead equalization); and an achievable crossover frequency of 0.25 rad/sec. The reduction is attributed to the IFR nature of the experimental task, the increased demands of the other tasks in the experiment (the Ref. 7 data assumes "easy" tasks in the other axes), and the need for considerable phase margin without generating lead-dictated by the low coherency of the experimental task. (Eq. A-25)
g. $\Omega_4 = 0.1$	The parafoveal/foveal crossover frequency ratio is taken at the low end of the $0 \leq \Omega \leq 0.5$ criterion range. The pilot is hypothesized to be able to devote minimal attention (as distinct from scanning) to position because of his concentration on attitude. η_{e_4} and Ω_4 define $\eta_4 = 0.351$ (Eq. A-26). η_4 and η_2 define $\eta_1 = 0.065$ which, together with $\overline{T}_{d_1}$ defines $\overline{T}_{s_1} = 6.15$ sec (Eqs. A-18 and A-31). $\overline{T}_{s_1}$ and $\overline{f}_s$ define $\nu_1 = 0.102$ (Eq. A-17) and this, together with ν_2 defines $\nu_4 = 0.398$ (Eq. A-14). ν_4 and $\overline{f}_s$ determine $\overline{T}_{s_4} = 1.58$ sec (Eq. A-17). $\overline{T}_{s_4}$ and η_4 define $\overline{T}_{d_4} = 0.555$ sec (Eq. A-31), consistent with the position task demands — more than minimal attention.
h. $S_4 = 24.5$	This value for the position display is a consequence of the foregoing assumptions (Eq. A-29), and clearly violates the $4 \leq S \leq 8$ criterion used in the preexperimental predictions. Since position loop crossover frequencies are on the order of 0.25 rad/sec (see next Section), the sample frequency parameters observed for the position display fall in the range of $15 \leq S \leq 30$, approximately.

SECTION V

DESCRIBING FUNCTION ANALYSIS

Three Priority IV runs (Subject: RG) were examined more closely than the rest to determine the significant differences among the three motion conditions. These runs were Nos. 226, 227, and 228, selected because they represented the best performance achieved on Configuration No. 6 for the three motion conditions. Histograms of the dwell times and sampling intervals, as well as the link fractions were presented in Section IV. These runs, representing respectively the FB, MBL, and MBA motion conditions were analyzed by NASA-ARC personnel for equivalent describing functions in the longitudinal and lateral tasks. The word, "equivalent", is used to indicate that the pilot model used in the analysis assumes only visual motion cues. The data for 6 additional runs on Configuration No. 6 is given in Appendix C. The results were judged to provide reasonably accurate results in the mid-frequency range, but poorer results at higher frequencies because of the relatively small amounts of high frequency power in the simulated vehicle motions. Figure 24 shows a series pilot model structure for the two tasks analyzed. In this model, Y_{p_θ}, Y_{p_φ}, Y_{p_x}, and Y_{p_y} include both display and stick gains.

Figures 25 and 26 show the frequency response plots of the simulated VTOL pitch and roll response. It is clear, on comparing these two figures, that the pilot must generate more lead for control of pitch attitude than for roll. This is reflected in Figs. 27 and 28 which show the inner-loop describing functions for pitch and roll for the three motion conditions. Y_{p_θ} shows roughly 10-20 deg more lead than Y_{p_φ} in the crossover region; Table XL lists the crossover frequencies, phase margins and performance in inner and outer loops of both the longitudinal and lateral tasks. Inner-loop crossover is at roughly the same frequency and phase margin in both pitch and roll.

Figures 29 and 30 show the outer-loop describing functions. In the longitudinal position control task, the pilot describing function shows lag in the crossover region, while the lateral control task shows lead in the FB and MBA cases, and essentially zero phase for the MBL condition.

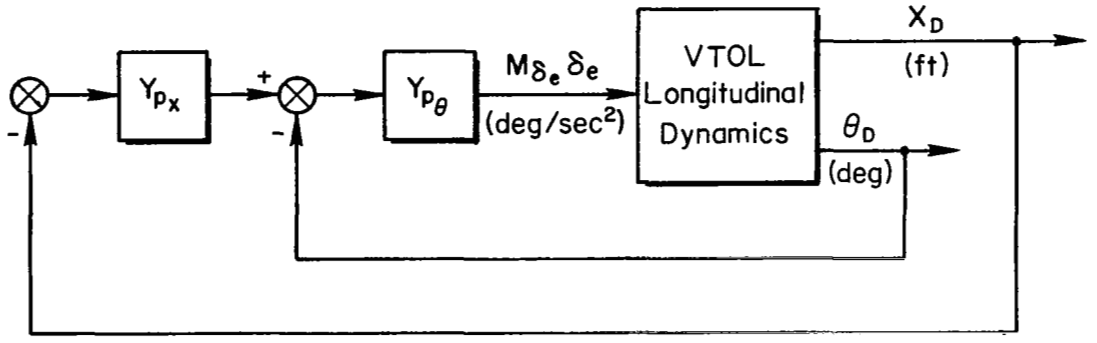

$$\frac{\theta_D}{M_{\delta_e}\delta_e}(s) = \frac{(0.1)}{(.620)[-.458, .568]} \qquad \frac{X_D}{M_{\delta_e}\delta_e}(s) = \frac{.563}{(0)(.620)[-.458, .568]}$$

*a) Longitudinal Task**

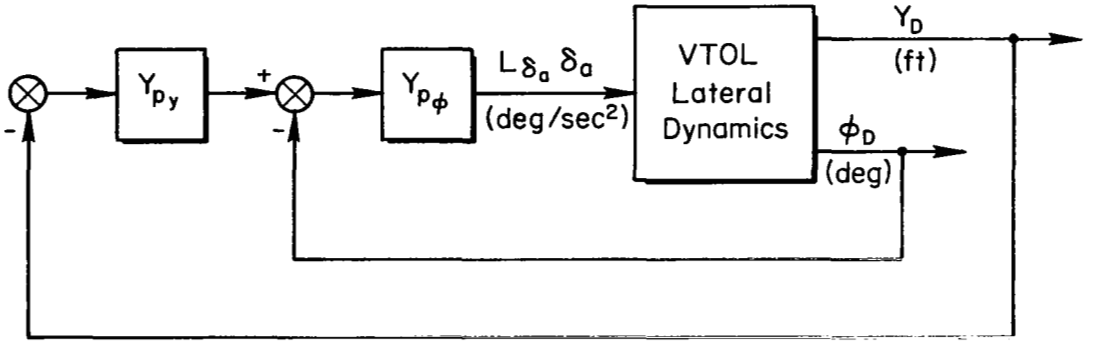

$$\frac{\phi_D}{L_{\delta_a}\delta_a} = \frac{(0.1)}{(.830)[-.234, .491]} \qquad \frac{Y_D}{L_{\delta_a}\delta_a} = \frac{.563}{(0)(.830)[-.234, .491]}$$

*b) Lateral Task**

*$(s + 1/T)$ written as $(1/T)$; $[s^2 + 2\zeta\omega s + \omega^2]$ written as $[\zeta, \omega]$

Figure 24. Series Model Closed-Loop Structure, Configuration 6

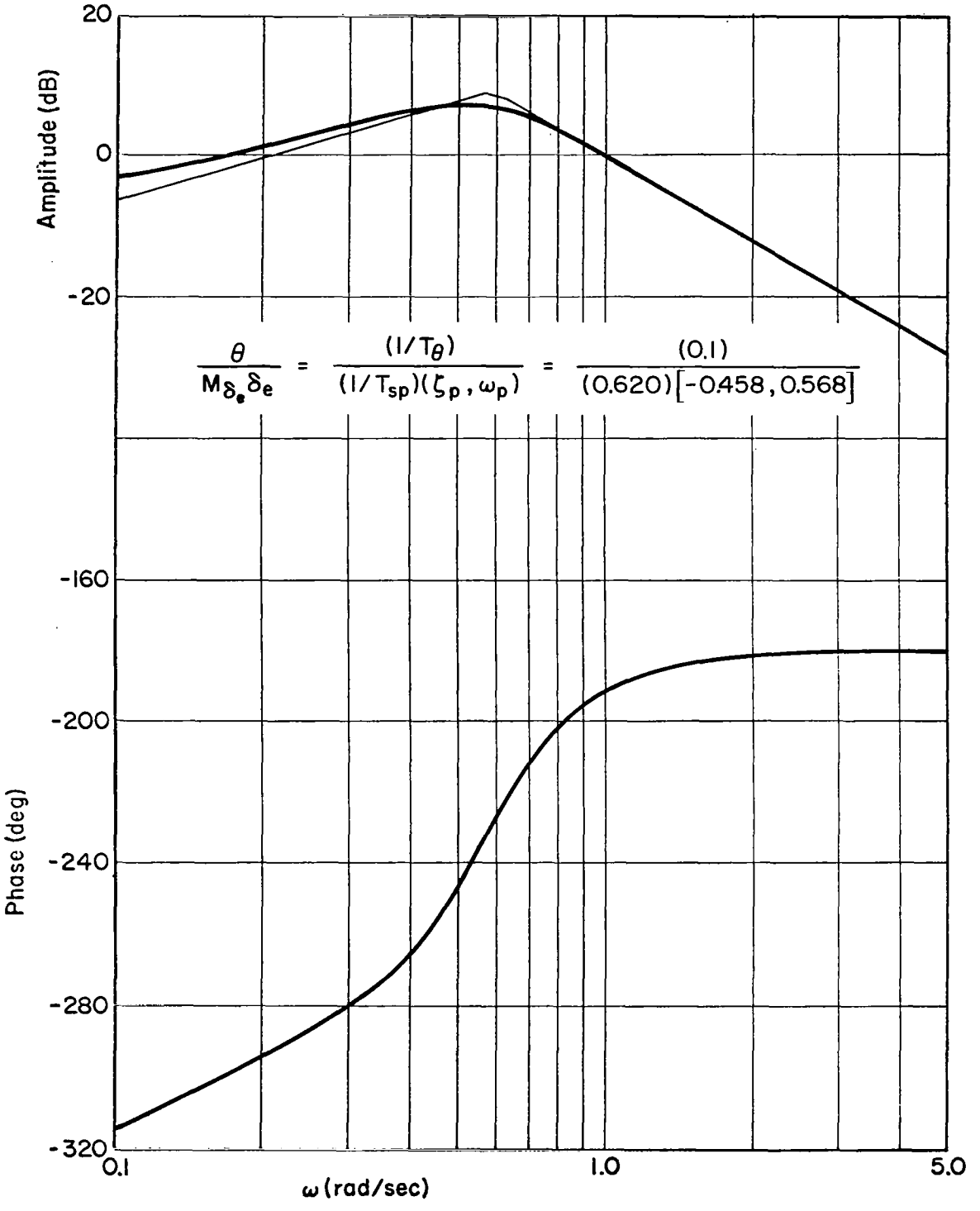

Figure 25. Open-Loop Transfer Function, Y_θ, Configuration 6

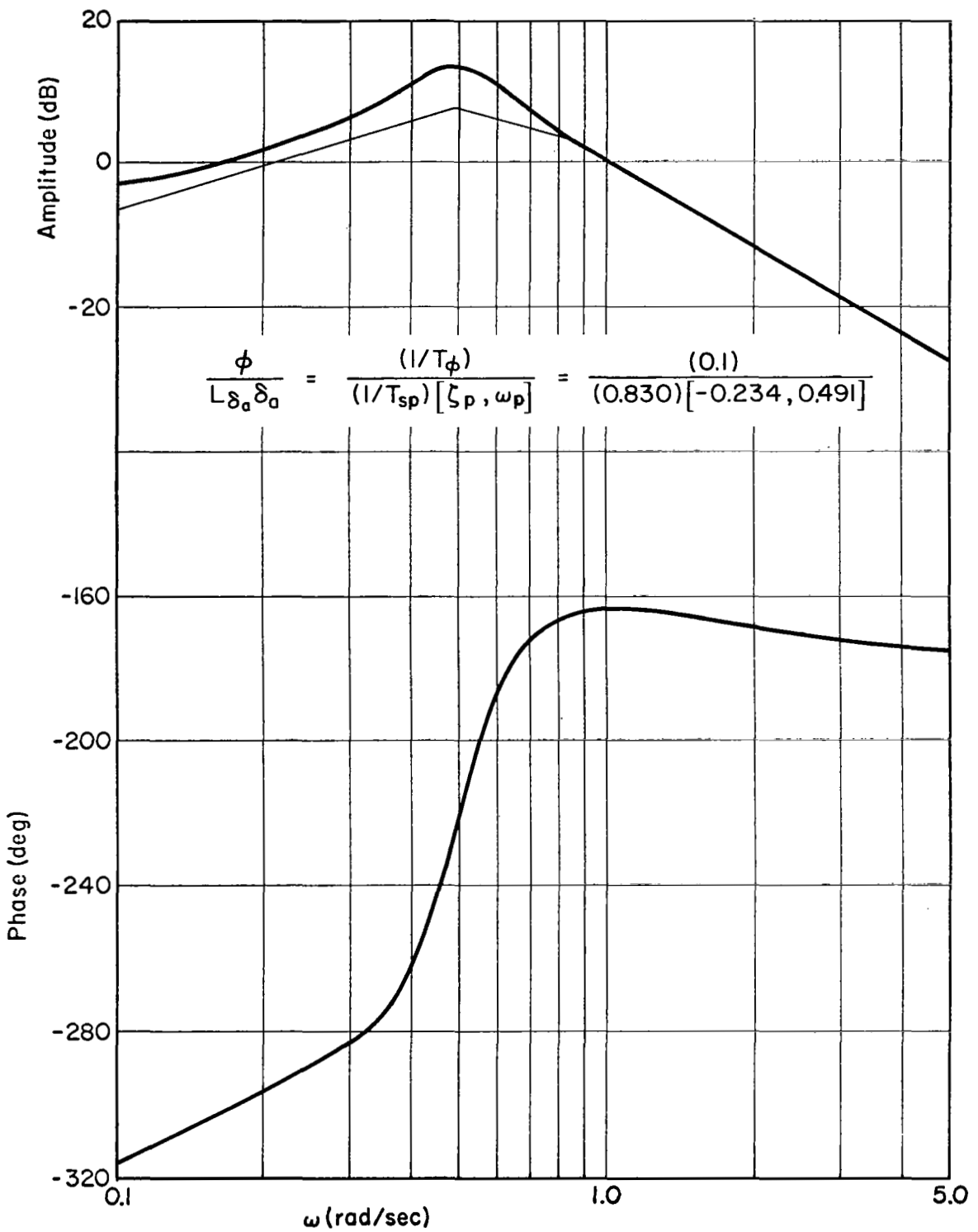

Figure 26. Open-Loop Transfer Function, Y_φ, Configuration 6

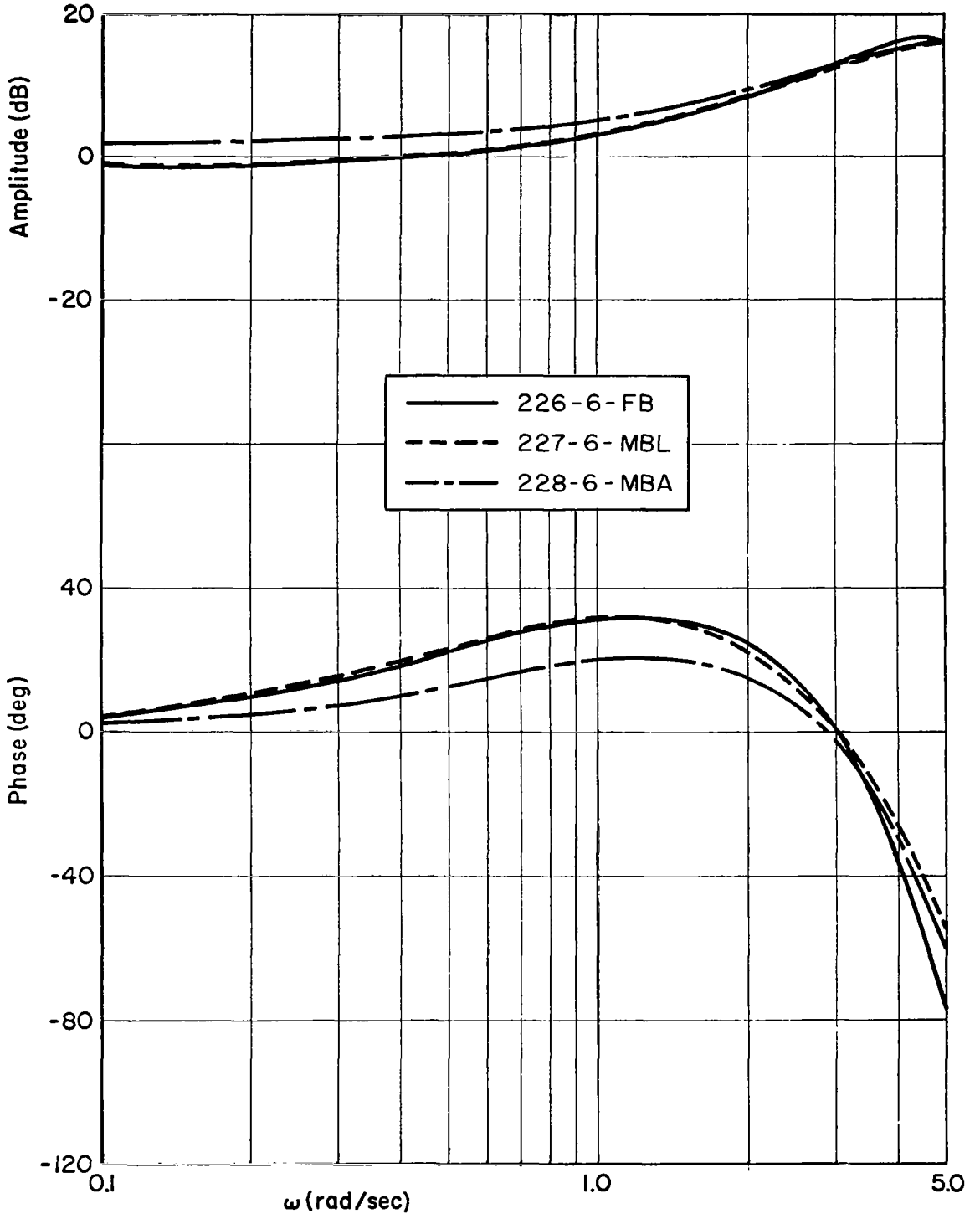

Figure 27. Pilot Describing Functions, Y_{p_θ}, Configuration 6

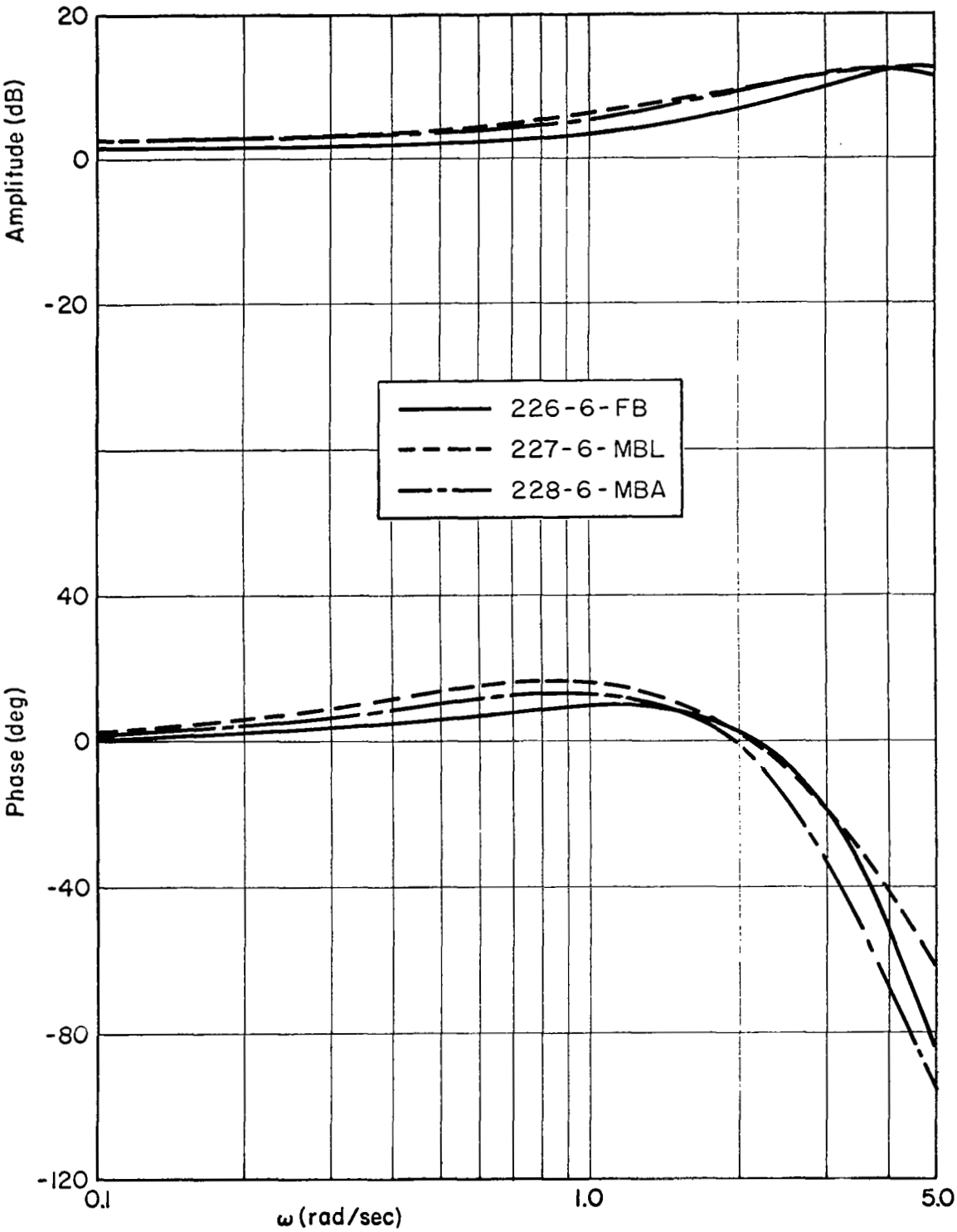

Figure 28. Pilot Describing Function, Y_{p_φ}, Configuration 6

TABLE XL

CROSSOVER FREQUENCIES, PHASE MARGINS AND PERFORMANCE FOR THREE EXAMPLE RUNS* RELATIVE TO PREDICTIONS

RUN NO.	226	227	228	PREDICTIONS	
	FB	MBL	MBA	FB	MBL
Longitudinal Task					
ω_{c_θ} (rad/sec)	1.37	1.41	1.55	1.5	2.25
φ_{m_θ} (deg)	27	27	17	11	18
σ_θ (deg)	0.80	0.84	0.54	0.80‡	0.73
ω_{c_x} (rad/sec)	0.13	0.24	0.19	0.5	0.5
φ_{m_x} (deg)	68	47	38	53	22
σ_x (ft)	3.13	2.53	1.92	1.1‡	1.3
Lateral Task					
ω_{c_φ} (rad/sec)	1.27	1.64	1.56	1.5	2.25
φ_{m_φ} (deg)	27	23	22	25	28
σ_φ (deg)	0.92	0.65	0.63	1.28	0.97
ω_{c_y} (rad/sec)	0.29	0.28	0.23	0.5	0.5
φ_{m_y} (deg)	55	36†	54	37	17
σ_y (ft)	2.01	2.13	2.41	1.8	1.8
Vertical Task					
σ_z (ft)	1.05	1.45	0.84	0.16	0.16
Overall Task					
σ_{disp} (ft)	3.87	3.61	3.19	2.1‡	2.2

*Subject was RG.
†No phase lead; see Fig. 30.
‡Scanning remnant not included in calculations; see Appendix A.

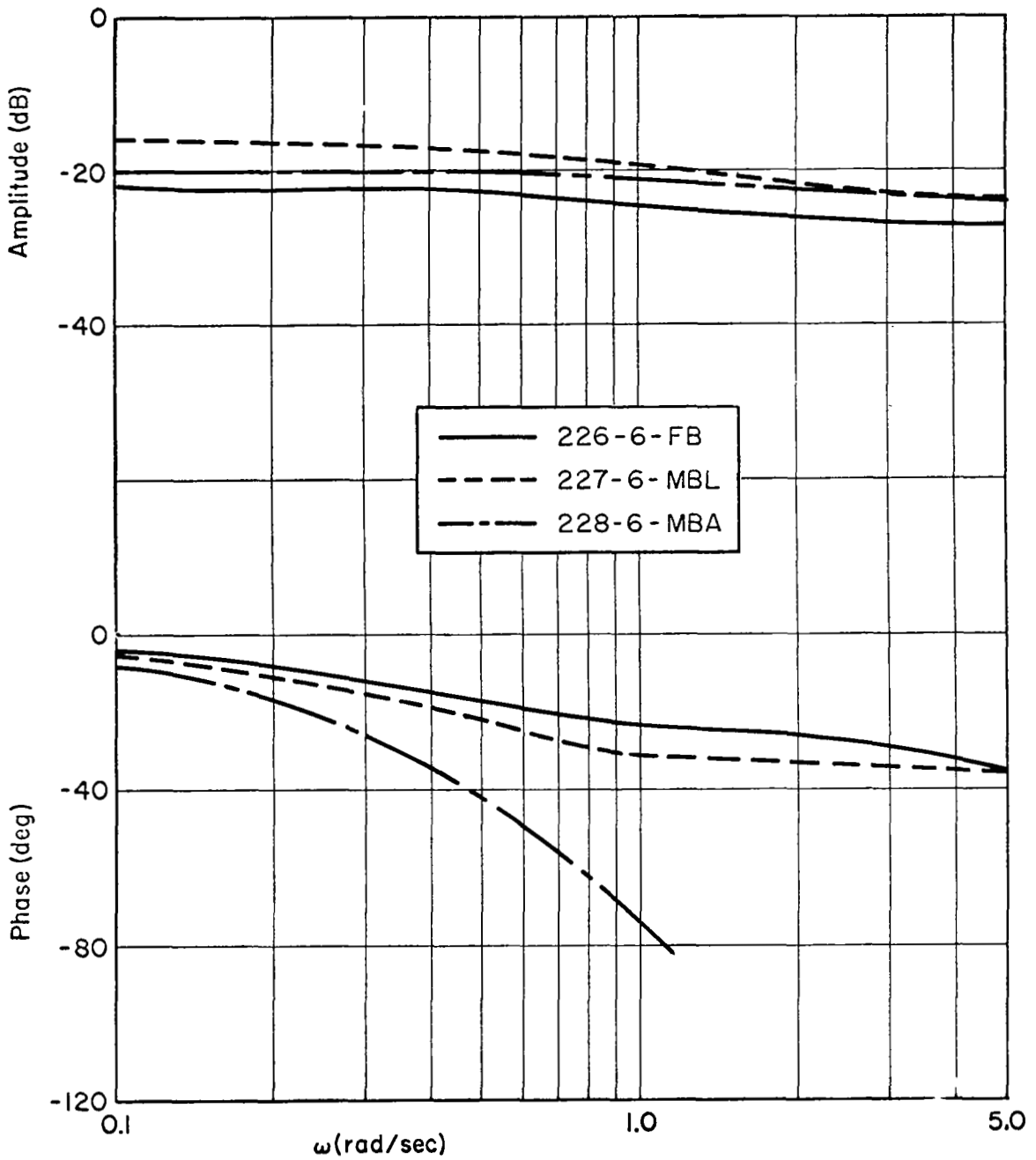

Figure 29. Pilot Describing Function, Y_{p_x}, Configuration 6

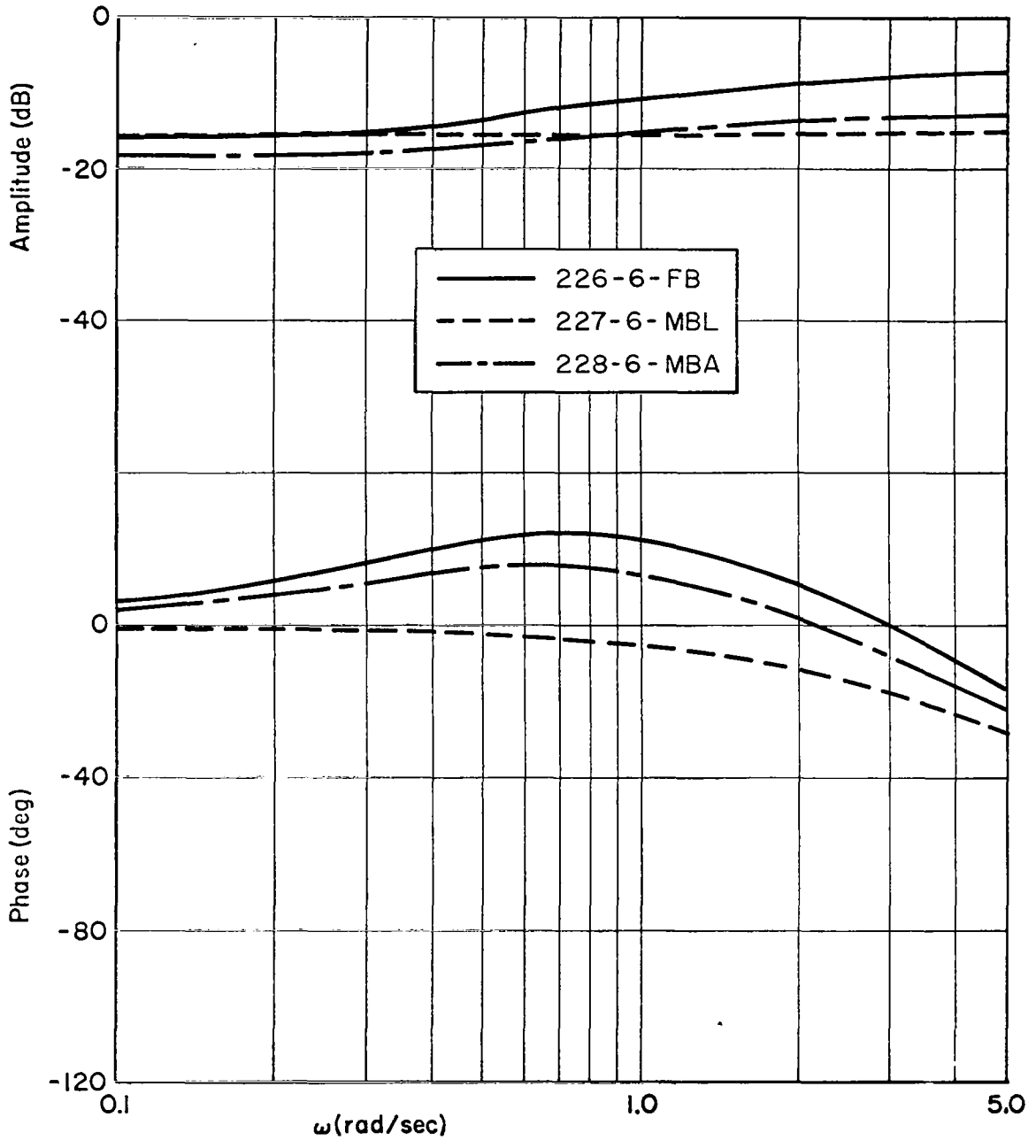

Figure 30. Pilot Describing Function, Y_{p_y}, Configuration 6

The pilot gains are generally somewhat higher, laterally, resulting in somewhat higher crossover frequencies. Lateral position control is easier than longitudinal position control. Table XL shows that the predicted loop crossover frequencies were optimistic in all cases, a result consistent with the observed performance discussed in Section III. This is particularly true in the outer (position) loops.

The overall performance (σ_{disp}) listed for each of the three motion conditions in Table XL shows relatively small run-to-run improvement with the fixed-base condition (FB) being worst and the moving-base (angular motion only) condition (MBA) being best. The MBL condition shows better performance relative to fixed base by virtue of improvement in the longitudinal position control performance (σ_x) — both the lateral (σ_y) and vertical (σ_z) performance deteriorate, the latter fairly substantially. The improvement is achieved primarily because of the increased outer-loop crossover frequency, ω_{c_x}, resulting from a pilot gain increase in the outer loop of almost 6 dB (see Fig. 29). Reference to the inner- and outer-loop dwell fractions (Fig. 16) shows that the former has decreased by 17 percent, the latter increased by 29 percent in the MBL condition. Figure 21 shows that the inner-loop sampling variability parameter, δ, has increased by 95 percent in this condition. These factors are evidence that the pilot need generate less lead, visually in the MBL condition relative to FB, and that the pilot-introduced remnant due to scanning in the inner loop is markedly reduced. In the lateral task, the pilot is able to increase his inner-loop crossover frequency substantially by virtue of a roll attitude gain increase of approximately 5 dB, and thus improve his roll attitude control, indicated by σ_φ. But he has relaxed his outer-loop control as evidenced by his reduced crossover frequency (ω_{c_y}), phase margin (φ_{m_y}), and performance (σ_y). He has also deteriorated in altitude control (σ_z). Apparently he has not only used the angular motion cues to improve overall performance, but also traded a small decrement in lateral position control and a larger decrement in vertical position control for the longitudinal task improvement. Thus the magnitude of the reduction in σ_x is not entirely attributable to motion. Some portion, to use a current phrase, is due to a change in priorities.

The MBA condition shows a further improvement in longitudinal position control attributable to greater pitch attitude control precision and a reduction (apparently) in his scanning remnant in this task—his position control performance (σ_x) improves despite a reduction in pilot gain in the outer loop (Fig. 29). This condition shows a further deterioration in lateral position control performance (σ_y) attributable to a reduction in outer-loop gain. Altitude performance improves markedly although the scanning behavior changes relatively little. Apparently the subject is able to pay more attention (as distinct from scanning) to altitude and longitudinal position control in the MBA condition; in the former task this is accomplished by (apparently) an increase in his parafoveal gain on the altitude task in the latter by an increase in position display dwell fraction.

Table XLI presents a comparison of the attitude crossover frequencies obtained in similar (but less demanding) tasks and those measured in this experiment. The current experiment shows much lower frequencies, primarily because of the high pilot workload due to separate display scanning. But the percentage change in this frequency with motion condition is comparable with previous data, at least in roll, and the phase margins are closely comparable, suggesting that the pilot uses similar attitude loop closure criteria in the three experiments, workload permitting.

Considering the limitations imposed by the small data sample, and lack of a stable performance level (as evidenced by the trend in performance improvement with motion condition being attributable to one or two tasks instead of all three), the describing functions obtained for these runs agree reasonably well with the performance achieved, pilot commentary and opinion, and the measured scanning behavior. Some of the performance changes evidenced must be attributed to changes in variables which cannot be measured (e.g., effective dwell fractions); further, the differences among the three performance conditions are quite small due either to the very great difficulty of the task and/or because of the small angular motion magnitudes already

TABLE XLI

ATTITUDE LOOP CROSSOVER FREQUENCY COMPARISON

VARIABLE	MOTION CONDITION (% CHANGE)	REF. 15 DATA*		REF. 1 DATA†			CURRENT DATA	
		PILOT A	PILOT B	PILOT GB	PILOT RG	PILOT MJ	ROLL	PITCH
ω_c (rad/sec)	FB	2.0	1.6	2.6	2.3	2.2	1.27	1.37
	MBL	2.3	2.3	3.2	3.3	3.0	1.64	1.41
	Δ (%)	15.0	43.8	12.3	43.5	36.3	29.0	3.0
ϕ_m (deg)	FB	26	34	30	25	30	27	27
	MBL	27	33	30	25	25	23	27
	Δ (%)	3.9	−3.0	≐0	≐0	−16.7	−14.8	≐0

$$^{*}Y_c = \frac{K}{s(s+0.33)} \quad , \quad \text{Flight versus Ground Test}$$

$$^{\dagger}Y_c = \frac{K}{s^2} \quad , \quad \text{Motion Simulator}$$

discussed in Section III. In Run 228, the magnitudes of the rms tilting of the cab in pitch and roll (0.54 and 0.63 degree, respectively) are essentially equivalent to utricular thresholds (Ref. 1) suggesting that even utricular threshold effects are important for this run.

SECTION VI

SUMMARY

The major results of this experimental program relate to the important role played by linear motion (or its absence) in task performance, the presence of vestibular threshold effects, and the decrements in pilot opinion and performance arising out of the need for display sampling and scanning in the simulated VTOL hovering task. In addition a large body of data was obtained on the effects of motion on pilot display scanning behavior.

A. LINEAR MOTION CUES

In the simulated task there was a clear-cut preference for the angular motion only condition over the full motion (angular and linear simulator movement) condition, as evidenced by pilot commentary, opinion and performance. This result was unanticipated and can probably be ascribed to two contributing causes:

1. Use of the g-vector tilt cue as an indicator of vehicle attitude, especially when not fixating on the attitude display.

2. Absence of a tendency to vertigo, "confusion", and "distraction" in the MBA condition as opposed to the MBL condition (wherein the apparent tilt of the g-vector is considerably less and unrelated to attitude, but rather to disturbances and pilot location effects).

The data indicate the former reason to be of greater importance than the latter, although the vertigo tendency undoubtedly contributes to the performance and rating decrements observed in the easiest (and least motion sensitive) configuration.

Certain configurations intended to be sensitive to the presence or absence of linear motion cues were not, to any significant extent. Pilot location effects were undetectable because of the low values of pitch acceleration. Performance across motion conditions for a

configuration having low control sensitivity and heave damping was more strongly affected by the lateral and longitudinal task differences, according to the subjects. However, there was commentary to the effect that jerkiness in vertical motion is "disconcerting," and one subject claimed to use this cue to regulate his collective control inputs.

B. VESTIBULAR THRESHOLD EFFECTS

The angular rate amplitudes (rms) were less than the estimated effective angular rate thresholds (2.6 deg/sec in pitch, 3.2 deg/sec in roll, per Ref. 1) and certainly of a magnitude where such effects are significant, per the results of Refs. 13 and 14. This is true even for the more difficult vehicle configurations, implying that the angular rate cues were only effective at the peak angular rates. This resulted in smaller motion versus no-motion performance and opinion differences than observed in past experiments on similar configurations. Scanning behavior differences and describing function differences were likewise smaller than predicted or previously observed. For some of the subjects, and configurations, even the rms attitudes were small enough to render the g-vector tilt cue in the MBA motion condition smaller than the utricular threshold (0.01g or 0.573 deg of tilt per Ref. 1) for much of the time. The small angles and angular rates are a result of the much lower outer (position) loop gains adopted by the pilots when using separated instrument displays — larger angles are incompatible with the motion simulator limits of these gain levels. To obtain this level of attitude control precision required the changes in the attitude display and control sensitivity made in the shakedown runs.

C. VFR-IFR DIFFERENCES AND SCANNING BEHAVIOR

The necessity for scanning separated instrument displays as opposed to VFR conditions or an integrated display caused a considerable decrement in pilot opinion and performance. The describing function data indicate lower crossover frequencies than predicted (preexperimental predictions of loop closure parameters were predicated on scanning behavior, however, pilot rating predictions were based upon data for VFR conditions, there being a dearth of equivalent IFR data). The

opinion decrement was so great (on the order of 2 to 4 points) to render the Cooper-Harper rating scale useless for detecting motion differences. The interpretation of the scale was modified to allow greater differentiation across motion conditions. The rating data given in this report are thus not directly comparable with past rating data.

Pilot scanning behavior reveals that the primary attention is to vehicle attitude, while the altitude control task is all but ignored, relatively speaking. Dwell times on the altitude display are close to the minimum values observed in past scanning measurements, and the sampling interval quite long. The position display dwells are somewhat longer and very frequent while the attitude display dwells are the longest of all — occasionally several seconds in duration. The primary effect of motion on scanning behavior is to reduce the attitude display dwell times and dwell fractions while the position and altitude displays receive a greater fraction of the pilot's foveal scan. There is relatively little difference between the MBL and MBA scanning behavior, indicating that the dominant cause of the behavior change is the presence of an angular rate cue in the moving base cases — a result fully in accord with predictions. The scanning frequency is generally higher than observed in past scanning measurements. The measured look (or scan) rate in one run exceeded two looks per second with a more typical value being 1.5 looks/second.

D. MOTION FIDELITY EFFECTS

All simulator axes used in the experiment were compensated for simulator dynamic response lags based on earlier measurements of simulator response, and no washouts were used. In some runs, the effects of angular motion lags (relative to the displayed value) were varied to determine the subject's sensitivity to such motion lags. Preexperimental predictions were that a 0.1 sec time constant would be significant while the experimental value was 0.2 sec. On the other hand, the attitude loop crossovers measured were on the order of 1.5 rad/sec — lower than the predicted crossover of 2.25 rad/sec. This difference in crossover frequency plus vestibular threshold

effects are felt to account for most, if not all, of the difference between predicted and observed results — both imply reduced sensitivity to high frequency motion lags.

E. MULTIMODALITY PILOT MODEL IMPLICATIONS

As a test of the multimodality pilot model, the experimental results provide less than a satisfactory check because of the overriding effects of VFR-IFR differences and the effective vestibular thresholds in the experimental task. However, the model was successful in predicting performance and rating trends, and it was not contradicted.

The beneficial effects of the g-vector tilt cue were unanticipated. It can be speculated that this effect would be less important in tasks where a visual attitude cue is available at all times, i.e., in an integrated display. In the experimental task, the tilt cue provides an attitude indication even when the pilot is looking elsewhere. This apparently permits him to spend more time monitoring the position display.

REFERENCES

1. Stapleford, R. L., R. A. Peters, and F. R. Alex, Experiments and a Model for Pilot Dynamics with Visual and Motion Inputs, NASA CR-1325, May 1969.

2. Allen, R. W., W. F. Clement, and H. R. Jex, Research on Display Scanning, Sampling, and Reconstruction Using Separate Main and Secondary Tracking Tasks, NASA CR-1569, July 1970.

3. Weir, David H., and Richard H. Klein, The Measurement and Analysis of Pilot Scanning and Control Behavior During Simulated Instrument Approaches, NASA CR-1535, June 1970.

4. Clement, W. F., and L. G. Hofmann, A Systems Analysis of Manual Control Techniques and Display Arrangements for Instrument Landing Approaches in Helicopters; Vol. I. Speed and Height Regulation, Systems Technology, Inc., Tech. Rept. 183-1, July 1969.

5. Williams, P. R., and M. B. Kronholm, Technical Report on Simulation Studies of an Integrated Electronic Vertical Display, United Aircraft Corp., Norden Div., Rept. No. 1161 R 0021, 31 Dec. 1965.

6. Miller, D. P., and E. W. Vinje, Fixed-Base Flight Simulator Studies of VTOL Aircraft Handling Qualities in Hovering and Low-Speed Flight, AFFDL-TR-67-152, Jan. 1968.

7. Craig, S. J., and A. Campbell, Analysis of VTOL Handling Qualities Requirements; Part I. Longitudinal Hover and Transition, AFFDL-TR-67-179, Oct. 1968.

8. Vinje, E. W., and D. P. Miller, Analytical and Flight Simulator Studies to Develop Design Criteria for VTOL Aircraft Control Systems, AFFDL-TR-68-165, Apr. 1969.

9. Fry, E. G., R. K. Grief, and R. M. Gerdes, Use of a Six-Degree-of-Freedom Motion Simulator for VTOL Hovering Tasks, NASA TN D-5383, Aug. 1969.

10. Stewart, J. D., Personal Communication [Concerns vertical motion simulator response not given in Ref. 9], 3 Oct. 1969.

11. Wingrove, Rodney C., Frederick G. Edwards, A Technique for Identifying Pilot Describing Functions from Routine Flight-Test Records, NASA TN D-5127, May 1969.

12. Bendet, J. S., and A. G. Piersol, Measurement and Analysis of Random Data, John Wiley and Sons, Inc., New York, 1966.

13. Bergeron, H. P., The Effects of Motion Cues on Compensatory Tracking Tasks, Paper No. 70-352, presented at the AIAA Visual and Motion Simulation Technology Conference, Cape Canaveral, Fla., Mar. 16-18, 1970.

14. Bergeron, H. P., Personal Communication [Concerns amplitudes of the motion variables reported on in Ref. 13], 3 Sept. 1970.

15. Szalai, K. J., and D. A. Deats, An Airborne Simulator Program to Determine if Roll-Mode Simulation Should be a Moving Experience, Paper No. 70-351, presented at the AIAA Visual and Motion Simulation Technology Conference, Cape Canaveral, Fla., Mar. 16-18, 1970.

16. McRuer, Duane, Dunstan Graham, Ezra Krendel, and William Reisener, Jr., Human Pilot Dynamics in Compensatory Systems — Theory, Models, and Experiments with Controlled Element and Forcing Function Variations, AFFDL-TR-65-15, July 1965.

17. McDonnell, John D., Pilot Rating Techniques for the Estimation and Evaluation of Handling Qualities, AFFDL-TR-68-76, Dec. 1968.

18. Stapleford, R. L., S. J. Craig, and J. A. Tennant, Measurement of Pilot Describing Functions in Single-Controller Multiloop Tasks, NASA CR-1238, Jan. 1969.

19. Anderson, Ronald O., An Additional or Alternate Method of Specifying Hover Flying Qualities, FDCC TM-69-2, 20 June 1969 (preliminary information).

APPENDIX A

PREEXPERIMENTAL ANALYSES

Prior to the actual running of the experiment, extensive preexperimental analyses were conducted to provide a basis for comparison of the results obtained. The objective was to provide estimates of the pilot performance, opinion, and display scanning behavior in the experimental task using the multimodality pilot model developed in Ref. 1 and display sampling theory (Ref. 2). This appendix outlines the methods of analysis used and the results of the analysis with no modifications based on experimental results. The task situation analyzed consists of two multiple loop (lateral and longitudinal dynamics) and two single loop (vertical and directional dynamics) tasks. Since the directional task was deleted from the program (see Section II.A.3) that portion of the analysis is omitted from this appendix, although it does affect the predicted scanning traffic.

PILOT MODELS

In this subsection three categories of pilot models are presented. First is the usual model for fixed-base cases; second is the multimodality pilot model; and finally, the modeling of pilot scanning behavior — the "switched gain" model.

Loop Topology and Pilot Models — Fixed Base

The loop structure for the longitudinal task is shown in Fig. A-1 for control of pitch attitude and horizontal position. In this series model the pilot makes position corrections by mentally biasing his pitch attitude reference up or down an amount dependent upon his gain and lead computations of the position error. His internal pitch command, θ_x, minus the actual pitch attitude then gives him an internal pitch attitude error. This is operated on by a gain, a lead, and a time delay.

The pilot's time delay depends upon the amount of lead that he has to provide. It is assumed that this is primarily dependent upon the

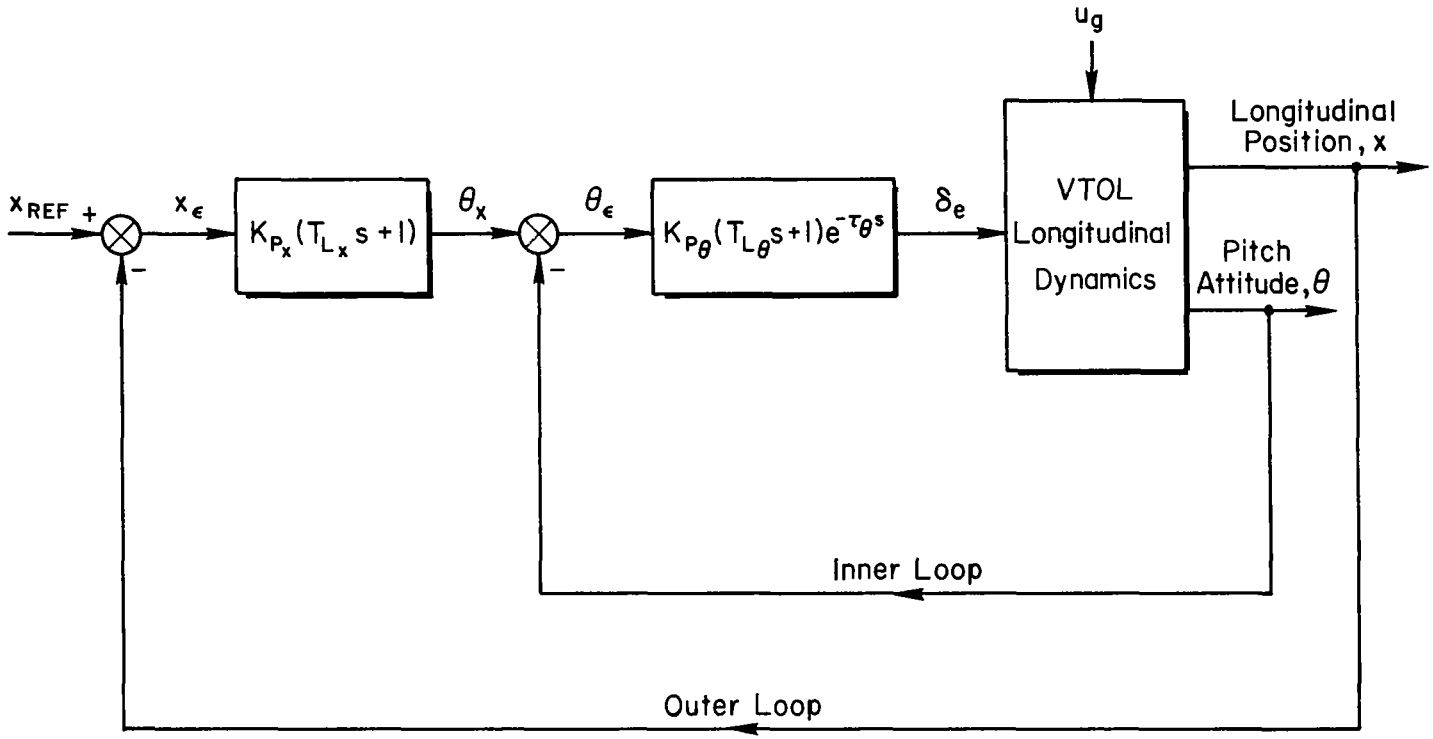

Figure A-1. Series-Loop Model for Pilot Control of Longitudinal Dynamics in Hover

lead time constant in the θ-loop, T_{L_θ}. The relationship* between time delay and lead time constant is given in Fig. A-2 (Refs. 16 and 17). A convenient approximation to the data in Fig. A-2 is given by the expression

$$\tau_o \doteq 0.33 + \frac{1}{8} T_L \qquad \text{(A-1)}$$

which is valid for $T_L \leq 1$ sec. In this example, $\tau_o = \tau_\theta$ and $T_L = T_{L_\theta}$.

A typical Bode plot for the $\theta \rightarrow \delta_e$ inner-loop closure is sketched in Fig. A-3. This shows the amplitude and phase of the open-loop transfer function. The airframe response modes are the phugoid, ω_p, and the short-period, $1/T_{sp}$. The $\theta \rightarrow \delta_e$ transfer function has a lead at $1/T_\theta$ and the pilot lead, $1/T_{L_\theta}$, is also indicated. In the following analyses it is always assumed that the pilot lead cancels the short-period real root, $1/T_{sp}$. This provides a long stretch of K/s-like response along which the pilot can select his crossover frequency. The phase portion of Fig. A-3 illustrates the differences between those cases where the phugoid mode is stable or unstable. In the unstable cases the system is conditionally stable, thus constraining the pilot's crossover frequency.

The effective open-loop dynamics for the outer loop with a reasonable inner-loop crossover frequency are sketched in Fig. A-4. This shows the closed-loop modes from the inner-loop closure, the oscillatory mode at ω_p', and the real root at $1/T_\theta'$ which has been driven close to the zero at $1/T_\theta$. Also shown in Fig. A-4 is the pilot lead, $1/T_{L_X}$, which will normally be required to provide additional phase margin for a reasonable outer-loop crossover frequency. The crossover frequency parameters assumed are based upon past experience with VFR vehicle control tasks.

The pilot model for lateral control of bank angle and lateral position has the same form as for the longitudinal axis just discussed.

---

*Note that Eq. A-1 does not include a term to account for the time delay dependence on forcing function bandwidth ($\Delta\tau = 0.08\omega_i$) (Ref. 16). This is because this term would be small for the effective input bandwidth after it passes through the vehicle dynamics.

The same adjustment rules with respect to pilot lead and time delay relationships therefore apply.

The pilot model for altitude control with collective is shown in Fig. A-5. This is a single-loop situation where the altitude dynamics consist of two poles, a free s and a root dependent upon the effective

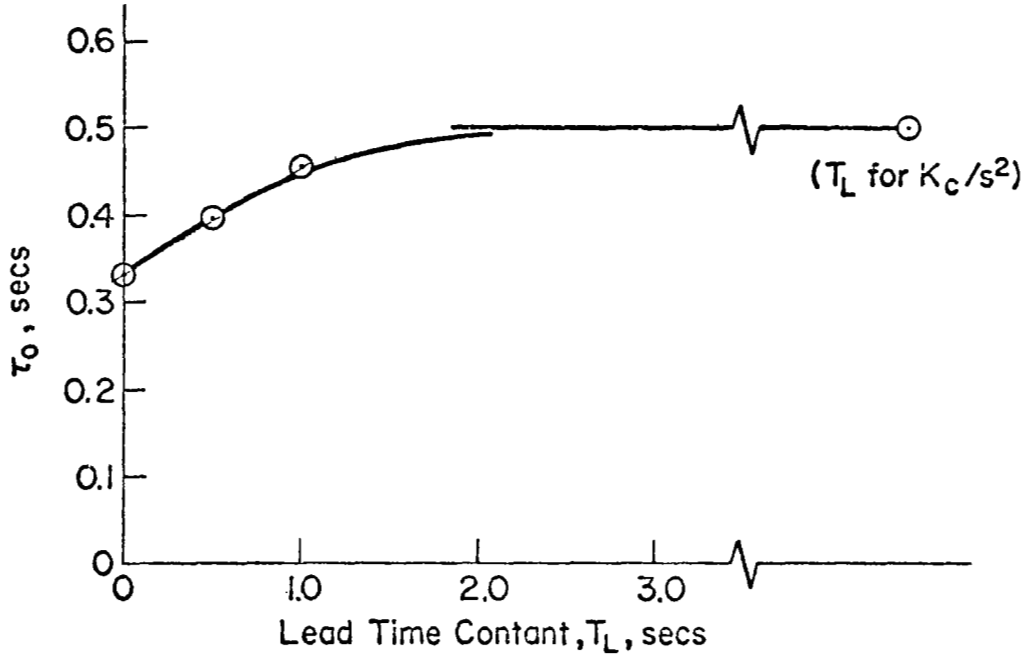

Figure A-2. Effect of T_L on τ_o

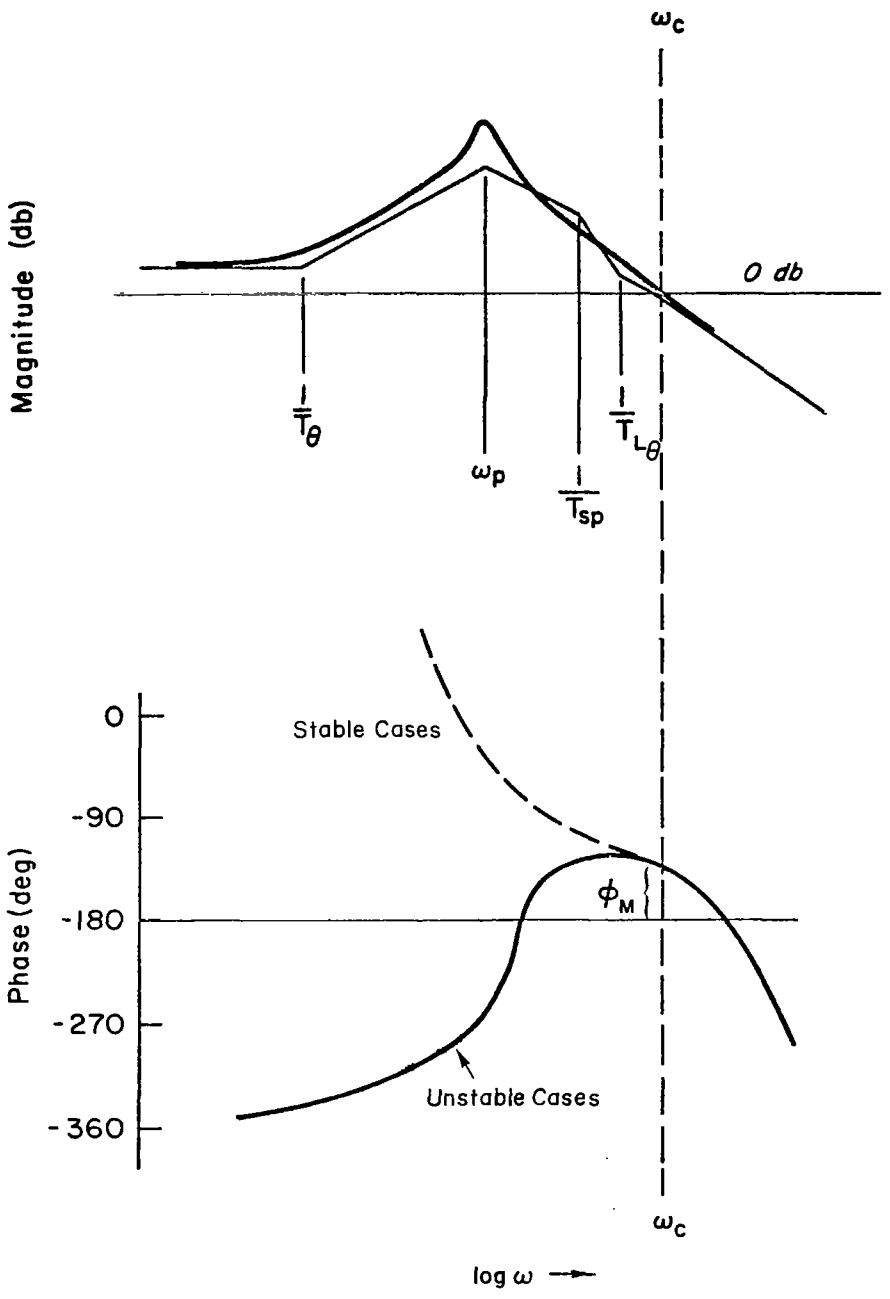

Figure A-3. Typical Bode Plot for $\theta \rightarrow \delta_e$ Closure

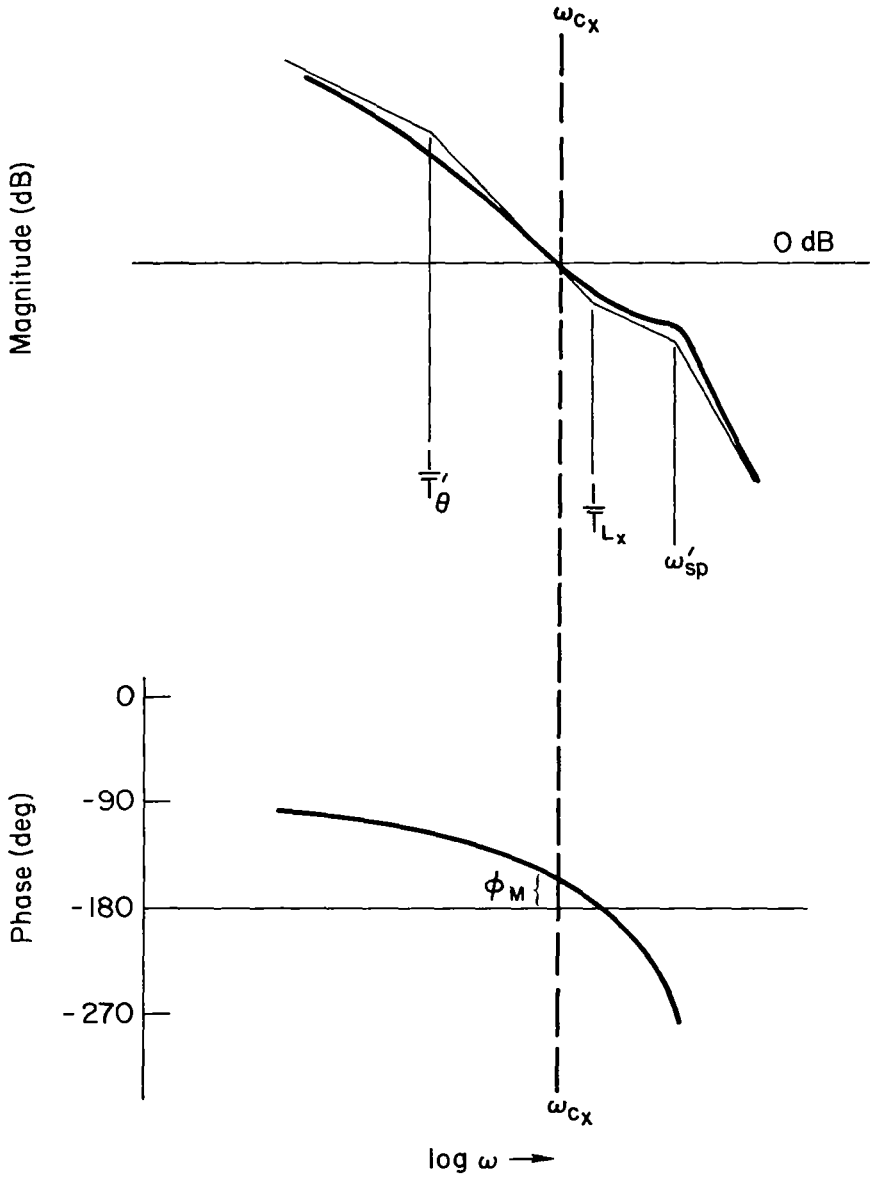

Figure A-4. Typical Bode Plot for $x \rightarrow \delta_e|_{\theta \rightarrow \delta_e}$ Closure

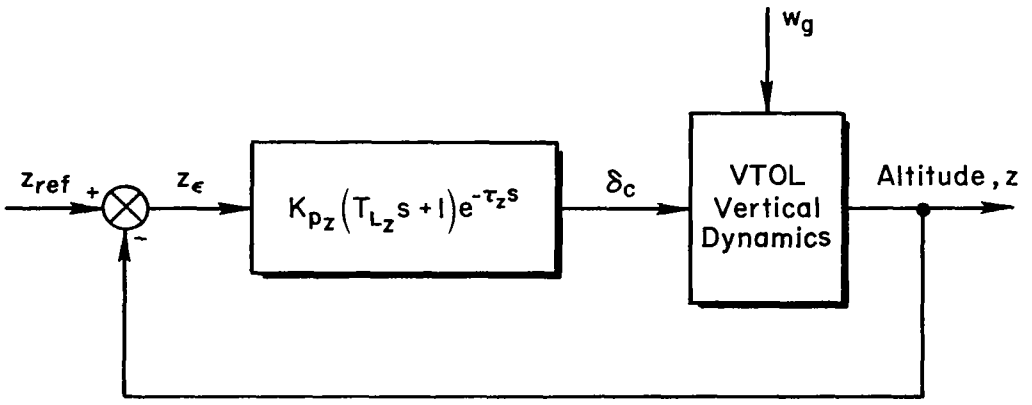

Figure A-5. Model for Pilot Control of Vertical Dynamics in Hover

heave mode damping. The pilot model is a simple lead and time delay where the lead is selected to cancel the real root in the altitude dynamics (Ref. 17). Again, the lead time delay relationship is given by Fig. A-2 and Eq. A-1. In this single-loop situation, the pilot uses the collective control to try and null out the altitude errors from the altitude display. Here the vertical gust provides the excitation.

Pilot Models — Moving Base

The pilot model to take into account moving-base motion effects derives from interpretations of data in Ref. 1. This data suggests the model shown in Fig. A-6 for the visual and motion path operations for the longitudinal task. This figure shows the pilot's output responding to the visually displayed pitch angle and position error signals, and the pitch rate picked up by his vestibular senses. The motion channel describing function is a pure lead and a time delay, τ_m. This form is consistent with the Ref. 1 data over the frequency range of interest in the experiment. τ_m was found to be about 0.16 sec for the two extreme controlled element forms, $K/s(s+10)$ and K/s^2. These extremes are similar to those found in the θ/δ_e and φ/δ_a transfer functions in this experiment.

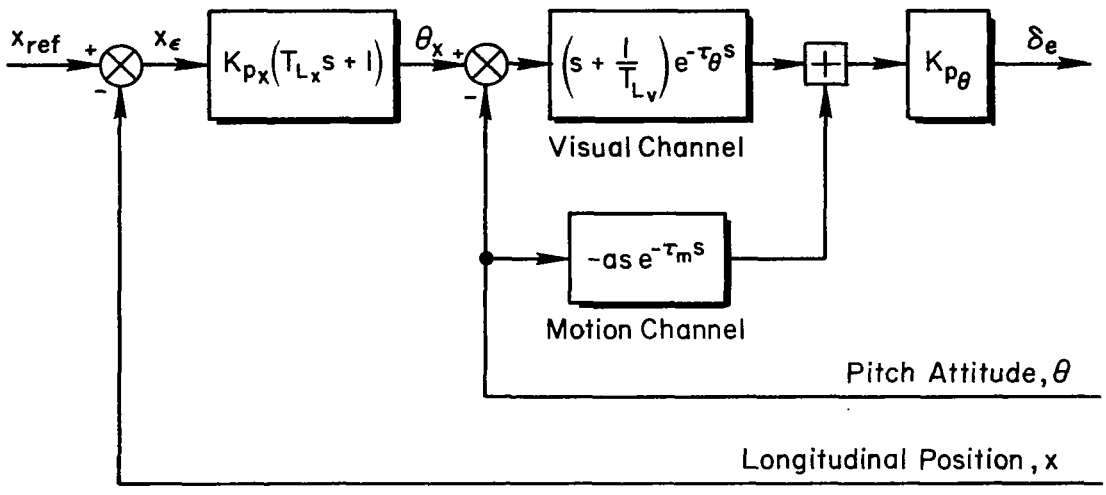

Figure A-6. Multimodality Pilot Model for Control of Longitudinal Dynamics in Hover

In Fig. A-6, the pilot's visual channel operation on the pitch angle has a lead and time delay term similar to the fixed base model. However, for the same configuration, less visual pilot lead will be required because the motion channel is providing some of the lead. However, this reduced visual lead also reduces the lead available to control the vehicle position, since it is in series with the direct position lead generation in the series pilot model. The pilot's visual channel lead time constant, T_{L_V}, and time delay, τ_θ, on pitch angle are assumed to be interrelated in the same fashion as for the fixed-base case discussed earlier, that is, the relationship given in Fig. A-2 and Eq. A-1.

The overall operation on pitch angle is given by the sum of the visual and motion channels, that is,

$$Y_{p_\theta} = K_{p_\theta}\left[as e^{-\tau_m s} + \left(s + \frac{1}{T_{L_V}}\right)e^{-\tau_\theta s}\right] \qquad (A\text{-}2)$$

$$= K_{p_\theta}\left[as + \left(s + \frac{1}{T_{L_V}}\right)e^{-\tau_1 s}\right]e^{-\tau_m s} \qquad (A\text{-}3)$$

where $\tau_1 = \tau_\theta - \tau_m$. Using an approximation for the time delay given by

$$e^{-\tau_1 s} \doteq \left(\frac{s - 4/\tau_1}{s + 4/\tau_1}\right)^2 \tag{A-4}$$

yields the form

$$Y_{p_\theta} \doteq \underbrace{K_{p_\theta}(a+1)}_{\text{gain}}\left(s + \frac{1}{T_{L_\theta}}\right)\frac{\left[s^2 + 2\zeta_1\omega_1 s + \omega_1^2\right]}{(s + 4/\tau_1)^2}\, e^{-\tau_m s} \tag{A-5}$$

The question now arises as to how the visual channel lead time constant, T_{L_V}, and the motion channel gain, a, are selected. From Fig. 20 of Ref. 1 it is noted that the pilot transfer function magnitudes in the visual and motion channels are equal at a frequency, ω_M, which depends on the controlled element dynamics. For controlled elements of the form, K/s^2, ω_M is approximately 2.0 rad/sec; for $K/s(s + 10)$ elements, ω_M ranges between 5.5 and 9.0 rad/sec. For the controlled elements in this experiment, the former figure (ω_M = 2.0 rad/sec) is assumed to apply to the $M_q = 0$ case which has similar frequency response characteristics; while ω_M is chosen to be 9 rad/sec for the $M_q = -4$ situation for the same reason. The intermediate cases are assigned intermediate values. The parameters a and T_{L_V} are then selected according to:

a. Magnitude of Visual Channel = Magnitude of Motion Channel at frequency ω_M

b. Overall lead time constant, T_{L_θ} = Short-period time constant, T_{sp}

The resulting values for the parameters of the moving-base pilot model pertinent to each of the controlled element forms given in Table I of the main text are given in Table A-I. (Note that $M_q = -0.5$ is included since it corresponds to $L_p = -0.5$.)

TABLE A-I

COMPARISON OF FIXED-BASE AND MOVING-BASE PILOT MODEL PARAMETERS FOR CONTROL OF VTOL ATTITUDE

VTOL PARAMETERS		PILOT MODEL, Y_{p_θ}, PARAMETERS						
		FIXED BASE		MOVING BASE				
M_q	$\frac{1}{T_{sp}}$	τ_θ	$\frac{1}{T_{L_\theta}}$	ω_M	a	$\frac{1}{T_{L_v}}$	τ_1	ζ_1 , ω_1
0	0.62	0.48*	0.62	2	1.18	1.24	0.27	0.083 , 14.07
-0.5	0.83	0.46*	0.83	2.5	1.20	1.64	0.246	0.093 , 15.43
-1	1.16	0.44	1.16	3	1.25	2.27	0.225	0.115 , 16.53
-4	4.01	0.36	4.01	9	1.22	6.28	0.19	0.084 , 17.61

*Taken from Fig. A-2.

The pilot model forms for the outer-loop position control tasks and for control of altitude are assumed invariant, going from fixed-base to moving-base conditions. The analysis therefore predicts no difference between moving base, angular motion only (MBA), and moving base, linear and angular motion (MBL) conditions.

"Switched Gain" Model for Display Scanning

Up to this point, the pilot models have assumed full attention to be paid to each of the three control tasks (longitudinal, lateral and vertical) in the experiment. To estimate the performance expected in the experimental situation where all tasks are controlled simultaneously, requires consideration of the pilot's scanning behavior, that is, how the pilot is likely to divide his time between the various displays and the resultant effects on his performance.

STI has hypothesized a "Switched Gain" model to account for the pilot's scanning behavior (Refs. 2 and 4). This model is not completely validated in that it has been verified experimentally for only a few controlled element types. The preexperimental analysis procedure outlined in the paragraphs which follow contains some implicit extensions

of the "Switched Gain" model; both the dynamics (requiring the pilot to generate lead) and the cues (motion feedbacks) differ from those cases where the model has been verified before.

The Switched Gain model hypothesizes that the pilot uses a quasi-random scan pattern over the various displays provided him. On each display he spends a finite dwell time gathering information so as to control the error signal on that display. He can also gather information from that display even while looking at the other displays if he uses his parafoveal vision; however, the information gained this way has a lower effective gain than when he is directly fixating the display. This gain switching takes place at quasi-random time intervals and has two important effects:

1. The effective pilot gain in each loop, given by the time average of his foveal/parafoveal gains, is smaller than it would be if he were devoting full attention to each display, thus he is not closing each loop as tightly as he could if he had single-loop control of that display. Further, there is a small time delay penalty (Ref. 2) for the attention-switching required to control all the loops.

2. This quasi-random finite-dwell sampling produces remnant in each channel sampled. This remnant has generally been found to be much greater than the remnant normally present in single-loop control, that is, if he were spending full time on a display with no other distractions. Finally, the power spectral density of the scanning remnant associated with a display scale with the variance of the displayed signal (Ref. 2) and that this interdependence significantly affects the total system.

Effect of Scanning Remnant on System Stability. Figure A-7 presents the system structure for the longitudinal task including the effects of scanning remnant. The pilot describing functions operating on the position and attitude errors and their divisions into visual and motion channels are the same as discussed above. An extra time delay, τ_s, is added for display scanning. Scanning noise components, n_x and n_θ, are shown to model the scanning remnant. There is no scanning remnant associated with the motion

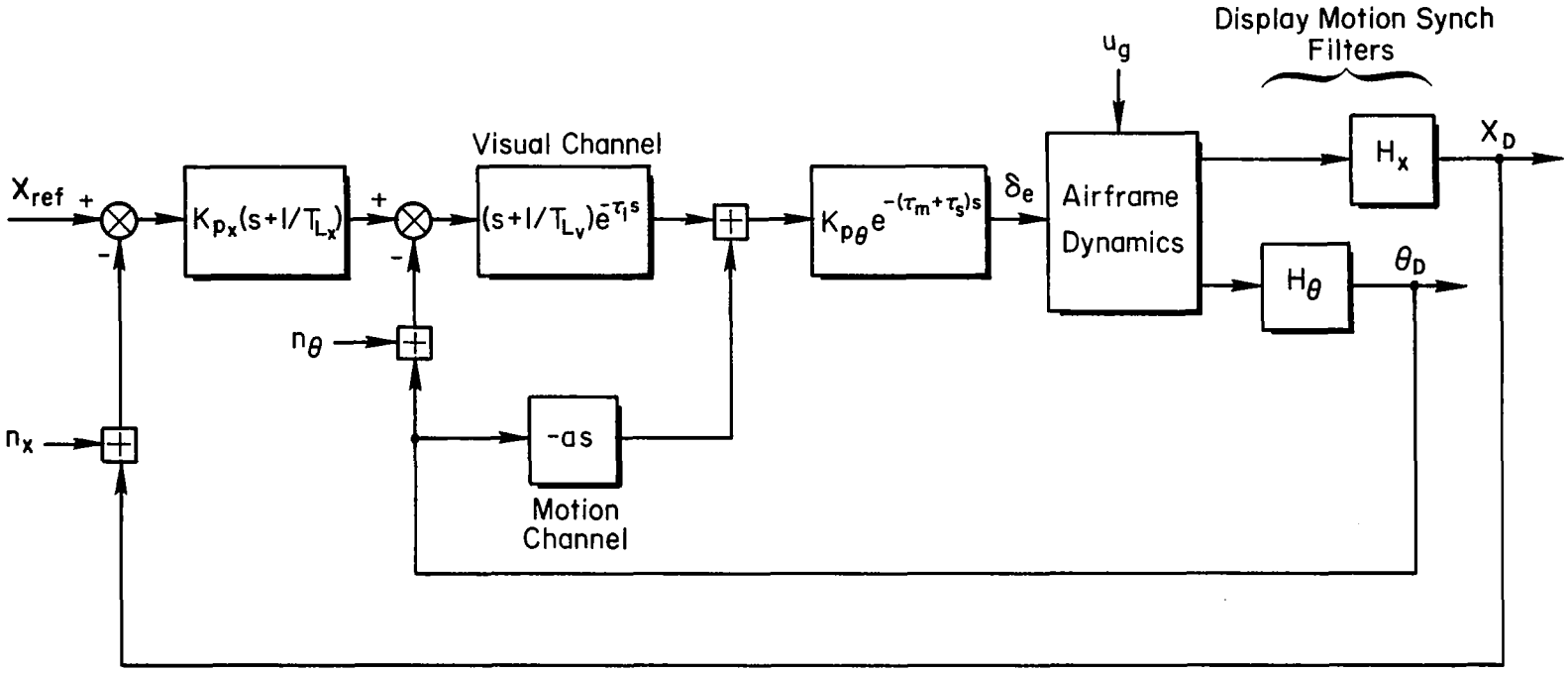

θ_D , X_D – Display (and simulator) motion quantities

n_θ , n_x – Scanning "Noise", introduced at pilot's visual inputs

u_g – Gust inputs , σ_g = 3 ft/sec , rms

$\tau_m + \tau_s$ – Pilot delay in vestibular modality (fixed) plus delay due to sampling

$\tau_\theta = \tau_m + \tau_1 + \tau_s$ – Pilot delay in visual modality (variable, depending on equalization requirements)

Figure A-7. Longitudinal Task Loop Topology

channel since that channel is presumably "wired in" at all times. The signals that the pilot is scanning in this model are the outputs of the display motion synchronization filters. Recall that the purpose of these filters was to synchronize the visual display with the sensed motions. In the experiment, the same objective was accomplished by lead compensation of the simulator motions. Note that each of the system outputs, x_d and θ_d, depend on three inputs, the gust input, u_g, and the two scanning remnant terms, n_x and n_θ. The scanning remnant noises are independent of each other and of the displayed signal (Ref. 4). Thus the system output variances ($\sigma^2_{x_D}$ and $\sigma^2_{\theta_D}$) can be written as:

$$\sigma^2_{x_D} = \sigma^2_{x_{u_g}} + \int_o^\infty \left|\frac{x_D}{n_x}\right|^2 \Phi_{n_x n_x}(\omega)d\omega + \int_o^\infty \left|\frac{x_D}{n_\theta}\right|^2 \Phi_{n_\theta n_\theta}(\omega)d\omega \qquad \text{(A-6)}$$

$$\sigma^2_{\theta_D} = \sigma^2_{\theta_{u_g}} + \int_o^\infty \left|\frac{\theta_D}{n_x}\right|^2 \Phi_{n_x n_x}(\omega)d\omega + \int_o^\infty \left|\frac{\theta_D}{n_\theta}\right|^2 \Phi_{n_\theta n_\theta}(\omega)d\omega \qquad \text{(A-7)}$$

where x_D/n_x is the closed-loop transfer function between the pilot's position display remnant and the system output

$\Phi_{n_x n_x}$ is the power spectral density of the n_x scanning remnant [(units of x)^2/rad/sec]

$\sigma^2_{x_{u_g}}$ and $\sigma^2_{\theta_{u_g}}$ are system responses to u_g and can be computed once the loop describing functions are selected (they are independent of remnant effects)

Equations A-6 and A-7 may be rewritten in matrix form as

$$\begin{bmatrix} 1 - \int_o^\infty \left|\frac{x_D}{n_x}\right|^2 \frac{\Phi_{n_x n_x}(\omega)}{\sigma^2_{x_D}}\,d\omega & -\int_o^\infty \left|\frac{x_D}{n_\theta}\right|^2 \frac{\Phi_{n_\theta n_\theta}(\omega)}{\sigma^2_{\theta_D}}\,d\omega \\ -\int_o^\infty \left|\frac{\theta_D}{n_x}\right|^2 \frac{\Phi_{n_x n_x}(\omega)}{\sigma^2_{x_D}}\,d\omega & 1 - \int_o^\infty \left|\frac{\theta_D}{n_\theta}\right|^2 \frac{\Phi_{n_\theta n_\theta}(\omega)}{\sigma^2_{\theta_D}}\,d\omega \end{bmatrix} \begin{bmatrix} \sigma^2_{x_D} \\ \sigma^2_{\theta_D} \end{bmatrix} = \begin{bmatrix} \sigma^2_{x_{u_g}} \\ \sigma^2_{\theta_{u_g}} \end{bmatrix} \qquad \text{(A-8)}$$

where the unknowns to be solved for are $\sigma^2_{x_D}$ and $\sigma^2_{\theta_D}$.

The terms on the right-hand side are the closed-loop responses to the gust inputs. The square matrix on the left-hand side is called the coherence matrix. The scanning remnant terms appear in it normalized by the variance of the displayed signal to which each remnant term adds; as indicated earlier, each of these scanning remnants scales with this variance. Thus the ratio, Φ_{nn_i}/σ_i^2 is independent of the variance, σ_i^2. This means that all of the elements in the coherence matrix depend upon loop closure parameters, and the normalized scanning remnant.

With scanning remnant effects included there is the possibility of an instability in the mean-square sense. This is different than the classical dynamic instability which can occur due to loop closures being so tight such that the pilot drives a response mode unstable. The nature of these two instability characteristics is sketched in Fig. A-8. This is a sketch of error variance versus crossover gain (taken from Ref. 2). If there were no scanning remnant, the pilot could use a fairly high gain and close in the region with the indicated stability margin from the dynamic instability boundary. However, when scanning remnant is present, he must reduce his gain such that he gets a larger error just due to this reduced gain, but in addition, there is an increment due to the forced switching of his attention around the display panel, and as indicated in Fig. A-8, the system can go unstable at a gain lower than the maximum gain for dynamic stability. This instability in

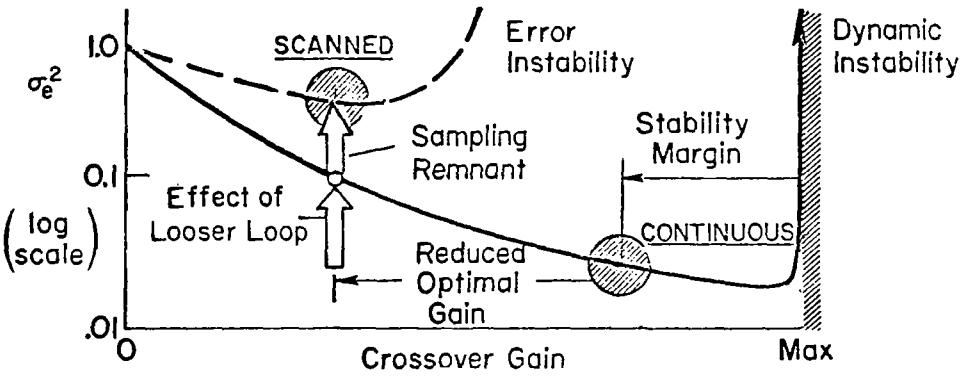

Figure A-8. Sketch of Scanning Implications on Gain and Performance

the mean-square sense manifests itself by the determinant of the coherence matrix becoming negative. Thus the loop closures must be selected so that the diagonal terms are always positive and sufficiently greater than the off-diagonal terms that the determinant of the coherence matrix is greater than zero. And generally it is found that it must be a fair amount greater than zero.

Scanning Terminology. For a given period of time corresponding to an experimental run length, T_R, the pilot spends a total time T_i fixating the ith instrument and a time T_{other}, looking elsewhere, thus:

$$T_R = \sum_{i=1}^{M} T_i + T_{other} \tag{A-9}$$

where M is the total number of instruments (displays). The time, T_i, is given by:

$$T_i = \sum_{k=1}^{N_i} T_{d_{i_k}} \tag{A-10}$$

where N_i is the number of times he looks at the ith instrument, and $T_{d_{ik}}$ is the time duration of the kth dwell on the ith instrument. The total number of looks during the run is obviously:

$$N = \sum_{i=1}^{M} N_i + N_{other} \tag{A-11}$$

where N_{other} numbers the looks elsewhere. The overall scanning frequency is given by:

$$f_s = \frac{N}{T_R} \tag{A-12}$$

The look fraction, ν_i, on the ith instrument is given by

$$\nu_i = \frac{N_i}{N} \tag{A-13}$$

There is a constraint on the look fractions such that

$$\sum_{i=1}^{M} \nu_i + \nu_{other} = 1 \tag{A-14}$$

where ν_{other} is the look fraction elsewhere. The <u>average</u> foveal dwell time is given by:

$$\overline{T}_{d_i} = \frac{1}{N_i} \sum_{k=1}^{N_i} T_{d_{i_k}} = \frac{T_i}{N_i} \tag{A-15}$$

The foveal dwell fraction is the fraction of time spent looking foveally at the ith instrument:

$$\eta_i = \frac{T_i}{T_R} = \frac{\overline{T}_{d_i}}{\overline{T}_{s_i}} \tag{A-16}$$

where $\overline{T}_{s_i}$ is the average time between looks at the ith instrument (or display sample interval) given by:

$$\overline{T}_{s_i} = \frac{T_R}{N_i} = \frac{T_R}{\nu_i N} = \frac{1}{\nu_i f_s} = \frac{1}{\overline{f}_{s_i}} \tag{A-17}$$

where $\overline{f}_{s_i}$ is the average look rate at (or scan rate of) the ith instrument. Note that $f_s = 1/\overline{T}_{s_i}\nu_i$ for i = 1, $\cdots$M. Obviously, there is an additional constraint on the scanning behavior which is that the sum of the dwell fractions (including time spent looking elsewhere than at the instruments) must be equal to unity:

$$\sum_{i=1}^{M} \eta_i + \eta_{other} = 1 \qquad \text{(A-18)}$$

If the task is very demanding, η_{other} will approach zero, as will T_{other}, ν_{other}, N_{other}, etc. In processing the scanning statistics, looks elsewhere (including blinks) are treated as an additional instrument — thus all terms in this development subscripted "other" are zero in the processing of scanning statistics (Appendix B).

Switched Gain Model Parameters. In the Switched Gain model for scanning behavior, the pilot is hypothesized to operate at one level of gain while looking at the instrument foveally, and another, lower level of gain while looking at it parafoveally. It is assumed that the lead and/or lag equalization, and the effective time delays are unchanged at each level of gain. Since the pilot operates in a K/s-like crossover region, the pilot gain adopted is proportional to the crossover frequency. Thus a foveal crossover frequency, $\omega_{c_{f_i}}$, and a parafoveal crossover frequency, $\omega_{c_{p_i}}$, for the ith instrument can be defined. Further, an effective dwell fraction can be defined according to:

$$\eta_{e_i} = \eta_i + (1-\eta_i)\frac{\omega_{c_{p_i}}}{\omega_{c_{f_i}}} = \frac{\omega_{c_{a_i}}}{\omega_{c_{f_i}}} \qquad \text{(A-19)}$$

where $\omega_{c_{a_i}}$ is the average crossover frequency for the ith instrument with both foveal and parafoveal viewing. The ratio, $\omega_{c_{p_i}}/\omega_{c_{f_i}}$ (called Ω_i), is generally one half or less.

The effective average dwell time can be defined as:

$$\bar{T}_{d_{e_i}} = \bar{T}_{d_i} + (\bar{T}_{s_i} - \bar{T}_{d_i})\frac{\omega_{c_{p_i}}}{\omega_{c_{f_i}}} \qquad \text{(A-20)}$$

Both the effective dwell time and the effective dwell fraction are greater than their foveal equivalents due to the additional information obtained between fixations on a given instrument due to parafoveal viewing.

There is an additional constraint on the pilot's scanning times which is a consequence of the need to sample a variable being displayed several times per average period. This is denoted by S_i, the sample frequency parameter of the ith instrument:

$$S_i = \frac{P_{c_i}}{\bar{T}_{s_i} - \bar{T}_{d_i}} = \frac{\omega_{s_i}}{\omega_{c_{a_i}}(1-\eta_i)} \qquad \text{(A-21)}$$

where P_{c_i} is the average period of the displayed signal, usually equal to $2\pi/\omega_{c_{a_i}}$, when the displayed signal power is concentrated in the region of crossover. $\bar{T}_{s_i} - \bar{T}_{d_{f_i}}$ is the average time between the end of a dwell and the next return to that instrument. Thus S_i is the ratio of the average period of the displayed signal to the average time-away from the display. Reference 2 found that $4 \leq S_i \leq 8$ with most values of S_i near 4.

Scanning Remnant Spectra Modeling. The form of the power spectral density of the scanning remnant introduced at the ith display is given in Ref. 4 as:

$$\Phi_{n_i n_i}(\omega) = \frac{(1-\eta_{e_i})}{\eta_{e_i}} \left(\frac{4(1-\delta_i)}{\pi \bar{T}_{d_{e_i}}}\right)\left(\frac{1}{\omega^2 + (2/\bar{T}_{d_{e_i}})^2}\right) \sigma_i^2 \qquad \text{(A-22)}$$

where σ_i is the rms display motion at the ith display

δ_i is a parameter related to the pilot's scan pattern variability. This is generally about 0.7.

This modeling of the remnant due to scanning is discussed in Ref. 2. It is dependent upon the effective dwell times on the pertinent displays, $\bar{T}_{d_{e_\theta}}$ of $\bar{T}_{d_{e_x}}$, the sampling variability parameters, δ_θ or δ_x, and the

effective dwell fractions, η_{e_θ} of η_{e_x}, on each display. The model is that of white noise passed through a simple lag filter with time constant of $\overline{T}_{d_{e_\theta}}/2$ (or $\overline{T}_{d_{e_x}}/2$). The rms level of the scanning remnants are given by

$$\sigma_{n_\theta} = \sqrt{\frac{(1-\eta_{e_\theta})(1-\delta_\theta)}{\eta_{e_\theta}}}\ \sigma_{\theta_D} \qquad \text{(A-23)}$$

or

$$\sigma_{n_x} = \sqrt{\frac{(1-\eta_{e_x})(1-\delta_x)}{\eta_{e_x}}}\ \sigma_{x_D} \qquad \text{(A-24)}$$

Therefore the scanning noise scales with the signal amplitude on each display as well as with the effective dwell fractions on each display, η_{e_θ} and η_{e_x}.

Switched Gain Model Algorithm. The selection of the switched gain model parameters for the various loop closures is an iterative process. It starts with a system survey where each of the control tasks is analyzed to define the range of possible pilot behavior in terms of the equalizations adopted, the crossover frequencies attained, and the dominant modes of display motion, using the quasi-linear pilot model adjustment rules. The ground rules for this analysis have already been discussed. Past experience (Ref. 4) would indicate that the phase and gain margins should be larger than would be the case if there were no scanning remnant. The desired outputs of this step include the foveal crossover frequency, $\omega_{c_{f_i}}$ (not necessarily the best achievable), a range of possible crossover frequencies, $\omega_{c_{a_i}}$ (restricted because of the conditional stability character of some loops and/or the need — based on past experimental observation — of considerable phase margin in these loops), and the dominant display motion frequencies (usually, but not always, the same as the achievable crossover frequencies).

On the basis of the preceding step, select the effective dwell fractions, η_{e_i}, and achievable crossover frequency, $\omega_{c_{a_i}}$, for each

loop in the several tasks. In particular, following a typical iterative sequence:

a. Select ω_{ca_i} based on reasonable values of η_{e_i} in each loop, according to

$$\eta_{e_i} = \frac{\omega_{ca_i}}{\omega_{cf_i}} \tag{A-25}$$

where ω_{cf} is close to the foveal values obtained fixed and moving base from Ref. 1 (i.e., dependent upon past experimental results modified, if necessary, by the results of the system survey).

b. Select $\Omega_i = \omega_{cp_i}/\omega_{cf_i}$ for each loop such that $\Omega_i \leq 0.5$ (typical value from Ref. 4) and compute the foveal dwell fractions, η_{f_i}, according to the equation:

$$\eta_i = \frac{\eta_{e_i} - \Omega_i}{1 - \Omega_i} \tag{A-26}$$

Some iteration may be necessary to satisfy the constraint that:

$$\sum \eta_i \leq 1 \tag{A-27}$$

In this step, it is assumed that the dwell fraction on the attitude ball and the position display (CRT) are effective for both the inner-loop tasks, and both of the outer-loop tasks. (If this were not true, there would be relatively little advantage in using these combined displays.)

c. Select reasonable values for the sampling frequency parameter, S_i, for each loop (display) based on the achieved crossover frequency for each display (modified, if necessary, if another mode is more dominant), according to:

$$4 \leq S_i \leq 8 \tag{A-28}$$

$$S_i = \frac{\omega_{s_i}}{\omega_{ca_i}(1 - \eta_{f_i})} \tag{A-29}$$

where

$$\omega_{s_i} = \frac{2\pi}{\overline{T}_{s_i}} \tag{A-30}$$

thus defining the average return time, $\overline{T}_{s_i}$.

d. Compute the average foveal dwell time according to

$$\overline{T}_{d_i} = \eta_i \overline{T}_{s_i} \tag{A-31}$$

This dwell time should exceed 0.4 sec, based on past experimental results. If it doesn't, some readjustment in the parameters computed up to this point will be necessary.

e. Compute the effective dwell time according to:

$$\overline{T}_{d_{ei}} = \eta_{e_i} \overline{T}_{s_i} = \eta_{e_i} \frac{1}{\overline{f}_{s_i}} \tag{A-32}$$

and the total average display scanning rate:

$$f_s = \sum_i \overline{f}_{s_i} \tag{A-33}$$

This latter value typically ranges between 1 and 1.3 "looks" per second, and serves as a gross check on the computations to this point.

f. Define the scanning remnant power spectral densities according to Eq. A-22. At this point, a tentative definition of the closed-loop parameters in each loop and the scanning behavior has been obtained.

g. Compute the coherence matrix to check for stability in the mean-square sense. This requires computation of the closed-loop responses to scanning remnant and gust inputs. If the coherence matrix is stable, the iteration is complete. If not, the scanning parameters must be readjusted starting with the first step, definition of the η_{e_i}. It may turn out that no solution satisfying all constraints can be obtained. The implication is clear — the configuration is too demanding.

h. Define the rms power for each display variable — this is the pilot performance. If the performance is very bad in one or more axes, while good in the remainder, it is likely that the system can be reiterated to improve the results.

EXAMPLE CALCULATIONS

In this subection, the results of the system survey of the various loops that the pilot must close to control all three tasks, are summarized. From these considerations are derived the postulated scanning traffic for these cases. Two example calculations for the extreme cases of the longitudinal dynamics are presented.

Assumptions and Ground Rules

To simplify the calculations and also to ease configuration comparisons, the following ground rules are followed:

a. All calculations are based on one scanning traffic set for the fixed-base cases and a slightly different set for the moving-base cases.

b. An additional time delay penalty due to scanning the display panel was added into each task. This amounted to τ_s equal to 0.05 sec (Ref. 2). See Fig. A-7 for the location of this τ_s in the longitudinal task model.

c. The pilot's lead in the pitch attitude closure is always adjusted to cancel the short-period real root. This is accomplished directly for the fixed-base cases whereas for the moving-base cases, the blend of the visual and motion pathways is used to accomplish this cancellation. In addition, this lead selection is applied to the lateral dynamics cases as appropriate.

d. The pilot's position lead, T_{L_X}, was set equal to one sec for all cases, both the longitudinal dynamics cases and the corresponding side deflections in the lateral cases. While this step may seem somewhat arbitrary, it does considerably simplify the resulting comparisons, and we shall estimate the consequences of other position lead values in a later section.

The loop crossover frequencies are based on the results of Ref. 1, which used the same simulator used in these experiments. In a single-loop roll control task Ref. 1 measured about 3.3 rad/sec moving base and 2.2 rad/sec fixed base. These numbers were fairly constant for a wide range of controlled element types from the extremes of no low frequency lead required to a very large amount of low frequency lead required. While these figures may be somewhat less than the absolute best that can be achieved for single-loop tasks, they nevertheless seem to reflect typical pilot loop closure tightness. Therefore these two crossover frequencies are used as reflecting the upper limits that the pilots will use if they could put full attention on the pitch angle or the bank angle task. Further, these two numbers indicate that the pilot can increase his crossover frequency by roughly 50 percent from fixed base to moving base, and this shall be reflected in all loop closures. Based on the foregoing and a careful survey of the loop closures across all the configurations, pitch angle closures of 1.5 rad/sec fixed base and 2.25 rad/sec moving base were assumed. These also apply to the lateral dynamics. A further rationale for the lower values is the recommendation in Ref. 4 that larger than normal stability margins (gain and phase) should be allowed to provide room for the effects of display scanning which can excite lightly damped closed-loop modes.

The outer or position loop was always closed at 0.5 rad/sec, both lateral and longitudinal. Again, this is based on the system survey of the likely loop closures and, in addition, is based on the Ref. 18 results where the outer loop was closed about 0.8 to 0.9 rad/sec. (The Ref. 18 situation landing approach control of pitch and altitude is quite similar to the longitudinal task here, control of pitch and position.) The selection of pilot lead in the position loop ($T_{I_X} = 1.0$ sec) is consistent with the measured data in Ref. 18 for a similar task. These data indicate that the outer loop lead time constant does not get much larger than this value.

The altitude loop can be closed at a fairly low crossover frequency, 0.4 rad/sec. This value is far lower than what one would expect for simple single loops with good damping characteristics. However, this value is forced by scanning limitations as shown in the next subsection.

Scanning Traffic

The fixed-base and moving-base scanning traffic parameters are shown in Table A-II for the three display instruments. The pitch and roll angles are on one combined display and the forward and lateral positions are combined on another display. A key assumption used in the predictions here is that when the pilot fixates the combined display, he gathers both pieces of information with no scanning penalty. This is based on the discussion in Appendix C of Ref. 4 where pertinent experimental data was examined and this conclusion drawn. In Table A-II the second column labeled $\omega_{c_{a_i}}$ is the actual crossover frequency at which the various loops were closed. The other quantities in the table are all discussed in detail in the next subsection. The basic constraint, of course, is that the foveal dwell fractions, η_i, must sum to 1 or less. The following points are noted:

a. The pilot spends better than 75 percent of his time observing the displays pertinent to the multiloop lateral and longitudinal tasks. This leaves relatively little time available to scan the altitude display, and is the major reason for the relatively low crossover frequency in this loop.

b. The overall display scanning rate given by the sum of the f_{s_i} numbers falls between 0.91 and 1.14 looks per second. This is a little low because the scanning traffic was originally computed including a directional control task. The Ref. 3 results for an all-axis landing approach task with ILS display (no flight director) showed overall scanning rates ranging between 1.02 and 1.36. Thus, the average number of fixations per second around the display seems to be typical, perhaps a little low.

c. The higher pitch attitude crossover frequency for the moving-base case demands a more frequent scanning ($\overline{f}_{s_\theta}$) of the attitude ball display, but less time is spend fixating it ($\overline{T}_{d_f}$) on each "look" because much of the lead is generated using motion cues.

TABLE A-II

SCANNING TRAFFIC FOR ALL CASES

A. Fixed-Base

Inst.	ω_{ca_i}	ω_{cf_i}	η_{e_i}	Ω_i	η_i^*	S_i	$\bar{f}_{s_i}$	$\bar{T}_{d_i}$	$\bar{T}_{de_i}$	δ_i	$2/\bar{T}_{de_i}$	σ_{n_i}/σ_i
θ , φ	1.5	1.97	0.763	0.5	0.525	4	0.455	1.15	1.67	0.7	1.2	0.305
x , y	0.5	0.798	0.627	↓	0.254	↓	0.237	1.07	2.65	↓	0.757	0.423
z	0.4	0.696	0.575	↓	0.150	↓	0.216	0.695	2.66	↓	0.752	0.471
					0.929		0.908					

B. Moving-Base

Inst.	ω_{ca_i}	ω_{cf_i}	η_{e_i}	Ω_i	$\eta_{f_i}^*$	S_i	$\bar{f}_{s_i}$	$\bar{T}_{d_i}$	$\bar{T}_{de_i}$	δ_i	$2/\bar{T}_{de_i}$	σ_{n_i}/σ_i
θ , φ	2.25	2.95	0.763	0.5	0.525	4	0.682	0.771	1.12	0.7	1.79	0.305
x , y	0.5	0.798	0.627	↓	0.254	↓	0.237	1.07	2.65	↓	0.757	0.423
z	0.4	0.696	0.575	↓	0.150	↓	0.216	0.695	2.66	↓	0.752	0.471
					0.929		1.135					

*The sum of the foveal dwell fractions is less than unity because the analysis originally included the directional control task, the scanning traffic for which is not shown. In effect, a $\eta_{other} = 0.071$ is assumed.

Example Cases (M_q = −4 and 0)

The two extremes of difficulty for longitudinal tasks illustrate the loop closures and coherence matrix aspects of this study. Figures A-9 through A-12 illustrate the inner- and outer-loop closures for the fixed- and moving-base cases for M_q = −4. Figures A-13 through A-16 illustrate the inner- and outer-loop closures for the fixed- and moving-base cases for M_q = 0. In both instances, the motion fidelity filters were assumed to be equal to a first-order lag at 10 rad/sec for angular motion (H_θ) and a second-order lag, at 5 rad/sec, with a damping ratio of 0.7 of critical (H_x). Table A-III summarizes the crossover frequency, gain

TABLE A-III

LOOP CLOSURE SUMMARY

	FIXED-BASE	MOVING-BASE
M_q = −4		
Attitude Loop		
Crossover Frequency	1.5 rad/sec	2.25 rad/sec
Gain Margin	7 dB	6 dB
Phase Margin	46 deg	39 deg
Position Loop		
Crossover Frequency	0.5 rad/sec	0.5 rad/sec
Gain Margin	9 dB	11.5 dB
Phase Margin	17 deg	17 deg
M_q = 0		
Attitude Loop		
Crossover Frequency	1.5 rad/sec	2.25 rad/sec
Gain Margin	+3 dB −7 dB	+4 dB −12 dB
Phase Margin	11 deg	18 deg
Position Loop		
Crossover Frequency	0.5 rad/sec	0.5 rad/sec
Gain Margin	4 dB	10 dB
Phase Margin	53 deg	22 deg

$$Y_{p_\theta} H_\theta \frac{N^\theta_{\delta_e}}{\Delta} = \frac{10K_\theta(.1)(4.012)(-9.75)(-9.75)}{[.195,.223](4.012)(9.75)(9.75)(10)}$$

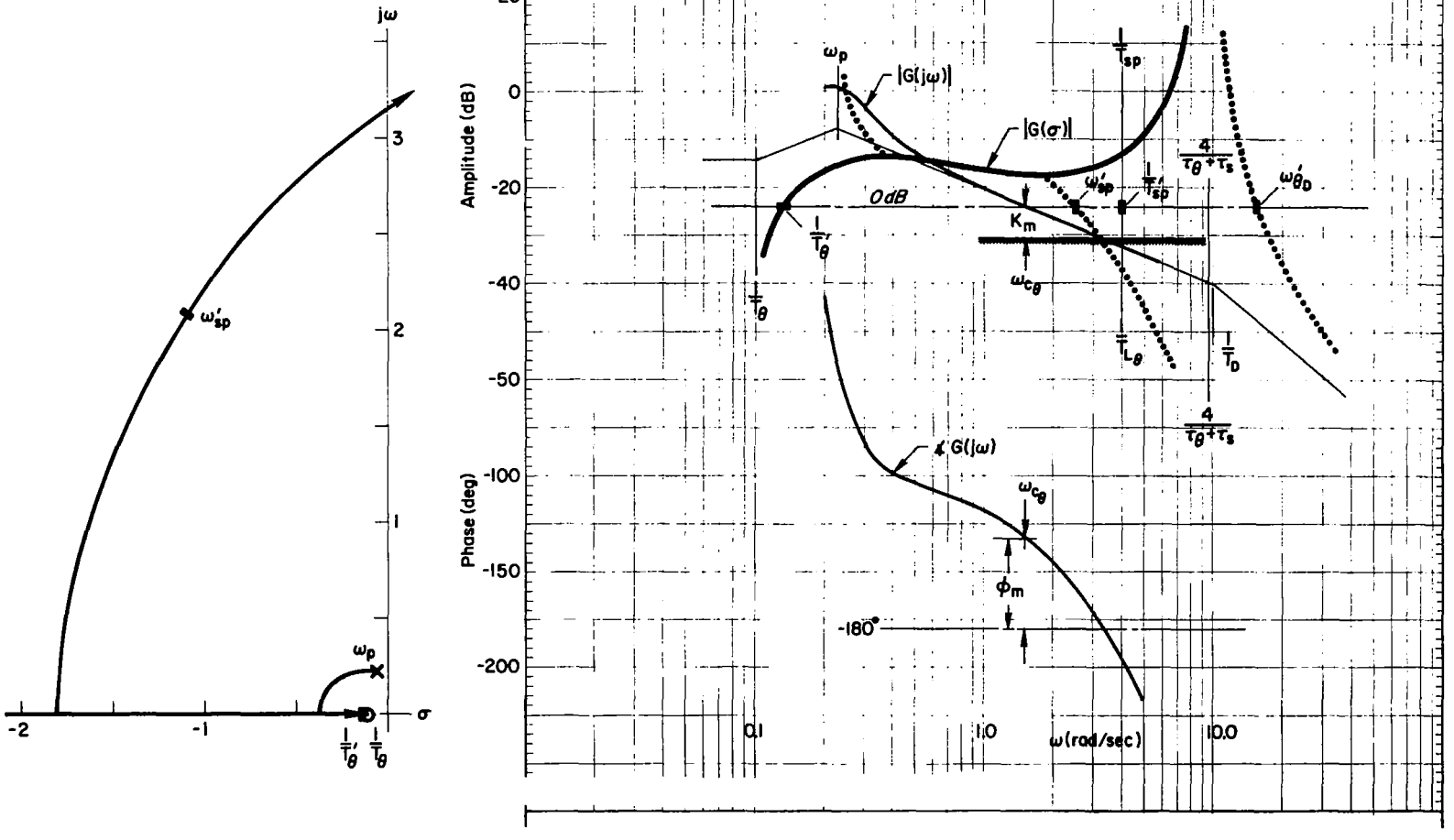

Figure A-9. System Survey for Pitch Attitude Closure, $\theta \rightarrow \delta_e$, Fixed Base, $M_q = -4$

$$\left(\frac{1}{T_D}\right)\left(\frac{4}{\tau_1}\right)^2\left(\frac{4}{\tau_m+\tau_s}\right)^2 Y_{p_x} Y'_{p_\theta} H_x \frac{N^x_{\delta_e}}{\Delta'} = \frac{-805\,K_{p_x}K_{p_\theta}(1)(1.24)(10)(-14.8)(-14.8)(-19)(-19)}{(0)(.321)(.62)[.196,2.573][.7,5][.644,14.533][.911,31.299]}$$

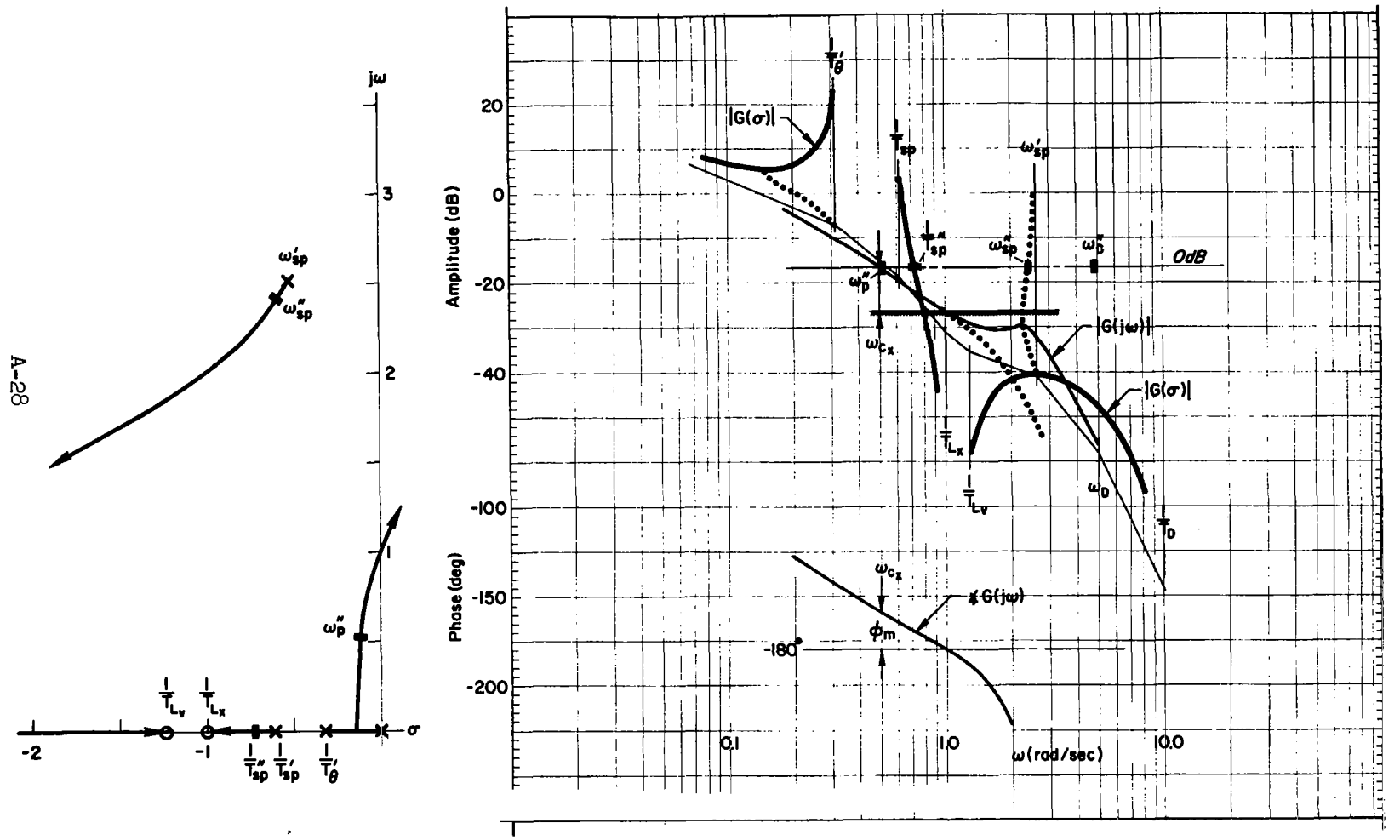

'Figure A-10. System Survey for Longitudinal Position Closure, $x \rightarrow \delta_e\big]_\theta \rightarrow \delta_e$, Fixed Base, $M_q = -4$

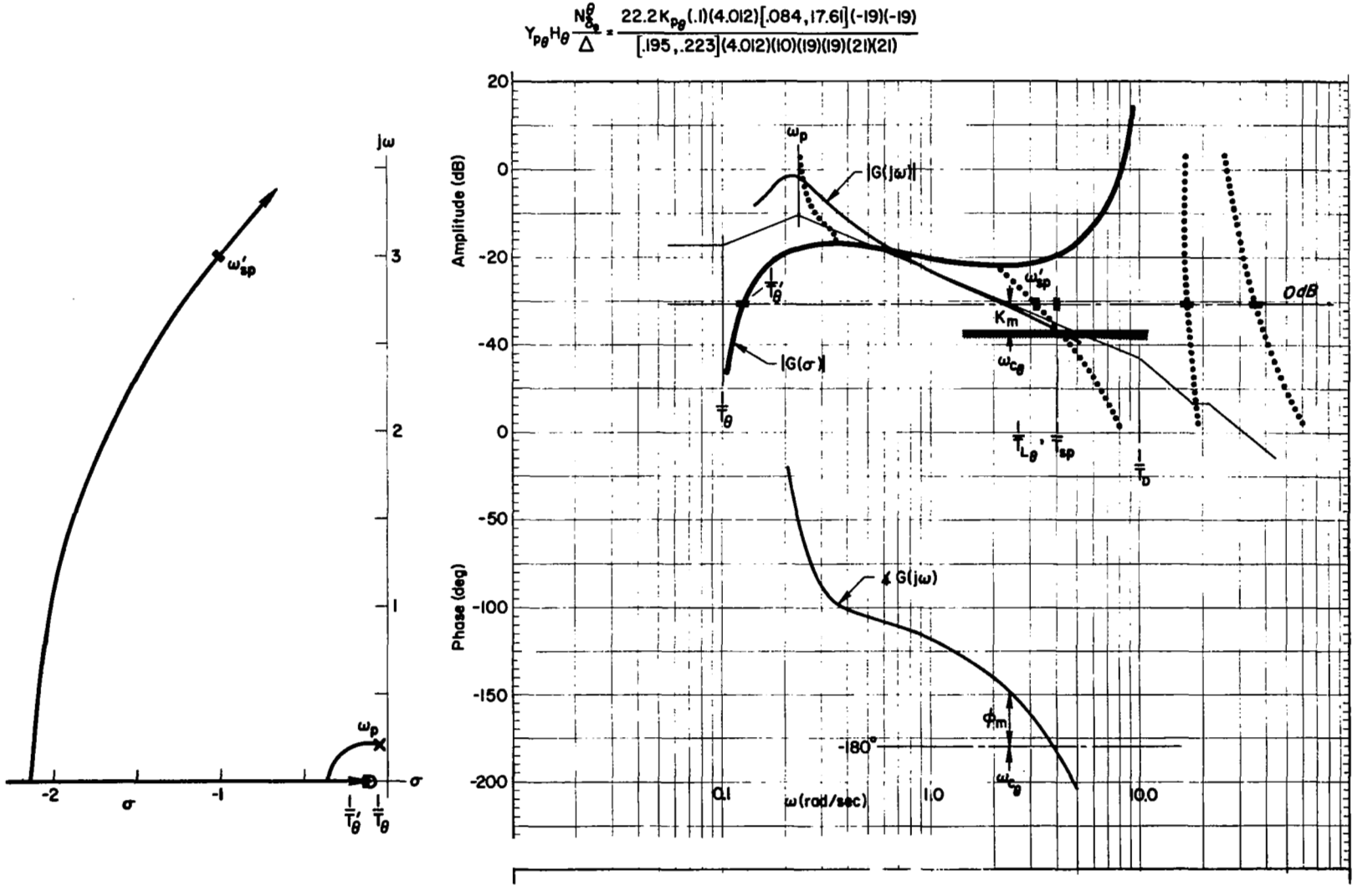

Figure A-11. System Survey for Pitch Attitude Closure, $\theta \rightarrow \delta_e$, Moving Base, $M_q = -4$

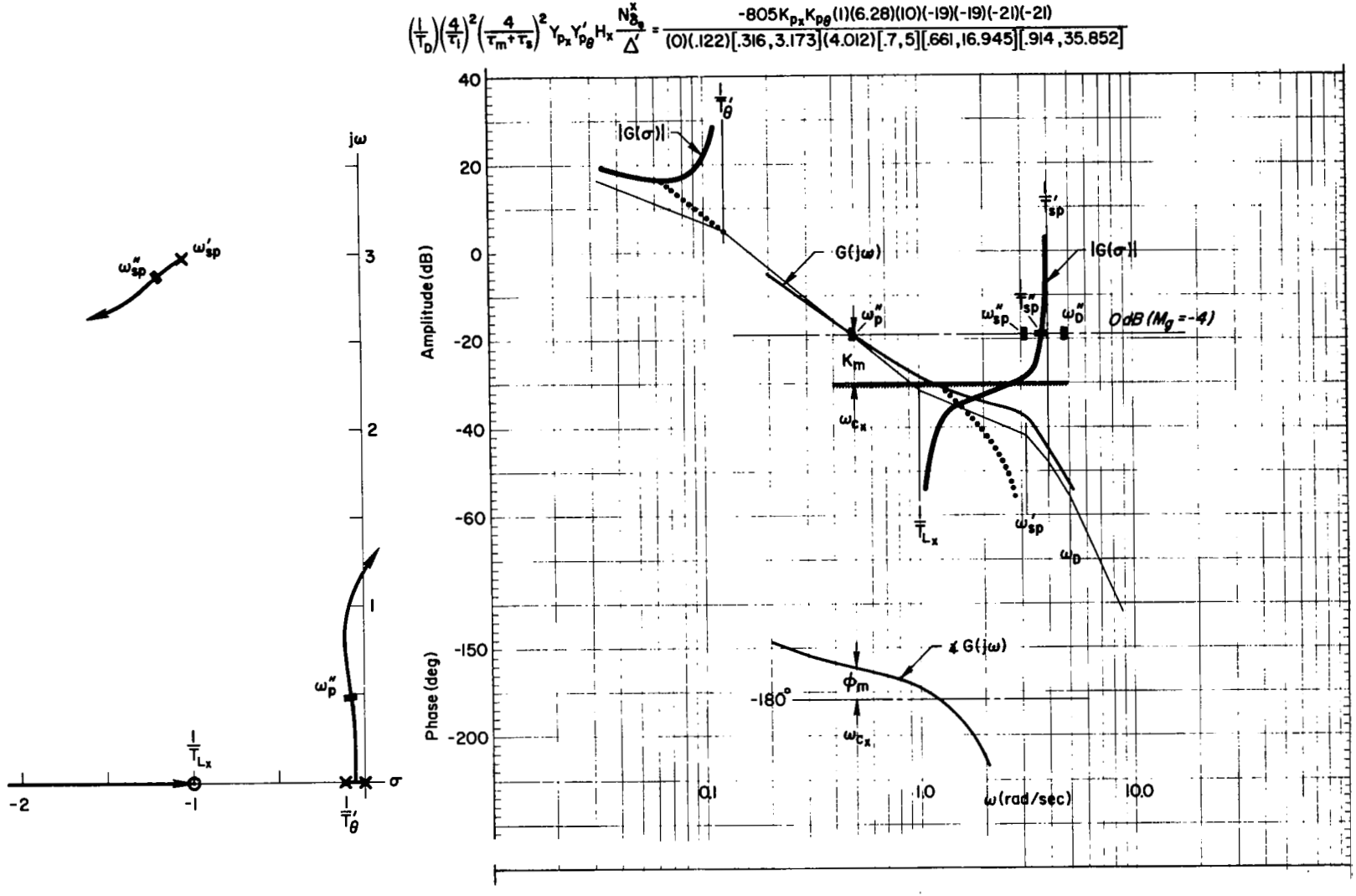

Figure A-12. System Survey for Longitudinal Position Closure, $x \rightarrow \delta_e \big| \theta \rightarrow \delta_e$, Moving Base, $M_q = -4$

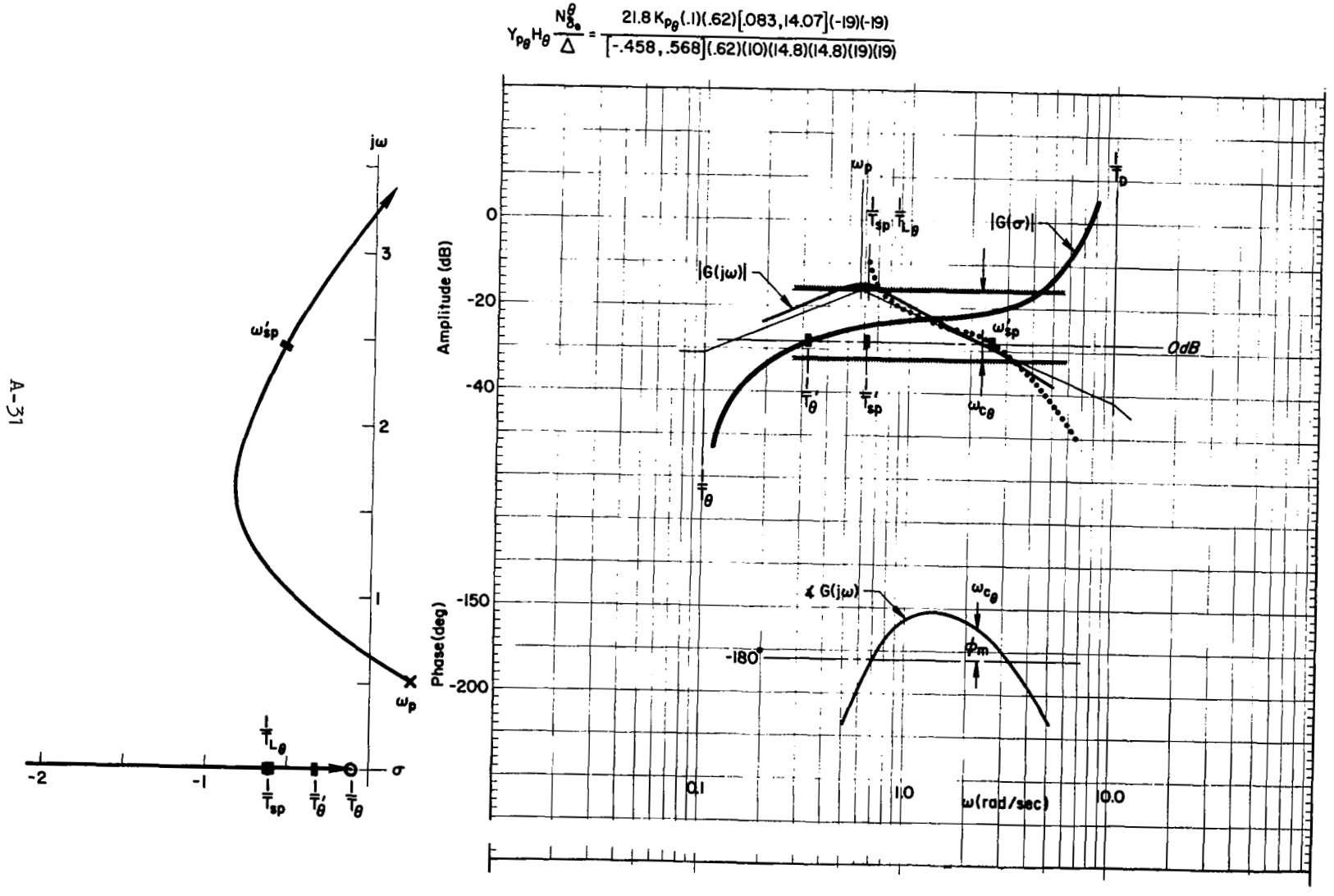

Figure A-13. System Survey for Pitch Attitude Closure, $\theta \rightarrow \delta_e$, Fixed Base, $M_q = 0$

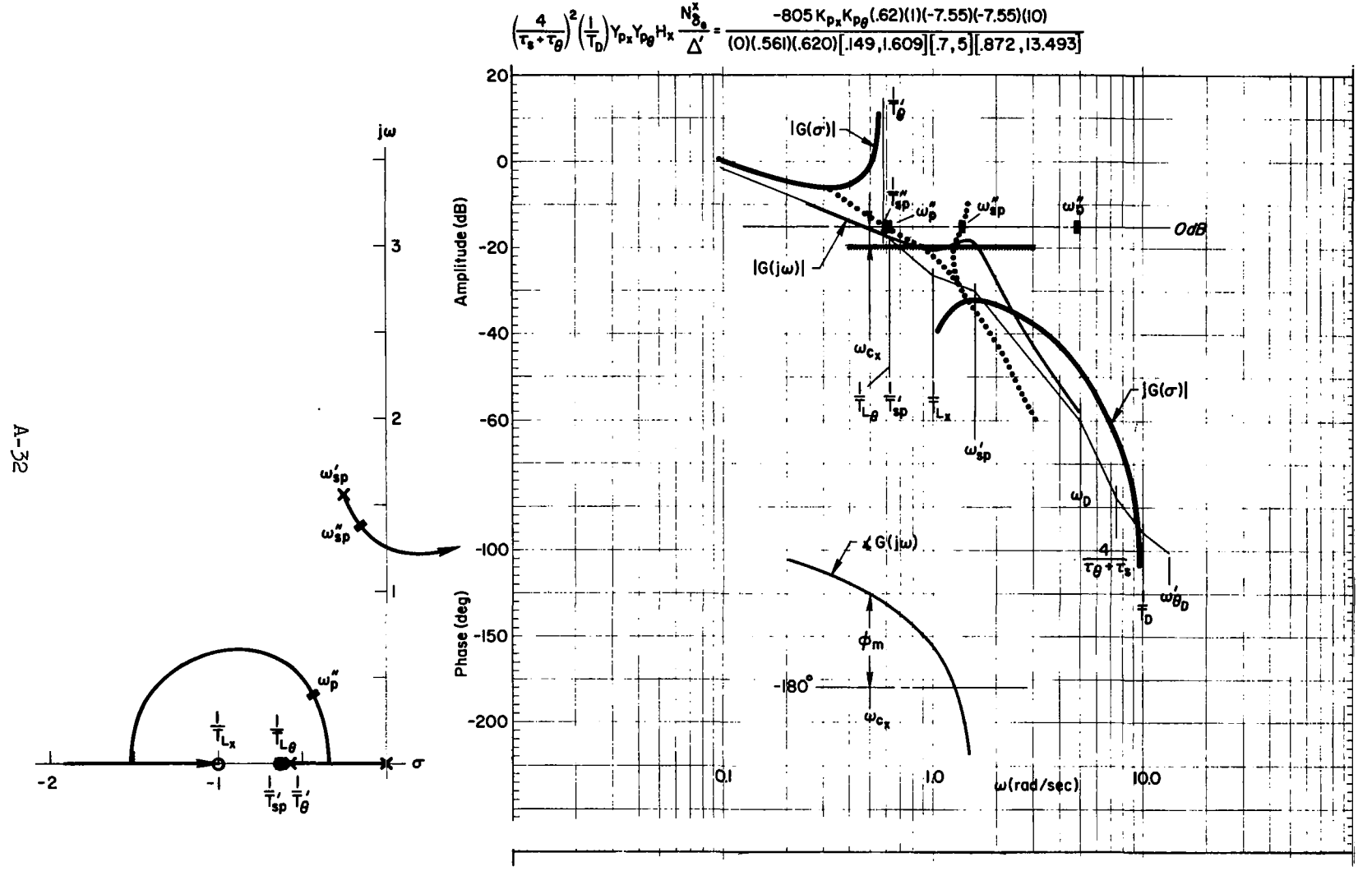

Figure A-14. System Survey for Longitudinal Position Closure, $x \rightarrow \delta_e\big|_\theta \rightarrow \delta_e$, Fixed Base, $M_q = 0$

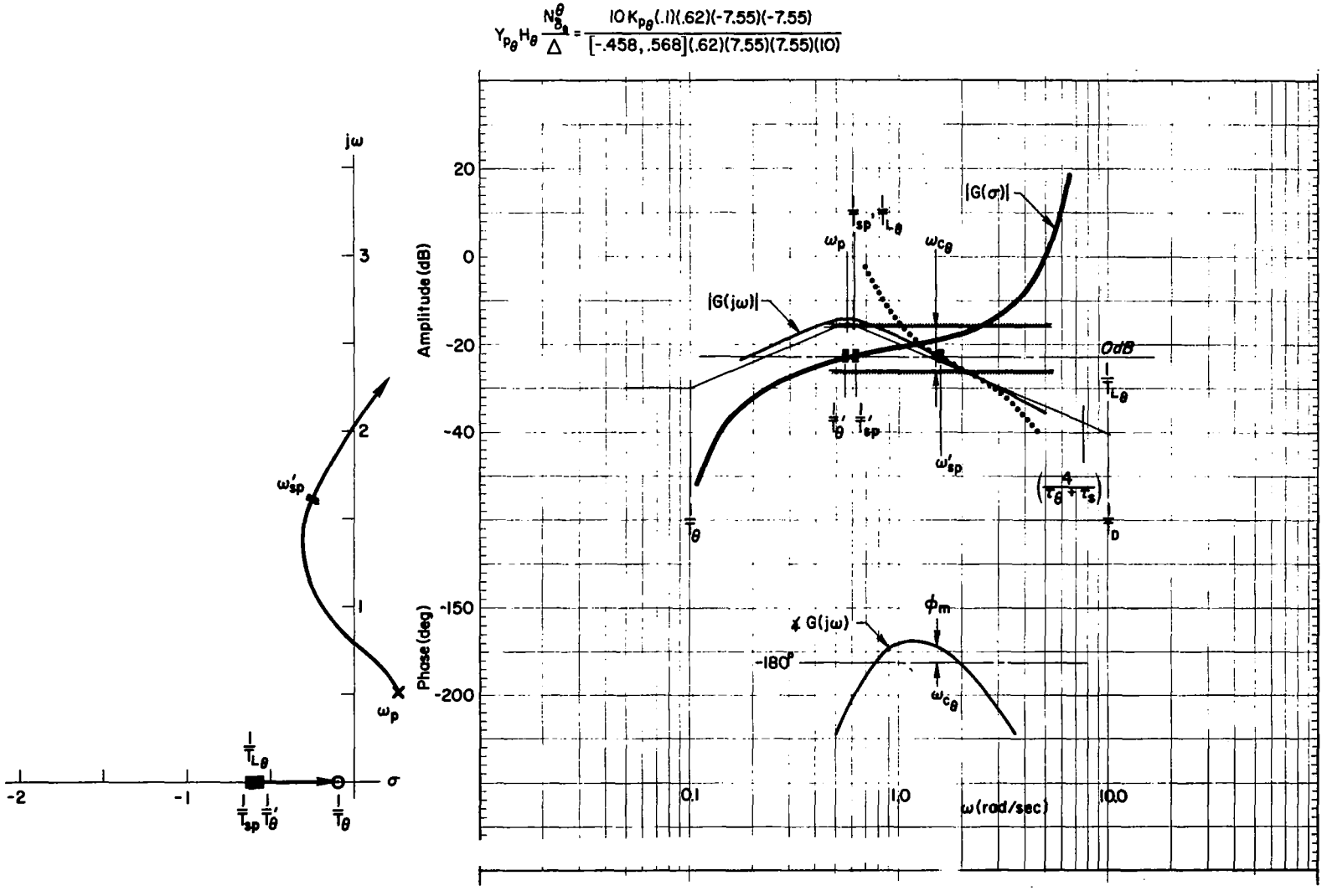

Figure A-15. System Survey for Pitch Attitude Closure, $\theta \rightarrow \delta_e$, Moving Base, $M_q = 0$

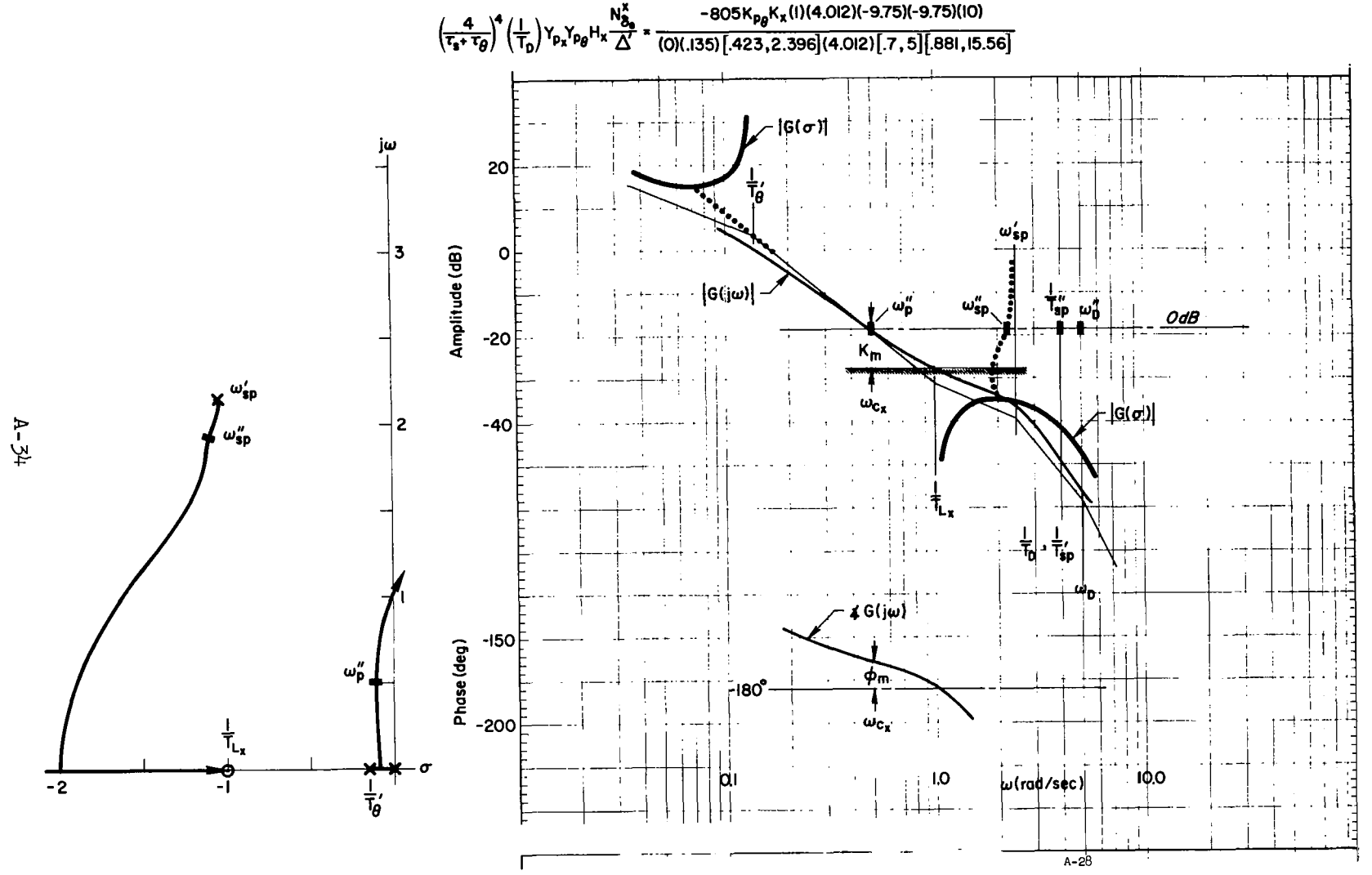

Figure A-16. System Survey for Longitudinal Position Closure, $x \rightarrow \delta_e\big|_\theta \rightarrow \delta_e$, Moving Base, $M_q = 0$

margin, and phase margin for these eight cases. All of these quantities are similar both fixed and moving base for the $M_q = -4$ case. However, the higher inner-loop crossover frequency moving base should provide somewhat better performance.

For the $M_q = 0$ cases, the inner loops are conditionally stable. This is reflected in the gain margins having positive and negative components, that is, the positive component indicates how much gain increase would produce instability, whereas the negative indicates how much gain decrease would produce instability. Note the attitude loop phase margin is very small fixed base and somewhat larger moving base. Both these values are quite a bit less than the phase margin achieved for the $M_q = -4$ case attitude loop. On the other hand, the fixed base position loop phase margins are considerably larger for $M_q = 0$ than for $M_q = -4$. The moving base position loop phase margins for these two values of M_q are essentially the same (as are the gain margins). The fixed-base position loop gain margin for the $M_q = 0$ case is quite a bit smaller than it is for $M_q = -4$ case.

Of these four cases, the largest differences occur between fixed and moving base for $M_q = 0$. For moving base the increased attitude loop crossover frequency and phase margin has given much better damping to the closed-loop phugoid mode even after the position loop is closed. The fixed-base phugoid mode is very lightly damped and at low frequency, and leads to difficulty in establishing stability in the mean-square sense.

Coherence Matrix Stability ($M_q = 0$ Cases)

The effects of these loop closures on the stability of the coherence determinant for $M_q = 0$ is illustrated in Eq. A-34 for fixed base and Eq. A-35 for moving base. These equations are numerical forms of Eq. A-8. Note that the coherence determinant for the fixed-base case has a negative element in the lower right corner, that is, the pitch response to the remnant on the pilot's pitch perception is larger than one. This same component for the moving-base case shown in Eq. A-35 is much smaller (0.175 versus 1.34). This large difference in stability is due to the

very low phase margin in the pitch attitude loop for the fixed-base case. The moving-base case short-period mode has larger damping and natural frequency compared with the fixed-base case (see the closed-root loops on the root loci in Figs. A-14 and A-16) due to the reduced effective time delay from obtaining pitch attitude lead via motion sensors. Further, closing the fixed-base case at a different attitude loop crossover frequency would not help significantly since his achievable phase margin is highly constrained due to the conditionally stable nature of this loop (see Fig. A-13).

Thus, for the most difficult longitudinal case, the addition of motion cues significantly improves the gust response performance (see the right hand column vectors in Eqs. A-34 and A-35) and further prevents an instability in the mean-square sense. If the pilots stabilize the $M_q = 0$ fixed-base cases, they will most likely have to put a higher percentage of the scanning traffic on the pitch display than shown here since this reduces the size of the pitch perception remnant.

$M_q = 0$, Fixed Base

$$\begin{bmatrix} 1 - 0.18 & -0.515 \\ -0.62 & \underbrace{1 - 1.34}_{\text{pitch response to remnant inserted on pitch perception}} \end{bmatrix} \begin{bmatrix} \sigma_{x_D}^2 \\ \sigma_{\theta_D}^2 \end{bmatrix} = \begin{bmatrix} (3.28)^2 \text{ ft}^2 \\ (2.4)^2 \text{ deg}^2 \end{bmatrix} \qquad \text{(A-34)}$$

$M_q = 0$, Moving Base

$$\begin{bmatrix} 1 - 0.25 & -0.363 \\ -0.155 & 1 - 0.175 \end{bmatrix} \begin{bmatrix} \sigma_{x_D}^2 \\ \sigma_{\theta_D}^2 \end{bmatrix} = \begin{bmatrix} (2.97)^2 \text{ ft}^2 \\ (1.32)^2 \text{ deg}^2 \end{bmatrix} \qquad \text{(A-35)}$$

Effects of Motion Fidelity Filters

In the Priority III runs of the experiment, interest is focused on the effects of simulator response lags, in particular, angular response lags. It is assumed, for simplicity, that a simple lag can be applied directly to the pilot's motion sensing describing function, viz.:

$$Y_{p_\theta} = K_{p_\theta}\left[asF + \left(s + \frac{1}{T_{I_V}}\right)e^{-\tau_1 s}\right]e^{-(\tau_m + \tau_s)s} \qquad \text{(A-36)}$$

where $F = b/(s+b)$ (high frequency lag) or

$F = 1$ (no filter)

Figure A-17 shows the effects of a low pass filter on the pilot's pitch equalization, Y_{r_θ}, for the $M_q = -4$ case. A 1/2 sec time constant is used. The low pass filter causes a slight amplitude increase (1 dB) and approximately 12 deg less phase margin. These slight changes should have little effect since the phase margin is big to begin with (39 deg) and the gain change can easily be adapted out.

Figure A-18 shows the effects of a low pass filter on the pilot's pitch equalization for the $M_q = 0$ case. The low pass filter has a 0.1 sec time constant. There is a very slight amplitude rise but, more important, a 7 deg loss of phase. This value reduces the phase margin from 18 deg to 11 deg which is the same as that obtained fixed base. Recall from the earlier discussion that the fixed-base case was very difficult to control. This relatively small amount of low pass filtering should have a significant effect on the pilot's control capabilities, and hovering precision.

The analysis therefore predicts a 0.1 sec lag to be significant in controlling Configuration 6, and a 0.5 sec lag to be relatively insignificant for Configuration 1, if it is assumed that only a small discrepancy between visual and motion cues results. If this discrepancy is too large, disorientation may result, leading to the pilot's downrating the configuration on that account.

ESTIMATED PERFORMANCE, PILOT RATINGS AND COMMENTARY

This subsection presents and discusses the estimated performance measures, pilot opinion differences, and pilot commentary for the various configuration and motion conditions. The performance measures presented below are not the full story. One reason is that a pilot may make up for bad dynamics by extreme equalization thereby achieving the same

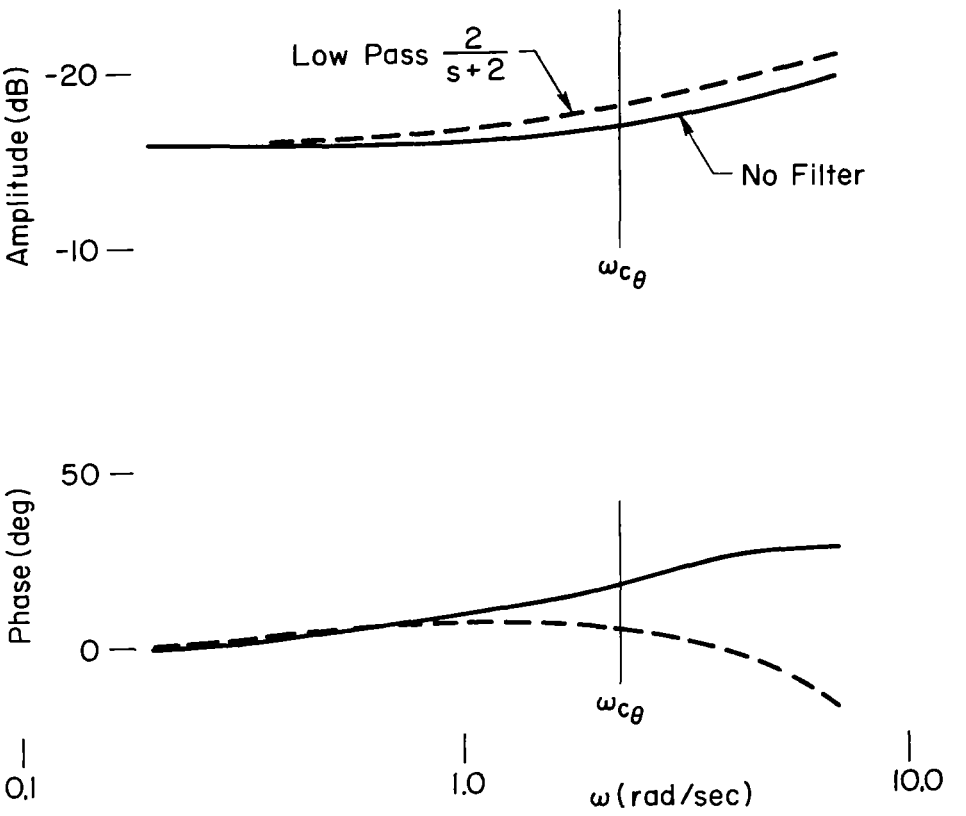

Figure A-17. Effects of Motion Fidelity Filters on Pilot Pitch Equalization ($M_q = -4$)

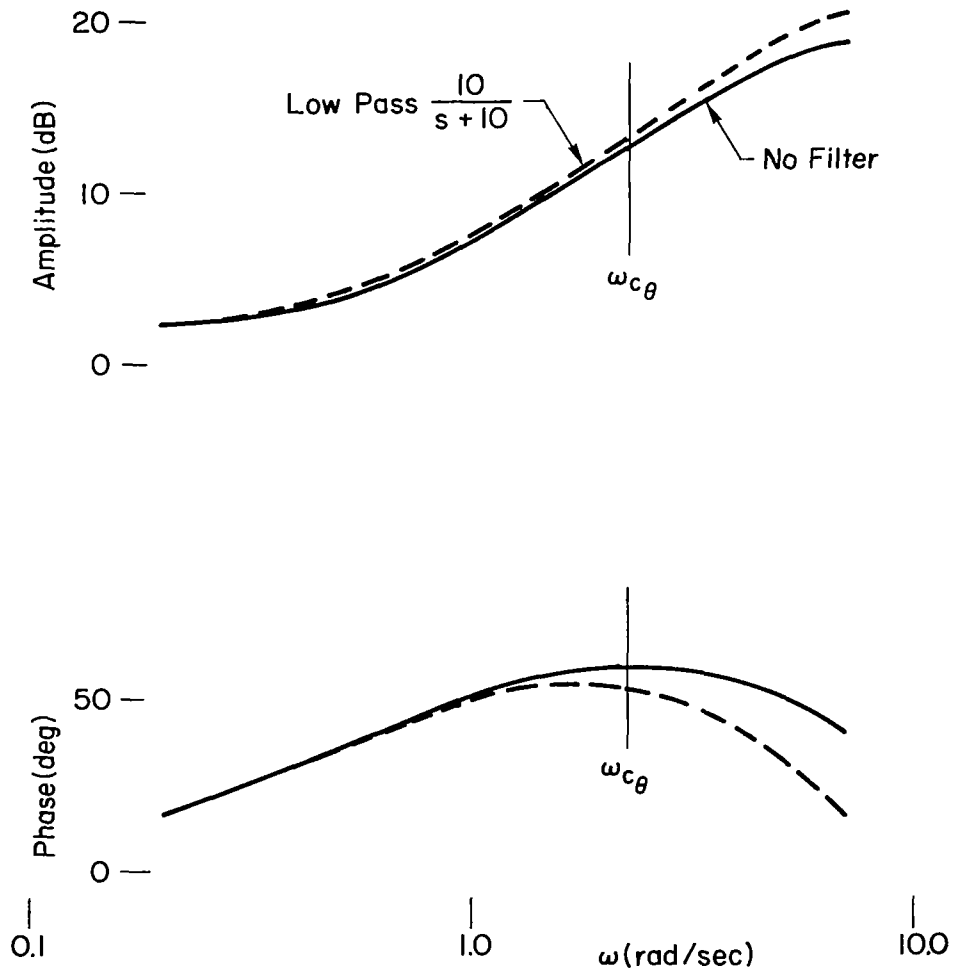

Figure A-18. Effect of Motion Fidelity Filters on Pilot Pitch Equalization ($M_q = 0$)

performance but yet he is working much harder in one instance. Thus, the pilot opinion results take a weighted sum of the achieved performance as well as the required pilot actions and should give a better overall assessment of the configuration and the fixed to moving base differences.

The primary emphasis in the following discussion is on fixed base to moving base differences, rather than the absolute values of performance or opinion. The scanning traffic used is that of Table A-II while the loop closure parameters are dictated by the assumptions and ground rules of the preceding subsections, viz.:

- Inner-loop crossover (longitudinal and lateral tasks) is at 1.5 rad/sec (FB) and 2.25 rad/sec (MBA and MBL).
- Inner-loop lead cancels the short-period pole at $1/T_{sp}$.
- Outer-loop crossover (longitudinal and lateral tasks) is at 0.5 rad/sec with outer-loop lead time constant fixed at $T_{L_x} = T_{L_y} = 1$ sec.
- Vertical task lead cancels the heave mode pole at $-(Z_w + Z_{\dot{w}})$, with crossover at 0.4 rad/sec.

Performance Measures

A summary of the computed normalized (by the pertinent gust input level) rms values for the various motion quantities is listed in Table A-IV. The phase margin and crossover frequency for each loop is included. For the ratios of the rms values to the gust input rms levels, the upper numbers in each block are the responses without scanning, while the lower values include the scanning remnant.

Fixed Base, Moving Base Comparisons for Good Lateral Dynamics. The closure parameters for Configuration 1 fixed and moving base were discussed earlier in this appendix. There was little difference in the estimated phase margins, but (referring to Table A-IV) significant differences in the rms position excursions, going from fixed to moving base. The stick deflection pitch rate and pitch position differences are minor with the moving base situation generally being smaller. The estimated pilot closure of altitude to collective has a low crossover frequency, large phase margin, and small position excursions — this task was estimated to

TABLE A-IV

NORMALIZED RMS PERFORMANCE MEASURE SUMMARY*

CONFIGURATION		LONGITUDINAL									VERTICAL				
		ω_{c_x}	φ_{m_x}	ω_{c_θ}	φ_{m_θ}	$\frac{\sigma_x}{\sigma_{u_g}}$	$\frac{\sigma_u}{\sigma_{u_g}}$	$\frac{\sigma_\theta}{\sigma_{u_g}}$	$\frac{\sigma_q}{\sigma_{w_g}}$	$\frac{\sigma_{M_{\delta_e}\delta_e}}{\sigma_{u_g}}$	ω_{c_z}	φ_{m_z}	$\frac{\sigma_z}{\sigma_{w_g}}$	$\frac{\sigma_w}{\sigma_{w_g}}$	$\frac{\sigma_{Z_{\delta_e}\delta_e}}{\sigma_{w_g}}$
1, 4, 9	FB	0.5	17	1.5	46	0.667 0.984	0.313 0.377	0.300 0.550	0.193	0.790	0.4	74	0.0934 0.0984	0.0550	0.151
	MBA & MBL		17	2.25	39	0.594 0.820	0.280	0.267 0.484	0.167	0.744					
2, 5, 10	FB		28	1.5	33	0.894 1.150	0.407	0.417 0.717	0.344	0.570					
	MBA & MBL		15	2.25	33	0.884 1.243	0.420	0.394 0.674	0.263	0.500					
3, 6, 11	FB		53	1.5	11	1.093	0.517	0.800	0.944	1.280					
	MBA & MBL		22	2.25	18	0.990 1.250	0.454	0.440 0.727	0.347	0.640					
7	FB, MBA & MBL	Same as Configuration 1										72	0.347 0.367	0.161	0.153
8	FB, MBA & MBL	Same as Configuration 1										71	1.022 1.080	0.292	0.157

*ω_{c_x}, ω_{c_θ}, ω_{c_z} in rad/sec; φ_{m_x}, φ_{m_θ}, φ_{m_z}, σ_θ in deg; σ_x, σ_z in ft; σ_u, σ_w, σ_{u_g}, σ_{w_g} in ft/sec; σ_q in deg/sec; $\sigma_{M_{\delta_e}\delta_e}$ in deg/sec^2; $\sigma_{Z_{\delta_e}\delta_e}$ in ft/sec^2.

TABLE A-IV* (Concluded)

CONFIGURATION		LATERAL								
		ω_{c_y}	φ_{m_y}	ω_{c_φ}	φ_{m_φ}	$\frac{\sigma_y}{\sigma_{v_g}}$	$\frac{\sigma_v}{\sigma_{v_g}}$	$\frac{\sigma_\varphi}{\sigma_{v_g}}$	$\frac{\sigma_p}{\sigma_{v_g}}$	$\frac{\sigma_{L_{\delta_a\delta_a}}}{\sigma_{v_g}}$
1, 2, 3 7, 8, 9 10 & 11	FB	0.5	17	1.5	46	0.667 0.984	0.313 0.377	0.300 0.550	0.193	0.790
	MBA & MBL		17	2.25	39	0.594 0.820	0.280	0.267 0.484	0.167	0.744
4, 5, 6	FB		37	1.5	25	0.990 1.282	0.440	0.490 0.914	0.454	0.647
	MBA & MBL		17	2.25	28	0.960 1.283	0.450	0.430 0.696	0.287	0.520

*ω_{c_y}, ω_{c_φ} in rad/sec; φ_{m_y}, φ_{m_φ}, σ_φ in deg; σ_y in ft; σ_v, σ_{v_g} in ft/sec; σ_p in deg/sec; $\sigma_{L_{\delta_a\delta_a}}$ in deg/sec^2.

be a much smaller load on the pilot. The expectation was that the pilot's primary effort will be on the longitudinal and lateral tasks. Table A-IV indicates that for Configuration 1, the loop closure parameters and estimated performance are the same for both the longitudinal and lateral tasks.

For Configuration 2, the fixed base/moving base comparisons for the longitudinal task show relatively small differences with moving base being slightly better (smaller estimated longitudinal position excursions). Pitch rate and stick deflections were both estimated to be significantly smaller moving base, reflecting the benefit of the motion cues on performance. The relatively large position excursions estimated for the moving base situation are probably due to the low phase margin, φ_{m_X}, in the position loop closure. This could be improved if the pilot uses a larger position loop lead than assumed for these calculations (T_{L_θ} = 1 sec). If he uses, for example, T_{L_θ} = 1.6 sec moving base, he will achieve the same phase margin as for fixed base, leading to a higher damping of the dominant position modes of response, and better performance in the form of smaller position excursions.

The closure parameters for Configuration 3 were discussed (p. A-35) where it was noted that the coherence matrix was unstable. Thus the prediction is that the pilot will have a very difficult time controlling the longitudinal task. If the remnant effect is ignored, Table A-IV predicts a better longitudinal response to gusts, moving base — much lower pitch and pitch rate response. Configuration 3 is therefore estimated to be quite sensitive to motion cue effects, primarily due to the small phase margin estimated for the inner, pitch loop closure.

Overall, the estimated pilot closures and performance in the longitudinal task shows that motion cues will be of positive benefit for Configurations 1, 2, and 3, and will be of greatest benefit for the most difficult (Configuration 3). Even so, the performance will deteriorate going from Configuration 1 to Configuration 3, moving base.

Fixed Base, Moving Base Comparisons for Bad Lateral Dynamics. When the lateral dynamics are bad (Configurations 4, 5, and 6) control over these dynamics is significantly worse than for Configurations 1, 2,

and 3 (Table A-IV). The rms lateral position deflections are nearly as large as the longitudinal excursions for Configuration 3. It will be harder for the pilot to contend with deteriorated longitudinal dynamics. Consequently it was estimated that Configuration 6 would have the poorest performance (assuming that it is controllable at all — the longitudinal task has an unstable coherence matrix), particularly fixed base; and would have the poorest pilot opinion.

Vertical Dynamics Cases. The damping of the vertical mode is reduced from Configuration 1 to 7 to 8 such that the vehicle becomes more gust sensitive. This shows up in the predicted performances in that for the same crossover frequency and essentially the same phase margin the rms altitude deviations increase markedly as does the rms altitude rates. However, the rms stick deflections are essentially unchanged. Thus the relatively large deterioration in performance for Configurations 7 and 8 may force a redistribution of scanning attention to the vertical axis display. No fixed to moving base differences were predicted in the vertical mode since all the available data indicate that only angular cues produce significant differences. However, Configurations 7 and 8 will still have fixed and moving base differences due to motion cue sensing of the longitudinal and lateral motions. The pilot will be able to divert more attention to the vertical task moving base because the motion cues are helpful in the other two tasks.

Effects of Pilot Location. Configurations 9 through 11 are intended to identify, by performance comparisons with Configurations 1 through 3, the effects of pilot location. The pilot's being located in front of the c.g. will provide coupling between pitch angle motions and vertical deflections that he can sense. Pitching motions involved in controlling the longitudinal dynamics produce vertical deflections which are sensed via the utricles.

As discussed in Ref. 1 the utricular sensors have a passband of about 1.5 rad/sec. Thus, due to the crossfeed effects of the pilot's location in front of the c.g., his utricles would be sensing $\ell_x \ddot{\theta}$ for low frequencies. This may be of some help in controlling the moving base cases. However this cue is not much different than sensing $\dot{\theta}$ via the semicircular canals.

The latter is good over a wide frequency range and was the basis of our model in which these cues are used to help provide lead in controlling pitch. It is not clear whether the linear cues will give a unique indication of pitching motions such that the likely effects could be easily predicted. In addition, the pilot is confronted with the task of trying to sort out those portions of the altitude motions which are in response to altitude gusts from those portions which are due to pitch angle feeding into the altitude display and simulator motions. He may use a cross controlling technique between the elevator and collective to offset the ℓ_x effect. With all these possibilities, plus the lack of any data which show any significant effects of utricular cues, the best estimate was that location effects are minimal.

Pilot Ratings

The predicted pilot ratings were based largely upon some work in Ref. 19 where a pilot rating formula that weights position excursions, pitch rate, and the various leads required was presented. The pilot rating formula was developed specifically for a hovering VTOL using a contact analog display (i.e., VFR conditions). For the experimental situation, the formula used was:

$$PR = 3.0 + \underbrace{\Delta T_{L_z}}_{1.2} + \underbrace{2.5(T_{L_\theta} + T_{L_\varphi})}_{6.5} + \underbrace{1.25(\Delta\sigma_x + \Delta\sigma_y)}_{5.0} \qquad \text{(A-37)}$$

Maximum Values →

where the Δ terms refer to changes in altitude lead and horizontal position excursions from the Configuration No. 1 condition, fixed base. The formula has rating penalties based on horizontal position excursions and visual lead generation in the various tasks (penalties for angular rates are small for the levels in this experiment). The factor of 3.0 is an estimate of the general set effects, the position lead generation requirements, and the effects of controlling all axes simultaneously.

The estimated pilot ratings resulting from this formula are given in Table A-V, wherein the ratings given are rounded off to the nearest half rating point modified by further interpretations of loop closures and scanning traffic. The change in the visual lead requirements going from fixed to moving base is such as to reduce the rating penalty and improve the rating for the moving base cases.

Pilot Commentary

Estimated pilot commentary is given in Table A-VI for Configurations 1, 2, and 3, for fixed and moving base conditions. For Configurations 4, 5, and 6, comments concerning the lateral task should be equivalent to those for the longitudinal task, Configuration 3. In particular, for Configuration 6, the predicted commentary should reflect incipient loss of control.

PREEXPERIMENTAL ANALYSIS SUMMARY

The analyses discussed in this appendix have made use of a multimodality (motion as well as visual cues) pilot model, modified to take account of display scanning effects. The predicted scanning behavior, performance and pilot ratings have been outlined. The results of the analysis may be qualitatively summarized as follows:

Configuration Effects

1. The configurations selected should range from easily controllable (Configuration 1) to marginally controllable (Configuration 6), especially fixed base. The range of cases selected should be a severe test of the multimodality pilot model.

2. Moving base simulator excursions may exceed simulator limits for difficult cases, presuming an input gust level of 3 ft/sec in all axes. A reduction in this level of excitation may be necessary for running the experiment.

3. The effects of locating the pilot forward of the center of gravity should be minor, at least with regard to performance. However, his rating may reflect this change due to the cross coupled motion.

TABLE A-V

ESTIMATED PILOT RATINGS, FIXED BASE

	$1.25\Delta\sigma_x$*	$1.25\Delta\sigma_y$*	$2.5T_{L_\theta}$	$2.5T_{L_\varphi}$	ΔT_{L_z}	TOTAL	TOTAL + 3	PREDICTED
1, 9	0	0	0.6	0.6	0	1.2	4.2	4
2, 10	0.6	0	2.1	0.6	0	3.3	6.3	6.5
3, 11	∞	0	3.25	0.6	0	∞	∞	8
4	0	1.2	0.6	3	0	4.8	7.8	7
5	0.6	1.2	2.1	3	0	7	10	8.5
6	∞	1.2	3.25	3	0	∞	∞	9 – 10
7	0	0	0.6	0.6	0.5	1.7	4.7	4.5
8	0	0	0.6	0.6	1.2	2.4	5.4	5.0

*$\sigma_{u_g} = \sigma_{v_g} = 3$ ft/sec, rms.

TABLE A-V (Concluded)

ESTIMATED PILOT RATINGS, MOVING BASE

	$1.25\Delta\sigma_x$*	$1.25\Delta\sigma_y$*	$2.5T_{L_\theta}$	$2.5T_{L_\varphi}$	ΔT_{L_z}	TOTAL	TOTAL + 3	ESTIMATED PILOT RATING
1, 9	-0.6	-0.6	0.4	0.4	0	-0.4	2.6	2.5
2, 10	0.9	-0.6	1.1	0.4	0	1.8	4.8	5
3, 11	0.9	-0.6	2	0.4	0	2.7	5.7	6
4	-0.6	1.1	0.4	1.5	0	2.4	5.4	5.5
5	0.9	1.1	1.1	1.5	0	4.6	7.6	7.5
6	0.9	1.1	2	1.5	0	5.5	8.5	8.5
7	-0.6	-0.6	0.4	0.4	0.5	0.1	3.1	3
8	-0.6	-0.6	0.4	0.4	1.2	0.8	3.8	3.5

*Assumes $\sigma_{u_g} = \sigma_{v_g} = 3$ ft/sec, rms.

TABLE A-VI

PREDICTED PILOT COMMENTS

CONFIG.	TECHNICAL FEATURES OF PREDICTED CLOSURES	TRANSLATION INTO LIKELY PILOT COMMENTS
1	No low frequency lead in pitch or roll required. Low frequency lead in position required. Loops not conditionally stable.	1. Pitch and roll are easy to control and positions require some anticipation. 2. Good performance 3. Not too sensitive in any axis. 4. Moving base position can be controlled somewhat better than fixed base.
2	Low frequency lead required in pitch and x, y positions. Motion cues lessen visual lead needs. Pitch loop conditionally stable.	Fixed Base: 1. Must avoid wrong corrections on pitch display since stick reversal errors can produce large excursions. 2. Must anticipate pitch motions. 3. Tight pitch control necessary Moving Base: 1. Pitch control not as sensitive as for fixed base, can anticipate pitch motions more confidently. However must still anticipate position changes.
3	Low frequency lead required in pitch especially fixed base where phase margin is very low. Pitch loop conditionally stable. Motion cues lessen visual lead needs.	Fixed Base: 1. Must monitor pitch very closely. Avoid stick reversal errors. 2. Can't keep both position and pitch well controlled as both require much anticipation. Moving Base: 1. Pitch task significantly easier than for fixed base. Can keep all motions reasonably well controlled (nearly as good as Configuration 2). 2. Must still avoid stick reversal errors.

Motion Effects

1. Motion effects should range from moderate for easy cases to very significant for the most difficult tasks. The moving/fixed base performance differences should range from small to substantial. However, pilot opinion moving base should always be better than fixed base since it is a weighted sum of both performance and the pilot's actions necessary to achieve that performance, i.e., heroic efforts fixed base might produce the same performance measures as moving base but the pilot's opinion will reflect these extreme efforts.

2. For moving-base cases the pilot model uses angular motion cues to aid in pitch and roll control. This results in a lower effective time delay compared to fixed-base cases.

3. There should be minor differences between moving base runs with angular motion only (MBA), and those with linear and angular motion (MBL).

4. The effects of simulator lag should be most easily felt on the most difficult configuration (where motion cues are of the greatest benefit).

Display Scanning Behavior

1. The separated displays used in this multiloop multi-axis task situation require pilot scanning. The switched gain model predicts reduced crossover frequencies due to this attention sharing (reduced from the values that could be achieved in each loop if it were controlled as a single-axis task).

2. The pilot should spend a large percentage of the time on pitch and position displays. For the very difficult configuration he should devote an even larger fraction of attention to the pitch and roll display at least for the fixed-base cases.

3. For the moving-base cases the higher pitch attitude crossover frequency demands more frequent scanning of the attitude display but less time is spent fixating it on each look because much of the lead is generated using vestibular cues.

4. The pilot's display scanning generates remnant which can have an important effect on the potential stability of each loop. The reduced crossover frequencies mentioned above are beneficial in preventing this scanning remnant from exciting lightly damped modes and causing potential instabilities in the mean-square sense. For a configuration where both longitudinal and lateral dynamics are extremely difficult, the model predicts an incipient loss of control for the fixed-base cases. This condition is alleviated for the moving-base case due to the lower effective time delay.

APPENDIX B

PERFORMANCE AND SCANNING DATA FOR CONFIGURATIONS 1, 3, 4, AND 6

Tables B-I through B-XII list the performance for these configurations for each subject for the Priority I, II, and IV experiments. Some of the Priority III data is also included where that data is pertinent to be a zero motion lag condition. The data is annotated in many cases to indicate why certain runs were repeated, and parentheses are used to indicate those data points not used in the performance averages presented in the main body of the report. Certain additional runs on these configurations were made which are not given. These involve errors in setup (e.g., GB ran six runs on Configuration 6 where L_p was inadvertently set to zero instead of -0.5) or procedure.

Table B-XIII presents the scanning data obtained from the Priority IV experiment.

TABLE B-I

CONFIGURATION NO. 1 PERFORMANCE, SUBJECT RG

PERFORMANCE VARIABLE	MOTION CONDITION	WARMUP 15 DEC.	WARMUP 17 DEC.	PRIORITY II 17 DEC.	PRIORITY IV 18 DEC.		AVERAGED PERFORMANCE
Run No.	FB	—	—	168	222	225*	
	MBL	—	—	167	223		
	MBA			169	224		
σ_q (deg/sec)	FB	0.230	0.232	0.185	0.289	0.270	0.22
	MBL	0.161	0.268	0.200	0.207		0.21
	MBA			0.192	0.254		0.22
σ_θ (deg)	FB	0.430	0.457	0.421	0.355	0.545	0.44
	MBL	0.265	0.394	0.386	0.332		0.34
	MBA			0.316	0.475		0.40
σ_u (ft/sec)	FB	0.589	0.776	0.704	0.431	0.787	0.66
	MBL	0.414	0.584	0.700	0.468		0.54
	MBA			0.503	0.570		0.54
σ_x (ft)	FB	3.611	2.828	2.510	1.220	2.496	2.5
	MBL	1.398	2.010	2.452	1.401		1.8
	MBA			1.936	1.981		2.0
σ_φ (deg)	FB	0.524	0.561	0.479	0.423	0.542	0.51
	MBL	0.361	0.424	0.317	0.354		0.36
	MBA			0.405	0.506		0.46
σ_y (ft)	FB	2.096	1.871	2.147	1.292	1.251	1.7
	MBL	1.876	1.500	1.366	1.330		1.5
	MBA			1.190	1.671		1.4
σ_w (ft/sec)	FB	0.543	0.468	0.510	0.427	0.445	0.48
	MBL	0.420	0.431	0.427	0.415		0.42
	MBA			0.470	0.469		0.47
σ_z (ft)	FB	1.118	1.028	1.210	0.759	1.069	1.0
	MBL	0.914	1.152	1.053	0.901		1.0
	MBA			0.861	0.942		0.9
σ_{disp} (ft)	FB	4.323	3.543	3.518	1.932	2.989	3.0
	MBL	2.512	2.760	2.997	2.131		2.6
	MBA			2.430	2.757		2.6
PR	FB	6.5	7.0	7.0	6.0	7.0	6.7
	MBL	6.0	6.5	6.5	6.5		6.4
	MBA			6.25	6.5		6.4

*This additional run was made because of EPR calibration problems on Run 222.

TABLE B-II

CONFIGURATION NO. 1 PERFORMANCE, SUBJECT EF

PERFORMANCE VARIABLE	MOTION CONDITION	WARMUP 9 DEC	WARMUP 10 DEC	PRIORITY I, CONFIG. 9 10 DEC		WARMUP 11 DEC	PRIORITY II, CONFIG. 1 11 DEC		WARMUP 16 DEC	PRIORITY II 16 DEC		PRIORITY IV 17 DEC		PRIORITY IV 18 DEC		AVERAGED PERFORMANCE
RUN NO.	FB	—	—	59	60	—	75	76	—	158*	159	183†	189	190†	191	
	MBL	—	—	57	58	—	73	74	—		160		185		193	
	MBA						71	72			161		184		192	
σ_q (deg/sec)	FB	0.259	—§	0.214	0.226	0.445	0.408	0.376	0.232	(0.284*)	0.295	(0.294†)	0.198	0.165†	0.156	0.27
	MBL	0.386	—§	0.375	0.432	0.477	0.454	0.378	0.218		0.417		0.266		0.226	0.34
	MBA						0.410	0.303			0.503		0.235		0.237	0.36
σ_θ (deg)	FB	0.458	(0.606§)	0.394	0.365	0.423	0.397	0.333	0.340	(0.496*)	0.444	(0.468†)	0.343	0.280†	0.304	0.37
	MBL	0.650	(0.507§)	0.616	0.638	0.429	0.428	0.374	0.331		0.493		0.397		0.361	0.47
	MBA						0.440	0.388			0.517		0.333		0.311	0.40
σ_u (ft/sec)	FB	0.664	(0.489§)	0.529	0.443	0.521	0.547	0.487	0.498	(0.759*)	0.618	(0.666†)	0.542	0.383†	0.451	0.52
	MBL	0.788	(0.560§)	0.777	0.717	0.510	0.553	0.463	0.460		0.603		0.542		0.502	0.59
	MBA						0.532	0.513			0.501		0.492		0.376	0.48
σ_x (ft)	FB	1.946	(2.927§)	1.559	1.100	1.704	2.404	1.308	1.533	(2.234*)	2.156	(2.362†)	2.620	1.235†	1.697	1.8
	MBL	2.372	(1.926§)	2.419	1.908	1.822	1.440	1.351	1.603		1.769		2.480		1.518	1.9
	MBA						1.384	1.398			1.235		1.853		1.695	1.5
σ_ψ (deg)	FB	0.562	(0.578§)	0.653	0.544	0.631	0.620	0.539	0.811	(0.596*)	0.552	(0.688†)	0.387	0.484†	0.499	0.57
	MBL	0.751	(0.755§)	0.730	0.959	0.684	0.482	0.586	0.560		0.611		0.494		0.503	0.64
	MBA						0.481	0.447			0.695		0.547		0.414	0.52
σ_y (ft)	FB	1.311	(2.634§)	1.536	1.552	1.513	2.307	1.581	1.639	(2.598*)	1.658	(2.727†)	1.672	1.843†	1.796	1.7
	MBL	2.120	(2.170§)	1.843	2.288	2.409	2.367	1.881	1.829		1.622		2.465		2.268	2.1
	MBA						1.735	1.987			1.546		1.744		1.360	1.7
σ_w (ft/sec)	FB	0.467	(0.400§)	0.490	0.515	0.517	0.645	0.569	0.531	(0.553*)	0.548	(0.519†)	0.497	0.582†	0.655	0.55
	MBL	0.606	(0.430§)	0.474	0.538	0.577	0.476	0.631	0.437		0.473		0.612		0.510	0.53
	MBA						0.519	0.443			0.489		0.458		0.718	0.52
σ_z (ft)	FB	2.104	(2.857§)	1.783	1.584	1.726	2.098	2.312	1.356	(1.509*)	1.633	(2.657†)	1.143	1.536†	1.610	1.7
	MBL	2.600	(1.192§)	2.310	2.260	1.618	1.841	2.517	1.084		1.400		1.696		1.437	1.9
	MBA						2.150	1.512			1.205		1.088		1.599	1.5
σ_{disp} (ft)	FB	3.151	(4.865§)	2.823	2.476	2.859	3.937	3.091	2.622	(3.744*)	3.173	(4.480†)	3.311	2.698†	2.949	3.0
	MBL	4.108	(3.137§)	3.819	3.739	3.427	3.327	3.421	2.663		2.778		3.886		3.084	3.4
	MBA						3.090	2.862			2.228		2.767		2.698	2.7
PR	FB	4.0	(4.0§)	3.5	3.5	3.0	4.5	4.0	5.0	—	6.0	(4.0†)	4.0	—	—	4.2
	MBL	4.0	(3.75§)	4.5	4.0	4.0	4.0	4.0	4.0		5.0		4.5		—	4.2
	MBA						4.0	4.0			4.5		4.0		—	4.1

*Strap interference with collective.

†Altitude loop open for first 5 sec.

‡Tape recorder not on.

§Low stick gains.

TABLE B-III

CONFIGURATION NO. 1, SUBJECT GB

PERFORMANCE VARIABLE	MOTION CONDITION	WARMUP 9 DEC	WARMUP 10 DEC	PRIORITY I, CONFIG. 1 10 DEC		WARMUP 12 DEC	PRIORITY I, CONFIG. 9 12 DEC				WARMUP 15 DEC	PRIORITY II 15 DEC		PRIORITY IV 17 DEC	PRIORITY IV 18 DEC		AVERAGED PERFORMANCE
RUN NO.	FB	—	—	51	52	—	103	104	125*		—	129	141	173	206	219	
	MBL	—	—	53	54	—	105	106	123*	126*	—	128	140	174	207	220	
	MBA			55	56				124*			127	139	175	208	221	
σ_q (deg/sec)	FB	0.078	0.093	0.062	0.073	0.071	0.047	0.092	0.073		0.115	0.072	0.062	0.105	0.069	0.049	0.08
	MBL	0.109	0.077	0.066	0.076	0.073	0.061	0.083	0.079	0.037	0.100	0.071	0.067	0.107	0.104	0.062	0.08
	MBA			0.074	0.063				0.052			0.126	0.174	0.136	0.082	0.100	0.10
σ_θ (deg)	FB	0.214	0.197	0.239	0.221	0.152	0.144	0.209	0.174		0.232	0.179	0.231	0.263	0.225	0.181	0.20
	MBL	0.212	0.219	0.224	0.229	0.225	0.229	0.237	0.288	0.157	0.230	0.215	0.168	0.214	0.168	0.210	0.22
	MBA			0.234	0.199				0.177			0.303	0.273	0.256	0.227	0.235	0.24
σ_u (ft/sec)	FB	0.519	0.489	0.569	0.570	0.400	0.351	0.436	0.360		0.467	0.407	0.581	0.601	0.453	0.410	0.47
	MBL	0.519	0.560	0.550	0.564	0.504	0.555	0.539	0.655	0.480	0.495	0.516	0.415	0.419	0.504	0.463	0.52
	MBA			0.476	0.512				0.377			0.705	0.587	0.605	0.393	0.432	0.51
σ_x (ft)	FB	3.351	2.662	3.107	3.161	2.740	2.191	2.493	2.071		2.312	1.920	3.000	3.156	2.573	2.114	2.6
	MBL	3.079	3.263	2.945	3.150	3.161	3.233	2.695	3.469	3.339	2.486	2.428	3.425	2.012	—	2.584	2.9
	MBA			2.863	3.803				2.308			3.836	3.146	3.102	3.200	1.937	3.0
σ_φ (deg)	FB	0.327	0.338	0.314	0.304	0.312	0.296	0.372	0.350		0.265	0.339	0.346	0.324	0.269	0.324	0.32
	MBL	0.310	0.190	0.318	0.317	0.356	0.298	0.313	0.430	0.349	0.242	0.262	0.370	0.317	0.547	0.241	0.32
	MBA			0.213	0.349				0.324			0.330	0.387	0.356	0.365	0.290	0.33
σ_y (ft)	FB	2.467	2.880	2.675	2.820	2.201	2.781	2.360	1.794		1.880	2.203	1.658	2.137	2.833	1.906	2.3
	MBL	2.333	2.818	2.319	3.560	2.593	1.867	2.269	2.985	2.465	2.145	2.107	2.477	1.826	2.268	1.866	2.4
	MBA			3.031	2.778				3.120			1.620	2.315	2.349	2.963	2.521	2.6
σ_w (ft/sec)	FB	0.440	0.400	0.442	0.428	0.470	0.364	0.486	0.486		0.363	0.555	0.347	0.465	0.393	0.386	0.43
	MBL	0.442	0.430	0.535	0.372	0.374	0.488	0.503	0.509	0.476	0.408	0.452	0.491	0.267	0.430	0.394	0.44
	MBA			0.391	0.482				0.437			0.478	0.371	0.371	0.502	0.351	0.42
σ_z (ft)	FB	2.256	1.388	1.905	1.906	1.741	1.077	1.704	2.293		1.040	3.069	0.864	1.813	2.300	1.869	1.7
	MBL	1.762	1.606	2.516	1.400	1.185	1.793	2.439	1.966	2.751	1.791	2.379	2.771	1.578	1.802	1.642	2.0
	MBA			1.977	2.578				2.322			2.292	1.587	1.503	2.261	1.043	1.9
σ_{disp} (ft)	FB	4.734	4.160	4.521	4.645	3.923	3.701	3.832	3.573		3.156	4.237	3.585	4.220	4.465	3.405	4.0
	MBL	4.247	4.601	4.515	4.956	4.257	4.142	4.285	4.981	4.979	3.740	3.999	5.054	3.142	—	3.585	4.3
	MBA			4.614	5.369				4.522			4.753	4.216	4.172	4.912	3.346	4.5
PR	FB	4.5	4.5	6.0	6.0	4.5	4.5	4.5	5.5		4.0	5.5	4.75	4.5	4.0	4.0	4.8
	MBL	—	4.5	6.0	6.0	4.5	4.0	4.5	6.5	5.5	4.25	5.0	5.0	4.0	4.5	4.5	4.9
	MBA			5.5	5.0				5.0			5.0	4.5	3.5	4.0	3.5	4.5

*Runs made at subject's request.

TABLE B-IV

CONFIGURATION NO. 3 PERFORMANCE, SUBJECT RG

PERFORMANCE VARIABLE	MOTION CONDITION	PRIORITY II 15 DEC.
Run No.	FB	144
	MBL	143
	MBA	142
σ_q (deg/sec)	FB	1.122
	MBL	0.656
	MBA	0.663
σ_θ (deg)	FB	1.352
	MBL	0.605
	MBA	0.724
σ_u (ft/sec)	FB	1.185
	MBL	0.676
	MBA	0.928
σ_x (ft)	FB	4.146
	MBL	3.137
	MBA	3.515
σ_φ (deg)	FB	0.578
	MBL	0.368
	MBA	0.517
σ_y (ft)	FB	2.392
	MBL	1.772
	MBA	2.398
σ_w (ft/sec)	FB	0.419
	MBL	0.440
	MBA	0.489
σ_z (ft)	FB	1.090
	MBL	1.524
	MBA	1.448
σ_{disp} (ft)	FB	4.909
	MBL	3.912
	MBA	4.495
PR	FB	9.5
	MBL	9.0
	MBA	9.25

TABLE B-V

CONFIGURATION NO. 3 PERFORMANCE, SUBJECT EF

PERFORMANCE VARIABLE	MOTION CONDITION	PRIORITY I, CONFIG. 11 11 DEC.		PRIORITY I, CONFIG. 3 11 DEC.		PRIORITY II 16 DEC.	PRIORITY IV 18 DEC.	AVERAGED PERFORMANCE
Run No.	FB	77	78	87	88*	157	200	
	MBL	79	80	91	92	155	202	
	MBA			89*	90	156	201	
σ_q (deg/sec)	FB	1.128	1.242	1.250	(1.248*)	0.937	1.179	1.15
	MBL	1.129	1.117	1.237	1.015	1.009	0.981	1.08
	MBA			(0.981*)	0.842	0.960	0.862	0.89
σ_θ (deg)	FB	0.811	1.016	1.253	(1.747*)	0.779	0.957	0.96
	MBL	0.660	0.735	1.039	0.590	0.832	0.671	0.76
	MBA			(0.665*)	0.663	0.736	0.628	0.67
σ_u (ft/sec)	FB	0.662	0.914	1.035	(1.296*)	0.719	0.839	0.83
	MBL	0.686	0.703	0.881	0.490	0.843	0.604	0.70
	MBA			(0.740*)	0.695	0.690	0.616	0.67
σ_x (ft)	FB	1.844	3.520	2.796	(3.769*)	1.782	3.492	2.7
	MBL	2.758	2.431	2.152	1.676	2.766	2.913	2.5
	MBA			(3.920*)	2.643	1.755	2.689	2.4
σ_φ (deg)	FB	0.483	0.351	0.392	(0.601*)	0.559	0.379	0.43
	MBL	0.364	0.404	0.456	0.405	0.382	0.307	0.39
	MBA			(0.390*)	0.348	0.323	0.339	0.34
σ_y (ft)	FB	2.238	2.217	3.496	(3.391*)	2.249	2.321	2.5
	MBL	2.730	1.776	3.102	2.237	2.835	1.708	2.4
	MBA			(3.917*)	2.038	1.832	2.882	2.3
σ_w (ft/sec)	FB	0.663	0.672	0.410	(0.589*)	0.465	0.593	0.56
	MBL	0.710	0.663	0.596	0.572	0.455	0.647	0.61
	MBA			(0.484*)	0.595	0.491	0.717	0.60
σ_z (ft)	FB	2.234	2.563	1.838	(3.230*)	1.741	1.435	2.0
	MBL	2.185	2.073	1.970	1.910	1.320	1.932	1.9
	MBA			(2.650*)	2.161	1.374	1.569	1.7
σ_{disp} (ft)	FB	3.660	4.886	4.840	(6.011*)	3.357	4.431	4.2
	MBL	4.454	3.655	4.258	3.386	4.175	3.890	4.0
	MBA			(6.143*)	3.976	2.885	4.242	3.7
PR	FB	7.0	7.5	8.0	(8.0*)	7.5	—	7.5
	MBL	7.0	6.5	8.0	6.5	6.5	—	6.9
	MBA			(7.5*)	7.5	6.0	—	6.8

*Subject checking attitude ball for sticking.

TABLE B-VI

CONFIGURATION NO. 3 PERFORMANCE, SUBJECT GB

PERFORMANCE VARIABLE	MOTION CONDITION	PRIORITY I, CONFIG. 3 9 DEC.		PRIORITY I, CONFIG. 11 10 DEC.		PRIORITY II 15 DEC.	PRIORITY IV 18 DEC.		AVERAGED PERFORMANCE
Run No.	FB	39	40	49	50	136	215		
	MBL	35	36	51	52	138	217	218*	
	MBA	37	38			137	216		
σ_q (deg/sec)	FB	0.996	0.803	0.860	0.951	0.890	0.869		0.90
	MBL	0.743	0.741	0.685	0.681	0.714	0.692	0.621	0.70
	MBA	0.675	0.855			0.558	0.615		0.68
σ_θ (deg)	FB	1.099	0.743	0.814	0.897	0.757	0.739		0.84
	MBL	0.653	0.698	0.624	0.684	0.637	0.733	0.572	0.66
	MBA	0.590	0.652			0.493	0.572		0.58
σ_u (ft/sec)	FB	0.554	0.719	0.765	0.829	0.781	0.666		0.72
	MBL	0.775	0.722	0.676	0.811	0.684	0.954	0.688	0.76
	MBA	0.735	0.801			0.594	0.733		0.72
σ_x (ft)	FB	3.824	2.545	3.207	2.939	2.949	2.111		2.9
	MBL	3.108	2.354	2.378	3.022	2.813	4.124	3.075	3.0
	MBA	3.610	3.553			2.447	2.980		3.2
σ_φ (deg)	FB	0.287	0.309	0.420	0.419	0.451	0.317		0.37
	MBL	0.276	0.389	0.354	0.339	0.407	0.323	0.306	0.34
	MBA	0.360	0.399			0.368	0.266		0.35
σ_y (ft)	FB	2.715	3.029	3.301	2.757	3.143	2.200		2.9
	MBL	2.414	3.253	2.528	2.207	1.903	2.374	2.878	2.5
	MBA	3.334	2.835			2.291	2.799		2.8
σ_w (ft/sec)	FB	0.713	0.398	0.504	0.497	0.482	0.422		0.50
	MBL	0.374	0.393	0.395	0.507	0.430	0.593	0.395	0.44
	MBA	0.431	0.436			0.568	0.495		0.48
σ_z (ft)	FB	1.166	1.513	1.814	2.075	2.407	2.349		1.9
	MBL	1.678	1.783	1.173	2.095	2.018	3.421	1.772	2.0
	MBA	1.926	2.160			2.139	3.005		2.3
σ_{disp} (ft)	FB	4.832	4.235	4.947	4.523	4.795	3.848		4.5
	MBL	4.278	4.393	3.663	4.288	3.951	5.860	4.569	4.4
	MBA	5.278	5.033			3.977	5.075		4.8
PR	FB	8.5	8.0	8.5	7.5	8.0	7.5		8.0
	MBL	6.5	6.5	8.0	6.5	7.0	7.5	7.0	7.0
	MBA	5.5	5.5			7.0	6.5		6.1

*Rerun because of EPR calibration drift on Run 217.

TABLE B-VII

CONFIGURATION NO. 4 PERFORMANCE, SUBJECT RG

PERFORMANCE VARIABLE	MOTION CONDITION	PRIORITY II 17 DEC.	PRIORITY III 19 DEC.		AVERAGED PERFORMANCE
Run No.	FB	171			
	MBL	170			
	MBA	172	247	248	
σ_q (deg/sec)	FB	0.190			0.19
	MBL	0.299			0.30
	MBA	0.224	0.299	0.208	0.24
σ_θ (deg)	FB	0.336			0.34
	MBL	0.580			0.58
	MBA	0.491	0.377	0.404	0.42
σ_u (ft/sec)	FB	0.538			0.54
	MBL	0.927			0.93
	MBA	0.777	0.669	0.694	0.71
σ_x (ft)	FB	2.049			2.0
	MBL	2.882			2.9
	MBA	2.625	3.090	2.373	2.7
σ_φ (deg)	FB	1.593			1.59
	MBL	0.655			0.66
	MBA	0.634	0.596	0.593	0.61
σ_y (ft)	FB	2.931			2.9
	MBL	2.675			2.7
	MBA	2.162	1.603	1.585	1.8
σ_w (ft/sec)	FB	0.498			0.50
	MBL	0.491			0.50
	MBA	0.448	0.545	0.490	0.50
σ_z (ft)	FB	1.758			1.8
	MBL	1.644			1.6
	MBA	1.286	1.177	1.271	1.2
σ_{disp} (ft)	FB	3.985			4.0
	MBL	4.262			4.3
	MBA	3.636	3.674	3.124	3.5
PR	FB	9.75			9.8
	MBL	9.0			9.0
	MBA	8.5	8.5	8.5	8.5

TABLE B-VIII.

CONFIGURATION NO. 4 PERFORMANCE, SUBJECT EF

PERFORMANCE VARIABLE	MOTION CONDITION	PRIORITY I 11 DEC		PRIORITY II 16 DEC		PRIORITY IV 18 DEC		PRIORITY III 19 DEC				AVERAGED PERFORMANCE
RUN NO.	FB	85	86*	148		198	203					
	MBL	81	82	150	151	197	205					
	MBA	83	84	149		199	204	229†	230	231	238	
σ_q (deg/sec)	FB	0.503	(0.408*)	0.209		0.169	0.419					0.33
	MBL	0.433	0.480	0.488	0.534	0.274	0.260					0.41
	MBA	0.530	0.510	0.384		0.302	0.218	(0.299†)	0.232	0.337	0.278	0.35
σ_θ (deg)	FB	0.363	(0.417*)	0.350		0.263	0.373					0.33
	MBL	0.366	0.423	0.518	0.554	0.424	0.345					0.44
	MBA	0.472	0.382	0.439		0.231	0.268	(0.395†)	0.281	0.285	0.316	0.33
σ_u (ft/sec)	FB	0.559	(0.778*)	0.602		0.431	0.645					0.56
	MBL	0.532	0.541	0.783	0.783	0.664	0.459					0.63
	MBA	0.705	0.498	0.699		0.280	0.374	(0.551†)	0.433	0.386	0.404	0.47
σ_x (ft)	FB	2.339	(4.868*)	2.036		2.843	3.122					2.6
	MBL	1.880	1.592	2.505	2.936	2.522	2.072					2.3
	MBA	2.891	2.080	2.333		1.644	1.524	(1.934†)	2.407	1.773	1.647	2.0
σ_φ (deg)	FB	0.801	(0.969*)	1.206		1.133	1.164					1.08
	MBL	0.961	0.895	1.042	0.932	0.845	0.890					0.93
	MBA	0.926	0.753	0.833		0.647	0.759	(0.741†)	0.722	0.724	0.768	0.77
σ_y (ft)	FB	1.722	(2.408*)	2.389		2.553	1.955					2.2
	MBL	2.311	1.672	1.672	1.643	3.552	1.416					1.8
	MBA	1.844	2.560	2.149		1.197	1.433	(2.752†)	1.550	1.534	1.934	1.8
σ_w (ft/sec)	FB	0.550	(0.608*)	0.563		0.644	0.805					0.64
	MBL	0.496	0.527	0.463	0.494	0.500	0.590					0.51
	MBA	0.566	0.694	0.534		0.740	0.698	(0.554†)	0.454	0.481	0.375	0.57
σ_z (ft)	FB	1.519	(2.075*)	1.641		1.659	1.709					1.6
	MBL	1.340	1.378	1.738	1.247	1.591	1.742					1.5
	MBA	1.437	2.086	1.372		1.779	1.579	(1.830†)	1.442	1.812	0.728	1.5
σ_{disp} (ft)	FB	3.277	(5.814*)	3.542		4.158	4.060					3.8
	MBL	3.267	2.688	3.477	3.588	4.637	3.055					3.5
	MBA	3.717	3.903	3.456		2.701	2.621	(3.829†)	3.205	2.963	2.642	3.1
PR	FB	8.0	(8.0*)	7.0		—	—					7.5
	MBL	7.0	6.5	7.0	6.5	—	—					6.8
	MBA	7.5	7.5	6.0		—	—	—	5.0	5.0	5.5	6.1

*Subject said he was inattentive to longitudinal task.

†No pitch simulation drive.

TABLE B-IX

CONFIGURATION NO. 4 PERFORMANCE, SUBJECT GB

PERFORMANCE VARIABLE	MOTION CONDITION	PRIORITY I 9 DEC.		PRIORITY II 15 DEC.	PRIORITY IV 17 DEC.	PRIORITY IV 18 DEC.	AVERAGED PERFORMANCE
Run No.	FB	41	42	132	180	214	
	MBL	45	46	130	182*	213	
	MBA	43	44	131	179	212	
σ_q (deg/sec)	FB	0.121	0.057	0.086	0.082	0.067	0.08
	MBL	0.117	0.096	0.117	0.066	0.071	0.09
	MBA	0.064	0.088	0.115	0.088	0.086	0.09
σ_θ (deg)	FB	0.214	0.194	0.224	0.218	0.255	0.22
	MBL	0.291	0.226	0.208	0.237	0.249	0.24
	MBA	0.208	0.231	0.286	0.184	0.326	0.25
σ_u (ft/sec)	FB	0.535	0.527	0.453	0.491	0.602	0.52
	MBL	0.713	0.529	0.440	0.523	0.461	0.53
	MBA	0.510	0.605	0.569	0.448	0.709	0.57
σ_x (ft)	FB	3.356	2.898	2.371	2.345	4.016	3.0
	MBL	3.701	3.126	2.535	2.575	2.463	2.9
	MBA	2.845	3.477	2.611	2.194	3.660	3.0
σ_φ (deg)	FB	0.690	0.767	0.879	0.707	0.906	0.79
	MBL	0.613	0.752	0.550	0.589	0.524	0.61
	MBA	0.614	0.579	0.550	0.528	0.462	0.55
σ_y (ft)	FB	2.766	2.949	2.861	2.358	2.096	2.6
	MBL	2.810	2.691	1.782	2.024	2.148	2.3
	MBA	3.537	2.366	1.557	1.192	2.647	2.3
σ_w (ft/sec)	FB	0.375	0.434	0.516	0.460	0.501	0.46
	MBL	0.462	0.392	0.418	0.492	0.433	0.44
	MBA	0.480	0.378	0.437	0.366	0.538	0.44
σ_z (ft)	FB	1.591	1.729	2.225	2.335	2.744	2.1
	MBL	2.455	1.814	2.069	2.408	1.833	2.1
	MBA	2.702	1.885	2.701	1.105	2.719	2.2
σ_{disp} (ft)	FB	4.631	4.482	4.331	4.064	5.296	4.6
	MBL	5.256	4.506	3.726	4.065	3.747	4.3
	MBA	5.283	4.609	4.066	2.730	5.272	4.4
PR	FB	7.5	6.5	8.25	7.0	7.25	7.3
	MBL	7.0	6.5	8.0	6.0	6.5	6.8
	MBA	6.0	5.5	7.75	5.5	6.0	6.2

*Run 181 lost due to equipment failure.

TABLE B-X

CONFIGURATION NO. 6 PERFORMANCE, SUBJECT RG

PERFORMANCE VARIABLE	MOTION CONDITION	WARMUP 15 DEC.	PRIORITY II 15 DEC.	WARMUP 17 DEC.	PRIORITY IV 18 DEC.	PRIORITY III 19 DEC.		AVERAGED PERFORMANCE
Run No.	FB	—	145	—	226			
	MBL	—	147	—	227			
	MBA		146		228	253*	257*	
σ_q (deg/sec)	FB	0.837	0.954	0.813	0.790			0.85
	MBL	0.636	0.657	0.663	0.820			0.69
	MBA		0.596		0.618	(0.675*)	(0.624*)	0.61
σ_θ (deg)	FB	0.887	1.021	0.889	0.795			0.90
	MBL	0.610	0.628	0.694	0.840			0.69
	MBA		0.540		0.542	(0.568*)	(0.602*)	0.54
σ_u (ft/sec)	FB	0.762	0.863	0.784	0.725			0.78
	MBL	0.651	0.635	0.738	0.851			0.72
	MBA		0.625		0.542	(0.673*)	(0.801*)	0.58
σ_x (ft)	FB	4.535	2.244	3.057	3.130			3.2
	MBL	2.155	2.857	2.489	2.531			2.5
	MBA		2.354		1.924	(4.068*)	(4.192*)	2.1
σ_φ (deg)	FB	0.952	1.043	0.943	0.919			0.96
	MBL	0.621	0.741	0.638	0.645			0.66
	MBA		0.664		0.628	(0.612*)	(0.617*)	0.65
σ_y (ft)	FB	2.948	1.958	2.206	2.013			2.3
	MBL	1.812	2.420	2.620	2.127			2.2
	MBA		1.967		2.408	(2.481*)	(2.259*)	2.2
σ_w (ft/sec)	FB	0.436	0.580	0.567	0.412			0.50
	MBL	0.354	0.461	0.448	0.443			0.43
	MBA		0.442		0.417	(0.475*)	(0.634*)	0.43
σ_z (ft)	FB	1.721	2.198	1.906	1.052			1.7
	MBL	0.666	1.798	1.676	1.454			1.4
	MBA		1.196		0.839	(1.223*)	(2.154*)	1.0
σ_{disp} (ft)	FB	5.676	3.702	4.226	3.867			4.4
	MBL	2.894	4.154	3.984	3.611			3.7
	MBA		3.292		3.194	(4.919*)	(5.226*)	3.2
PR	FB	9.5	10	9.75	9.75			9.8
	MBL	9.0	9.75	9.5	9.5			9.4
	MBA		9.25		9.0	(9.0*)	(9.5*)	9.1

*Performance decrement suggests different "set" for Priority 3 runs.

TABLE B-XI

CONFIGURATION NO. 6 PERFORMANCE, SUBJECT EF

PERFORMANCE VARIABLE	MOTION CONDITION	WARMUP 9 DEC	WARMUP 10 DEC	PRIORITY I 10 DEC		WARMUP 11 DEC	WARMUP 16 DEC	PRIORITY II 16 DEC	PRIORITY IV 17 DEC	PRIORITY IV 18 DEC	PRIORITY III 19 DEC		AVERAGED PERFORMANCE
RUN NO.	FB	—	—	67	68	—	—	153	187	196			
	MBL		—	69	70*	—	—	152	188	195			
	MBA			65	66			154	186	194	239	245	
σ_q (deg/sec)	FB	0.815	1.008	1.235	0.981	1.174	0.891	1.199	1.188	0.723			1.02
	MBL		0.872	0.930	(1.135*)	1.068	0.796	1.137	0.836	0.693			0.91
	MBA			1.079	0.860			1.066	0.882	0.718	0.706	0.767	0.87
σ_θ (deg)	FB	0.865	1.042	1.264	0.945	0.918	0.867	1.362	1.095	0.588			0.99
	MBL		0.894	0.874	(0.978*)	0.761	0.562	0.726	0.694	0.575			0.73
	MBA			0.877	0.803			0.633	0.602	0.476	0.484	0.669	0.65
σ_u (ft/sec)	FB	0.824	0.832	1.028	0.893	0.839	1.126	1.163	1.021	0.654			0.93
	MBL		0.807	0.851	(0.824*)	0.728	0.580	0.786	0.751	0.617			0.73
	MBA			0.774	0.851			0.638	0.599	0.433	0.497	0.570	0.62
σ_x (ft)	FB	2.453	2.130	2.937	2.236	2.367	4.259	3.504	4.651	3.215			3.1
	MBL		1.925	3.116	(4.352*)	2.719	2.107	2.853	3.335	3.190			2.8
	MBA			2.199	2.812			2.158	2.981	3.618	2.614	2.718	2.7
σ_φ (deg)	FB	1.002	0.997	1.101	0.870	1.055	0.784	1.348	1.297	1.114			1.06
	MBL		0.669	0.849	(0.890*)	0.757	0.679	0.643	0.849	0.669			0.73
	MBA			0.611	0.506			0.726	0.683	0.540	0.550	0.698	0.62
σ_y (ft)	FB	2.908	3.492	4.156	3.057	3.045	3.839	3.165	2.516	2.211			3.2
	MBL		3.873	3.220	(4.752*)	4.155	1.772	1.544	3.075	2.760			2.9
	MBA			2.195	3.286			2.058	2.274	1.708	2.213	2.451	2.3
σ_w (ft/sec)	FB	0.582	0.496	0.594	0.411	0.684	0.514	0.669	0.478	0.443			0.54
	MBL		0.646	0.630	(1.083*)	0.554	0.501	0.472	0.478	0.686			0.57
	MBA			0.728	0.525			0.606	0.488	0.774	0.442	0.501	0.58
σ_z (ft)	FB	3.888	2.599	3.243	1.646	3.292	2.010	3.355	2.005	1.331			2.6
	MBL		3.715	3.359	(4.266*)	3.517	1.685	1.299	1.609	2.124			2.5
	MBA			3.402	2.196			1.924	1.576	1.948	2.019	2.744	2.3
σ_{disp} (ft)	FB	5.439	4.846	6.035	4.130	5.071	6.076	5.792	5.656	4.122			5.2
	MBL		5.701	5.600	(7.728*)	6.085	3.228	3.495	4.813	4.722			4.8
	MBA			4.608	4.851			3.548	4.067	4.450	3.975	4.574	4.3
PR	FB	8.0	8.0	9.0	9.0	7.0	9.0	9.5	9.5	—			8.6
	MBL		6.5	9.0	(8.0*)	6.5	8.0	8.5	8.5	—			7.8
	MBA			6.5	6.5			8.0	7.5	—	—	6.5	7.0

*Subject complained of fatigue.

TABLE B-XII

CONFIGURATION NO. 6 PERFORMANCE, SUBJECT GB

PERFORMANCE VARIABLE	MOTION CONDITION	WARMUP 9 DEC	WARMUP 10 DEC	WARMUP 12 DEC	PRIORITY I 12 DEC		WARMUP 15 DEC	PRIORITY II 15 DEC	PRIORITY IV 17 DEC	PRIORITY IV 18 DEC	AVERAGED PERFORMANCE
RUN NO.	FB	—	—	—	119	120	—	134	176	210	
	MBL	—	—	—	117	118	—	135	177	209	
	MBA				121	122		133	178	211	
σ_q (deg/sec)	FB	—	0.988	1.238	1.237	0.827	1.057	0.923	1.155	1.013	1.06
	MBL	0.859	0.831	0.890	0.743	0.803	0.699	0.586	0.722	0.836	0.77
	MBA				0.645	0.698		0.694	0.649	0.652	0.67
σ_θ (deg)	FB	—	1.023	1.213	1.310	0.855	1.012	0.707	0.922	0.845	0.99
	MBL	0.895	0.836	0.816	0.677	0.821	0.640	0.562	0.655	0.715	0.73
	MBA				583	0.643		0.555	0.527	0.581	0.58
σ_u (ft/sec)	FB	—	0.967	1.245	1.219	0.818	1.100	0.757	0.874	0.788	0.97
	MBL	0.934	0.836	0.863	0.925	0.959	0.718	0.669	0.634	0.723	0.81
	MBA				0.733	0.859		0.619	0.602	0.744	0.71
σ_x (ft)	FB	—	3.331	4.077	3.386	2.174	3.650	2.902	2.895	2.738	3.1
	MBL	4.233	2.895	3.015	3.305	3.032	2.281	1.981	2.209	2.387	2.8
	MBA				3.338	3.532		2.831	2.228	3.707	3.1
σ_φ (deg)	FB	—	0.887	1.013	1.078	1.106	0.804	0.821	1.028	0.745	0.94
	MBL	0.740	0.797	0.896	0.673	0.629	0.479	0.635	0.666	0.606	0.68
	MBA				0.619	0.582		0.602	0.684	0.627	0.62
σ_y (ft)	FB	—	2.681	2.997	2.874	2.821	1.910	2.299	2.536	2.446	2.6
	MBL	2.512	2.892	2.884	1.984	2.098	1.845	2.115	2.049	2.279	2.3
	MBA				2.629	2.506		2.314	2.588	2.652	2.5
σ_w (ft/sec)	FB	—	0.386	0.529	0.375	0.523	0.440	0.468	0.477	0.408	0.45
	MBL	0.500	0.538	0.353	0.382	0.476	0.384	0.461	0.415	0.409	0.44
	MBA				0.551	0.414		0.452	0.434	0.570	0.48
σ_z (ft)	FB	—	1.916	2.754	1.843	2.341	2.449	2.779	2.407	2.472	2.4
	MBL	2.933	3.176	1.164	1.489	2.161	2.293	2.927	2.230	1.382	2.3
	MBA				2.773	2.500		2.616	2.418	3.026	2.7
σ_{disp} (ft)	FB	—	4.686	5.761	4.808	4.262	4.792	4.629	4.539	4.426	4.7
	MBL	5.762	5.180	4.331	4.132	4.273	3.724	4.119	3.749	3.578	4.3
	MBA				5.074	5.000		4.496	4.185	5.471	4.9
PR	FB	—	9.5	9.5	8.75	9.0	9.0	9.25	9.5	9.0	9.2
	MBL	8.0	9.5	8.5	8.0	8.0	8.5	8.75	8.5	9.0	8.5
	MBA				8.0	8.5		8.5	8.5	9.0	8.5

TABLE B-XIII

INDIVIDUAL RUN EPR DATA

RUN NUMBER	CONFIG.	SUBJECT	INSTRUMENT NO. 1 (ALTIMETER)							INSTRUMENT NO. 2 (ATTITUDE BALL)							INSTRUMENT NO. 4 (POSITION DISPLAY)							ALL INSTRUMENTS			PILOT RATING*	PERFORMANCE σ_{disp}
			N_1	T_{d_1}	σ_{Td_1}	η_1	ν_1	$\bar{f}_{s_1}$	$\bar{T}_{s_1}$	N_2	T_{d_2}	σ_{Td_2}	η_2	ν_2	$\bar{f}_{s_2}$	$\bar{T}_{s_2}$	N_4	T_{d_4}	σ_{Td_4}	η_4	ν_4	$\bar{f}_{s_4}$	$\bar{T}_{s_4}$	T_R	N	f_s		
184	1-MBA	EF	14	0.35	0.08	0.048	0.081	0.139	7.10	85	0.58	0.14	0.491	0.494	0.846	1.18	73	0.63	0.14	0.461	0.424	0.726	1.38	100.5	172	1.711	4.0	2.77
185	1-MBL	EF	20	0.33	0.06	0.066	0.109	0.198	5.04	91	0.59	0.19	0.535	0.495	0.903	1.11	73	0.55	0.11	0.399	0.397	0.724	1.38	100.8	184	1.826	4.5	3.89
186	6-MBA	EF	15	0.31	0.05	0.045	0.088	0.148	6.76	85	0.75	0.31	0.632	0.497	0.838	1.19	71	0.46	0.07	0.323	0.415	0.700	1.43	101.4	171	1.686	7.5	4.07
187	6-FB	EF	10	0.30	0.03	0.030	0.060	0.098	10.21	84	0.82	0.36	0.674	0.500	0.823	1.22	74	0.41	0.07	0.296	0.440	0.725	1.38	102.1	168	1.646	9.5	5.66
188	6-MBL	EF	13	0.31	0.05	0.040	0.074	0.129	7.76	86	0.72	0.29	0.616	0.491	0.852	1.17	76	0.46	0.08	0.344	0.434	0.753	1.33	100.9	175	1.734	8.5	4.81
189	1-FB	EF	15	0.49	0.23	0.072	0.088	0.148	6.75	84	0.63	0.20	0.520	0.491	0.830	1.20	72	0.57	0.14	0.408	0.421	0.712	1.41	101.2	171	1.690	4.0	3.31
191	1-FB	EF	15	0.40	0.13	0.060	0.085	0.148	6.75	86	0.62	0.17	0.528	0.486	0.849	1.18	73	0.56	0.13	0.404	0.412	0.721	1.39	101.2	177	1.748	—	2.95
192	1-MBA	EF	21	0.36	0.08	0.074	0.116	0.208	4.80	90	0.60	0.20	0.532	0.497	0.892	1.12	70	0.57	0.11	0.394	0.387	0.694	1.44	100.9	181	1.795	—	2.70
193	1-MBL	EF	18	0.37	0.08	0.066	0.098	0.178	5.63	92	0.57	0.16	0.521	0.500	0.908	1.10	73	0.57	0.09	0.409	0.397	0.720	1.39	100.4	184	1.815	—	3.09
194	6-MBA	EF	17	0.31	0.04	0.053	0.101	0.169	5.91	84	0.76	0.36	0.636	0.500	0.836	1.20	66	0.47	0.09	0.308	0.393	0.657	1.52	100.5	168	1.672	—	4.45
195	6-MBL	EF	17	0.30	0.05	0.050	0.090	0.169	5.92	93	0.66	0.33	0.607	0.495	0.924	1.08	76	0.45	0.09	0.338	0.404	0.755	1.33	100.7	188	1.867	—	4.72
196	6-FB	EF	12	0.28	0.04	0.033	0.069	0.121	8.24	87	0.74	0.33	0.650	0.500	0.880	1.14	74	0.42	0.08	0.315	0.425	0.749	1.34	98.9	174	1.760	—	4.12
197	4-MBL	EF	12	0.31	0.09	0.037	0.065	0.119	8.43	91	0.58	0.17	0.524	0.495	0.900	1.11	80	0.55	0.12	0.436	0.435	0.791	1.26	101.1	184	1.819	—	4.64
198	4-FB	EF	14	0.32	0.05	0.045	0.075	0.139	7.17	92	0.65	0.26	0.594	0.495	0.916	1.09	78	0.46	0.08	0.356	0.419	0.777	1.29	100.4	186	1.852	—	4.17
199	4-MBA	EF	20	0.29	0.03	0.059	0.101	0.200	4.99	99	0.52	0.13	0.514	0.497	0.992	1.01	80	0.53	0.12	0.427	0.402	0.802	1.25	99.8	199	1.994	—	2.70
200	3-FB	EF	14	0.33	0.08	0.046	0.076	0.139	7.18	89	0.66	0.27	0.586	0.481	0.886	1.13	76	0.47	0.11	0.353	0.411	0.756	1.32	100.5	185	1.841	—	4.43
201	3-MBA	EF	16	0.35	0.06	0.055	0.086	0.158	6.32	91	0.64	0.29	0.576	0.492	0.900	1.11	76	0.48	0.11	0.364	0.411	0.751	1.33	101.2	185	1.829	—	4.24
202	3-MBL	EF	18	0.32	0.04	0.057	0.089	0.179	5.59	100	0.53	0.13	0.525	0.493	0.994	1.01	83	0.50	0.10	0.414	0.409	0.825	1.21	100.6	203	2.017	—	3.89
203	4-FB	EF	15	0.33	0.07	0.049	0.081	0.149	6.72	93	0.65	0.23	0.597	0.503	0.923	1.08	77	0.46	0.10	0.354	0.416	0.764	1.31	100.7	185	1.836	—	4.06
204	4-MBA	EF	19	0.34	0.05	0.063	0.098	0.189	5.30	95	0.56	0.17	0.529	0.490	0.944	1.06	77	0.52	0.09	0.401	0.397	0.765	1.31	100.6	194	1.928	—	2.62
205	4-MBL	EF	16	0.33	0.06	0.053	0.082	0.161	6.23	97	0.53	0.15	0.514	0.495	0.973	1.03	82	0.52	0.10	0.430	0.418	0.823	1.22	99.7	196	1.967	—	3.06
222	1-FB	RG	27	0.42	0.09	0.114	0.169	0.269	3.72	69	0.71	0.27	0.488	0.431	0.687	1.45	61	0.64	0.12	0.392	0.381	0.608	1.65	100.4	160	1.594	6.0	1.93
223	1-MBL	RG	27	0.47	0.11	0.127	0.173	0.269	3.71	74	0.74	0.33	0.547	0.474	0.738	1.36	54	0.60	0.11	0.323	0.346	0.538	1.86	100.3	156	1.556	6.5	2.13
224	1-MBA	RG	29	0.48	0.07	0.139	0.184	0.290	3.45	71	0.70	0.27	0.496	0.449	0.710	1.41	56	0.64	0.08	0.360	0.354	0.560	1.78	99.9	158	1.581	6.5	2.43
225	1-FB	RG	28	0.47	0.09	0.131	0.190	0.280	3.57	61	0.81	0.37	0.491	0.415	0.610	1.64	56	0.67	0.10	0.373	0.381	0.560	1.79	100.1	147	1.469	7.0	2.99
226	6-FB	RG	13	0.35	0.08	0.062	0.142	0.181	5.53	62	1.12	0.74	0.699	0.488	0.623	1.61	45	0.52	0.08	0.234	0.354	0.452	2.21	99.5	127	1.276	9.75	3.70
227	6-MBL	RG	29	0.39	0.08	0.114	0.172	0.291	3.44	83	0.70	0.27	0.580	0.491	0.833	1.20	55	0.55	0.08	0.302	0.325	0.552	1.81	99.7	169	1.695	9.5	3.61
228	6-MBA	RG	30	0.39	0.08	0.118	0.179	0.300	3.33	79	0.70	0.35	0.552	0.470	0.790	1.27	58	0.57	0.10	0.328	0.345	0.580	1.72	99.9	168	1.681	9.0	3.20
176	6-FB	GB	9	0.36	0.11	0.029	0.055	0.080	12.52	73	0.83	0.42	0.601	0.500	0.729	1.37	65	0.57	0.12	0.370	0.445	0.649	1.54	100.2	146	1.458	9.5	4.54
177	6-MBL	GB	8	0.33	0.09	0.026	0.057	0.080	12.52	69	0.89	0.53	0.610	0.489	0.689	1.45	64	0.57	0.10	0.364	0.454	0.639	1.57	100.2	141	1.407	8.5	3.75
178	6-MBA	GB	9	0.41	0.15	0.036	0.071	0.090	11.17	63	0.96	0.61	0.600	0.500	0.627	1.60	54	0.68	0.23	0.364	0.429	0.537	1.86	100.5	126	1.254	8.5	4.19
209	6-MBL	GB	8	0.40	0.13	0.032	0.062	0.079	12.67	65	0.99	0.44	0.632	0.500	0.641	1.56	57	0.60	0.16	0.336	0.438	0.562	1.78	101.4	130	1.282	9.0	3.58
210	6-FB	GB	11	0.38	0.10	0.042	0.080	0.110	9.12	68	0.96	0.44	0.653	0.496	0.678	1.47	57	0.53	0.13	0.303	0.416	0.568	1.76	100.3	137	1.366	9.0	4.43
211	6-MBA	GB	18	0.66	0.30	0.120	0.137	0.182	5.43	64	0.94	0.54	0.608	0.489	0.648	1.54	46	0.57	0.13	0.264	0.351	0.466	2.15	98.75	131	1.327	9.0	5.47

*Pilot ratings were not taken for Runs 191 to 205 for fear of disturbing the EPR system calibration. This fear proved groundless in later runs.

APPENDIX C

DESCRIBING FUNCTION ANALYSIS FOR SUBJECT EF

Following completion of the analysis presented in Section V, NASA-ARC personnel analyzed six additional runs for "equivalent" (visual cues only assumed) describing functions. These data are presented in this Appendix as they do not materially alter the conclusions of Section V. The subject in these runs was EF and the Configuration was No. 6.

Figures C-1 through C-8 illustrate the describing function data. The inner-loop describing functions (Y_{p_θ} and Y_{p_φ}) show more lead in the crossover region for the pitch control task than for roll as a consequence of the more unstable dynamics. The describing functions for the outer-loop tasks (Figs. C-5 through C-8) show somewhat more variability than those in the main text. A trend emerges from consideration of both sets of data: Y_{p_y} shows a generally leading characteristic in the crossover frequency region for both subjects; while Y_{p_x} is more variable — sometimes lead, sometimes lag; and when lagging, sometimes a nonminimum phase characteristic (which may or may not be real — there is little high-frequency power in the displacement signals upon which to establish the higher frequency characteristics of the describing functions).

Table C-I lists the crossover and performance data for all nine runs together with predicted behavior. There is considerable scatter, but some trends emerge: first, this subject (EF) generally has a higher inner-loop crossover frequency than RG — generally in accord with expectations — his (EF's) attitude display look fractions and dwell fractions are generally greater (see Table B-XIII). Second, his outer-loop crossover frequencies are essentially the same as RG's, but with (9 times out of 12) greater phase margins and poorer performance. This suggests greater pilot remnant for EF. It is probably safe to conclude that the short measurement interval (relative to the frequencies in the outer loop) is a major contributor to the data scatter in the outer-loop tasks, in particular, his achieving best performance on a fixed-base run in one instance (Run No. 196).

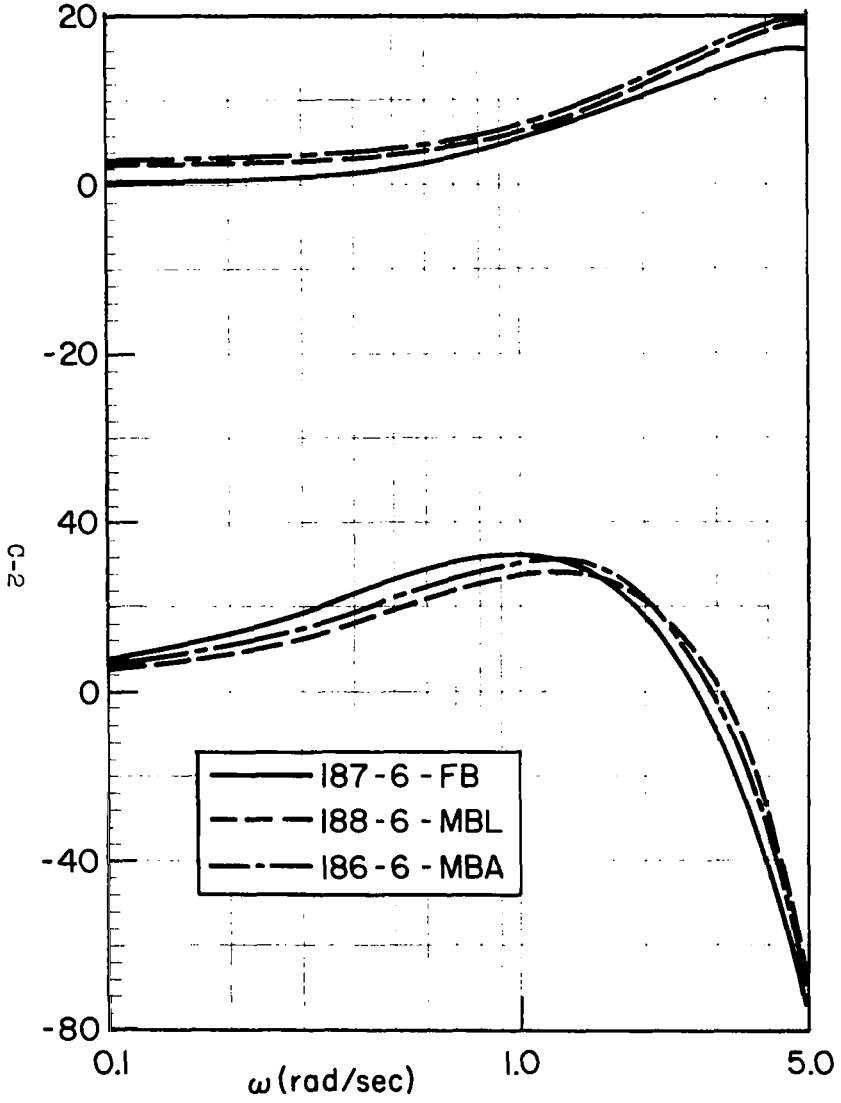

Figure C-1. Y_{p_θ} Describing Functions, EF,
17 December 1969

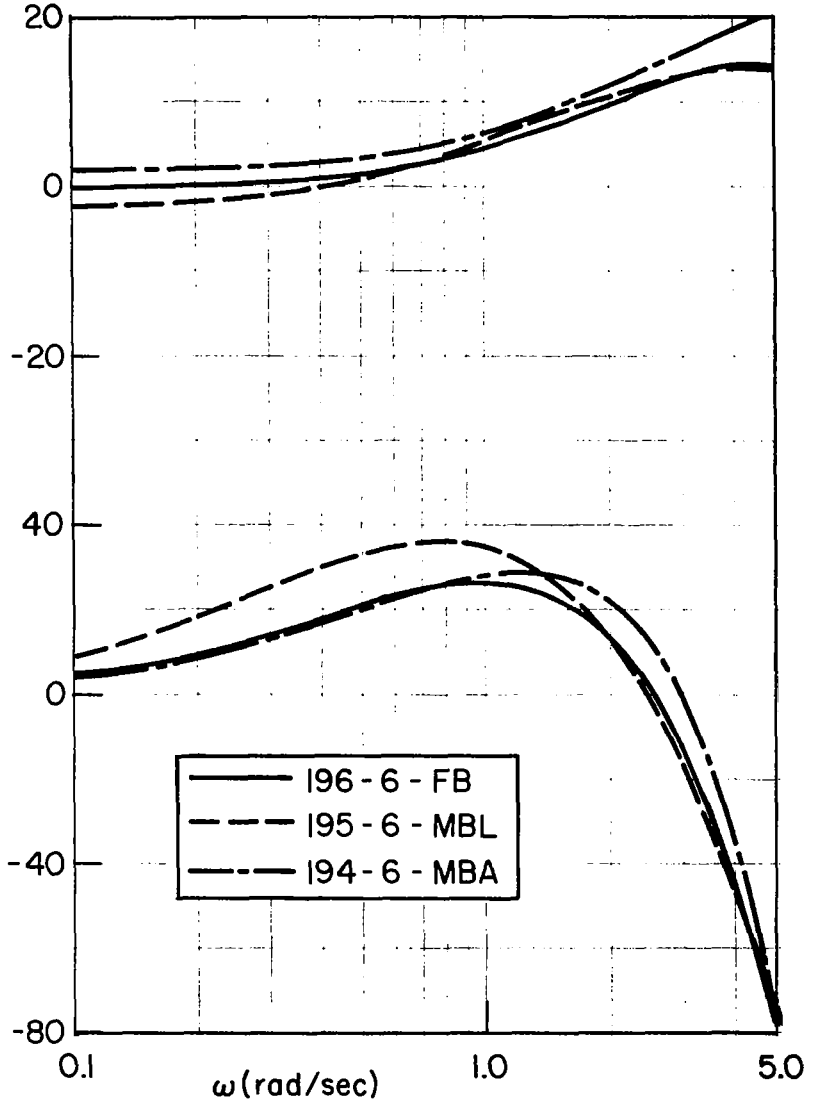

Figure C-2. Y_{p_θ} Describing Functions, EF,
18 December 1969

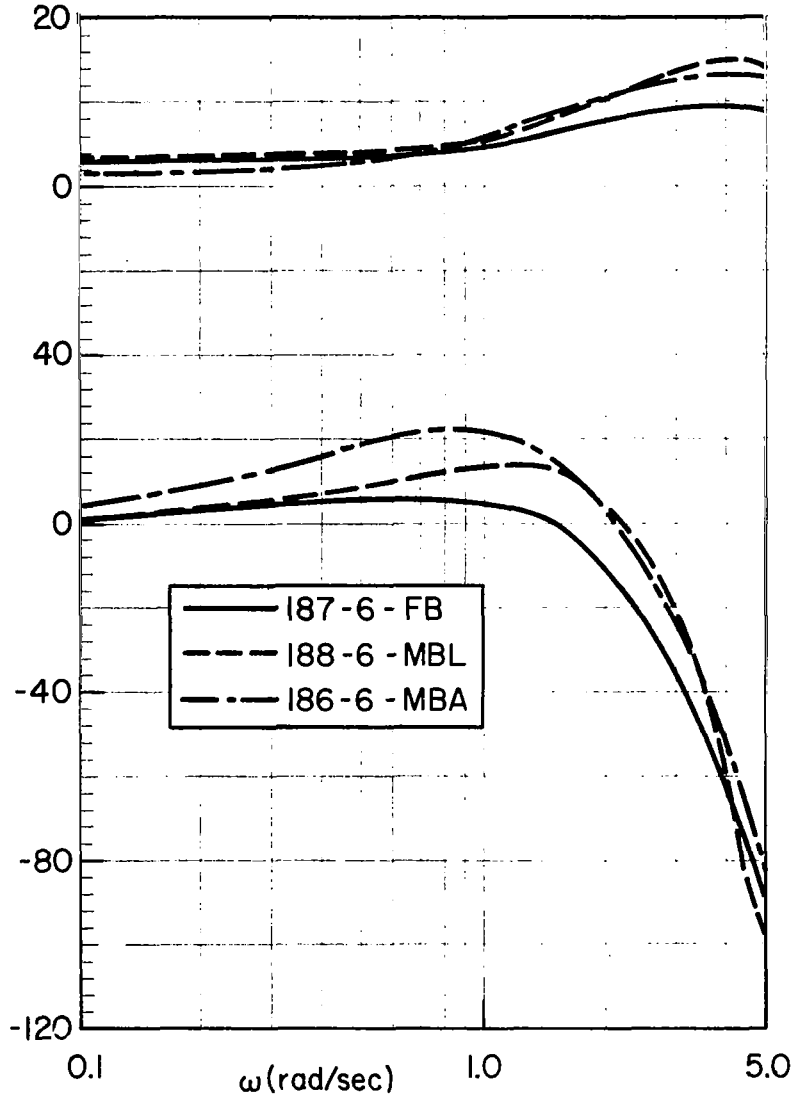

Figure C-3. Y_{p_φ} Describing Functions, EF,

17 December 1969

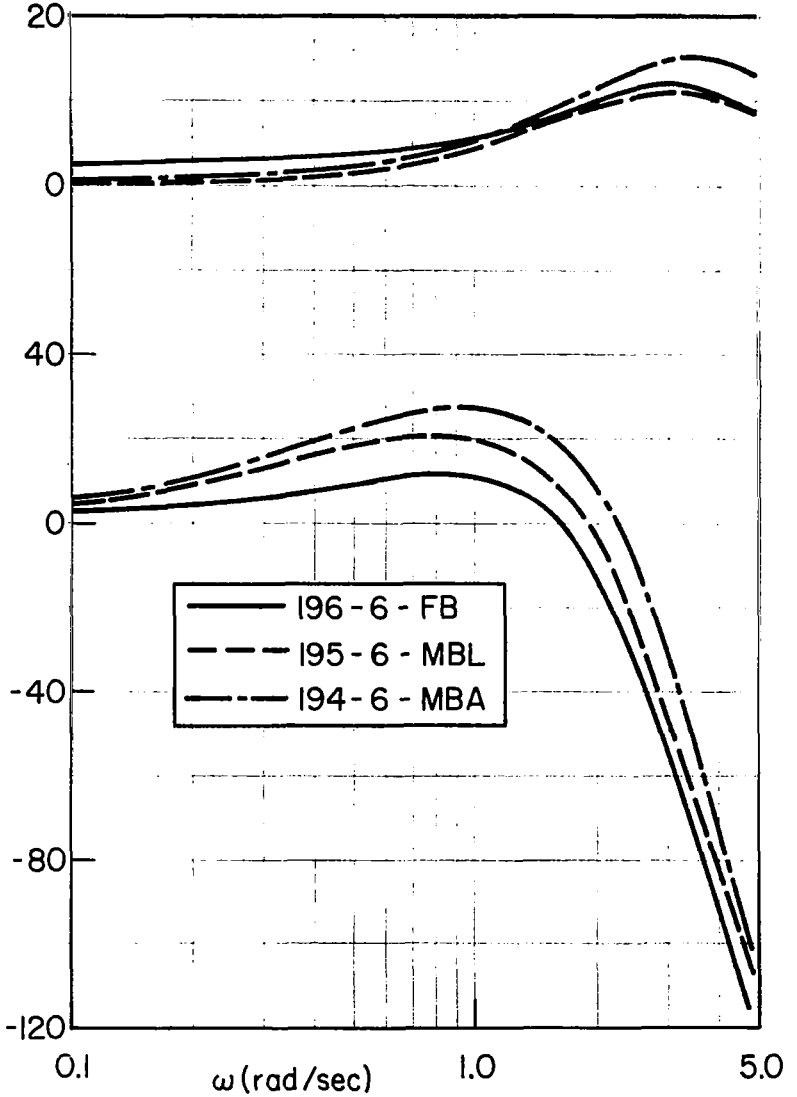

Figure C-4. Y_{p_φ} Describing Functions, EF,

18 December 1969

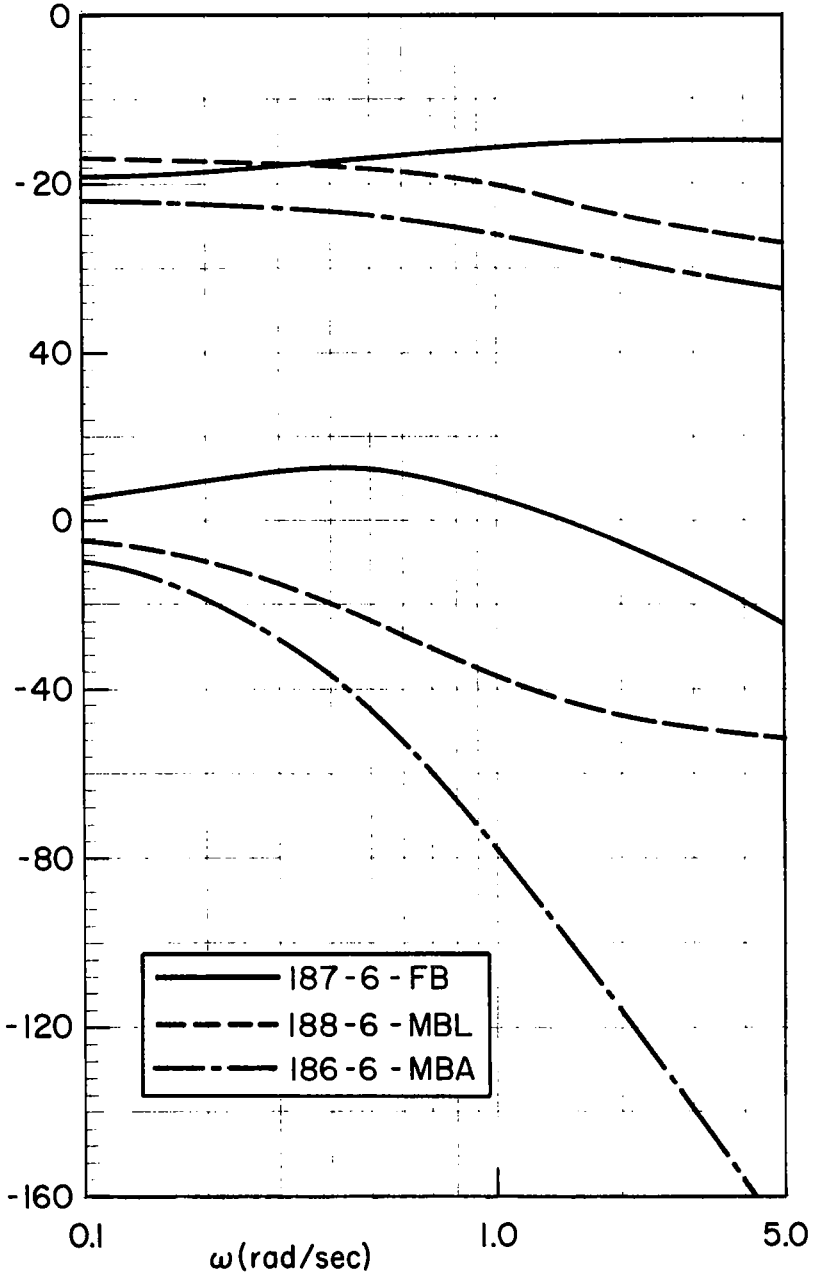

Figure C-5. Y_{p_x} Describing Functions, EF, 17 December 1969

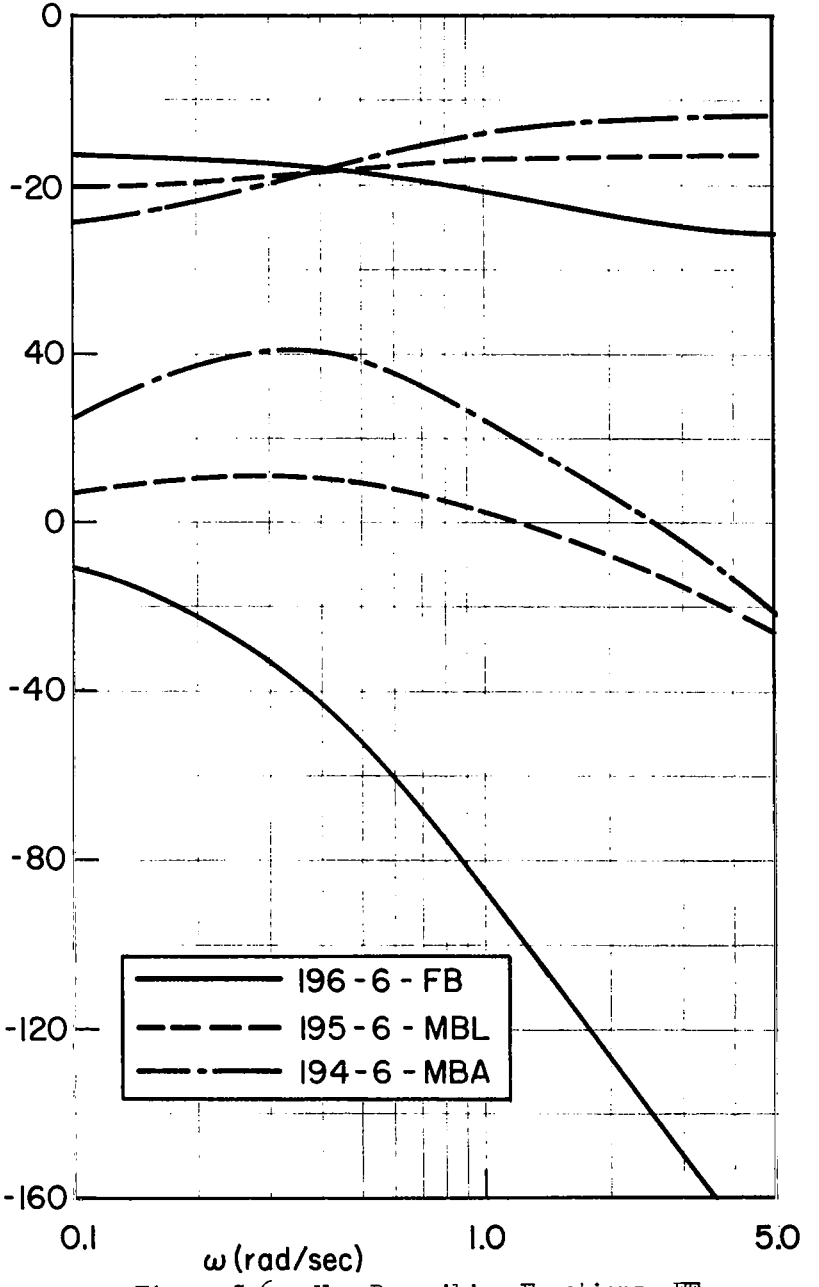

Figure C-6. Y_{p_x} Describing Functions, EF, 18 December 1969

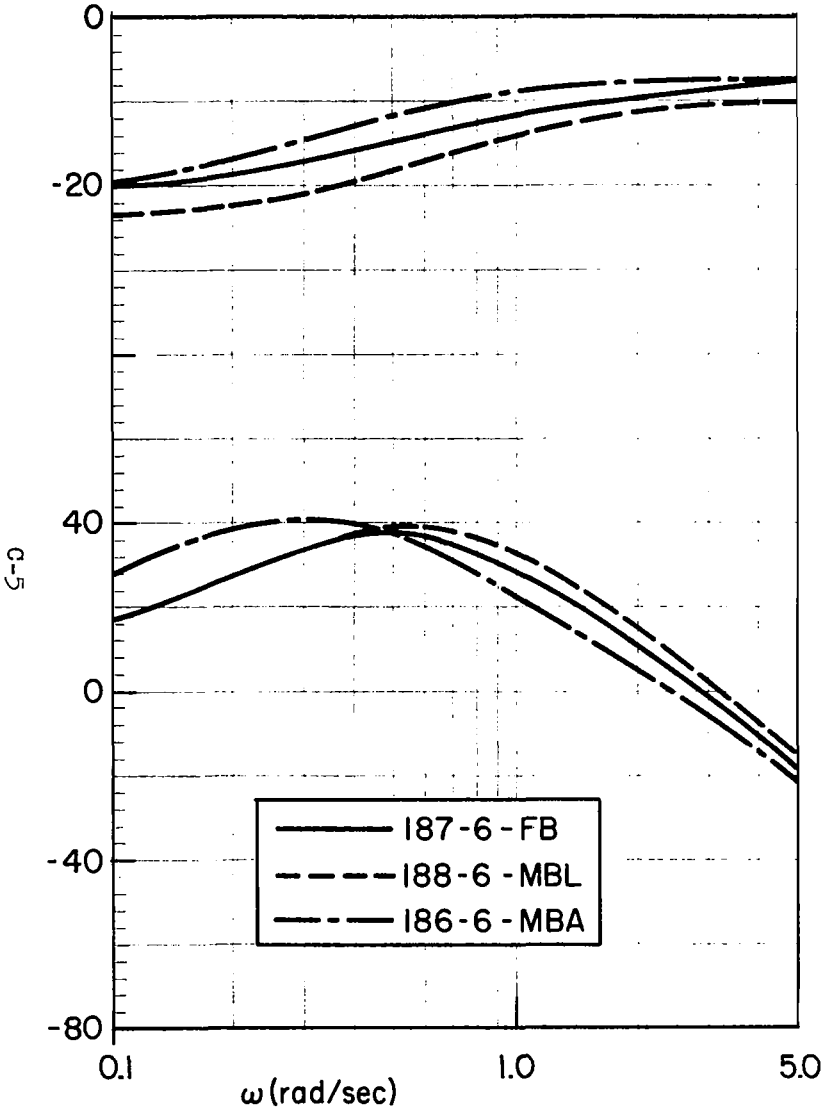

Figure C-7. Y_{p_y} Describing Function, EF,

17 December 1969

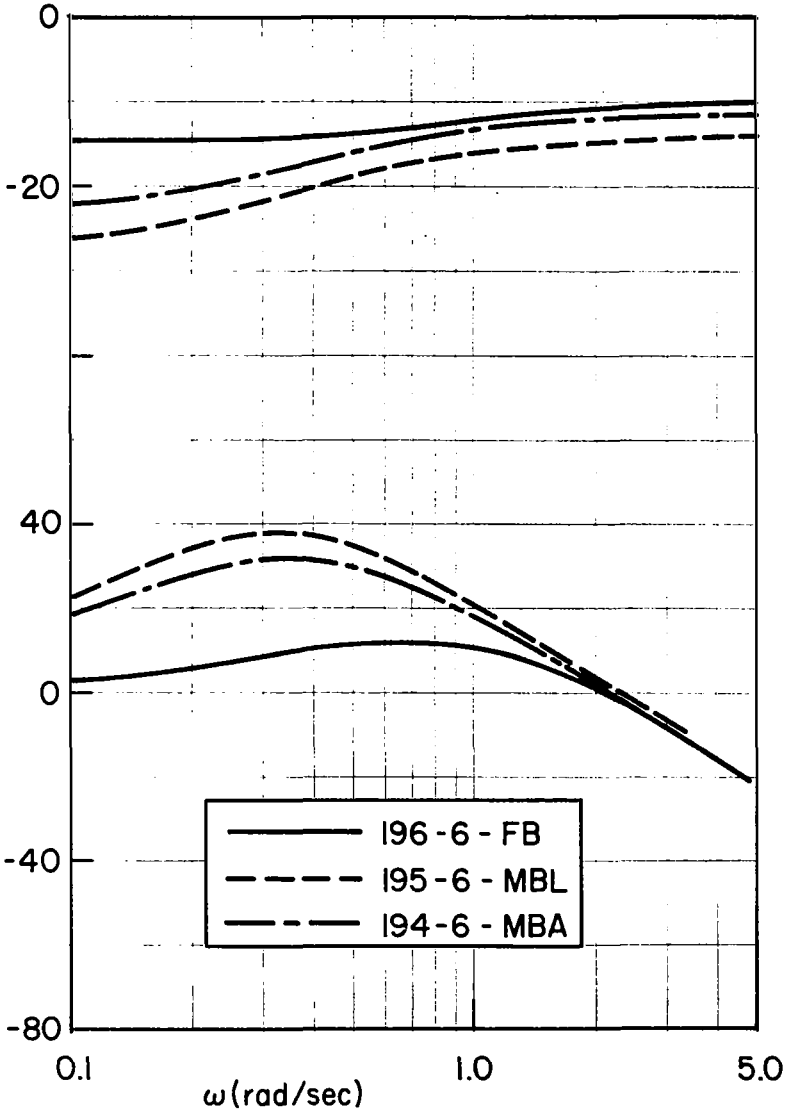

Figure C-8. Y_{p_y} Describing Function, EF,

18 December 1969

TABLE C-I

CROSSOVER FREQUENCIES, PHASE MARGINS AND PERFORMANCE FOR NINE EXAMPLE RUNS* RELATIVE TO PREDICTIONS

	226	227	228	187	188	186	196	195	194	PREDICTIONS	
	FB	MBL	MBA	FB	MBL	MBA	FB	MBL	MBA	FB	MBL
Longitudinal Task											
ω_{c_θ} (rad/sec)	1.37	1.41	1.55	1.78	1.82	2.00	1.65	1.90	2.10	1.5	2.25
φ_{m_θ} (deg)	27	27	17	21	22	21	18	30	20	11	18
σ_θ (deg)	0.80	0.84	0.54	1.10	0.69	0.60	0.59	0.58	0.48	0.80‡	0.73
ω_{c_x} (rad/sec)	0.13	0.24	0.19	0.21	0.24	0.15	0.24	0.19	0.15	0.5	0.5
φ_{m_x} (deg)	68	47	38	71	38	48	30	82	95	53	22
σ_x (ft)	3.13	2.53	1.92	4.65	3.34	2.98	3.22	3.19	3.62	1.1‡	1.3
Lateral Task											
ω_{c_φ} (rad/sec)	1.27	1.64	1.56	1.40	1.65	1.70	1.65	1.52	1.78	1.5	2.25
φ_{m_φ} (deg)	27	23	22	19	24	27	15	28	30	25	28
σ_φ (deg)	0.92	0.65	0.63	1.30	0.85	0.68	1.11	0.67	0.54	1.28	0.97
ω_{c_y} (rad/sec)	0.29	0.28	0.23	0.24	0.16	0.34	0.33	0.10	0.20	0.5	0.5
φ_{m_y} (deg)	55	36†	54	76	78	74	42	100	85	37	17
σ_y (ft)	2.01	2.13	2.41	2.52	3.08	2.27	2.21	2.76	1.71	1.8	1.8
Vertical Task											
σ_z (ft)	1.05	1.45	0.84	2.01	1.61	1.58	1.33	2.12	1.95	0.16	0.16
Overall Task											
σ_{disp} (ft)	3.87	3.61	3.19	5.66	4.81	4.07	4.12	4.72	4.45	2.1‡	2.2

*Subject was RG for Runs 226, 227, and 228; EF for the remaining runs.
†No phase lead; see Fig. 30.
‡Scanning remnant not included in calculations; see Appendix A.

NASA-Langley, 1971 —— 2